92

Advances in Biochemical Engineering/Biotechnology

Series Editor: T. Scheper

Advances in Biochemical Engineering/Biotechnology

Series Editor: T. Scheper

Recently Published and Forthcoming Volumes

Microscopic Techniques
Volume Editor: Rietdorf, J.
Vol. 95, 2005

Regenerative Medicine II
Clinical and Preclinical Applications
Volume Editor: Yannas, I.V.
Vol. 94, 2005

Regenerative Medicine I
Theories, Models and Methods
Volume Editor: Yannas, I.V.
Vol. 93, 2005

Technology Transfer in Biotechnology
Volume Editor: Kragl, U.
Vol. 92, 2005

Recent Progress of Biochemical
and Biomedical Engineering in Japan II
Volume Editor: Kobayashi, T.
Vol. 91, 2004

Recent Progress of Biochemical
and Biomedical Engineering in Japan I
Volume Editor: Kobayashi, T.
Vol. 90, 2004

Physiological Stress Responses
in Bioprocesses
Volume Editor: Enfors, S.-O.
Vol. 89, 2004

Molecular Biotechnology of Fungal
β-Lactam Antibiotics and Related Peptide
Synthetases
Volume Editor: Brakhage, A.
Vol. 88, 2004

Biomanufacturing
Volume Editor: Zhong, J.-J.
Vol. 87, 2004

New Trends and Developments
in Biochemical Engineering
Vol. 86, 2004

Biotechnology in India II
Volume Editors: Ghose, T.K., Ghosh, P.
Vol. 85, 2003

Biotechnology in India I
Volume Editors: Ghose, T.K., Ghosh, P.
Vol. 84, 2003

Proteomics of Microorganisms
Volume Editors: Hecker, M., Müllner, S.
Vol. 83, 2003

Biomethanation II
Volume Editor: Ahring, B.K.
Vol. 82, 2003

Biomethanation I
Volume Editor: Ahring, B.K.
Vol. 81, 2003

Process Integration in Biochemical
Engineering
Volume Editors: von Stockar, U.,
van der Wielen, L.A.M.
Vol. 80, 2003

Microbial Production of L-Amino Acids
Volume Editors: Faurie, R., Thommel J.
Vol. 79, 2003

Phytoremediation
Volume Editor: Tsao, D.T.
Vol. 78, 2003

Chip Technology
Volume Editor: Hoheisel, J.
Vol. 77, 2002

Modern Advances in Chromatography
Volume Editor: Freitag, R.
Vol. 76, 2002

History and Trends in Bioprocessing
and Biotransformation
Vol. 75, 2002

Technology Transfer in Biotechnology

From Lab to Industry to Production

Volume Editor: Udo Kragl

With contributions by
A. Aivasidis · J. Büchs · V. I. Diamantis · K. Drauz · J. Hubbuch · W. Hummel · A. Karau · A. Knoll · M.-R. Kula · W. Leuchtenberger · A. Liese · B. Maier · M. Müller · K. Nöh · M. Oldiges · T. Schubert · K. Schügerl · R. Takors · J. Thömmes · H. Tscherrig · D. Vasic-Racki · D. Weuster-Botz · R. Wichmann · W. Wiechert · M. Wolberg · J. Wöltinger

Springer

Advances in Biochemical Engineering/Biotechnology reviews actual trends in modern biotechnology. Its aim is to cover all aspects of this interdisciplinary technology where knowledge, methods and expertise are required for chemistry, biochemistry, micro-biology, genetics, chemical engineering and computer science. Special volumes are dedicated to selected topics which focus on new biotechnological products and new processes for their synthesis and purification. They give the state-of-the-art of a topic in a comprehensive way thus being a valuable source for the next 3–5 years. It also discusses new discoveries and applications.

Special volumes are edited by well known guest editors who invite reputed authors for the review articles in their volume.

In references *Advances in Biochemical Engineering/Biotechnology* is abbreviated as *Adv Biochem Engin/Biotechnol* as a journal.

Visit the ABE home page at springeronline.com

Library of Congress Control Number 2004114230

ISSN 0724-6145
ISBN 3-540-22412-2 **Springer Berlin Heidelberg New York**
DOI 10.1007/b14094

Springer is a part of Springer Science+Business Media
springeronline.com

Printed in The Netherlands

Typesetting: Fotosatz-Service Köhler GmbH, Würzburg
Cover: KünkelLopka GmbH, Heidelberg; design & production GmbH, Heidelberg

Printed on acid-free paper 02/3141xv – 5 4 3 2 1 0

Series Editor

Professor Dr. T. Scheper

Institute of Technical Chemistry
University of Hannover
Callinstraße 3
30167 Hannover, Germany
scheper@iftc.uni-hannover.de

Volume Editor

Professor Dr. Udo Kragl

University of Rostock, Institute of Chemistry
Dept. Analytical, Technical & Environmental Chemistry
Albert-Einstein-Str. 3A
18059 Rostock, Germany
udo.kragl@chemie.uni-rostock.de

Editorial Board

Advances in Biochemical Engineering/Biotechnology Also Available Electronically

For all customers who have a standing order to Advances in Biochemical Engineering/Biotechnology, we offer the electronic version via SpringerLink free of charge. Please contact your librarian who can receive a password for free access to the full articles by registering at:

springerlink.com

If you do not have a subscription, you can still view the tables of contents of the volumes and the abstract of each article by going to the SpringerLink Homepage, clicking on "Browse by Online Libraries", then "Chemical Sciences", and finally choose Advances in Biochemical Engineering/Biotechnology.

You will find information about the

– Editorial Board
– Aims and Scope
– Instructions for Authors
– Sample Contribution

at springeronline.com using the search function.

Prof. Christian Wandrey

Foreword

In 1974, when Prof. Christian Wandrey was working on the final stages of his PhD thesis on heterogeneous catalysis at the Institute for Technical Chemistry at the Technical University of Hannover, Prof. Dr. Karl Schügerl, at that time director of the institute, suggested that he should work on biocatalysis as the topic for his habilitation since enzymes seemed to be better catalysts than precious metals. We met on a memorable summer afternoon in 1974 at an autobahn service area between Hannover and Brunswick to discuss a project proposal and I was expected to contribute the necessary biochemical support. My first thought was to formulate a somewhat negative reply but, in the course of the discussion, the quantitative reaction engineering approach seemed to me to be an interesting and promising approach. So for three decades, a lasting fruitful scientific cooperation in the field of biocatalysis began. The first visible success was the development of the enzyme-membrane reactor (together with Degussa) for a technical process. These years were a time of intensive work with the enthusiastic commitment of all participants. However, at the same time, it was a great pleasure and Prof. Wandrey and I were awarded the Technology Transfer Prize by the German Research Ministry.

With the choice of the topic for his habilitation, Prof. Wandrey's career in the field of biotechnology started. The work with enzymes and enzyme reactors has been continuous up to now, with changing focuses and group leaders as the following chapters will show. In addition, there were other additional focuses. So, after Prof. Wandrey had moved to the Research Center at Jülich in the1980s, the anaerobic production of biogas was worked on intensively for some time. Technical chemists succeeded in introducing strictly anaerobic bacteria such as *Methanosarcina barkerii* into continuous cultures and in examining these cultures in pilot reactors for the reduction of different defined waste-products. These first attempts were also applied in the industry and were awarded the Phillipp Morris prize in 1987. From the 1990s, the activities of Prof. Wandrey shifted to the aerobic production of high value products like amino acids or proteins by means of microbial processes or animal cell cultures. These topics are still relevant.

To guarantee the necessary expertise und to remain competitive at an international level, networks and long-term cooperation are still needed in research work today. Jülich was a particularly convenient location, where – together

with Prof. Hermann Sahm and other scientists at the Institute of Biotechnology 1 – common interests in the production of amino acids, metabolic flux analysis and modeling could be followed. The support within the scope of the BMBF-project "Biocatalysis" as well as the BioRegio competition and co-operation with industry were helpful and encouraging. New challenges arise today in the development and the use of "designer bugs" for sustainable production or biological oxidation and reduction processes.

At a very early stage in Jülich, he started to study the production of monoclonal antibodies by means of animal cell cultures. At that time, nobody could foresee that pharmaceutical substances based on antibodies would become, as it is today, an ever growing field of industrial biotechnology. This decision made by Prof. Wandrey also helped my research group, which was involved with the isolation and purification of proteins, by giving us access to this kind of product and represented the basis of our studies on moving bed adsorption and mass transport in porous materials. I am very happy that after my retirement these activities are still being carried out at the Institute of Biotechnology 2, in order to maintain and expand this know-how. The cell culture group deals, in addition to protein production – another highly relevant topic – with the expansion of somatic cells.

For me the common denominator of all work and interests of Prof. Wandrey seemed to be always the reaction engineering approach to identify the limiting steps for speed or selectivity and to process modelling. By simulation, a great deal of process optimization can be speeded up as well as rational scale up and robust processes can be easily achieved. Naturally the efforts to extend and make useable the basic knowledge for a detailed understanding of all the process steps is also part of his interests.

After his 60th birthday, Prof. Wandrey is still facing five years of active and fruitful research work. The younger scientists who have come from this research group will have to meet future challenges – their contributions to this special volume show that they are well equipped for these tasks. Finally I would like to congratulate Prof. Wandrey heartily on the impressive successes which have led to many honors. I will remember the pleasant and inspiring co-operation over so many years and I am eagerly looking forward to new and exciting results which will be presented by his research group.

June 2004 Maria-Regina Kula

Contents

Adv Biochem Engin/Biotechnol (2005) 92: 1–48
DOI 10.1007/b98920

Extraction of Primary and Secondary Metabolites

K. Schügerl (✉)

Institute for Technical Chemistry, University Hannover, Callinstrasse 3,
30167 Hannover, Germany
Schuegerl@iftc.uni-hannover.de

Abstract Several new methods besides the usual organic solvent extraction have been developed over the last few years for the extraction of primary and secondary metabolites. These are: alcohol extraction with various biocompatible solvents, recovery of carboxylic acids and antibiotics with reactive extraction, dissociation extraction, aqueous two-phase extraction, and supercritical and near critical fluid extraction. Extraction and re-extraction processes are integrated into a single step by emulsion liquid membrane and solid supported liquid membrane extractions. These extraction processes are discussed and compared in this review, along with extraction with reversed micelles, and reactive extraction with the formation of a third phase at the organic-aqueous interface.

Keywords Reactive extraction · Emulsion liquid membrane · Solid supported liquid membrane · Aqueous two-phase system · Reversed micelles

Abbreviations

Adogen 381	Bis(tridecyl)amine
Adogen 283	Di-tri-decyl amine, branched
Adogen 368	Tri C_8, C_{10}, C_{12} amine isomers with straight chain
Adogen 464	Tri-octyl-methyl ammonium chloride
Ala	Alanine
Alamine 336	Tri-*n*-(C_8-C_{10})-amine
Aliquate336	Tricapryl methyl ammonium chloride
AmAc	Amyl acetate
Amberlite LA-1	Sec. amine with highly branched chains
Amberlite LA-2	*N*-lauryl-*N*-trialkyl methylamine
AOT	Bis(2-ethyl-hexyl) sodium sulfo succinate
6-APA	6-Amino penicillanic acid
APPT	Hydroxy propyl starch polymer
Arg	Arginine
ATPS	Aqueous Two Phase System
BuOH	Butanol
CBO	Carbon-bonded oxygen
Chevron 25	Mixture of C_8 and C_9 alkylated aromatics
Cyanex 923	Mixture of tri-alkyl phosphine oxides
DOA	Dioctyl amine
D2EHPA	Di-(2-ethyl hexyl) phosphoric acid
D2EHPA(S)	Di-(2-ethyl hexyl)mono thiophosphoric acid
DITDA	Di-iso-tri-decylamine
DNNS	Di-nonyl-naphthalenesulfonate
DTAC	Dodecyl-thrimethyl ammonium chloride
ECA4360J	Surfactant
EO-PO	Ethylene oxyde-propylen oxide copolymer
EtAc	Ethyl acetate
Gly	Glycine
HEC	Hydroxy methyl cellulose
His	Histidine
HoeF2562	Di-iso-tridecylamine
Hostarex A327	50:50 Mixture of tri-*n*-octyl/tri-*n*-decylamine
Ile	Isoleucine
IP	Ion-pair
ISOPAR	Paraffinic kerosene
K_D	Dissociation coefficient
Leu	Leucine
MCl_2	Methylene dichloride
MeOH	Methanol
Met	Methionine
MIBK	Methyl-isobutyl ketone
MPEG	Methoxy polyethylene glycol
NP	Nonyl-phenol ethoxylate
PAA	Phenyl acetic acid
PBO	Phosphorus-bonded oxygen
PEG	Polyethylene glycol
PEI	Polyethylene imine
Phe	Phenylalanine

pK_a	$Log K_D$ of acids
pK_b	$Log K_D$ of bases
PPG	Polypropylene glycol
PTFE	Polytetrafluoro ethylene
PVDF	Polyvinilidene difluoride
SCF	Supercritical fluid
Ser	Serine
Shellsol A	Medium fraction of aromatic hydrocarbons
Shellsol H	Medium fraction of aliphatic hydrocarbons
Span 80	Surfactant
TBP	Tri-butyl phosphate
Thr	Theronine
TOA	Tri-octyl amine
TOMAC	Tri-octyl-methyl-ammonium chloride
TOPO	Trictyl-phosphine oxide
Trp	Tryptophan
Tyr	Tyrosine
Val	Valine

1 Introduction

Extraction is an important separation technique in chemistry and biotechnology. It is usually applied in biotechnology as the first step in the recovery of primary and secondary metabolites.

Extraction competes with many other separation methods, including adsorption, precipitation, chromatography, distillation, membrane separation, crystallisation, ion exchange, and electrodialysis. Adsorption has the disadvantage of low loading capacity, so it is applied if other techniques are less effective (such as in case of cephalosporin C). In spite of its low selectivity, precipitation is used as the first step of recovery for many compounds, for instance citric acid. Chromatography and crystallisation are used for purification, not for the first step of product recovery. Distillation is employed for temperature stable metabolites like acetic acid. Ion exchange and electrodialysis are utilised for the separation of low molecular primary metabolites such as lactic acid. Membranes are often used to separate cells, and as the first stage of product recovery, but they are not very selective and are impaired by fouling from proteins, which are ingredients of the cultivation medium. Membranes are often combined with other separation methods, which have higher selectivity.

The main problem with the recovery of primary and secondary metabolites by extraction is the complexity of industrial cultivation media, meaning that several by-products are extracted as well as the desired main product. Various alternative extraction techniques, like reactive extraction and aqueous two-phase extraction, have been investigated in order to improve the selectivity

of the product recovery. A decrease in production costs can be obtained by integrating downstream processing stages by performing extraction and re-extraction in a single stage, for example by using emulsion liquid membrane or solid supporting liquid membrane techniques.

If product inhibition prevails, an increase in productivity can be obtained using in situ recovery of the products. In the case of in situ extraction, the toxic effect of the solvent on the cells can be reduced by using membranes to avoid direct contact between cells and solvent. In some cases, the phase separation is not possible or it is a slow process. This problem can be overcome by separating the phases with a membrane.

This review is a status report on solvent extraction and its various alternatives. The equilibrium distribution coefficient K_D of the product in solvent is decisive for the recovery of primary and secondary metabolites by solvent extraction. To determine K_D, basic investigations are performed with model systems using only a single solute in a chemically well defined aqueous feed (F) by applying a chemically well defined solvent (S). The distribution equilibrium and sometimes the kinetics of the extraction process are determined by measuring the concentrations of the solute in the extract (E) and sometimes in the raffinate (R). For in situ product recovery, the biocompatibility of the solvent is important. For these investigations the growth rate, viability of the microorganisms, and the product formation are determined in the presence of solvents.

This review is divided into two main sections, two phase systems and three phase systems, and these are subdivided according to the various types of extraction techniques. Different solutes are discussed in these subsections.

2
Two-Phase Systems

The microorganisms are separated from the cultivation medium by filtration or centrifugation. The product is extracted from the cell free cultivation medium by solvent/extractant. During the extraction, only the aqueous feed phase and the organic solvent/extractant phases are present. No third phase is formed.

2.1
Solvent Extraction

Cultivation of microorganisms is performed in aqueous media. The microorganisms are separated from the cultivation medium at the end of the production process. The product is extracted from the cell free medium by an organic solvent. The main problem is how to extract a hydrophilic compound from the aqueous phase into an organic phase with high efficiency. Several organic solvents have been tested, and the distribution equilibrium of the solutes between

water and solvent were determined. In the following, the recoveries of different metabolites by solvent extraction are discussed.

2.1.1 Alcohols

Industrial alcohols are formed from petrochemical sources. Edible ethanol must be produced by fermentation. During the 1970s, research into microbial alcohol production from renewable sources was intensified because of the energy crisis. During this time several investigations were carried out on ethanol and butanol production and recovery from cultivation media. The recovery of ethanol from the cell free cultivation media was performed by distillation.

In situ removal of ethanol and butanol during the cultivation is necessary for high productivity, because cell growth and product formation are inhibited at high alcohol concentrations. Solvent extraction was considered to be one possible solution for maintaining the alcohol concentration in the cultivation medium at a low level.

The main problem was that common organic solvents with high distribution coefficients for alcohols were toxic to the cells, and solvents which were biocompatible had low distribution coefficients. Therefore, large numbers of different compounds were tested for their suitability as solvents in terms of their distribution coefficients and biocompatibility. Daugulis et al investigated 1500 compounds [1–6] for their suitabilities as extractants. Other research groups (for example [7, 8]) also tested a large number of solvents. The main interest was in improving the productivity of the process by reducing the product inhibition. This was performed by in situ extraction of the alcohols during the cultivation. The microorganisms were retained in the bioreactor by the membrane. The product was extracted in situ from the cell free cultivation medium, and the medium was recycled into the reactor or the cells in direct contact with the solvent. In Table 1 some solvents are listed that are relatively useful for the in situ extraction of ethanol and butanol. The aqueous and organic solvent phases are sometimes separated by a membrane in order to avoid the direct contact of the cells with the solvent. Some of these investigations are described in Table 2.

Ethanol was formed by the cultivation of *Saccharomyces cerevisiae* or *Zymomonas mobilis.* The ethanol productivity was improved using in situ extraction by a factor of 2.5–3.0 [4, 26, 28, 52].

Butanol is produced by *Clostridium acetobutylicum,* which forms acetone, ethanol, acetate, butyrate and a small amount of acetoin. The equilibrium distribution coefficients of acetone in these solvents are lower than those of butanol (Table 3). At particular cultivation conditions the K_D values in *n*-decanol are: 6.5 (butanol), 4.65 (butyrate), 0.7 (acetone), and 0.45 (ethanol) [37]. Because acetone, ethanol and butyrate are co-extracted, a separation step by fractionated distillation is necessary after their recovery.

Table 1 In situ extraction of ethanol and butanol by various solvents

Ethanol		Butanol	
Solvent	Reference	Solvent	Reference
Dodecanol	[9–13]	*n*-decanol	[37, 38]
Higher iso-alcohols	[9, 14]	*n*-hexanol	[38]
Higher *n*-alcohols	[9, 15, 16]	Iso-nonanol	[38]
Tributyl phosphate	[13, 14, 17, 18]	Iso-decanol	[38]
Dibutyl phtalate	[18, 19]	Methylbenzoate	[38]
2-tert-butyl phenol	[18]	Tetradecanol	[38]
Dodecane	[20]	Diisobutyl ketone	[38]
Fluoro carbons	[21]	Mesitylen	[38]
Higher iso-acids	[20]	Anisol	[38]
n-decanol	[22]	Xylene	[38]
Heptanal	[23]	Dibutyl phthalate	[38, 39]
Tributyl phosphate + ISOPAR M(paraffin)	[17, 24]	Benzyl benzoate + oleyl alcohol (multiple extractants, theory)	[40]
Oleyl alcohol	[4, 6, 25, 27, 31]		
Oleic acid	[28, 29]	Oleyl alcohol (theory)	[41]
With immobilised cells:		Poly(propylene glycol)	[42]
Sec-octanol + Poropak Q	[30]	Oleyl alcohol	[43, 44]
Poly(propylene glycol)1200	[31]	Oleyl alcohol (model)	[45]
o-isopropylphenol	[31–34]	Oleyl alcohol(comparison)	[46]
o-tert butylphenol	[31–34]		
oleyl ester	[35]	2,3-butanediol extracted by dodecanol	[47]
n-dodecanol	[8]		
Tri-*n*-butyl phosphate/ ISOPAR N, extractive distillation	[36]		

Table 2 In situ membrane extraction of ethanol and butanol by various solvents

Ethanol		Butanol	
Solvent	Reference	Solvent	Reference
Sec octanol	[48]	2-ethyl hexan	[55]
Propylene glycol		Oleyl alcohol	[56]
Ethylene glycol	[49]	Ethylene glycol (comparison)	[57]
Tributyl phosphate (Model)	[50, 51]		
Dibutyl phthalate	[52]		
Caprylic acid/octane ester formation with immob lipase	[53]		
Ester formation with immob lipase	[54]		

Table 3 Experimental values of K_D for acetone and butanol for various solvents [38]

Solvents	T (°C)	K_D (acetone)	K_D (butanol)
Ethyl ether	20	0.76	5.14
n-Hexanol	20	0.67	9.47
	40	1.19	14
Iso-nonanol	20	0.63	7.73
	40	0.87	8.69
Iso-decanol	20	0.41	5.86
Tetradecanol	40	0.61	5.22
Di-isobutyl-ketone	20	0.72	2.55
Anisole	20	0.85	0.99
	40	1.04	1.77
Phenetol	20	0.68	0.88
Xylene	20	0.49	0.53
Mesitylene	20	0.38	0.47
Methylbenzoate	20	0.79	1.84
Di-butylphthalate	20	0.52	1.21

Although product concentrations are low in continuous cultivation, by recirculating the microorganisms the product concentration can be improved. For example without recycling at D=0.1 h^{-1}, 3.81 g l^{-1} butanol, 1.92 g l^{-1} acetone, 0.36 g l^{-1} ethanol, and 1.27 g l^{-1} butyrate were obtained. With recycling at D=0.1 h^{-1}, 14,1 g l^{-1} butanol, 6.73 g l^{-1} acetone, 1.19 g l^{-1} ethanol, and 1.28 g l^{-1} butyrate were obtained, while 10.27 g l^{-1} butanol, 5.66 g l^{-1} acetone, 0.76 g l^{-1} ethanol and no butyrate were attained at D=0.4 h^{-1} [57]. At these high product concentrations the inhibition is considerable. Therefore, in situ extraction is necessary. Butanol is formed from butyrate. Its concentration should be high in the cultivation medium. The feed phase is sometimes saturated by butyrate in order to improve the productivity. The butanol productivity was increased with in situ extraction by a factor of 1.5–1.6 [39, 42, 43]. With four stage extraction [37] and with membrane extraction [56] the productivity was increased by a factor of four compared to standard cultivation conditions. Because of the large differences between the boiling points of the applied solvents and solutes, recovery of the alcohols from the extract is performed by fractionated distillation.

2.1.2 Acids

Aliphatic carboxylic acids are formed during aerobic cultivation as intermediates of the metabolic pathway. Special modifications of the tri-caboxylic acid pathway produce some of these acids in relatively high yields. The most important products are acetic, lactic and citric acids. Acetic acid is produced by the species *Acetobacter*, and it is recovered through a combination of extraction

Table 4 K_D values of solvents for acetic acid [59]

Solvents	Range of K_D
n-Alcohols (C_4–C_8)	1.68–0.64
Ketones (C_4–C_{10})	1.20–0.61
Acetates (C_4–C_{10})	0.89–0.17
Ethers (C_4–C_8)	0.63–0.14

and azeotropic distillation [58]. If one uses high boiling point solvents, acetic acid and co-extracted water are taken overhead. With low boiling point solvent, the acetic acid comes as a still residue, which may contain heavy impurities. Some K_D values of different solvents with regard to acetic acid are shown in Table 4. In each case, the lowest molecular weight member shows the highest value of K_D. Although they give high K_D values, alcohols tend to esterify with acetic acid and are therefore seldom used. Ketones have the next highest K_D but they do not have good azeotropic properties for removing water by subsequent azeotropic distillation. Hence acetates and ethers are the more commonly used solvents [59]. In the present of salts, and with increasing salt concentration, the K_D value increases, which can be explained by the "salting out" effect [60]. Acetic acid was extracted by decyl-alcohol through a membrane [61].

Lactic and citric acids are precipitated as Ca-salts in the cultivation medium, and after their separation, the free acids are obtained with sulphuric acid.

The extraction equilibria of citric, tartaric and malic acids in *n*-octanol, *n*-heptanol, 1-pentanol and 2-pentanol were determined. These extractions cannot compete with the salt precipitation because of their low equilibrium constants: K_D=0.102 (*n*-octanol) and K_D=0.237 (*n*-hexanol) for citric acid [62].

In order to improve the extraction efficiencies of higher carboxylic acids, they were converted to their esters using oleyl alcohol in the presence of lipase. This oleyl ester formation of butyric and propionic acids resulted in increases in distribution coefficients by factors of 4–15 [63, 64].

2.1.3 Secondary Metabolites

The most important secondary metabolites in bulk biotechnological production are the antibiotics. Standard handbooks cover the recovery of antibiotics [64–69]. Most antibiotics are secreted by the cells into the broth. The cells are removed from the broth by filter press or rotary filter and the product is recovered from the cell free broth by extraction or adsorption.

Penicillin recovery has been investigated by several researchers. The first reports on the extraction of penicillin from the cultivation medium by means of amyl acetate and 10% phosphoric acid at 3 °C [70] and in amyl acetate, cyclohexyl acetate and methylcyclohexanone [71] were published in 1946. Later, the extraction was carried out in centrifugal extractors [72–74]. Various other

Table 5 Solvent extraction of some antibiotics [76]

Product	Medium	Solvent	pH	Reference
Actinomycin	cake	1MeOH+2MCl_2	2.5	[77]
Adriamycin	cake	acetone	acidic	[78]
Bacitracin	cult medium	n-BuOH	7.0	[79]
Chloramphenicol	cult medium	EtAc	alkaline	[80]
Clavulanic acid	cult medium	*n*-BuOH	2.0	[81]
Cyclheximid	cult medium	MCl_2	3.5–5.5	[82]
Erythromycin	cult medium	AmAc	alkaline	[83]
Fusidic acid	cult medium	MIBK	6.8	[84]
Griseofulvin	cake	BuAc, MCl_2	7.0	[84]
Macrolides (general)	cult medium	MIBK, EtAc	alkaline	[86]
Nisin	cult medium	$CHCl_3$, sec-octanol	4.5	[87]
Oxytetracycline	cult medium	BuOH		[88]
Penicillin	cult medium	BuAc, AmAc	2.0	[89]
Salinomycin	cake	BuAc	9.0	[90]
Tetracycline	cult medium	BuOH		[91]
Tylosin	cult medium	AmAc, EtAc		[92]
Virginiamycin	cult medium	MIBK	acidic	[93]
Cephalosporin C (chemically modified)	cult medium	4-methylpentanon *n*-butanol		[94]

MeOH (methanol), AmAc (amylacetate), BuOH (butylalcohol), BuAc (butylacetate) EtAc (ethylacetate), $MeCl_2$ (methylene-dichloride), MIBK (methyl-isobutylketone) $CHCl_3$ (chloroform), mash (cult medium with cells), cult medium (cell free medium), cake (medium-free cells).

methods have been developed [75], but the original method using a centrifugal extractor is preferred in the industry.

If the product is a weak acid with a low dissociation constant (pK_a), the value of the pH of the cultivation medium must be reduced considerably below the pK_a value in order to be able to extract the product using organic solvents.

If the product is a weak base with a high dissociation constant (pK_b), the pH of the cultivation medium must be increased above the pK_b value by two units in order to be able to extract the product from the broth by organic solvent.

If the product is very soluble in water, the cultivation medium must be salt saturated (salting out) in order to increase the degree of extraction with the organic solvent.

Carbon-bonded oxygen-bearing extractants (alcohols, esters and ketones) are often used for the recovery of polar compounds. Apolar extractants (petrolether, methylene dichloride, ethylene dichloride) are applied for the extraction of lipophilic compounds. The main problem with the carbon-bonded oxygen-bearing extractants is their relatively high solubility in the cultivation medium. With increasing molecular weight, their solubility in the aqueous phase decreases, but their tendency to form stable emulsion increases [76].

Solvent extractions of some antibiotics are described in Table 5 .

Table 6 Distribution coefficients for penicillin G at pH 4 between aqueous solutions and organic solvents [70, 71]

Solvent	Distribution coefficient
Methyl-cyclohexane	180
Dimethyl-cyclohexane	160
Methyl-cyclohexanol	80
Cyclohexyl acetate	62
Furfuryl acetate	44
Methyl-isobutyl ketone	33
Dimethyl-phthalate	30
2-Ethyl hexanol	26
Amyl acetate	20
Diethyl oxalate	20

Penicillin aside, only a few antibiotics are recovered by extraction. Earlier publications on tetracycline and cephalosporin extractions do not have practical relevance any longer, since nowadays tetracycline is recovered by precipitation and cephalosporin by adsorption.

Penicillin can be recovered by various organic solvents at low pH and at low temperature (see Table 6). The mycelium free cultivation medium is cooled down to 0–3 °C, acidified by sulphuric acid (pH 2.0–3.0) and penicillin G and/or V are extracted by amyl acetate or butyl acetate in centrifugal (Podbielnak, Luwesta or Alfa-Laval) extractors. In order to repress the formation of emulsion, de-emulsifier is added to the cultivation medium. In some factories the cell containing cultivation medium is extracted by amyl acetate in a counter current extraction decanter (Westfalia, Oelde) [76].

The organic solution is added at pH 6 to an aqueous buffer solution to produce a penicillin-rich aqueous solution. Water-soluble penicillin anions are present at this pH. After re-acidification, it is re-extracted with butyl acetate or amyl acetate [95–97]. Modern strains yield high product concentration in the cultivation medium, so the potassium salt can be precipitated after the first extraction step.

2.2 Reactive Extraction

Smith and Page [98] first pointed out that long chain aliphatic amines form hydrophobic ion pair complexes with organic acids, which can be extracted by organic solvents. King et al [99–102] systematically investigated the formation of these complexes with a large number of long chain amines and long chain alkyl phosphine oxides. They determined the equilibrium distribution coefficients of acetic acid and several other carboxylic acids with these amines and phosphine oxides in various organic solvents. This separation technique for the recovery of acetic acid with TOPO (tri-octyl phosphine oxide) [103, 104] and of various organic acids with long chain aliphatic amines [105–107] was patent-

Table 7 Examples of the influence of the acetic acid concentration in the aqueous phase on the distribution coefficient with 22 wt% TOPO in Chevron 25 [100]

Aqueous acetic acid concentration	K_D
0.189	3.12
1.27	1.33
3.20	0.76
7.45	0.45

ed. The equilibrium distribution coefficients of several aliphatic carboxylic acids with tri-iso-octylamine and iso-decanol as modifier and in Shellsol T as diluent were determined [108–109]. Wojtech and Mayer [110] used a 4/1 mixture of nonyl-phenol/Hostarex A 327 (50:50 mixture of tri-*n*-octyl/tri-n-decylamine) with a distribution coefficient of 300 to remove acetic acid from waste water. This mixture was also used for the extraction of butyric, malonic and lactic acids, and their distribution coefficients was increased by factors of 10–100 by complex formation. The combination of extractants, diluents, and acid concentration has a considerable influence on the distribution coefficients [111–113]. With the development of Cyanex 923 (a mixture of tri-alkyl phoshine oxides) the efficiency of the extraction was improved [114]. A comparison of the equilibrium distributions of acids with different extractants indicates that their efficiency depends on the acid and its concentration: TOPO>TBP (tributyl phosphate)>TOA (tri-octyl amine) for dilute and concentrated acetic acid. For propionic acid, the order of succession is different: TOA>TBP>TOPO [114]. The influence of the acid concentration on K_D is shown in Table 7. The extraction power increases with dilution of the acid [115].

The recovery of acids with amines from waste water is especially efficient. The K_D values are influenced by the type of extractant as well (Table 8).

The extraction of organic acids with a carbon-bonded oxygen (CBO) donor is not selective enough. The solvation numbers of aliphatic carboxylic acids extracted with phosphorous-bonded oxygen (PBO) donor extractants sometimes indicate a stoichiometric association between an individual phosphoryl

Table 8 Examples of the influence of extractant on the K_D of acetic acid in water with 30 vol% secondary and/or tertiary amines in a chloroform diluent system at 0.04 wt% acid concentration [100]

Amines		K_D
Secondary	Amberlite LA-1	4.48
	Amberlite LA-2	9.86
Tertiary	Adogen 381	32.11
	Adogen 368	7.79
	Alamine 336	9.6

group and an individual carboxyl group. Due to successful competition between the solvating phosphoryl groups and the water molecules at the interface, the organic adducts with alkylphosphates are hydrated with one or more water molecules. This causes the high distribution ratios of the acids. The best results can be achieved with high-molecular weight aliphatic amine extractants or by combining them with PBO extractants. When using aliphatic amine (secondary or tertiary amine) extractants, proton transfer occurs during the extraction, and the acid prevails in the organic phase as an amine-acid ion pair. They are therefore called ion-pair (IP) extractants. They are less soluble in water than CBO- and PBO-extractants and yield the highest partition coefficients. Because of the rather high prices of the extractants, a low solubility in aqueous solutions is desired. The low solubility is obtained by the long hydrophobic tails of the PBO- and IP-extractants. High selectivity can be obtained by choosing suitable operational conditions (pH-value, ion strength). Low toxicity would be desired. However, most of these extractants are toxic to organisms. The ideal extractants are inexpensive, selective, biocompatible and have low solubilities in water. Unfortunately, these ideal properties cannot be realized. The toxicities of these extractants restricts their application to industrial use.

The recovery of aliphatic carboxylic acids with CBO-extractants is not economical. PBO- and IP-extractants are preferred because of their high partition coefficients and low solubilities in the aqueous solutions. Extractions of single aliphatic carboxylic acids with PBO- and IP-extractants have been investigated by several groups. Various solvents/diluents were used for the extractants. If paraffin was used as solvent, the complex often formed a third phase at the interface. To avoid this third phase formation, polar co-solvents (modifiers) were added to the system.

The extraction chemistry of carboxylic acids was theoretically discussed by Kertes and King [102]. They distinguished between three extraction types:

- Acid extraction can be carried out by solvation with carbon bonded oxygen-bearing (CBO) extractants.
- Acid extraction by solvation with phosphorous-bonded oxygen bearing (PBO) extractants.
- Acid extraction by proton transfer or ion-pair (IP) formation, the extractants being high molecular weight aliphatic amines.

Let us now consider the corresponding relationships.

The mass action law equilibrium for the extraction of monocarboxylic acid by a strong solvating extractant, such as an organo-phosphorous compound, is strongly influenced by the dissociation of the acid in the aqueous solution

$$HS \overset{K}{\rightleftharpoons} H^+ + S^- \tag{1}$$

The dissociation constant K is given by

$$K = \frac{[H^+][S^-]}{[HS]} \tag{2}$$

The acid in the aqueous phase HS_a forms the complex $HSEx_{no}$ in the organic phase with n moles (solvation number) of the solvating extractant Ex_o in the organic phase

$$HS_a + nEx_o \overset{K_{on}}{\rightleftarrows} HSEx_{no} \tag{3}$$

The equilibrium constant K_{en} complex formation is given by

$$K_{en} = \frac{[HSEx]_o}{[HS]_a\,[Ex]_o^n} \tag{4}$$

The distribution ratio D_c on a molar concentration basis is given by

$$D_c = \frac{C_{HS_{ot}}}{C_{HS_{at}}} = \frac{[HSEx_n]_o}{[HS]_a + [S^-]_a} = \frac{K_{en}\,[HS]_a\,[Ex]_o^n}{[HS]_a + K\,[HS]_a/[H^+]_a} = \frac{K_{en}\,[Ex]_o}{1 + K/[H^+]_o} \tag{5}$$

These equations neither take the free acid nor the dimer into account, since in the presence of strongly solvating agents no unsolvated acid monomer and dimer are present.

The Mass Action Law Equilibrium between the proton bearing organic compound HS in the aqueous phase and the long chain aliphatic amine extractant in the organic phase is given by

$$HS_a + A_o \overset{K_{em}}{\rightleftarrows} AHS(HS)_{mo} \tag{6}$$

The equilibrium constant K_e is given by

$$K_e = \frac{[HSA]_o}{[HS]_a\,[A]_o} \tag{7}$$

In some cases this acid-base type reaction is not stoichometric. If the extractant takes acid in excess, the following relationships are valid:

$$AHS_o + mHS_a \overset{K_{em}}{\rightleftarrows} AHS(HS)_{em} \tag{8}$$

with the equilibrium constant

$$K_{em} = \frac{[AHS(HS)_m]_o}{[AHS]_o\,[HS]_o^m} \tag{9}$$

In several publications the equilibrium distribution coefficient K_D is used, which is defined empirically as the weight fraction of the solute in the solvent phase per its weight fraction in the aqueous phase. The relationship between the distribution ratio D_c and K_D is given by

$$D_c = K_D \frac{\rho_o}{\rho_a} \tag{10}$$

where ρ_o and ρ_a are the densities of the organic and aqueous phases.

In the case of acetic acid, the acid [HS] distributed between the aqueous (a) and organic (o) phases dissociates to anion S^- and proton H_3O^-, and reacts with the amine carrier A [116]:

Physical extraction (p):

$$HS_{a,p} \overset{k_p}{\rightleftharpoons} HS_{o,p} \tag{11}$$

$$k_p = [HS]_{o,p}\, V_o / [HS]_{a,p} V_a \tag{12}$$

Dissociation

$$HS_a + H_2O \overset{k_a}{\rightleftharpoons} H_3O + S_a^- \tag{13}$$

$$[HS]_a = \frac{c_o[HS]}{1 + 10^{(pH - pK_a)}} \tag{14}$$

where K_a is the dissociation coefficient of the acid in the aqueous phase.

Complex formation (V_a:V_o=1:1)

$$HS_a + (A)_o \overset{k_1}{\rightleftharpoons} (HSA)_o \tag{15}$$

$$k_1 = \frac{[HSA]_o}{[HS]_a\,[A]_o} \tag{16}$$

$$HS_a + (HSA)_o \overset{k_2}{\rightleftharpoons} ((HS)_2\,A)_o \tag{17}$$

$$k_2 = \frac{[(HS)_2\,A]}{[HS]_a^2\,[HSA]_o} \tag{18}$$

where k_1 and k_2 are the complex formation constants with one and two acid molecules. These relationships hold true for other acids as well.

Several research groups have investigated the reactive extraction of lactic acid. Some investigations are compiled in Table 7. Lactic acid inhibits cell growth and product formation by *Lactobacilli.* This is caused by the pH drop and its toxicity to the microorganisms. Especially at low pH the non-dissociated acid toxicity is high. Therefore, the in situ extraction of lactic acid has been investigated by several research groups. Common long chain amine and phosphorus-bonded oxygen bearing extractants are toxic to the microorganisms. By using immobilised cells and oleyl alcohol, or cells with co-immobilised soybean oil, the inhibition effect was reduced [119]. In Table 9 some investigations are presented.

The separation of different aliphatic carboxylic acids by reactive extraction depends on their dissociation constants (pK_a). The stabilities of PBO- and IP-acid complexes are influenced by the pH values of the solutions and the pK_a

Table 9 Investigations into the reactive extraction of lactic acid (–) without the cultivation of micro organisms

Microorganisms	Extractant	Solvent/diluent	Reference
Lactobacillus delbrückii, immobilised	Alamine 336	Oleyl alcohol	[117–120]
	TOPO	Dodecane	[117]
	Alamine 336	Co-immobilised Soybean oil/ Oleyl alcohol	[119]
Lactobacillus casei	Amberlite LA2	Kerosene, Butylacetate	[121, 122]
	HoeF2562	Kerosene, Butylacetate	[121, 122]
Lactobacillus salivarius, *Lactobacillus delbrückii*	Alamine 336	Kerosene, Butylacetate	[121, 122]
	Hostarex A237	Kerosene, Butylacetate	[121, 122]
	Cyanex 923	Kerosene, Butylacetate	[121, 122]
–	Alamine 336	Toluene	[123]
–	Tri-*n*-octylamine	Xylene	[124]
–	Trioctylamine	MIBK, Octanol, Decanol	[125]
Lactobacillus rhamonosus	TOMAC, TOPO, DOA, TOA, TBP	Oleyl alcohol, Butylacetate	[126]
–	TOA	MIBK	[127]
–	Trioctylammonium chloride	Oleyl alcohol	[128]
–	Alamine 336	MIBK	[129]
Lactobacillus amylovorus, membrane extraction	TOPO	Kerosene	[130]

values of the compounds. Separation of components is possible if their pK_a values are at least one pH unit apart, for example formic acid (pK_a=3.7) and acetic acid (pK_a=4.76). The separation of higher carboxylic acid homologues based on their pK_a values is not possible (pK_a values of propanoic, butyric, pentanoic, hexanoic, heptanoic, octanoic, … acids are in the range 4.85–5.0). The differences between, for instance propanoic acid (pK_a=4.85), lactic acid (pK_a= 3.86) and pyruvic acid (pK_a=2.49) are large enough for their separation. *Cis-trans*-isomers, such as maleic acid (pK_a=1.93; 6.14) and fumaric acid (pK_a= 3.03; 4.38), can also be separated by IP-extraction.

Citric acid is produced by *Aspergillus niger* and precipitated from the cultivation medium as Ca salt. After treating this salt with sulphuric acid, the free citric acid is recovered and the waste $CaSO_4$ is deposed of. To avoid the deposition of this contaminated $CaSO_4$, which cannot be used for any other purpose, an attempt was made to recover the acid by extraction. However, the distribution coefficients of citric acid in common organic solvents are low. For instance, following values were determined in 0.16 wt% aqueous feed: 0.29 (butanol), 0.1 (butylacetate), 0.1 (ethylether), 0.1 (methyl-isobutyl-ketone), 0.33 (methyl-

Table 10 Investigations into the reactive extraction of citric acid without cultivation of micro organisms (–)

Microorganism	Extractant	Diluent	Reference
Aspergillus niger	Trilaurylamine Trilaurylamine Trilaurylamine + diethylhexyl phosphoric acid Trilaurilamine	Oleic acid Octanol Hydrocarbon 2-Bromohexanone acid	[105–107]
–	TOPO	*n*-Heptane+*n*-octanol	[131]
–	TOPO	Shellsol H	
–	TBP	Di-iso-propylether	
–	TBP	MIBK	
–	TBP	Shellsol H	
–	Tri-iso-octyl amine	Shellsol H	
Aspergillus niger	Alamine 336	Isopar H Isopar H+MIBK *n*-Butyl chloride	[132]
Aspergillus niger	Trialkyl-phosphine oxide C_8–C_{10} tertiary amine Trioctylamine	Non-specified diluent Specified diluent	[133]
–	Hostarex A 324	Isodecanol	[134–136]
–	Trialkylamine	MIBK and other solvents	[137, 138]
Aspergillus niger	Tridodecylamine	Octanol	[139]
–	Trioctylamine	Octanol cyclohexanol isobutylalcohol petroleum ether	[140]
Aspergillus niger	Hostarex A327	Oleyl alcohol	[141]

ethyl ketone), and 0.21 (cyclohexanone) [98]. To improve the distribution coefficient, the hydrophobicities of the solutes were increased by creating phosphorous-bonded oxygen donor or long chain amine compounds of citric acid. The K_D values of some of these compounds indicate improved distribution coefficients: 2.3 (tri-butyphosphate), 2.7 (dibutyl phosphate), 4.4 (tributyl-phosphine oxide), 6.5 (tri-iso-octyl amine) [131]. Some investigations into the reactive extraction of citric acid are compiled in Table 10, while the extraction and separation of some carboxylic acids are described in Table 11.

Separating solutes with more than one charged group, which form approximately neutral zwitterions, is a difficult task. Typical compounds of this type are the amino acids. With the exception of threonine, all bifunctional amino acids have their pK_1 (COO^-) value between 2 and 3, and their pK_2 (NH_3^+) value between 9 and 10. This also holds true for trifunctional amino acids, with the exception of cystein that has pK_1=1.71 and pK_2=10.78, and histidine with pK_1=1.82.

Table 11 Investigations into the reactive extraction of various carboxylic acids without cultivation of micro organisms (–)

Microorganism	Acid	Extractant	Diluent	Reference
Lactobacillus casei, *Lactobacillus salivarius*, *Lactobacillus delbrückii*	Acetic, Lactic, Citric (separation)	Amberlite La-2, HoeF2562, Alamine 336, Hostarex A237, Cyanex 923	Kerosene, Butylacetate	[121, 122]
Propionibacterium acidopropionici	Propionic	Alamine 336	2-Octanol	[142, 143]
–	Propionic	TOA, TOPO, TBP	Hexane	[115]
Clostridium butyricum	Butyric	Hostarex A 327, Tri-hexylphosphate	Isodecanol, Isotridecanol, Oleyl alcohol	[144]
Clostridium tyrobutyricum	Butyric	Alamine 336	Oleyl alcohol	[145]
–	Succinic Tributylamine Tripentylamine Trioctylamine	Tripropylamine *n*-Heptane Octanol Octanol	Octanol	[146–148]
–	Succinic	Alamine 336	Chloroform, MIBK	[149]
–	Oxalic	Trioctylamine	*n*-Octanol, *n*-Octanol/ kerosene	[150]
–	Acetic, Lactic, Propionic, Butyric	Aliquate 336 and Alamine 336	2-Octanol or Kerosene	[151]
–	C_2–C_4 mono carboxylic, C_4 dicarboxylic, C_6 tricarboxylic	TOPO	Kerosene, *n*-Hexane, Isoctane, Cyclohexane, *n*-Heptane	[152]
–	C_1–C_4 mono carboxylic	Tri-*n*-octylamine	–	[153]
–	C_1–C_8 mono carboxylic, C_2–C_4 dicarboxylic, Citric	Octyl(phenyl)-*N*,*N*-diisobutyl-carbamoyl-methyl-phosphine	–	[154]
–	Acetic, Lactic, Propionic, Crotonic, Malic, Citric, Itaconic	TOPO	Hexane	[155]

Table 11 (continued)

Microorganism	Acid	Extractant	Diluent	Reference
Propionibacterium Acidipropionici (membrane extraction)	Propionic	Adogen 283	Oleyl alcohol	[156]
–	Salicylic	Amerlite LA-2	Xylene	[157–160]
–	Glucuronic, Gluconic, Glucanic (separation)	Trioctyamine	1-Butanol	[161]
–	Acetic acid (hollow fibre module)	Trioctylamine	MIBK *n*-octanol	[162]
Lactic acid (hollow fibre module)	Tri-*n*-octyl-phosphinoxide	Kerosene		[163]
	Trioctylamine	Xylene		[164]
Citric acid (hollow fibre module)	Tri-*n*-octyl-amine	MIBK		[165]
Valeric acid (UF module)	Tri-*n*-butyl-phosphate	Kerosene		[166]

The trifunctional amino acids differ only in their pK_3=(side group) values: 3.36 (aspartic acid), 4.25 (glutamic acid), 6,0 (histidine), 8.33 (cystein) 10.07 (tyrosine), 10.52 (lysine), and 12.40 (arginine). For the extraction of these compounds, quaternary ammonium ions, tertiary sulfonium ions, organic borid ions, organic sulfonic ions or dialkyl or diaryl phosphoric acids can be used. The extraction is performed at very low or very high pH values in order to eliminate the zwitterionic form. However, at very low pH values considerable co-extraction of H^+ ions occurs, and at very high pH values co-extraction of OH^- ions occurs. In Table 12 some investigations into the extractions of amino acids are described.

Phenylalanine exhibits zwitterionic character in neutral aqueous solution and is insoluble in the organic solvents commonly used in solvent extraction. Its extraction in organic solvents is only possible with the use of carriers. With a quaternary ammonium chloride carrier, which is a liquid anion exchanger (cationic surfactant), the prerequisite for the extraction is that a high fraction of the amino acid should be in the anionic form in the aqueous phase. Since pK_b=9.29, at least pH 10 is necessary for the high anion fraction. The re-extraction is usually performed in concentrated KCl solution. The Cl^- anion is transported back to the feed membrane phase.

Table 12 Investigations into the reactive extraction of amino acids

Amino acid	Extractant	Diluent	Reference
Tryptophane	TOMAC	Xylene	[167, 168]
Tyrosine	TOMAC	Xylene	[167, 168]
Phenylalanine	TOMAC	Xylene	[169]
Phenylalanine	Amberlite LA-2	Xylene	[170]
Phenylalanine	Adogen 464	Xylene	[170]
Leucine/Isoleucine separation	TOMAC, Aliquat 336	Decanol// Methylcyclohexane, Cyclohexanone	[171, 172]
Tryptophan/ Tyrosine separation	TOMAC	Xylene	[171, 172]
Aspartate/Lysine separation	TOMAC	Xylene	[171, 172]
Aspartate/Asparagine/ Lysine separation	TOMAC	Xylene	[173]
13 amino acids, $K_D=f(\text{pI})$	TOMAC	Kerosene, Hexane, Isooctane, Toluene	[174]
Glutamic acid	Naphtenic acid	Cyclohexane	[175]
Phenylalnine	D2EHPA	Paraffin	[176]
Arginine, Phenylalanine	DNNSA	Toluene	[177]
Alanine, Glycine,	D2EHPA(S)	Toluene	[178]
Aspartate mixture	D2EHPA	Toluene	
	Versatic	Toluene	
Phenylalanine	D2EHPA	*n*-Octane	
Phenylalanine	Aliquat 336	Colloidal liquid aphrons	[179]
Tryptophane	D2EHPA	*n*-Octanol	[180]
Phenylalanine (hollow fibre module)	Aliquat 336	Isodecanol/ Kerosene	[181]
	D2EHPA	Kerosene	[182]

Adogen 464, Aliquat 336, TOMAC (tri-octyl-methyl ammonium chloride), D2EHPA (di(2-ethyl hexyl) phosphoric acid), Amberlite LA-2 (*N*-lauryl-*N*-trialkyl methylamine), D2EHPA(S)-(di(2ethylhexyl)monothiophosphoric acid), DNNSA (dinonyl-naphthalen sulfonocacid).

When applying D2EHPA, the amino acid cations react with the secondary and/or tertiary amine carrier anions. By re-extracting at low pH values the amino-carrier complex is decomposed and the acid cation is freed.

Maas et al [182] produced L-phenylalanine using genetically modified *Escherichia coli* W3110 in continuous cultivation. The cells were separated through a membrane module and recycled to the reactor. L-phenyl alanine was

extracted from the cell free medium in extractor I and recycled to the reactor. The extraction was performed in counter current operation by D2EHPA in kerosene. The organic phase was recycled through extractor II, in which the re-extraction of L-phenylalanine was performed. Using this operation, the product inhibition was eliminated and L-phenylalanine was enriched by a factor of four.

2.2.1 Antibiotics

The most extensively investigated antibiotic is penicillin. As already pointed out, the classical extraction is carried out in the undissociated free state at pH 2.0–2.5: a pH range where penicillin G is unstable, so the extraction temperature is dropped to 2–3 °C. This low pH is necessary, because the pK_a is 2.75. The decomposition of penicillin G was investigated by Reschke and Schügerl [183] as a function of pH. Its stability was highest at pH 7. Below and above this pH value the stability quickly reduced. To avoid the extreme pH values, ion pairs of penicillin G and V anions with long chain amines and/or quaternary ammonium salts were formed at neutral pH. The physical and reactive extractions occur in parallel [183]:

Physical extraction:

$$K_{Ph} = \frac{C_{HP_o}}{C_{HP_a} C_{P_a}} \tag{19}$$

where is K_{Ph} the physical distribution constant, C_{HP} the concentration of penicillic acid and C_P that of the penicillin anion. K_{Ph} depends on the pH value:

$$K_{Ph} = C \frac{1}{1 + 10^{(pH - pK_s)}} \tag{20}$$

where

$$C = \frac{C_{HP_o}}{C_{HP_a}} \tag{21}$$

the partition coefficient.

The degree of extraction E is defined by

$$E = \frac{C_{HP_o}}{C_{HP_o} + C_{HP_a} + C_{P_a}} \times 100 \tag{22}$$

Hence

$$E = \frac{100}{1 + (1 + 10^{(pH - pK_s)})/C} \tag{23}$$

The ion-pair extraction with aliphatic amines in the organic phase with the penicillin anion is given by

$$A_o + P_a^- \overset{K_g}{\rightleftarrows} AHP_o \tag{24}$$

where A_o is the amine in the organic phase, P_a^- is the penicillin anion in the aqueous phase, and AHP_o is the ion-pair complex in the organic phase. This instantaneous reaction at the interface has an equilibrium constant K_G:

$$K_G = \frac{C_{AHP}}{C_A C_P C_H} \tag{25}$$

where the charge of the ions is omitted for simplicity.

We have simultaneous physical and chemical extractions. For the penicillin anion the following relationship holds true:

$$C_P = -0.5\left(\frac{C_{A,G} - C_{P,G}}{Z} + \frac{1}{K_G C_H}\right) + \left\langle 0.25\left(\frac{C_{A,G} - C_{P,G}}{Z} + \frac{1}{K_G C_H}\right)^2 + \frac{C_{P,G}}{K_G C_H Z}\right\rangle^{1/2} \tag{26}$$

with

$$Z = 1 + 10^{pK_s - pH} + 10^{pK_s - pH} C \tag{a}$$

$$C_{P,G} = C_P + C_{HP_a} + C_{HP_o} + C_{AHP} \tag{b}$$

the overall concentration of penicillin and

$$C_{A,G} = C_A + C_{AHP} \tag{c}$$

the overall concentration of the amine.

The distribution coefficient K is given by

$$K = \frac{C_{P,G}}{C_P(1 + 10^{pK_s - pH})} - 1 \tag{27}$$

and the degree of extraction

$$E = \left\langle 1 - \frac{C_P(1 + 10^{pK_s - pH})}{C_{P,G}} \right\rangle \times 100 \tag{28}$$

Sometimes the ion-pair complex consists of m amine and n acid molecules. In the case of co-extraction, the mass balances are modified as well. The relationships for these cases are given in [183].

Quaternary ammonium salts are used for extraction as well. The removal of the penicillin anion P^- from the aqueous phase occurs by ion exchange with the anion Cl^- of the ammonium salt $NR_4^+Cl_o^-$ dissolved in the organic phase. These ion exchange reactions are given by

$$NR_4^+ Cl_a^- \overset{K_G}{\rightleftarrows} NR_4^+ P_o^- + Cl_a^- \tag{29}$$

The equilibrium constant of this reaction is given by

$$K_G = \frac{C_{NR_4P} C_{Cl}}{C_{NR_4Cl} C_P} \tag{30}$$

Since $C_{NR_4P} C_{Cl}$, it follows that:

$$K_G = \frac{(C_{P,G} - C_P)^2}{C_{NR_{4Cl,G}} C_P - C_{P,G} C_P + C_P^2} \tag{31}$$

Around neutral pH, reaction (29) is independent of the pH value. At acidic pH, the dissociation of penicillin should be taken into account. This pH-independence has disadvantages – at high equilibrium constants, the re-extraction is difficult. It cannot be enhanced by a pH shift, unlike for the ion-pair reaction. It can only be accelerated by a consecutive reaction that removes the anion P^- from the equilibrium [183].

In Table 13 several investigations into penicillin extraction are listed. The best results were obtained with Amberlite LA-2 (a mixture of secondary amines (*N*-lauryl-*N*-tri-alkyl-methylamine with 11–13 carbon atoms) (Roehm and Haas AG) and with HoeF2562 (DITDA, di-iso-tridecylamine) (Hoechst AG) in Butanol: E=95% at pH 5, and for re-extraction at pH 8.5 $E \cong 100\%$. The application of DITDA is recommended, because the cost of DITDA is twenty-fold lower than that of LA-2 [191]. All of these extractants are toxic to the cells, so they cannot be used for in situ extraction.

The kinetics of the extraction can be evaluated and calculated by

$$-\frac{dC_P}{dt} = k_P a_P \left[C_P + 0.5 \left(\frac{k_A}{k_{AHP} K_G C_H} + \frac{k_A C_A}{k_P} - C_P \right) - \left\{ 0.25 \left(\frac{k_A}{k_{AHP} K_G C_H} + \frac{k_A C_A}{k_P} - C_P \right)^2 + \left(\frac{k_A C_P}{k_{AHP} K_G C_H} + \frac{k_A C_{AHP}}{k_P K_G C_H} - C_P \right) \right\}^{0.5} \right] \tag{32}$$

where a_p is the specific interfacial area, calculated using

$$a_P = \frac{6\varepsilon}{d_{32}(1-\varepsilon)} \tag{33}$$

The Sauter diameter d_{32} in the column and ε (the hold up of the organic phase) were measured.

The axial concentration profiles of the solutes in the extraction column could be mathematically simulated using the cascade model – N equally sized, ideally mixed stirred vessels – where N corresponds to the number of stages in the extraction column, the rate given by Eq. 31, and the specific interfacial area given by Eq. 32. The calculated and measured concentration profiles were in good agreement when the initial specific interfacial area was reduced in line with the increased Sauter diameter observed (smaller specific interfacial area)

Table 13 Investigations into the reactive extraction of penicillin G and V and other β-lactam antibiotics with long chain secondary and tertiary amines and quaternary ammonium chloride

Investigations	Reference
Distribution coefficients, degrees of extraction, kinetics	[183–185]
Extraction and re-extraction in Karr column	[186, 187]
Extraction in Pilot plant Karr column	[188–189]
Modeling of extraction in pilot plant	[190]
Testing various carriers	[191]
Re-extraction	[192]
Re-extraction in Karr column	[193]
Comparison of extraction in Karr-, Kühni- and pulsed -columns	[194]
Modeling of extractions in various columns	[195]
Extraction in mixer settler	[196]
Extraction in centrifugal extractors	[197]
Extraction from mycelium containing broth in counter-current extraction decanter	[198]
Extraction in three-phase reactor	[199]
Mathematical model for extraction and re-extraction	[200]
Extraction in stirred cell	[201]
Extraction with neutral phosphorous esters	[202]
Interfacial reaction kinetics	[203]
Effect of volume ratio of the phases	[204]
Extraction with quaternary ammonium chloride	[205–206]
Extraction of cephalosporin antibiotics	[94, 207, 208, 210]
Extraction of cephalosporin, cephalexin	[209]
Reactive extraction in membrane modules	[211–216]
Mathematical model for penicillin extraction	[217]

in the first stage (at the bottom). Pai et al [217] also developed a mathematical model for this multistage extraction using the cascade model. However, they could not compare their results with measurements of real systems.

If the cultivation time was too long, it was not possible to separate the phases in the counter current extraction decanter, because the protein content increased exponentially in the cultivation medium at the end of the cultivation. The phase separation could be accomplished by reducing the cultivation time (and therefore the protein content) [198].

Rindfleisch et al [212] extracted penicillin G from the cultivation medium at pH 5 using Amberlite LA-2 in isodecanol in the hollow fibre module in counter-current operation. The penicillin free medium was recycled. Penicillin G was re-extracted from the ion-pair-complex in counter current operation in a second hollow fibre module by a buffer solution at pH 8. The penicillin free organic phase was recycled into the first membrane module. The first aqueous and the second organic recycling loops were connected. Both of the

extraction loops were realised in Celgard X-10 microporous polypropylene hollow fibre modules of effective contact area 7 m^2. The conversion of penicillin G to 6-APA (6-amino penicillanic acid) and PAA (phenyl-acetic acid) by Pencillin G-amidase was performed at pH 8 in the stripping phase of the second membrane module. The separation of 6-APA and PAA was performed in an electro-dialysis module, and the 6-APA was converted into ampicillin using D-phenylglycine ethyl ester (PGE) and immobilized Penicillin G-amidase at pH 6.

2.3 Dissociation Extraction

Sharma et al [218–222] developed an extraction technique that utilises the difference between the dissociation coefficients of acids (pK_a) and bases (pK_b). This technique is particularly useful in the separation of close-boiling mixtures of organic acids/bases which have different dissociation constants and distribution coefficients. Wadekar and Sharma [218] developed the theory behind this, and presented a large number of examples. Anwar et al developed the following relationship for the separation factor:

$$a = \frac{D_A}{D_B} \cdot \frac{K_B}{K_A} \left[\frac{N(\delta+1) + T\left\{ \frac{1}{D_B} + \frac{K_A}{K_B} \cdot \frac{\delta}{D_A} \right\}}{N(\delta+1) + \mathrm{T}\left\{ \frac{K_B}{K_A} + \frac{1}{D_B} \cdot \frac{\delta}{D_A} \right\}} \right] \tag{34}$$

where

D_A and D_B	are the distribution coefficients of A and B
K_A and K_B	are the dissociation constants of A and B
α	is the separation factor
N	is the normality of the aqueous acid
δ	is the ratio of A to B in the organic phase
T	is the total amount of A, B in the organic phase.

The basic principle of this separation technique is similar to that for reactive extraction, which uses the differences in dissociation coefficients. However, only a few biotechnological examples are known of where main products can be separated from by-products in the cultivation medium by means of their different dissociation constant for amino acids (see Table 10). No example has been published in the literature on the use of dissociation extraction for the recovery of biotechnological products. Therefore, this technique will not be discussed any further in this review.

2.4 Aqueous Two-Phase Extraction

Aqueous two phase extraction is based on the discovery of Albertsson [223]. The aqueous solutions of two polymers, or a polymer and a salt, form two phases because of their mutual incompatibility. This aqueous two phase system (ATPS) is generally described by a bimodal curve which separates the two-phase area from the single phase zone (Fig. 1). The phase diagram gives the exact composition of the top and bottom phases. Two phases are only formed by compositions above the bimodal curve. Any two points on the same tie-line will have the same phase composition, but different volume ratios of the phases. At the plait point P, the compositions and volumes of the two phases are equal. The phase diagram depends on the polymer molecular weight, polymer concentration, pH, the temperature, and the dissolved salts.

The aim of the application of ATPS is to separate the cells (in the top phase) from the product (in the bottom phase). By continuous replacement of the bottom phase the product can be removed from the reactor in situ. The main application of this technique is the separation of cells from proteins. However, several investigations have been published on the separation of cells from

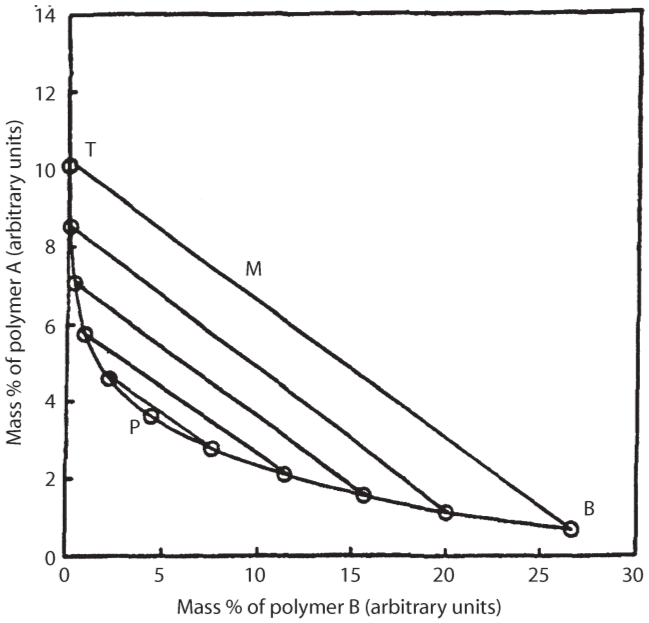

Fig. 1 Phase diagram for two polymers in water forming an aqueous two-phase system. T: top phase composition; B: bottom phase composition; M: mixture composition; P: plait point (critical point). The bimodal curve is the curve with circles along it; the tie lines are the straight lines connecting points (circles) on the bimodal curve

Table 14 Applications of ATPS for the separation of primary and secondary metabolites

Microorganisms	Product	Phase composition	Reference
Zymomonas mobilis	Ethanol	Dextran 500/PEG 6000	[225]
Arthrobacter simplex	Biotransformation: hydrocortisone to prednisolone	PEG8000/dextran T40 pluronicF68, PPG2025 MPEG5500/dextranT70	[226]
–	Penicillin G	PEG3350/salt	[227]
Brevibacterium flavum	*Lysine*, Phenylalanine, Glutamic acid	*PEG1540/salt*	[228]
–	Vancomycin	MPEG/dextran, PEG8000/ dextranT500	[229]
Clostridium acetobutylicum	A-B-E (aceton/ butanol/ethanol)	APPT/dextran, PEG/ dextran, PEG/APPT	[230]
Acremonium chrysogenum	Cephalosporin C/ desacetyl cephalo-sporin C separation	PEG600/sulfate, PEG/phosphate	[231]
Lactobacillus delbrücki subs *delbrückii*, *Lactobacillus lactis* subs *lactis*, *Lactobacillus lactis* subs cremonis	Lactic acid	PEG/dextran, PEG/HPS *i*, EO-PO/HPS	[232]
Streptomyces rimosus, *Streptomyces griseus*, *Streptomyces erythreus*	Oxy-/tetracyclin, Cycloheximid, Erythromycin A, Cephalosporin C	NP/water, OP/water	[233]
Lactobacillus casei	Lactic acid	PEG/dextran	[234]
Lactobacillus lactis	Lactic acid	PEI/PEG, PEI/HEC	[235]
Lactobacillus delbrückii subs *delbrücki i*, *Lactobacillus lactis* subs *lactis*, *Lactobacillus lactis* subs *cremoris*	*Lactic acid*	PEG/dextran, PEG/HPS, EO-PO/HPS	[236]
Review			[237]
Minireview			[238]

PEG (polyethylene-glycol); PPG (polypropylene-glycol); MPEG (methoxy-polyethylene-glycol); APPT (hydroxyl-propyl starch polymer), EO-PO (ethyleneoxid-propyleneoxide-copolymer); PEI (polyethylene-imine): HEC (hydroxymethyl-cellulose); NP (nonyl-phenol-ethoxylate); OP(octyl-phenol-ethoxylate).

primary and secondary metabolites [224]. Some applications of ATPS to the separation of low molecular products are listed in Table 14.

Dextran is non-toxic but very expensive. Low molecular PEG inhibits growth. The high concentrations of salts needed are toxic to the cells. PEI, ATPS, HPS EO-PO, HEC and high molecular PEG are non-toxic for *Lactobacilli.* Therefore, they can be used for the in situ recovery of lactic acid. However, high product recovery is difficult to obtain with biocompatible systems. In addition, the partition coefficients are strongly dependent on salt concentration and pH value, which can vary during the cultivation. Therefore, good results can only really be obtained in continuous culture under steady state conditions, in which the separation conditions can be kept constant.

Aqueous two phase extraction is too costly for the recovery of primary and secondary metabolites, even if dextran is recycled or replaced by salts.

2.5 Supercritical and Near Critical Fluid Extraction

Supercritical fluids are materials that exists as fluids above their critical temperature T_c and critical pressure P_c, respectively. Because of their low critical pressures, the following gases are suitable for supercritical fluid (SCF) extraction: CO_2 (31.2 °C, 48.1 bar), ethane (32.2 °C, 48.1 bar), propane (96.6 °C, 41.9 bar), butane (135.0 °C, 37.5 bar), pentane (196.6 °C, 37.5 bar).

The properties of these solvents are highly sensitive to changes in both pressure and temperature. A large number of investigations have dealt with SCF extraction (for examples, see [239–241]). SCF are generally suitable for the extraction of lypophilic compounds of low polarity, like esters, ethers, and lactones below 70–100 bars. The introduction of strong polar groups (such as -OH, -COOH) makes extraction difficult. Benzene derivatives with up to three -OH groups or two -OH groups and one -COOH group can be still extracted, but only above 100 bars. Benzene derivatives with three -OH groups and one -COOH group, as well as sugars and amino acids, cannot be extracted below 500 bars. SCF extraction is used in the food and mineral oil industries.

Carbon dioxide [242–245], ethane [243], propene [246], and propane (for the dehydration of ethanol) [247, 248] have been used for the extraction of ethanol from aqueous solution SCF. The solubility of ethanol in supercritical CO_2 increases with increasing ethanol concentration in the aqueous phase. At 10% ethanol concentration in the aqueous phase, the solubility amounts to 1.5 wt%, so a large amount of solvent is needed for the recovery of ethanol and so ethanol recovery with supercritical CO_2 is not economical. Lypophilic compounds, such as pyrethrins [249], hops, plant oils [250], digoxin, digitoxin [251], and steroids [252] have been extracted with supercritical CO_2, sometimes with co-solvents in order to increase the solubility of the solutes. A modified high pressure extraction is discussed in Chapter 4.

SCF extraction plays a minor role in biotechnology, because of the many hydrophilic products.

3
Three-Phase Systems

Over the last thirty years a variety of three phase systems have been developed for product recovery and enrichment, which have some advantages when compared to two phase systems. The three liquid phases consist of: the emulsion liquid membrane, the solid supported liquid membrane, and the inverse micelle systems. Aqueous-organic phase extraction across a solid membrane is not considered here, because the solid membrane does not take an active role in the extraction. However, aqueous-organic phase systems with the formation of a third phase at the interface will be discussed.

3.1
Emulsion Liquid Membrane

Two miscible aqueous phases are separated by a organic phase, which prevents the mixing of the two miscible liquids. This three phase system can be formed by emulsification of aqueous phase 1 in an organic phase at high stirrer speed (10,000 rpm) and by dispersing the emulsion in an aqueous phase 2 at low stirrer speed (200–300 rpm). The inner aqueous (acceptor) phase with a droplet diameter of about 0.1–1 mm forms a w/o-emulsion, and the emulsion with a droplet diameter of 1–5 mm forms a dispersion in the second aqueous (donor) phase. Sufficient stability of this emulsion/dispersion system is obtained by choosing suitable detergents. Because the organic phase separates the two aqueous phases, it is called a *liquid surfactant membrane* or a *emulsion liquid membrane*. Such systems were discovered by Li [253]. A carrier (extractant) is dissolved in the organic phase, and, for example, the pH value in the external aqueous phase is set to a high value at which transfer of the solute to the organic phase occurs. In this case the pH is set to a low value in the internal aqueous phase, so that the solute is extracted from the organic to the internal aqueous phase. The pH in the internal phase is maintained by counter carrier transport of protons and/or anions. For example, the amino acid anion is transferred from a 0.1 N KOH solution to the membrane phase if positively charged lipophilic carrier (Aliquat 336, tri-caprylyl-methyl-ammonium chloride) is added to the membrane. The amino acid anion reacts with the positively charged carrier at the membrane/donor interface. It is transported across the membrane as carrier complex. The amino acid is extracted from the membrane at the membrane/acceptor interface by protonation if 0.1 N HCl is present in the acceptor phase. The chloride anion in the acceptor phase is transported to the membrane/acceptor interface, where it is exchanged with the amine anion, which drives the amino acid transport against its concentration gradient [254] (Fig. 2). This is called *facilitated membrane* transport.

To recover the solute in the acceptor phase, the stirring is stopped in batch operation, which stops phase separation. In continuous operation, the emulsion

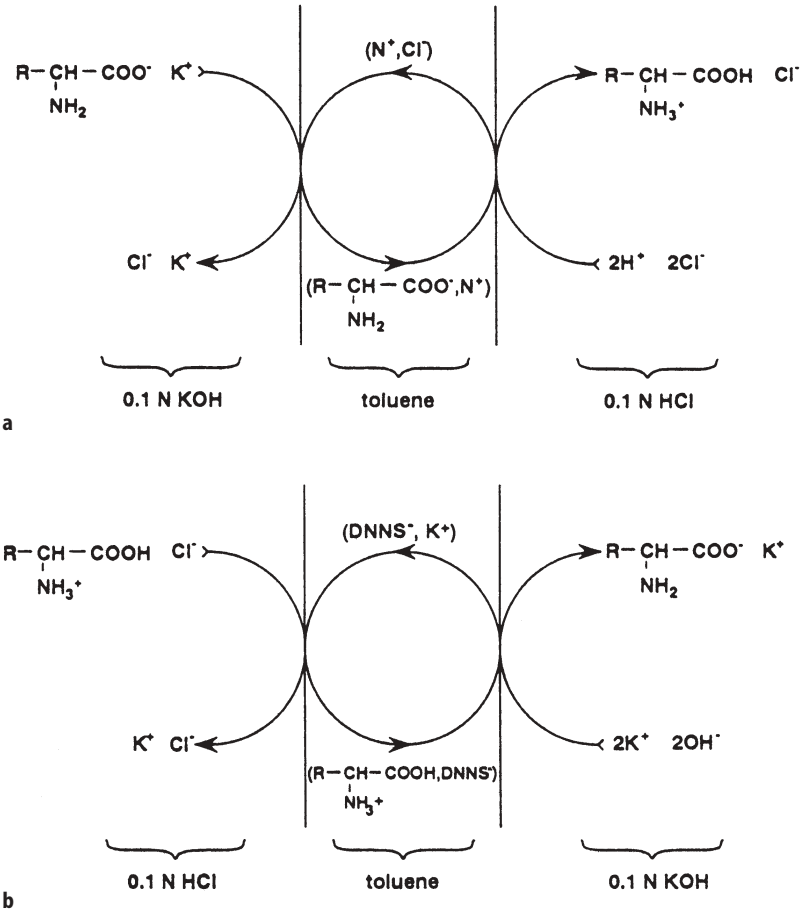

Fig. 2a–b Transport of amino acid through a toluene membrane layer: **a** from basic to acidic aqueous phase using a positively charged carrier; **b** from acidic to basic aqueous phase using negatively charged carrier [254]

phase is collected at the top of the column or in the upper layer of the settler of the mixer settler, and the water phase is withdrawn from the bottom. The solute from the inner aqueous phase is recovered by breaking the emulsion using electro-coalescence.

The liquid membrane technique can also be used for enantiomer-separation with immobilised enzymes in the inner phase. For example, to separate L-phenylalanine from D,L-phenylalanine, methylester α-chymotrypsin is immobilised in the liquid membrane emulsion [255]. D,L-amino acid methyl esters permeate from the donor aqueous phase at pH 6 through the membrane due their physical solubility. The enzyme encapsulated in the internal phase only reacts with the L-ester. The product L-phenylalanine is enriched in the acceptor phase

Table 15 Extraction of some acids by emulsion liquid membranes

Acid	Donor (external) phase	Carrier (extractant) phase	Acceptor (internal) phase	Reference
Lactic	Cultivation medium	Alamine 336/paraffin	Na_2CO_3soln	[256]
Lactic	Aqueous solution	TOA/kerosene, TBP/kerosene, DOA/kerosene, TOPO/kerosene	Na_2CO_3 soln	[257]
Lactic	Cult medium	Amberlite LA-2/ ShellsolT	Na_2CO_3 soln	[258, 259]
Lactic	pH 2.2	Alamine 336/ paraffin	Na_2CO_3 soln	[260, 261]
Lactic	Cult medium + H_2SO_4, pH 4.5	Hostarex A327/, kerosene Amberlite LA-2/ kerosene	Na_2CO_3 soln	[262]
Lactic		Alamine 336/Paraffin, *x* Amberlite LA-2/ kerosene	Na_2CO_3 soln	[263]
Lactic	Aqueous soln pH 7	Aliquat 336/*n*-octane	Na_2CO_3 soln, KCl, NaOH etc.	[264]
Citric	Cult medium, Aqueous soln pH 1.5	Alamin 336/heptane, Shellsol A	NaOH soln, Na_2CO_3 soln	[265]
L-phenyl-alanine	NaOH soln, pH 11	Aliquat 336/ decyl acohol	KCl soln	[266]
L-lysine		D2EHPA/vaselin oil	1 N HCl	[267]
L-phenyl-alanine	NaOH soln, pH 11	Aliquat 335/ decyl alcohol	conc NaCl soln	[268]
Phenyl-alanine	H_2SO_4 soln, pH 3.0	D2EHPA/Telura619/ paraffine	1.6 N HCl	[269]
Trp, Phe, Leu, Val, Gly	KOH soln, pH 11–12	TOMAC/kerosene	NaCl soln	[270]
L-Tryp-tophan L-Phenyl-alanine	aq soln, pH 3.0	D2EHPA/paraffin	HCl soln	[271]

Table 15 (continued)

Acid	Donor (external) phase	Carrier (extractant) phase	Acceptor (internal) phase	Reference
L-Phenyl-alanine	aq soln, pH 4	D2EHPA/kerosene	HCl soln	[272]
Gly, Val, Leu, Phe	KOHsoln, pH 11–12	TOMAC/kerosene	conc. NaCl	[273]
Trp, Met, Phe, Leu, Ile, Val	HCl pH 2.02	Crown-ethers	0.1 N LiOH soln	[274]
L-Tryp-tophan	pH 1.5–3.0	D2EHPA/kerosene, paraffin oil	HCl soln, pH 1.5–2.0	[275]
Minireview			[276]	

Aliquat (quaternary ammonium salt), TOMAC (quaternary ammonium salt), Hostarex A327 (tertiary amine); Alamin 336 (tertiary amine), Amberlite LA-2 (secondary amine), TOA (tri-*n*-octylamine), DOA (di-*n*-octylamine), D2EHPA (di-2-ethyl-hexyl-phosphoric acid), TOPO (tri-*n*-octylphosphine oxide), TBP (tributyl-phosphate) Paranox, Span, and/or ECA 11522 or 4360 are surfactants.

because it has zwitterionic character at pH 6. The unchanged D-ester and methanol permeate through the liquid membrane due to their physical solubility into the donor phase. To maintain a constant pH in the inner phase, Adogen 464 (an anion exchanger) is dissolved in the membrane phase. The carrier counter-transport hydroxide ions react with the protons produced in the acceptor phase. Only a small amount of L-acid is in the anionic form, which can be transported into the donor phase. Again, L-phenylalanine is recovered by ceasing the stirring and braking the emulsion by electro-coalescence.

The extractions of some acids using an emulsion liquid membrane are described in Table 15.

As Behr and Lehn [254] have shown, at pH 11 the amino acid anion replaces the chloride anion in quaternary ammonium chloride. The ion exchange complex is transported to the acceptor membrane interface, where the amino acid is protonated. The driving force for the separation is the chloride anion, which is transported from the acceptor phase to the donor phase. This is the case with the carriers Aliquat 336 and TOMAC. In another case, the amino acid anion forms an ion-pair complex with the carrier cation. In this case it is favourable to start with low pH values, because the uncharged amino acid is more soluble in the membrane phase. The ion-pair reaction occurs in the membrane phase. The ion-pair complex is transported to the acceptor interface, where the acid anion forms a salt with the base (NaOH). The OH^- or CO_3^-

Table 16 Investigations into penicillin extraction by emulsion liquid membranes

Donor phase	Membrane phase	Diluter	Acceptor phase	Reference
Citrate buffer soln, pH 6	Di-*n*-octylamine	*n*-butylacetate	NaOH soln, kerosene, ECA4360J	[277]
Citrate buffer soln, pH 5.3	Amberlite LA-2	*n*-butyl acetate, ECA4360J	Na_2CO_3 soln, pH 5.5	[278]
Citrate buffer soln	Amberlite LA-2	Kerosene, kerosene; BuAc dioctylamine, ECA4360J, Span 80	Na_2CO_3 soln	[279]
Penicillium chrysogenum, cult medium	Amberlite LA-2	Paraffin, Span 80, kerosene	Phosphate buffer pH 8	[280]

anions react with the carrier cation at the acceptor interface and are transported to the donor phase. This is the case for the tertiary and secondary amine carriers. If one uses D2EHPA, the amino acid cation reacts with the carrier anion at the donor interface. The amino acid-carrier complex is transported to the acceptor interface, where the acid cations become free at low pH and the protons form the carrier/proton complex, which is transferred back to the donor interface (Fig. 2).

The situation is more complex in the case of citric acid because of the three carboxyl groups with dissociation constants 3.13, 4.76 and 6.4. Boey et al [255] used three different pH values in the donor phase: 1.5, 3.30 and 4.8. The best results were obtained with the undissociated acid at pH 1.5, which has the highest solubility in the membrane phase. The acid solubility plays an important role in membrane transport for this carrier transport as well.

Table 16 discusses some investigations that were made into the extraction of penicillin G using emulsion liquid membranes. Also, a review of the recovery of β-lactam antibiotics using new techniques is given by Ghosh et al [281].

Barenschee et al [280] recycled the cell containing cultivation medium through a PTFE MF membrane module and removed the mycelium. The cell free medium was extracted in a pilot plant Kühni column in counter-current operation with the emulsion phase consisting of a liquid membrane (95% kerosene, 7.5% Span, 1% LA-2) and an acceptor phase (40 mM phosphate buffer, pH 8, and the enzyme Penicillin G-amidase). The penicillin G was enzymatically converted in the acceptor phase into 6-APA (6-amino penicillanic acid) and PAA (phenyl acetic acid). Because of the zwitterionic character of 6-APA, its re-extraction was not possible: it was enriched in this phase. PAA returned to the donor phase. It was used as precursor for the synthesis of penicillin G by *P chrysogenum.* The emulsion phase was continuously withdrawn at the top of the column, broken by electro-coalescence, and 6-APA was

then recovered. The 6-APA was converted to ampicillin using D-phenylglycine methylester and immobilised Penicillin G-amidase at pH 6 in a separate column. This process worked well with laboratory *Penicillium chrysogenum* strains. However, the penicillin concentrations of high-producing industrial strains were much higher. After enrichment of 6-APA in the acceptor phase, this caused emulsion instability.

3.2 Solid Supported Liquid Membrane

Hollow fibre membranes can be used for the physical separation of medium components. To make the chemical separation feasible, the pores of the solid membrane are saturated with a liquid that is highly specific to the required selective extraction.

Some emulsion liquid membrane systems are not stable enough to use for long operational periods. To improve their stability, they are combined with solid membranes, in which case the solid membrane is saturated with the liquid membrane. These systems are called "solid supported liquid membranes".

These membranes are used without a carrier [282–284] to separate alcohols. Butanol is extracted by a combination of Celgard 2500 microporous polypropylene membrane flat sheet membrane soaked with oleyl alcohol, tri-cresyl phosphate or butyl-phthalate, all of which are biocompatible. The recovery of butanol from the supported membrane is performed by pervaporation [282]. This system is suitable for in situ extraction during cultivation in order to avoid product inhibition. Butanol/isopropanol have been produced in a continuous process involving immobilised *Clostridium isopropylicum*, and these products have been extracted by a Celgard 2500 membrane soaked in oleyl alcohol. Recovery of butanol and isopropanol was performed by pervaporation. Using this technique, the butanol concentration was increased by a factor of fifty [283]. Ethanol has been produced by *Saccharomyces bayanus* in a semi-continuous process [284]. Using an iso-tri-decanol-prepared Teflon sheet, the ethanol was extracted in situ from the cultivation medium and recovered by pervaporation. The volumetric productivity was increased by a factor of 2.5.

When applying this technique to extract organic acids and antibiotics, the solid membrane is soaked in the extractants, which are dissolved in diluents, and the donor and acceptor phases are liquids. The chemistry of the separation is similar to that for emulsion liquid membranes. In Table 17 some examples of the extraction of organic acids and penicillin by solid supported liquid membranes are shown. Note that with dansylated amino acid, in which the amino group is blocked by derivatisation, extraction efficiencies <90% and enrichment factors of 100–1000 were obtained [294].

Similar relationships should exist for extraction with solid supported liquid membranes to those for emulsion liquid membranes. However, an additive mass transfer resistance of the hollow-fibre membrane must also be taken into account. In addition, the specific interfacial areas for the donor and acceptor

Table 17 Examples of the extraction of organic acids and penicillin by solid supported liquid membranes

Acid	Membrane	Organic membrane phase	Donor phase	Acceptor phase	Reference
Acetic	Polypropylene	MIBK	Aqueous	Water	[285]
Lactic ethyl-ester	Polypropylene	Polyorganic-siloxane (quaternary ammonium salt)	0.1 M NaoH	0.1 M NaOH	[286]
Lactic	Polypropylene	Aliquat 336/ Shellsol A	pH 6.3	NaCl soln	[287]
Succinic	Cellulose acetate	MIBK/butanol	Aqueous	Water	[288]
Acetic	Reg cellulose, Polypropylene	MIBK/xylene	Aqueous	Water, 2% NaOH	[289]
Pro-pionic	Polypropylene	TOPO/n-decane, TOPO/kerosene	Aqueous	NaOH soln	[290]
Acetic, Pro-pionic	Polysulfone, Polypropylene, Polyethylene	Alamine 304/ decane, Adogen 283/ decane, Amberlite LA-2/ decane,TOPO/ kerosene	Aqueous, Cultiv. medium	NaOH soln	[291]
Formic, Acetic, Propionic, *n*-Butyric	Teflon, PTFE	TOPO/kerosene	Aqueous pH<pK_a	NaOH soln	[292]
Lactic, Citric	PVDF	TOA/xylene	Aqueous	Na_2CO_3 soln	[293]
Citric	Polypro-pylene	TOA/MIBK	Aqueous	NaOH soln	[294]
Citric	PVDF	Alamine 336/ xylene	Aqueous	Na_2CO_3 soln	[295]
L-valine	Polypro-pylene, PTFE	Aliquate 336/ decanol	Cult medium, pH 12	NaCl pH 1.65	[296]
Dansylated Val, Phe, Trp, Met, Thr, Ser, Glu, Asp, Arg, Lys	PTFE	Di-*n*-hexylether	Aqueous pH 3.0	Buffer pH 10	[297]

Table 17 (continued)

Acid	Membrane	Organic membrane phase	Donor phase	Acceptor phase	Reference
Phenylalanine, Tyrosine	PTFE	Aliquate 336/ toluene	Aqueous pH 11	KCl soln	[298]
Penicillin G	Polypro-pylene	Amberlite LA-2/ decanol	Aqueous pH 6	Buffer pH 7.5	[299, 300]
Penicillin G	Teflon	Tetrabutyl-ammo-nium-hydrogen sulfate/*n*-decanol	Aqueous pH 6.5 pH 6.5	Buffer	[301]

PVDF (polyvinylidene difluoride), PTFE (polytetrafluoroethylene).

phases are much smaller than those for an emulsion liquid membrane, so the extraction process is much slower.

3.3 Extraction with Reversed Micelles

Reversed micelles are formed by surfactants in organic solvents. The polar groups (heads) of the surfactant molecules are directed towards the interior of the spherical aggregate, forming a polar core, and the aliphatic chains are directed towards the organic solvent. This is the reverse of the scenario for normal micelles in water (Fig. 3) [302].

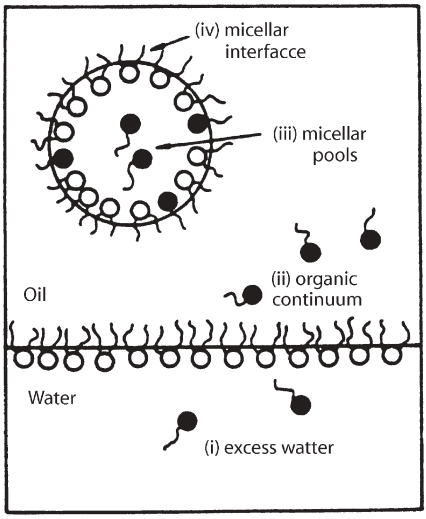

Fig. 3 Schematic picture of reversed micelle with four solubilisation environments in a two phase system at equilibrium [302]

Reversed micelles are mainly used for dissolving proteins in organic solvents [303]. The physical basis of the extraction of amino acids using reversed micelles, using model systems, has been investigated by Leodidis and Hatton [302, 304–306]. They used Aerosol-OT (bis(2-ehthyhexyl)sodium sulfo-succinate) (AOT) as surfactant in isooctane, as well as dodecyl-tri-methyl-ammonium chloride (DTAC) as surfactant in heptane/hexanol, and brought these organic phases into contact with a solution of amino acid in phosphate buffer (pH 6–6.5). After shaking these phases and the subsequent phase separation, the upper organic phase contained most of the amino acid, in reversed micellar solution.

Amino acids are essentially insoluble in organic solvents because of their zwitterionic nature. This means that amino acids that are dissolved in a reversed micellar solution are actually associated with the aggregates and are not dissolved in the solvent. Since they are zwitterions at neutral pH, they expected to have minimal interaction with the double layer formed inside the water pools of the reversed micelles. Amino acids associated with the surfactant interface are expected to reside close to the charged surfactant heads, with their hydrophobic tails mostly embedded in the surfactant sheath. The side chains of amino acids can be polar, non-polar, charged, bulky, short, or long. Any differences in interfacial behaviour can definitely be ascribed to different side chains, since the zwitterionic group is common to all molecules [302].

Leodidis et al [302, 304] evaluated the partition coefficients of amino acids between the aqueous and organic phases. They also considered the physicochemical basis of this phenomenon and found that the free energy transfer of a large number of amino acids from water to the surfactant interfaces of AOT/isooctane and DTAC/heptane/hexanol W/O microemulsions correlate well with the existing hydrophobicity scales. For amino acids, it is possible to calculate the partition coefficients (P_c^s) between water and the surfactant interface of AOT and DTAC-reversed micelles using simple phase-equilibrium experiments:

$$P_c^s = \frac{55.5 V_{a,in}}{N_{s,tot}\,(1 + R_C)} \left[\frac{C_{a,in} - C_{a,f}}{C_{a,f}} \right] \tag{35}$$

where $V_{a,in}$ is the initial volume of the aqueous phase before the contact, $N_{s,tot}$ the total number of moles of the surfactant, R_C the ratio of moles of alcohol (octanol, heptanol) to the moles of surfactant (AOT, DTAC) in the reversed micellar interface, $C_{a,in}$ and $C_{a,f}$ are the molar concentrations of the solute (amino acid) in aqueous phase before the phases are placed in contact (in) and for the final aqueous phase (f) [304].

In Table 18 some interfacial partition coefficients are compared. The partition coefficients depend strongly on the electrolyte concentration and type present in the system and on the interface curvature [305]. The solutes act as co-surfactants and expand the droplet interface and allow significant water uptake by the W/O microemulsion phase [306]. Arginine and tyrosine could

Table 18 Interfacial partition coefficients for some amino acids [304]

Compound	P_c^s (water → AOT)
Valine	4.6
Leucine	26.1
Isdoleucine	17.0
Proline	2.2
Phenylglycine	16.8
Tyrosine	9.0
Tryptophan	238.1
Methionine	19.2

also be separated by reversed micelle extraction, based on their different isoelectric points [307]. Hydrophilic amino acids are mainly solubilised in the water pool while hydrophobic amino acids are mainly incorporated into the interfacial region [308].

Cardoso et al [309–312] investigated amino acid partitioning in cationic reversed micelles. According to these authors, the solubilisation of amino acids is accomplished by an ion-exchange process between the amino acid and the surfactant counter ion. The assumed mechanism neglects the contribution of the structure of the reversed micellar interface to the solubilisation step. Based on this mechanism, a simple model was developed in order to be able to predict equilibrium concentrations for extractions of amino acids at different operating conditions. This model was applied to the solubilisations of amino acids with different structures, including aspartic acid (hydrophilic), phenylalanine (slightly hydrophobic), and tryptophan (a hydrophobic amino acid). Finally, the effect of the reversed micellar structure on the amino acid solubilisation was evaluated by modifying the reversed micellar structure.

An aqueous amino acid solution was brought into contact with an *n*-heptane solution containing TOMAC (tri-octyl ammonium chloride) as surfactant and hexanol as co-surfactant. The desired pH and the ionic strength of the aqueous solution were adjusted using KOH solution and by adding KCl, respectively. Equal volumes of aqueous and organic phases were shaken and emulsified, and after phase separation the phase volumes were measured. Transfer of water from the aqueous phase into the organic phase was observed and the amount of water was determined. The electrical conductivity of the organic phase indicated that the organic phase was a reversed micellar system. However, the solubilisation of the hydrophobic amino acids cannot be described by a simple ion exchange model. The hydrophobic contribution was evaluated by the determination of the interfacial partition coefficient and was taken into account in the model [309]. The influence of pH, initial amino acid concentration in the aqueous phase, surfactant and co-surfactant concentrations, and ionic strength on the solubilisation were determined [310]. The extraction and re-extraction of phenylalanine by cationic reversed micelles in hollow fibre contactors were

investigated and mathematically modelled. Simultaneous extraction/stripping of phenylalanine was performed using two hollow fibre modules in series [311]. The kinetics of the extraction and re-extraction of phenylalanine was evaluated using a diffusion cell. The extraction was carried out with 0.1 M KCl, and the re-extraction with 2 M KCl [312].

Hu and Gulari [313] investigated the extraction of the antibiotics neomycin and gentamycin by means of a reversed micelle system of sodium di-2-ethylhexyl phosphate surfactant and tributyl phosphate co-surfactant in isooctane solvent. The pH of the aqueous phase was adjusted to 8. After emulsion formation, phase separation was carried out by centrifugation. The reversed micelle phase was formed in the upper phase. The re-extraction was carried out with an aqueous solution of $CaCl_2$.

3.4 Reactive Extraction with the Formation of a Third Phase with an Enriched Solute-Extractant Complex at the Aqueous-Organic Interface

During reactive extraction the formation of a third phase at the aqueous-organic interface at high loading and in apolar diluents is suppressed by the addition of polar organic solvents (modifiers) to the system. Hartl and Marr [314, 315] recommend that the formation of this third phase, which contains the enriched solute-extractant complex, should be encouraged by selection of suitable extractor and diluent system. The third phase formation depends on the type of extractant and solute (Table 19), their concentrations, and the pH and ion strength in the aqueous phase. With decreasing pH the separation efficiency increases. Optimum efficiency was observed at pH 2. However, at this pH the co-extraction of acid was too high. Therefore, pH 2.5 seems to be optimal. The advantage of this method is the enrichment of the complex concentration in the third phase; disadvantages include the low degree of extraction and the technically difficult separation of the three phases [315].

Table 19 Third phase formation with 50 vol% extractant in ShellsolT. The acid concentration in the aqueous feed was 2 M (+: third phase formation; –: no third phase was formed; NI: not investigated). The HCl used to adjust the pH value was extracted as well [314]

Extractant\Acid	Formic	Acetic	Propionic	Lactic	HCl
Tri-butylamine	NI	NI	NI	–	–
Tri-hexylamine	+	+	+	+	+
Tri-*n*-octylamine	+	+	+	+	+
Tri-2-ethylhexylamine	+	–	–	–	+
Tri-iso-octylamine	+	+	–	+	+
Tri-*n*-octyl/decylamine	+	–	–	+	+
Di-dodecyl/tridecylamine	+	–	–	+	–
Di-iso-tridecylamine	–	–	–	+	–

4 Comparison of the Extraction Techniques

Several investigations have been published into the efficiency of the recovery of ethanol [5, 13, 26, 316] and butanol [44, 46] using solvent extraction. According to these investigations, the in situ solvent extractions of these alcohols are technically feasible and profitable. The production and recovery of penicillin G by solvent extraction has been considered by A.G. McKee & Co. [317, 318]. This process is used in various forms in industry. As already pointed out, acetic acid is recovered in industry by an extraction-fractionated distillation process [59]. No studies into the economy of reactive extraction processes, not even for citric acid, which was protected by patents [105–107], are known of. It is unknown whether this process was used industrially.

The aqueous two phase system is mainly used for polymer recovery. Some investigations have dealt with the extractive bioconversion of polymers (starch, cellulose, casein) to monomers. In these systems, the biocatalysts are immobilised in one of the phases and the low molecular product is extracted in situ into the other phase [237]. This is not well suited for the selective extraction of low molecular metabolites, so it will not be compared with the other extraction techniques.

We do not have enough information on the extraction of primary and secondary metabolites with reversed micelles to compare it with the other extraction processes.

A qualitative comparison of the other extraction techniques has been published by Hartl and Marr [315]. They considered reactive extraction (RE), emulsion liquid membrane extraction (LME), reactive extraction with the formation of a third phase (TPE), and a special version of high pressure extraction (HPE) used to recover some carboxylic acids. Solid supported liquid membrane extraction (SLME) has similar properties to emulsion liquid membrane extraction, but it is a much slower process. Table 20 compares these processes.

Table 20 Recoveries of some carboxylic acids with various extraction techniques (processes in deceasing efficiency: +++, ++, +, –)

	RE	LME	SLME	TPE	HPE
Concentration range	Intermediate	Low	Low	High	Low
Separation	+++	+++	+++	–	+
Enrichment	++	++	++	+++	+++
Selectivity	++	+	+	+++	+++
Co-extraction of water	+	–	–	++	+++
Solubility of Ex in water	++	+++	+++	–	+
Phase separation	++	++	NPS	–	+++
Re-extraction enrichment	+++	+	+	++	++
Economy	+++	+++	++	+	–

NPS: No phase separation is necessary.

Table 21 Suitabilities of the extraction techniques for various acids based on the obtained degree of recovery, enrichment and selectivity of the extraction (in decreasing suitability: +++, ++, +, –)

	RE	LME	SLME	TPE	HPE
Formic acid	+++	+++	+++	++	+
Acetic acid	+++	+++	+++	+	+++
Propionic acid	+++	+++	+++	–	+++
Lactic acid	+++	+++	+++	++	+++
Malic acid	++	++	++	++	–
Citric acid	+++	+	+	+++	–
Gluconic acid	+	–	–	–	–
Pyruvic acid	+++	+++	+++	+++	+
L-leucine	+	++	++	+	–

The HPE technique is a combination of reactive extraction and high pressure extraction. The acids are dissolved in a mixture of 4–5% extractant Amberlite LA-2 in supercritical CO_2 at 25 °C and 130 bar. 95–100% extraction yields were obtained in a continuous extraction column with acetic and lactic acids [315].

These extraction techniques are suitable for the recovery of organic acids, but their efficiency depends on the type of acid (Table 21).

RE, LME, SLME and HPE techniques are especially suitable for acid recovery at low acid concentrations. Additional enrichment is obtained during the re-extraction. LME is not suitable for product recovery at high acid concentrations, because of the limited capacity of the acceptor phase and because, at high product concentrations in the acceptor phase, the emulsion becomes instable due to the strong osmosis. The upper limit for mono-carboxylic acids is about 200 M. As the number of carboxylic groups increases, this limit drops. To recover the product, the emulsion must be broken (by electro-coalescence, say), which increases the separation costs. SLME is less sensitive for high product concentrations. The product recovery is easier than with LME. However, the rate of the extraction process is much lower, so the extraction process needs more time. Because of the low solubilities of the acids in supercritical CO_2, the HPE method can only deal with low product concentrations. TPE is only effective at high solute concentrations. The separation of the phases is the critical point of this process. On the other hand, at high solute concentrations a third phase can form during the RE process. Addition of a modifier is necessary. However, this increases the carrier losses due to the enhanced solubility of the carrier in the aqueous phase. RE is suitable for product recovery under varied operational conditions, which has been proved using complex cultivation media in different kinds of extraction equipment, including various types of extraction columns and centrifugal extractors, as well as a counter current extraction decanter on the pilot plant scale [76].

References

1. Kollerup F, Daugulis AJ (1985) Can J Chem Eng 63:919
2. Kollerup F, Daugulis AJ (1985) Biotechnol Bioeng 27:1335
3. Kollerup F, Daugulis AJ (1986) Can J Chem Eng 64:598
4. Bruce LJ, Axford DB, Ciszek B, Daugulis AJ (1991) Biotechnol Lett 13:291
5. Daugulis AJ, Axford DB, McLellan PJ (1991) Can Chem Eng 69:488
6. Bruce LJ, Daugulis AJ (1992) Biotechnol Lett 14:71
7. Chang HN, Yang JW, Park YS, Kim DJ, Han KC (1992) J Biotechnol 24:329
8. Gyamerach M, Glover J (1996) J Chem Technol Biot 66:145
9. Munson CL, King CJ (1983) ISEC'83, 500
10. Munson CL, King CJ (1984) Ind Eng Chem Proc Des Dev 23:109
11. Minier M, Goma G (1981) Biotechnol Lett 3:405
12. Minier M, Goma G (1982) Biotechnol Bioeng 29:1565
13. Gyamerach M, Glover J 1983) J Chem Technol Biot 66:145
14. Roddy JW (1981) Ind Eng Chem Proc Des Dev 20:104
15. Zacchi CI, Aly G, Wennersten R (1983) ISEC'83, 507
16. Wang HY, Robinson FM, Le SL (1981) Biotech Bioeng Symp 11:555
17. Eckles AJ, Ferster PJ, Tawlik WY, Tedder DW, Myerson AS (1984) Continuous fermentation and product recovery by liquid/liquid extraction. Poster, Sea Island, 1984
18. Park YS, Chang HN, Kim BH (1988) Biotechnol Lett 10:261
19. Ramalingham A, Finn RK (1977) Biotechnol Bioeng 19:583
20. Finn RK (1966) J Ferment Technol 44:305
21. Levy S (1981) Solvent extraction of alcohol from water solutions with fluorocarbon solvents. US Patent 4,260,836
22. Crabbe PG, Tse CW, Munro PA (1986) Biotechnol Bioeng 28:939
23. Essien DE, Pyle DL (1987) In: Verrall MS, Hudson MJ (eds) Separations for biotechnology. Ellis Horwood, Chichester, UK, p 320
24. Tedder DW (1983) US Patent 4,399,000
25. Job C, Blass E, Schertler C, Staudenbauer WL (1989) Ber Bunsenges Phys Chem 93:997
26. Daugulis AJ, Swaine DE, Kollerup F, Groom CA (1987) Biotechnol Lett 9:425
27. Jones TD, Havard JM, Daugulis AJ (1993) Biotechnol Lett 15:871
28. Jassal DS, Zhang Z, Hill GA (1994) Can J Chem Eng 72:822
29. Diaz M (1988) TIBTECH 6:126
30. Matsumura M, Märkl H (1984) Appl Microbiol Biot 20:371
31. Gianetto A. Ruggeri B, Specchia V, Sassi G, Forna R (1988) Chem Eng Sci 43:1891
32. Honda H, Taya M, Kobayashi T (1986) J Chem Eng Jpn 19:268
33. Tanaka H, Harada S, Kurosava H, Yama M (1987) Biotechnol Bioeng 39:22
34. Aires-Barros MR, Cabral JMS, Novais JM (1987) Biotechnol Bioeng 29:1097
35. Oliviera AC, Cabral JMS (1991) J Chem Technol Biot 52:219
36. Tedder DW, Tawflik WY, Poehlein SR (19986) ISEC'86 III: 659
37. Eckert G, Schügerl K (1987) Appl Microbiol Biot 27:221
38. Dupire S, Thyrion FC (1986) Solvent extraction of products from Aceton Butabol fermentation. ISEC'86, Vol III, p 613
39. Wayman M, Parekh R (1987) J Ferment Technol 65:295
40. Shi Z, Shimizu K, Iijima S, Morisue T, Kobayashi T (1990) Biotechnol Bioeng 36:520
41. Shimizu K, Matsubara M (1987) Chem Eng Sci 42:499
42. Darton WE, Daugulis AJ (1992) Appl Microbiol Biot 36:632
43. Roffler SR, Blanch HW, Wilke CR (1988) Biotechnol Bioeng 31:135
44. Roffler SR, Blanch HW, Wilke CR (1987) Biotechnol Progr 3:131

45. Roffler SR, Wilke CR, Blanch HW (1988) Biotechnol Bioeng 32:192
46. Groot WJ, van der Laans RGJM, Luyben KchAM (1992) Process Biochem 27:61
47. Eiterman MA, Gainer JL (1989) Appl Microbiol Biot 30:614
48. Vatai G, Tekic M (1991) Sep Sci Technol 26:1005
49. Bandini S, Gostoli C (1990) In: Pyle DL (ed) Separations for Biotechnology. SCI Elsevier, p 539
50. Fournier RL (1988) Biotechnol Bioeng 31:235
51. Naser SF, Fournier RL (1988) Biotechnol Bioeng 32:628
52. Chang HN, Yang JW, Park YS, Kim DJ, Han KC (1992) J Biotechnol 24:329
53. Burfeind J, Schügerl K (1999) Process Biochem 34:675
54. Aires-Barros MR, Cabral MR, Novais JM (1987) Biotechnol Bioeng 29:1097
55. Shukla R, Kang W, Sirkar KK (1989) Biotechnol Bioeng 34:1158
56. Jeon YJ, Lee YY (1989) Enzyme Microb Tech 11:575
57. Groot WJ, Baart de Faille T, Donck PB, van der Laans RGJM, Luyber KChAM (1991) Bioseparation 2:261
58. Schlote D, Gottschalk G (1986) Appl Microbiol Biot 24:1
59. King CJ (1983) In: Lo TC, Baird MHI, Hanson C (eds) Handbook of solvent extraction. Wiley, New York, p 567
60. Shah DJ, Tiwari KK (1981) Chem Eng Data 26:375
61. Bartels PV, Drost JCG, de Graauw J (1987) In: Proc 4th European Congress on Biotechnology, vol 2. Elsevier, Amsterdam, p 558
62. Kertes AS, King CJ (1986) Biotechnol Bioeng 28:268
63. Aires-Barros MR, Cabral JMS, Willson RC, Hamel JFP, Cooney CI (1989) Biotechnol Bioeng 34:909
64. Evans PJ, Wang HY (1990) Appl Microbiol Biot 32:393
65. Atkinson B, Mavituna F (1983) Biochemical engineering and biotechnology handbook. MacMillan, New York p 984
66. Hersbach GJM, Van der Beck CP, Van Dijk PWM (1984) In: Vandamme EJ (ed) Biotechnology of industrial antibiotics. Marcel Dekker, New York
67. Rigdway K, Thorpe EE (1983) In: Lo TC, Bairs MH, Hanson C (eds) Handbook of solvent extraction. Wiley, New York, p 583
68. Vandamme EJ (ed) (1984) Biotechnology of industrial antibiotics. Marcel Dekker, New York
69. Hatton TA (1985) In: Moo Young M, Cooney C, Humphrey AE (eds) Comprehensive biotechnology, vol 2. Pergamon, Oxford, UK, p 493
70. Whitmore FC, Wagner RB, Noll CI, Bassler GC, Fleming GH, Carnahan FI, Weisgerber CA, Oakwood TS, Herr CH, Patterson HAT, Haggard HH, Mraz RG, Hoover TB, Di Giorgio PA, Weisel CA, Lowell HL, Walter RN, Ropp WS (1946) Ind Eng Chem 38:942
71. Rowley D, Steiner H, Zimkin E (1946) J Soc Chem Ind 65:237
72. Anderson DW, Lau EF (1955) Chem Eng Prog 51:507
73. Todd D, Davies GR (1973) Filtr Separat 663
74. Todd DB, Podbielniak WJ (1965) Chem Eng Prog 61:69
75. Weatherley LR, Arnott L, Slaughter JC, Campell I (1991) T I Chem Eng–Lond Part C 69:83
76. Schügerl K (1994) Solvent extraction in biotechnology. Recovery of primary and secondary metabolites. Springer, Berlin Heidelberg New York, p 126
77. Vezina C, Sehgal SN (1984) Actinimycin. In: Ref. [67], p 629
78. White RJ, Stroshane RM (1984) Daunorubicin and adriamycin. In: Ref. [67], p 569
79. Miescher GM (1974) US Pat 3 795 663
80. Vining LC, Westlake DWS (1984) Choramphenicol. In: Ref. [67]
81. Butterworth D (1984) Clavulanic acid. In: Ref. [67]

82. Jost JL, Kominek LA, Hyatt GS, Wang HY (1984) Cylcoheximid. In: Ref. [67], p 531
83. Shreve RN, Brink JAS (1977) Chemical process industries. McGraw Hill, New York, p 777
84. van Daehne W, Jahnsen S, Kirk I, Larsen R, Lörk H (1984) Fusidic acid. In: Ref. [67]
85. Huber FM, Tietz AJ (1984) Griseofulvin. In: Ref. [67], p 551
86. Higashide Macrolides (1984) Macrolides. In: Ref. [67], p 452
87. Rayman K, Hurst A (1984) Nisin. In: Ref. [67], p 607
88. Sobin BA, Finlay AC, Kane JH (1977) US Pat 306 669
89. Hersbach GJM, Van der Beek CP, van Dijk PWM (1984) The penicillins. In: Ref. [67], p 45
90. Otake N (1984) Salomycin. In: Ref. [67], p 721
91. Podojil M, Blumauerova M, Vanek Z, Culik K (1984) The tetracyclines. In: Ref. [67], p 259
92. Gray PP, Bhuwapathanapun S (1984) Tylosin. In: Ref. [67], p 743
93. Biot AM (1984) Virginiamycin. In: Ref. [67], p 695
94. Ghosh AC, Mathur RK, Dutta NN (1997) Adv Biochem Eng Biot 56:111
95. Swartz RW (1979) In: Annual report on fermentation processes. Acad Press, New York 3:75
96. Podbielniak WJ, Kaiser HR, Ziegenhorn GJ (1970) Chem Eng Prog Symp Ser 100, 66:37
97. Queener S, Schwartz R (1979) In: Rose AH (ed) Economic biotechnology. Acad Press, New York, 3:35
98. Smith EL, Page JE (1948) J Soc Chem Ind 67:48
99. Wardell JM, King CJ (1978) J Chem Eng Data 23:144
100. Ricker NL, Michaels JN, King CJ (1979) J Sep Proc Technol 1:36
101. Ricker NL, Pittman EF, King CJ (1980) J Sep Proc Technol 1:23
102. Kertes ASA, King CJ (1986) Biotechnol Bioeng 28:269
103. Grinastead RR (1974) US Patent 3 816 574
104. Kanzler W (1981) Austrian Patent 365 080
105. Baniel AM (1981) Europ Patent EP 49429
106. Baniel AM, Blumberg R, Hajdu K (1981) US Patent 4 275 234
107. Alter JE, Blumberg R (1981) US Patent 4 251 671
108. Siebenhofer M, Marr R (1983) ISEC'83
109. Sibenhofer M, Marr R (1985) Chem Ing Tech 57:558
110. Wojtech B, Mayer M (1985) Chem Ing Tech 57:134
111. Schügerl K (1987) In: Verrall MS, Hudson MJ (eds) Separations for biotechnology. Ellis Horwood, Chichester, UK, p 260
112. Marr R, Hartl J (1991) BioEngineering 2:22
113. Schügerl K (1988) In: Li NN, Stratmann H (eds) Separation technology. p 336
114. Watson EK, Rickelton WA, Robertson AJ, Brown TJ (1986) ISEC'86 III 775
115. Fahim M, Quader A, Hughes MA (1992) Sep Sci Technol 27:1809
116. Schügerl K (1994) Solvent extraction in biotechnology. Recovery of primary and secondary metabolites. Springer, Berlin Heidelberg New York, p 84
117. Yannavar VM, Wang DIC (1987) Ann New York Acad Sci 506:523
118. Yannavar VM, Wang DIC (1991) Biotechnol Bioeng 37:544
119. Yannavar VM, Wang DIC (1991) Biotechnol Bioeng 37:716
120. Yannavar VM, Wang DIC (1991) Biotechnol Bioeng 37:1095
121. Siebold M, v. Frieling P, Joppien R, Rindfleisch D, Schügerl K, Röper H (1995) Process Biochem 30:81
122. v Frieling P, Schügerl K (1999) Process Biochem 34:685, erratum: (2000) Process Biochem 35:1077
123. San-Martin M, Pazos C, Coca J (1996) J Chem Technol Biot 65:281
124. Juang RS, Huang RH (1997) Chem Eng J 65:47
125. Han DH, Hong WH (1998) Sep Sci Technol 33:271

126. Tong Y, Hirata M, Takanashi H, Hano T, Matsumoto M, Miura S (1998) Sep Sci Technol 33:1439
127. Choudhuri B, Swaninathan T (1998) Bioprocess Eng 19:317
128. Hironaka M, Hirata M, Takanashi, Hano T, Miura S (2001) Sep Sci Technol 36:2927
129. Wasewar KL, Heesink ABM, Versteeg GF, Pangarkar VG (2002) J Biotechnol 97:59
130. Scheler C, Popovic M, Bajpai R (1997) Chem Ing Tech 69:951
131. Wennersten R (1980) ISEC'80 2:80–63
132. Wennersten R (1983) J Chem Technol Biot 33B:85
133. Yu-Ming J, Dao-Chen L, Yuan-Fu S (1983) ISEC'83 2:514
134. Rückl W, Siebehofer M, Marr R (1986) ISEC'86, 3:653
135. Bauer U, Marr R, Rückl W, Siebenhofer M (1988) Chem Biochem Eng Q 2:230
136. Bauer U, Rückl W, Siebenhofer M (1989) Ber Bunsenges Phys Chem 93:980
137. Bizek V, Horacek J, Kousova M, Heyberger A, Prochazka J (1992) Chem Eng Sci 47:1433
138. Bizek V, Horacek J, Kousova M (1993) Chem Eng Sci 48:1447
139. Wieczorek S, Brauer H (1998) Bioprocess Eng 18:75
140. Dinculescu D, Guzun-Stoica A, Dobre T, Foarea O (2000) Bioprocess Eng 22:529
141. Kilic M, Bayraktar E, Ates S, Mehmetoglu Ü (2002) Process Biochem 37:759
142. Lewis VP, Yang ST (1992) Biotechnol Prog 6:104
143. Gu Z, Glatz BA, Glatz CE (1998) Biotechnol Bioeng 57:454
144. Vandak D, Zigiva J, Sturdik E, Schlosser S (1997) Process Biochem 32:245
145. Wu Z, Yang ST (2003) Biotechnol Bioeng 82:93
146. Hong YK, Hong WH (2000) Bioprocess Eng 22:281
147. Hong YK, Hong WH (2000) Bioprocess Eng 22:477
148. Hong YK, Hong WH (2000) Bioprocess Eng 23:535
149. Tamada JA, Kertes AS, King CJ (1986) ISEC'86 3:631
150. Qin W, Cao Y, Luo X, Liu G, Dai Y (2001) Sep Purif Technol 24:419
151. Yang ST, White SA, Hsu ST (1991) Ind Eng Chem Res 30:1335
152. Hano T, Matsumoto M, Ohtake T, Sasaki K, Hori F, Kawano Y (1990) J Chem Eng Jpn 23:734
153. Chen F, Tanaka H, Naka Y, O'Shima E (1989) J Chem Eng Jpn 22:6
154. Clark GA, Gatrone RC, Horwitz EP (1987) Solvent Extr Ion Exc 5:471
155. Matsumoto M, Hano T, Hirata M, Miura S (1996) J Chem Technol Biot 67:260
156. Jin Z, Yang ST (1998) Biotechnol Prog 14:457
157. Schlichting E, Halwachs W, Schügerl K (1985) Chem Eng Prog 19:317
158. Haensel R, Halwachs W, Schügerl K (1986) Chem Eng Sci 41:135
159. Haensel R, Halwachs W, Schügerl K (1986) Chem Eng Sci 41:555
160. Schlichting E, Halwachs W, Schügerl K (1987) Chem Eng Commun 51:193
161. Hirth J, Bicker M, Vogel H (2003) Chem Ing Tech 75:294
162. Lee YM, Kang JS, Nam SY, Chol CH (2001) Sep Sci Technol 36:457
163. Scheker C, Popovic M, Bajpai R (1997) Chem Ing Tech 69:951
164. Juang RS, Huang RH (1997) J Membrane Sci 129:185
165. Basu R, Sirkar KK (1991) AIChE J 37:383
166. Rubio B, Escudero I, Ruiz MO, Cabezas JL, Alvarez JR, Coca J (2000) Sep Sci Technol 35:811
167. Kirgios I, Hänsel R, Rhein HB, Schügerl K (1986) ISEC'86 3:623
168. Kirgios I, Rhein HB, Hänsel R, Schügerl K (1986) Chem Ing Tech 58:908
169. Hänsel R, Halwachs W, Schügerl K (1986) Chem Eng Sci 41:1811
170. Schlichting E, Halwachs W, Schügerl K (1987) Chem Eng Commun 51:193
171. Schügerl K, Brandes A, Degener W, von Frieling P, Handojo L (1990) In: Sekine T (ed) Solvent extraction 1992. Elsevier, Amsterdam, p 1905

172. Schügerl K, Degener W, v Frieling P, Handojo L, Kirgios I (1990) In: Pyle DL (ed) Separation for biotechnology. Elsevier, Amsterdam, p 238
173. Handojo L, Degener W, Schügerl K (1990) In: Sekine T (ed) Solvent extraction 1992. Elsevier, Amsterdam, p 1785
174. Hano T, Ohtake T, Matsumono M, Kitayama D, Hori F, Nakasio F (1991) J Chem Eng Jpn 24:21
175. Wang SS, Chan CC (1992) Sep Sci Technol 27:1229
176. Boyadzhiev L, Atanassova I (1994) Process Biochem 29:237
177. Kelly NA, Lukhezo M, Reuben BG, Dunne LJ, Verrall MS (1998) J Chem Technol Biot 72:347
178. Liu YS, Dai YY, Wang JD (1999) Sep Sci Technol 34:2165
179. Scarpello JT, Stuckey DC (2000) Biotechnol Bioeng 69:469
180. Liu YS, Dal YY, Wang JD (2000) Sep Sci Technol 35:1439
181. Escalante H, Alonso AI, Ortiz I, Irabien A (1998) Sep Sci Technol 33:119
182. Maas D, Gerigk MR, Kreutzer A, Weuster-Botz D, Wubbolts M, Takors R (2002) Bioproc Biosyst Eng 25:85
183. Reschke M, Schügerl K (1984) Chem Eng J 28:B1
184. Reschke M, Schügerl K (1984) Chem Eng J 28:B11
185. Reschke M, Schügerl K (1984) Chem Eng J 29:B25
186. Reschke M, Schügerl K (1985) Chem Eng J 31:B19
187. Reschke M, Schügerl K (1986) Chem Eng J 32:B1
188. Müller B, Schlichting E, Bischoff L, Schügerl K (1987) Appl Microbiol Biot 26:36
189. Müller B, Schlichting E, Bishoff L, Schügerl K (1987) Appl Microbiol Biot 26:206
190. Müller M, Schlichtign E, Schügerk K (1988) Appl Microbiol Biot 27:484
191. Likidis Z, Schügerl K (1987) J Biotechnol 5:293
192. Likidis Z, Schügerl K (1988) Bioprocess Eng 3:79
193. Likidis Z, Schügerl K (1988) Chem Eng Process 23:61
194. Likidis Z, Schügerl K (1988) Chem Eng Sci 43:27
195. Likidis Z, Schügerl K (1988) Chem Eng Sci 43:1243
196. Likidis Z, Schügerl K (1987) Biotechnol Lett 9:229
197. Likidis Z, Schügerl K (1987) Biotechnol Bioeng 30:1932
198. Likidis Z, Schlichting E, Bishoff L, Schügerl K (1989) Biotechnol Bioeng 33:1385
199. Likidis Z, Reschke M, Scheper T (1987) Chem Ing Tech 59:522
200. Patniak PR (1992) J Biotechnol 23:95
201. Wang SS, Lee CJ (1995) Chem Eng J 58:285
202. Yang ZF, Yu SQ, Chen CY (1992) Chem Eng J 50:B39
203. Lee CJ, Wang SS (1995) J Chem Tech Biot 64:239
204. Lee KH. Lee WK (1954) Sep Sci Technol 29:601
205. Bora MM, Ghosh AC, Dutta NN, Mathur RK (1997) Can J Chem Eng 75:520
206. Harris TAJ, Khan S, Reuben BG, Shokoya T (1990) In: Pyle DL (ed) Separations for biotechnology. Elsevier, Amsterdam, p 172
207. Bora MM, Dutta NN, Bhattacharya RG (2000) J Chem Eng Data 45:399
208. Hano T, Matsumoto M, Ohtake T, Hori F (1992) J Chem Eng Jpn 25:293
209. Sahoo GC, Ghosh AC, Dutta NN (1997) Process Biochem 32:265
210. Ghosh AC, Mathur RK, Dutta NN (1997) 56:111
211. Yang ZF, Rindfleisch D, Scheper T, Schügerl K (1993) In: Patterson R (ed) 3rd Int Conf on Effective Membrane Processes—New Perspectives. British Hydromechanics Research Group, Cranfield, UK, p 49
212. Rindfleisch D, Syska B, Lazarova Z, Schügerl K (1997) Process Biochem 32:605
213. Juang RS, Lin YS (1998) J Membrane Sci 141:19

214. Sahoo GC, Borthakur S, Dutta NN, Dass NN (1999) Bioprocess Eng 20:117
215. Yang C, Cussler EL (2000) Biotechnol Bioeng 69:67
216. Lazarova Z, Syska B, Schügerl K (2002) J Membrane Sci 202:151
217. Pai RA, Doherty M, Malone M (2002) AIChE J 48:514
218. Wadekar VV, Sharma MM (1981) J Sep Proc Technol 2:1
219. Gaikar VG, Sharma VG (1984) J Sep Proc Technol 5:49
220. Gaikar VG, Sharma MM (1984) J Sep Proc Technol 5:53
221. Anwar MM, Arif AS, Pritchard DW (1995) Solvent Extr Ion Exc 13:127
222. Anwar MM, Arif AS, Pritchard DW (1998) Solvent Extr Ion Exc 16:931
223. Albertsson PA (1986) Partition of cell particles and macromolecules, 3rd edn. Wiley, New York
224. Huddleson JG, Lydiatt A (1990) Appl Biochem Biotechnol 26:249
225. Kühn I (1980) Biotechnol Bioeng 22:2393
226. Kaul R, Mattiasson B (1986) Appl Microbiol Biot 24:259
227. Yang WY, Chu IM (1990) Biotechnol Tech 4:191
228. Chu IM, Chang SL, Wang SH, Yang WY (1990) Biotechnol Tech 4:143
229. Lee CK, Sandler SI (1990) Biotechnol Bioeng 35:408
230. Kim YJ, Weigand WA (1992) Appl Biochem Biot 34/35:419
231. Yang WY, Lin CD, Chu IM, Lee CJ (1994) Biotechnol Bioeng 43:439
232. Planas J, Radstrom P, Tjerneld F (1996) Appl Microbiol Biot 45:737
233. Müller U, Merrettig-Bruns U, Hollmann D (1995) Chem Ing Techn 67:783
234. Katzbauer B, Cesi V, Narodoslawsky M, Moser A (1995) Chem Biochem Eng Q 9:79
235. Kwon YJ, Kaul R, Mattiasson B (1996) Biotechnol Bioeng 50:280
236. Planas J, Radström P, Tjerneld F, Hahn-Hägerdal (1996) Appl Microbiol Biot 48:45
237. Raghavarao KSMS, Guinn MR, Todd P (1998) Sep Purif Methods 27:1
238. Sinha J, Dey PK, Panda I (2000) Appl Microbiol Biot 54:476
239. Paulaitis ME, Krukonis VI, Kurnik RT, Reid RCX (1982) Rev Chem Eng 1:179
240. McHugh MA, Krukonis VJ (1986) Supercritical fluid extraction, principles and practice. Butterworth, Stoneham, MA
241. Randolph TW (1990) TIBTECH 8:78
242. Paulaitis EM, Gibert MI, Nahs CA (1981) Separation of ethanol-water mixtures with supercritical fluids. 2nd World Congress of Chem Eng
243. Kuk MS, Montagna JC (1983) Solubility of oxygenated hydrocarbons in supercritical carbon dioxide. Ann Arbor Science, Ann Arbor, MI
244. Brunner G, Kreim K (1985) Chem Ing Tech 57:550
245. Brunner G (1987) Chem Ing Tech 59:12
246. Victor JG (1983) ISEC'83, 2:511
247. Horizoe H, Tanimoto T, Yamamoto I, Kano Y (1993) J Chem Eng Jpn 26:482
248. Horizoe H, Tanimoto T, Kano Y (1993) J Chem Eng Jpn 26:490
249. Bunzenberger G, Lack E, Marr R (1984) Ger Chem Eng 7:2533
250. King MB, Bott TH, Chami JH (1987) In: Verrall MS (ed) Separations for biotechnology. Ellis Horwood, Chichester, UK, p 294
251. Adrian T, Freitag J, Maurer G (2000) Biotechnol Bioeng 69:561
252. Jarzebski AB, Malinowski JJ (1995) Process Biochem 30:343
253. Li NN (1968) US Patent 3 410 794
254. Behr JP, Lehn JM (1973) J Am Chem Soc 95:6108
255. Scheper T, Halwachs W, Schügerl K (1984) Chem Eng J 29:B31
256. Chaudhuri JB, Pyle DL (1990) In: Pyle DL (ed) Separation for biotechnology. Elsevier, Amsterdam, p 112
257. Hano T, Matsumoto M, Ohtake T, Sasaki K, Hori F, Kawano Y (1990) ISEC'90

258. Reisinger H, Marr R (1992) BIOforum 7–8:234
259. Reisinger H, Marr R (1993) Chem Ing Tech 65:198
260. Chaudhuri JB, Pyle DL (1992) Chem Eng Sci 47:41
261. Chaudhuri JB, Pyle DL (1992) Chem Eng Sci 47:49
262. Reisinger H, Marr R (1992) Chem Eng Technol 15:363
263. Schöller C, Chaudhuri JB, Pyle DL (1993) In: Logsdail DH, Slater MJ (eds) Solvent extraction in the processindustries 2. Elsevier, London, p 925
264. Lazarova Z, Peeva L (1994) Biotechnol Bioeng 43:907
265. Boey SC, del Cerro MCG, Pyle DL (1987) Chem Eng Res Des 65:218
266. Thien MP, Hatton TA, Wang DIC (1986) In: ISEC'86 (International Solvent Extraction Conference), Munchen, Germany, 11–16 September 1986
267. Yagodin GA, Yurtov EV, Golubkov AS (1986) ISEC'86
268. Thien MP, Hatton TA, Wang DIC (1988) Biotechnol Bioeng 32:604
269. Itoh H, Thien MP, Hatton TA, Wang DIC (1990) Biotechnol Bioeng 35:853
270. Hano T, Ohtake T, Matsumoto M, Kitayama D, Hori F, Nakashio F (1990) ISEC'90
271. Tulasi GL, Kumar S (1999) AIChE J 45:2534
272. Liu X, Liu D (1998) Sep Sci Technol 33:2598
273. Matsumoto M, Ohtake T, Hirata M, Hano T (1998) J Chem Technol Biot 73:237
274. Buschmann HJ, Mutihac L, Mutiac R (1999) Sep Sci Technol 34:331
275. Liu X, Liu D (2000) Sep Sci Technol 35:2707
276. Eyal AM, Bressler E (1993) Biotechnol Bioeng 41:287
277. Hano T, Ohtake T, Matsumono M, Ogawa SI, Hori F (1990) J Chem Eng Jpn 23:772
278. Lee SC, Lee WK (1992) J Chem Technol Biot 55:251
279. Lee KH, Lee CS, Lee WK (1994) J Chem Technol Biot 59:371
280. Barenschee T, Scheper T, Schügerl K (1992) J Biotechnol 26:143
281. Ghosh AC, Bora MM, Dutta NN (1998) Bioseparation 6:91
282. Matsumura M, Sueki M, Araki K, Kataoka H (1987) In: Neissel OM, van der Meer RR, Luyben KChAM (eds) Proc 4th European Congr on Biotechnology. Elsevier, Amsterdam, 2:453
283. Matsumura M, Takehara S, Kataoka H (1992) Biotechnol Bioeng 39:148
284. Christen P, Minier M, Renon H (1990) Biotechnol Bioeng 36:116
285. Sengupta A, Basu R, Prasad R, Sirkar KK (1988) Sep Sci Technol 23:1735
286. Yahaya G (2001) Sep Sci Technol 36:3563
287. Coelhoso IM, Cardoso MM, Viegas RMC, Crespo JPSG (2000) Sep Purif Technol 19:183
288. Prasad R, Sirkar KK (1987) AIChE J 33:1057
289. Sengupta A, Basu R, Sirkar KK (1988) AIChE J 34:1698
290. Ozdali F, Glatzu BA, Glatz CE (1996) Appl Microbiol Biot 44:710
291. Solichien MS, O'Brien D, Hammond EG, Glatz CE (1996) Enzyme Microbial Tech 17:23
292. Nuchnoi P, Yano T, Nishio N, Nagai S (1987) Ferment Technol 65:301
293. Juang RS, Lee SH, Huang RH (1998) Sep Sci Technol 33:2379
294. Basu R, Sirkar KK (1992) Solvent Extr Ion Exc 10:119
295. Sirman T, Pyle DL, Grandison AS (1990) In: Pyle DL (ed) Separation for biotechnology. Elsevier, Amsterdam, p 245
296. Deblay P, Minier M, Renon H (1990) Biotechnol Bioeng 35:123
297. Wiezorek P, Jönnson JA, Mathiasson L (1997) Anal Chim Acta 337:183
298. Adarkar JA, Sawant SB, Joshi JB, Pangarkar VG (1997) Biotechnol Prog 13:493
299. Lee CJ, Yeh HJ, Yang WJ, Kang CR (1993) Biotechnol Bioeng 42:527
300. Lee CJ, Yeh HJ, Yang WY, Kang CR (1994) Biotechnol Bioeng 43:309
301. Marchese J, Lopez JL, Quinn JA (1989) J Chem Tech Biotechnol 46:149
302. Leodidis EB, Hatton A (1990) J Phys Chem 94:6400

303. Luisi PL, Laane C (1986) TIBTECH June 153
304. Leodidis EB, Hatton A (1990) J Phys Chem 94:6411
305. Leodidis EB, Hatton A (1991) J Phys Chem 95:5943
306. Leodidis EB, Hatton A (1991) J Phys Chem 95:5957
307. Furusaki S, Kishi K (1990) J Chem Eng Jpn 23:91
308. Adachi M, Harada M, Shioi A, Sato Y (1991) J Phys Chem 95:7925
309. Cardoso MM, Barradas MJ, Carrondo MT, Kropner KH, Crespo GC (1988) Bioseparation 7:65
310. Cardoso MM, Barradas MJ, Kroner KH, Crespo JG (1999) J Chem Technol Biot 74:801
311. Cardoso MM; Viegas RMC, Crespo JPSG (1999) J Membrane Sci 156:303
312. Cardoso MM, Viegas RMC, Crespo JPSG (2000) Chem Eng Sci 55:2835
313. Hu Z, Gulari E (1996) J Chem Technol Biot 65:45
314. Hartl J, Marr R (1991) 4th World Congr Chemical Engineering, Karlsruhe, Germany, 16–21 June, Vol IV:19
315. Hartl J, Marr R (1993) Chem Ing Tech 65:810
316. Arnold SG, McLellan PJ, Daugulis AJ (1996) Can J Chem Eng 74:395
317. Swarz RW (1979) Annual reports of fermentation processes, vol 3. Acad Press, New York, p 75
318. Swarz RW (1985) In: Moo-Young M (ed) Comprehensive biotechnology, vol 3. Pergamon, Oxford, p 7

Received: March 2004

Adv Biochem Engin/Biotechnol (2005) 92: 49–76
DOI 10.1007/b98919

Biochemical Reaction Engineering and Process Development in Anaerobic Wastewater Treatment

Alexander Aivasidis (✉) · Vasileios I. Diamantis

Laboratory for Wastewater Management and Treatment Technologies, Department of Environmental Engineering, School of Engineering, Democritus University of Thrace, Vas. Sofias 12, Xanthi, 671 00 Greece
spiadou@env.duth.gr

Abstract Developments in production technology have frequently resulted in the concentrated local accumulation of highly organic-laden wastewaters. Anaerobic wastewater treatment, in industrial applications, constitutes an advanced method of synthesis by which inexpensive substrates are converted into valuable disproportionate products. A critical discussion of certain fundamental principles of biochemical reaction engineering relevant to the anaerobic mode of operation is made here, with special emphasis on the roles of thermodynamics, kinetics, mass and heat transfer, reactor design, biomass retention and recycling. The applications of the anaerobic processes are discussed, introducing the principles of an upflow anaerobic sludge bed reactor and a fixed-bed loop reactor. The merits of staging reactor systems are presented using selected examples based on two decades of research in the field of anaerobic fermentation and wastewater treatment at the Forschungszentrum Julich (Julich Research Center, Germany). Wastewater treatment is an industrial process associated with one of the largest levels of mass throughput known, and for this reason it provides a major impetus to further developments in bioprocess technology in general.

Keywords Wastewater anaerobic treatment · Upflow anaerobic sludge bed reactor · Fixed-bed loop reactor · Two-stage process · Methanization cascade

1 Introduction

In aerobic fermentation (for instance yeast production or isolation of single-cell bacterial protein), the production of biomass is usually the most important single factor. Although a high degree of substrate conversion is the primary aim in aerobic wastewater treatment (the activated sludge process), large amounts of biomass are simultaneously formed because of the aerobic nature of the phenomenon. The fundamental advantage of the aerobic treatment is that oxidative degradation of the carbon substances provides the energy required for propagation of the microorganisms that act as the biocatalyst. From the standpoint of achieving a high space-time yield, the limiting factor is often the supply of oxygen, a gas that is only slightly water-soluble.

In anaerobic fermentation, it is the formation of product that usually occupies the spotlight (generation of methane or of alcohols, ketones and organic acids). In this case, it is the energy that is usually limiting, resulting in relatively limited growth of the catalytic microorganisms compared to the aerobic case. Since the microorganisms serve as both reaction product and catalyst, it is advantageous to maintain a high catalyst concentration under an anaerobic regime as well. The fact that energy is rarely a limiting factor in the case of alternative aerobic fermentation must be paid for with considerable energy expenditure in the course of providing the oxygen supply. The energy limitation associated with anaerobic fermentation is a function of the formation of energy-rich products.

In analyzing the microbial formation of methane, two important aspects stand out: the fact that methane is derived from waste materials, and its applicability in the treatment of industrial wastewater. The anaerobic treatment of industrial wastewater has become increasingly important in recent years as a result of environmental-protection legislation, increased energy costs and problems with the disposal of excess sludge formed in aerobic treatment processes. Efforts are now being made to remove organic contaminants as far as possible without external resources of energy, taking advantage of the biogas produced, where the desired level of purification is ultimately achieved with the aid of a subsequent aerobic biological-clarification step. Actual research fields on anaerobic wastewater treatment consist of:

- New developments concerning integrated anaerobic-aerobic treatment systems.
- Development of staged reactor systems, and membrane applications.
- Treatment of low strength wastewater at lower temperatures.
- Treatment of recalcitrant and aromatic compounds.

2
Basic Principles

Developments in production technology have frequently resulted in the concentrated local accumulation of highly organic-laden wastewaters, a factor that it is therefore important to take into account with respect to the disposal technology. With conventional aerobic wastewater treatment (the activated-sludge process), the greater the organic load, the more problematic the process, since the required level of oxygen transfer rapidly approaches limits that are both technically and economically unattainable in practice.

The fundamental advantages of anaerobic wastewater treatment are:

1. Energy-intensive oxygen transfer is avoided.
2. The energy content of the resulting biogas can be put to further use.
3. Very little excess sludge is formed, while at the same time up to 95% of the organic contamination is converted into a combustible gas (Fig. 1), constituting a case of true disposal.

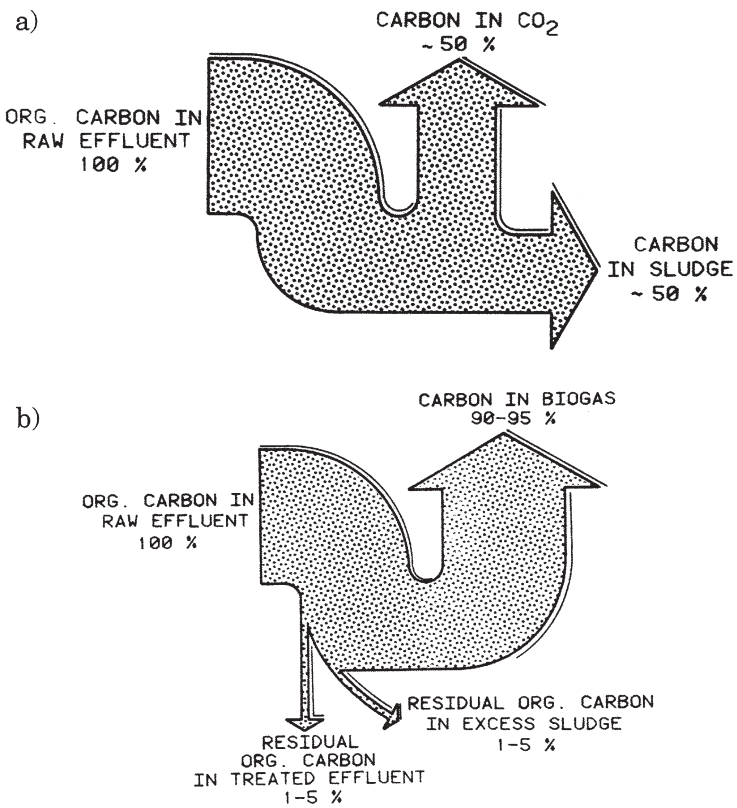

Fig. 1 Carbon balances in the **a** aerobic and **b** anaerobic microbial degradation of organic compounds

4. Heavy metals are not subjected to oxidative mobilization, but rather to reductive precipitation (as heavy-metal sulfides), facilitating their orderly disposal rather than wider dispersal.
5. Aerosol formation accompanying oxygen transfer is avoided.
6. Space-time yields (bioreactor performances) reach a level fundamentally unattainable in the activated-sludge process because of the limitations imposed by oxygen transfer.
7. Anaerobic biomass can be preserved without feed for long periods of time without any significant deterioration in its properties.

To acquire a beyond-empirical understanding of anaerobic wastewater treatment forces, one has to examine the interactions between the various microorganisms in a food chain more closely. The basic scheme is depicted in Fig. 2. In simplified terms, at least three groups of microorganisms are involved in the degradation of complex organic molecules. To begin with, biopolymers that cannot be directly utilized by the anaerobic organisms are first hydrolytically degraded to soluble monomers (amino acids, sugars and fatty acids). Acidogenic bacteria that form short chain fatty acids and alcohols ferment the latter. This is followed by acetic acid formation, with the simultaneous generation of hydrogen and carbon dioxide, a step referred to as acetogenesis. It is at this point that methane formation can commence. Indeed, tracer experiments have shown that ~70% of the methane produced in the overall process comes from the degradation of acetic acid [1], while the remainder arises from the reaction of hydrogen with carbon dioxide. The complete degradation chain is in reality

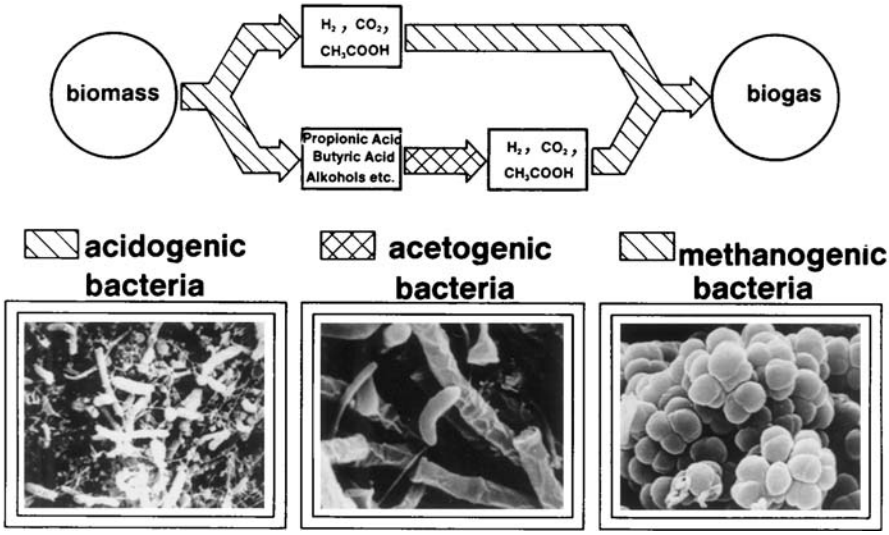

Fig. 2 Schematic representation of the course of anaerobic methane generation from complex organic substances

much more complicated, and requires balanced cooperation between the various microorganisms present, ensuring that there will be neither a shortage nor an accumulation of intermediates.

The central problem from a reaction-engineering point of view is finding a way to achieve high space-time yields. The more complex the substrate mixture from a chemical structure and particle size standpoint, the more difficult it becomes to meet this challenge. Furthermore, the growth of anaerobic microorganisms is a function of numerous factors, including residence time, temperature, redox potential, pH, and nutrient composition. Since the generation time for the microorganisms involved is comparatively long, the residence time of the catalyst must be uncoupled from the residence time of the substrate if one hopes to increase the space-time yield. To this end, various approaches are available for the retention and recycling of the catalytic biomass.

From a thermodynamic perspective, hydrogen is an particularly important "intermediate". If hydrogen utilization is not sufficiently effective, then the equilibrium position of the preceding steps is influenced in an unfavorable way.

Finally, the kinetics of the most important individual steps (Fig. 2) are so far quite inadequately understood. This is in part because of the complexity of the substrate mixture usually encountered in practice, but also because collecting reliable kinetic data is a very time consuming process, and possible only in the case of continuous cultivation.

3 Thermodynamics

As shown in Fig. 2, the anaerobic degradation of organic matter proceeds via a series of intermediate steps. In terms of both thermodynamics and kinetics, further degradation may be severely limited if intermediates are allowed to accumulate. The concentration of hydrogen takes on a regulative role by influencing the distribution of metabolic products formed by the fermentative bacteria [2–5]. This point is emphasized in Fig. 3 and reinforced by the equations in Scheme 1, involving the products of acidogenesis (acetic acid, propionic acid, and butyric acid) and the hydrogen produced from them.

While the decomposition of acetic acid is independent of the partial pressure of hydrogen, the degradation of propionic acid and butyric acid would be inhibited by a high partial pressure of hydrogen. At the same time, an adequate hydrogen partial pressure is necessary for the formation of methane from hydrogen and CO_2. This results in a narrow "thermodynamic window" within which the decisive reactions are able to proceed simultaneously (Fig. 4). Consequently, there must be a close relation between microorganisms that form hydrogen and those that instead utilize it (interspecies hydrogen transfer). Hydrogen transfer presupposes a spatial proximity on the part of the relevant microorganisms. In fact, if the population density

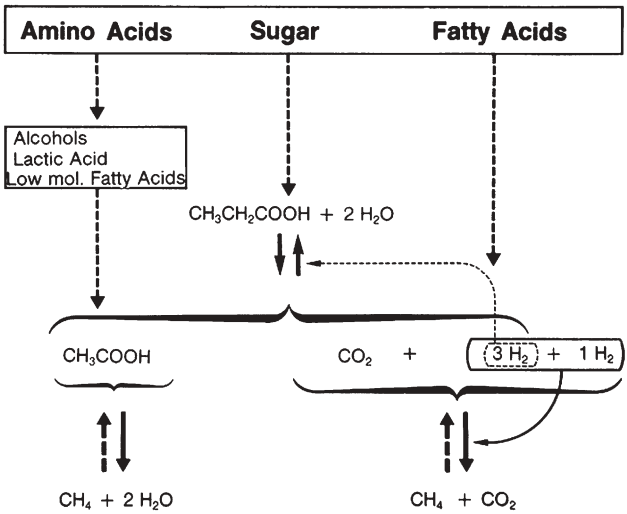

Fig. 3 Methane formation from acetic acid and the combination of hydrogen and carbon dioxide: the influence of hydrogen on propionic acid degradation

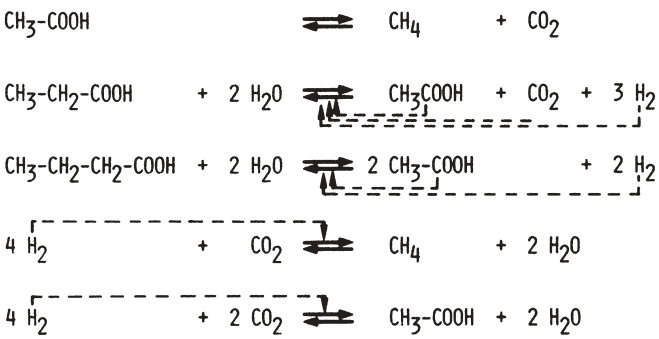

Scheme 1 Acidogenesis products and methane formation

is inadequate, vigorous stirring can actually interfere with this synergistic effect.

Figure 4 shows that propionic acid is poorly degradable in the presence of even a low partial pressure of hydrogen. If hydrogen utilization in a mixture culture is not sufficiently high, accumulation is observed, especially of propionic acid (and the wastewater reactor "turns acidic"). Since the activity of methanogenic microorganisms decreases significantly pH<5, a vicious circle is therefore likely to result.

However, the relationships are much more complex than this, because it is not only the propionic acid already present that may serve as an input to aceto-

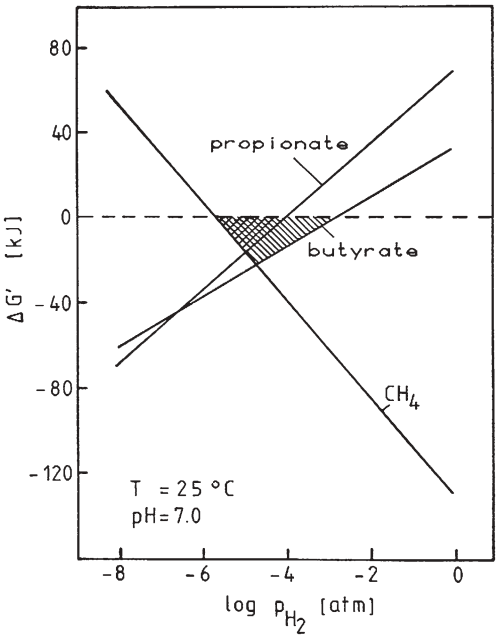

Fig. 4 "Thermodynamic window" for simultaneous methane formation from propionic acid, butyric acid, and H_2/CO as a function of hydrogen partial pressure

$$C_6H_{12}O_6 + 4\,H_2O \rightarrow 2\,CH_3COO^- + 2\,HCO_3^- + 4\,H^+ + 4\,H_2 \qquad \Delta G_R^0: -206.3\ \text{kJ}$$

$$C_6H_{12}O_6 + 2\,H_2 \rightarrow 2\,CH_3CH_2COO^- + 2\,H_2O + 2\,H^+ \qquad \Delta G_R^0: -358.1\ \text{kJ}$$

$$C_6H_{12}O_6 + 2\,H_2O \rightarrow CH_3CH_2COO^- + 2\,HCO_3^- + 3\,H^+ + 2H_2 \qquad \Delta G_R^0: -254.6\ \text{kJ}$$

$$C_6H_{12}O_6 + 2\,H_2O \rightarrow 2\,C_2H_5OH + 2\,HCO_3^- + 2\,H^+ \qquad \Delta G_R^0: -225.9\ \text{kJ}$$

$$C_6H_{12}O_6 \rightarrow 2\,CH_3CHOHCOO^- + 2\,H^+ \qquad \Delta G_R^0: -198.3\ \text{kJ}$$

Scheme 2 Fermentative conversions of carbohydrates in the presence of hydrogen

genesis, but also additional propionic acid derived from prior steps in the context of acidogenesis. The equations in Scheme 2 show that fermentative conversion of carbohydrates in the presence of hydrogen is directed mainly toward propionic acid, because this step links to the greatest change in the free energy (ΔG_R^o=–358.1 kJ/mol).

4 Kinetics

In practice, only continuously operated systems can be used for kinetics measurements, because batch-reactor experiments (shaken cultures) provide results that are poorly reproducible. This is due to the fact that in a batch experiment the reaction conditions change constantly over the course of the test period, resulting in the appearance and disappearance of various limitations. In a chemostatic operating mode the reactor is maintained at a steady state with respect to outlet conditions. The influence of various parameters can therefore be studied by varying either the residence time or the substrate composition. The basic procedure for collecting kinetic data can be illustrated by using the anaerobic degradation of acetic acid with a pure culture of *Methanosarcina barkeri* as an example. This example is also of practical importance, because most biogas comes from the degradation of acetic acid, and this reaction is regarded as the limiting step.

In studying the growth of *M. barkeri* (DSM 804), acetic acid was used as the sole source of carbon, with a defined mineral growth medium [6, 7]. An elemental analysis [%(m/m)] of *Methanosarcina barkeri* growing on this medium revealed carbon (46.85%), nitrogen (12.16%), hydrogen (6.69%), sulfur (1.05%), and phosphorus (0.91%). Since optimal growth of this particular microorganism is possible only over a very narrow pH range, the pH needs to be held constant. On the other hand, a pH shift should be expected during the conversion process [8].

A schematic representation of the experimental arrangement used in this study is shown in Fig. 5. The stirred-tank reactor was equipped with pH measuring and control devices, a redox indicator, two coordinated pumps for substrate dosing and product withdrawal, thermostatic control, a thermal

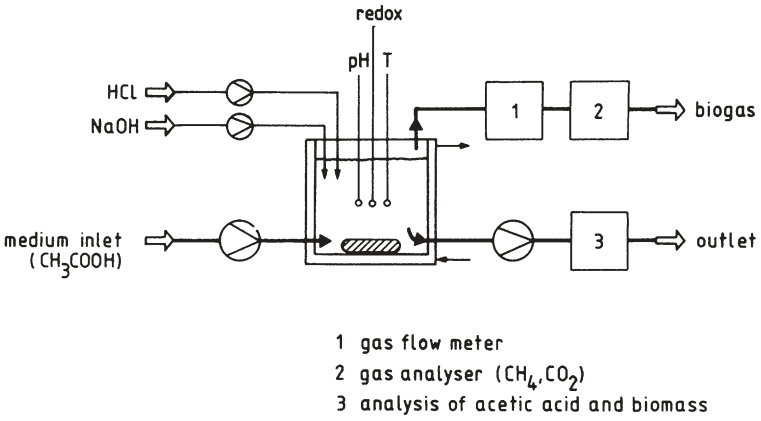

Fig. 5 Schematic representation of the experimental setup for obtaining kinetic data on the anaerobic degradation of acetic acid by *M. barkeri*

mass-flow meter (1), and a gas analyzer (2) for methane and carbon dioxide analysis. Substrate flow was determined with the aid of balance.

To establish a set of model parameters it was necessary to simultaneously solve the substrate and the biomass balances for a stationary state in a continuous stirred-tank reactor without biomass retention:

The mass balance for the substrate (where S=substrate concentration; X=cell dry-mass concentration; τ=mean residence time) is given by:

$$0 = \frac{1}{\tau}(S_0 - S) + \frac{\mu_{max}}{Y_{max}} \cdot \frac{S}{K_s + S} \cdot X \tag{1}$$

The mass balance for the biomass is given by:

$$0 = -\frac{1}{\tau} \cdot X + \mu_{max} \cdot \frac{S}{K_s + S} \cdot X \tag{2}$$

The model parameters (acetate degradation by *M. barkeri*) are:

μ_{max} is the maximum growth rate (0.528 d^{-1})
Y_{max} is the maximum growth-yield coefficient (2.104 g mol^{-1})
K_S is the Michaelis-Menten constant (0.0067 mol L^{-1})

The reaction conditions for continuous measurement are:

S_o is the initial substrate concentration (0.3; 0.6; 0.9 mol L^{-1} acetic acid)
pH = 6.3
T = 37 °C

This leads to the following equations for the two variables X and S, obtained by solving Eqs. 1 and 2 for the biomass concentration X and the substrate concentration S respectively:

$$X = f(\tau) = \frac{(S_0 - S)}{\tau \cdot \left(\frac{\mu_{max}}{Y_{max}} \cdot \frac{S}{K_s + S} \right)} \tag{3}$$

$$S = f(\tau) = \frac{K_S}{\mu_{max} \cdot \tau - 1} \tag{4}$$

The specific substrate consumption rate $r(S)$ is coupled to the substrate concentration S by the Monod kinetics (r_{max}=maximum specific substrate consumption rate):

$$r(S) = r_{max} \cdot \frac{S}{K_s + S} \tag{5}$$

The classical way of evaluating such kinetics is represented by methods that convert the non-linear kinetics into a straight line (easy to interpret graphi-

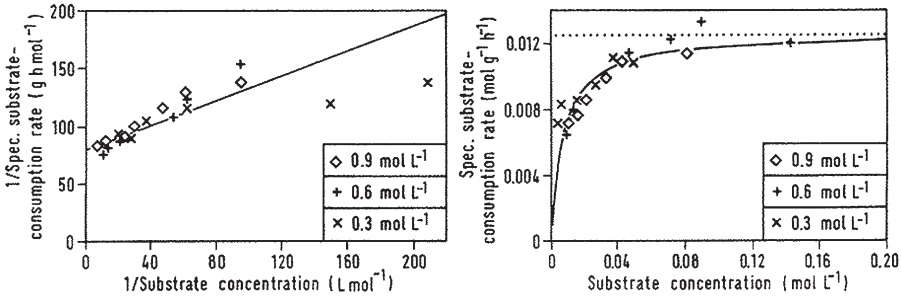

Fig. 6 Kinetics of substrate consumption

cally) by means of linear transformations. The best-known approach is the double reciprocal Lineweaver-Burke plot:

$$\frac{1}{r(S)} = \frac{K_s}{r_{max}} \frac{1}{S} + \frac{1}{r_{max}} \tag{6}$$

However, due to distortions, these transformations do not lead to statistically perfect statements [9]. The Lineweaver-Burke method is indeed the poorest of the linear transformations. For this reason, methods of non-linear optimization, such as the Rosenbrock method used below [10], are applied almost exclusively today. Figure 6 shows the substrate consumption kinetics calculated according to both methods with the following values: r_{max}= 0.0125 mol g^{-1} h^{-1} and K_S=0.0067 mol L^{-1}. It can be seen that, with linear plotting, the small substrate concentrations have an inappropriately large influence on the result.

Up to this point, it was possible to evaluate the data without any statement about the nature of the coupling between microbial growth and substrate consumption. If the maintenance metabolism is taken into consideration, the substrate consumption rate results from the growth of the biomass and its maintenance metabolism:

$$r(S) = \frac{\mu}{Y_{X/\Delta S}} = \frac{\mu}{Y_{max}} + m \tag{7}$$

where m is the maintenance metabolism coefficient, μ is the growth rate, and $Y_{X/\Delta S}$ is the yield coefficient (selectivity for incorporation of substrate in biomass).

Non-linear optimization of Eq. 7, 8

$$Y_{X/\Delta S} = Y_{max} \frac{\mu}{\mu + Y_{max} \cdot m} \tag{8}$$

results in the parameters Y_{max}=2.104 g mol^{-1} and m=0.0022 mol g^{-1} h^{-1} (Fig. 7).

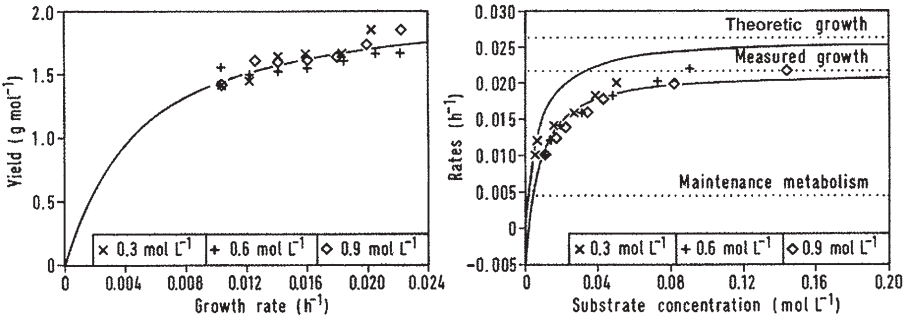

Fig. 7 Growth kinetics

The growth rate can then be calculated according to:

$$\mu = r_{\max} Y_{\max} \frac{S}{S + K_s} - mY_{\max} \tag{9}$$

or more briefly according to (Fig. 7, left)

$$\mu = \mu^*_{\max} \frac{S}{S + K_s} - b \tag{10}$$

where $\mu^*_{\max}$ is the true specific growth rate, and b is the specific maintenance metabolism rate.

The measurable growth represents the growth converted into biomass; the concept of true growth is a fictive growth including the maintenance metabolism [11]. The following values result for the parameters $\mu^*_{\max}=r_{\max}\cdot Y_{\max}=0.0263\ h^{-1}$, $K_S=0.0067$ mol L^{-1}, and $b=m\cdot Y_{\max}=0.0046\ h^{-1}$.

The minimum substrate concentration that just covers the requirements for maintenance metabolism can be calculated from Eq. 9 by setting $\mu=0$:

$$S_{\min} = \frac{m}{r_{\max} - m} K_S = 0.0014 \text{ mol L}^{-1} \tag{11}$$

5 Mass and Heat Transfer

The anaerobic treatment of wastewater occurs essentially without any heat of reaction, which means that heat-exchanging surfaces are unnecessary. Nevertheless, since a bioreactor operates above ambient temperature, insulation of the outer walls is advisable. In fact, simply warming the substrate up to reaction temperature meets the primary heat requirement. To some extent it is possible to utilize the heat capacity of the effluent flow for heating purposes. Heat losses can be compensated for without difficulty by combustion energy derived from the biogas produced. Therefore, operation of an anaerobic wastewater-treatment plant is at least self-sustaining from an energy standpoint.

Since no gaseous substrate (oxygen) is required, problems related to creating a large surface for material exchange are avoided. However, it is necessary that provision be made for the rapid removal of gaseous reaction products to ensure that as little of the "catalyst surface" as possible is blocked by gas bubbles. As a result of the residence times involved and the difference in densities between the emerging biogas and the liquid phase (which provides a stirring effect), mechanical stirring aimed at mixing the liquid phase can be more or less dispensed with. When mechanical stirrers are used, their primary purpose is to ensure homogeneous distribution of the catalyst or the suspension of solids.

6 Biomass Retention/Recycling

Achieving high performance in a reactor is not simply a function of the biomass activity. Because of the autocatalytic factor, the biomass concentration is important as well. The biomass concentration cannot be adjusted independently of the wastewater residence time in the bioreactor. Given the long generation time of anaerobic microorganisms, important components of the mixed population are always lost along with the partially treated water even at a residence time of several days if no precautions are taken with respect to biomass retention or external separation and return. In general, this requires increasing the particle size and/or the density difference relative to the liquid phase.

The most important methods for decoupling the residence times for liquid substrate and biomass in anaerobic wastewater treatment via internal retention are illustrated in Fig. 8.

A selection in favor of either flocculating or granule-forming microorganisms that sediment easily in a bioreactor is still accomplished in most cases by empirical optimization of the reaction conditions. Factors that influence the formation and maintenance of anaerobic granules include the liquid upflow velocity and hydraulic retention time, the characteristics of the substrate, the characteristics of seed sludge, the addition of polymers and cations (Ca^{2+}, Mg^{2+}, Fe^{2+}, Fe^{3+}, Al^{3+}), reactor temperature, and pH [12–14]. This principle of biomass retention is the basis for the Upflow Anaerobic Sludge Bed (UASB) reactor and the Expanded Granular Sludge Bed (EGSB) reactor [15–26].

Free biomass or pelletized biomass can be separated with the help of filtration techniques, depending on the pore size of the filter, although such filters easily become clogged [27–30]. Moreover, activity losses must be anticipated due to the mechanical shear stress involved in recirculating a microbial suspension.

One way to achieve an increase in the particle size, with a corresponding improvement in the separability of the liquid face, is to immobilize the biomass on a carrier material [31–41]. Evidence for the potential of this approach to microbial retention is available from nature, because most microorganisms in the environment are present in a fixed state. Nevertheless, adsorption

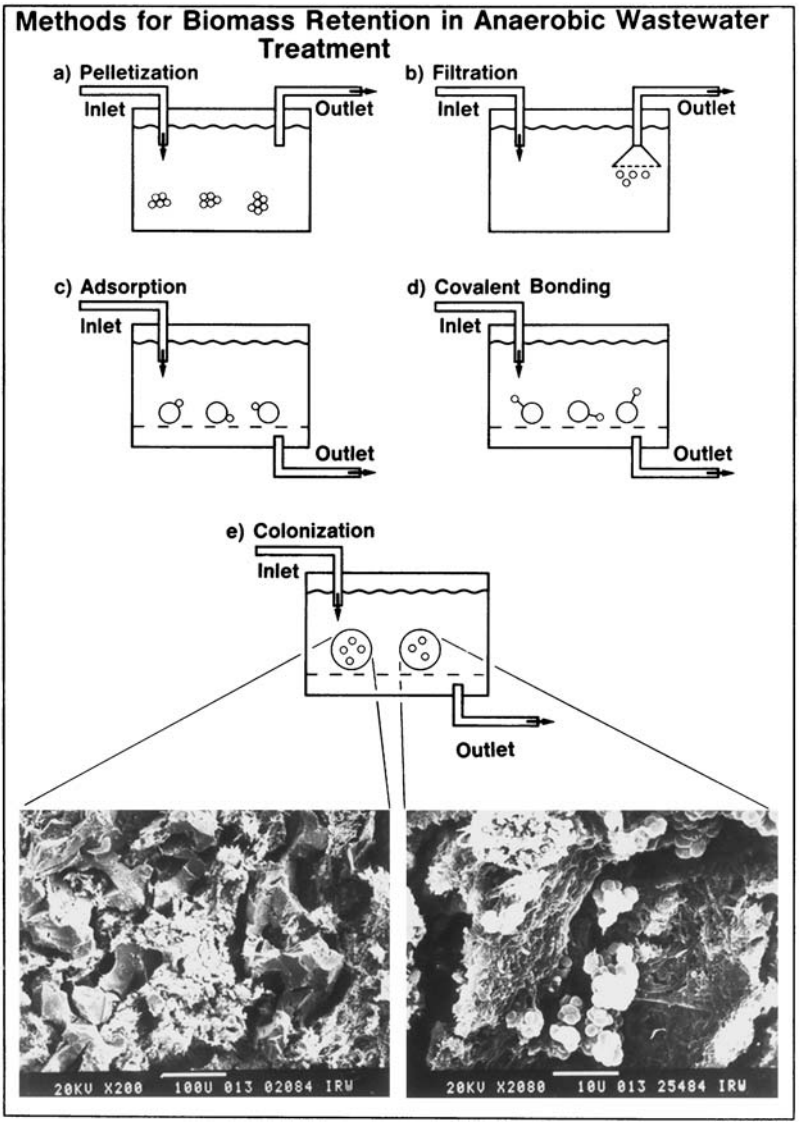

Fig. 8 Schematic representation of various approaches to biomass retention: **a** Flocculation-pelletization; **b** Filtration; **c** Immobilization through adsorption; **d** Immobilization through covalent bonding; **e** Immobilization through colonization on a macroporous carrier

presents the risk that the biomass might become detached as a consequence of shear forces.

The colonization of macroporous carriers with high surface areas lowers the risk of biomass detachment, while at the same time it substantially increases the amount of biomass that can be accumulated per unit volume [8, 42–48].

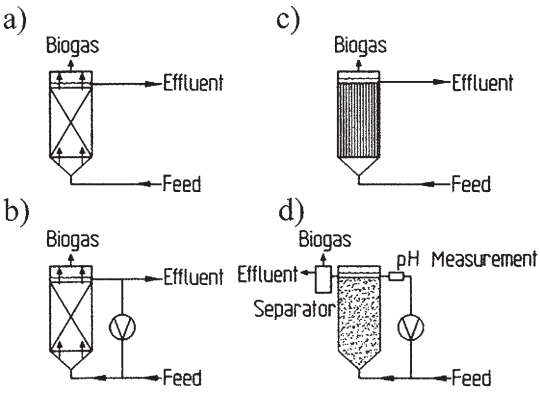

Fig. 9 Reactors for the immobilization of microorganisms in anaerobic wastewater treatment: **a** Fixed-bed reactor; **b** Fixed-bed loop reactor; **c** Fixed film reactor; **d** Fluidized bed reactor

Proper adjustment of the pore size of the carrier material permits the flow to partially penetrate the interior of the particles without also detaching the biomass. This has the further advantage that it facilitates the rapid removal of biogas as it is formed. A summary of common reactor configurations based on immobilized microorganisms is provided in Fig. 9.

In the case of external biomass recycling, sedimentation is achieved either by flocculation induced by chemical additives, or by increasing the separation area with the help of lamella separators. This technique is also known as the anaerobic contact process [49, 50]. It is also possible to increase the density difference by flotation [51], or to increase the gravitational field by centrifugation. The principles of external biomass recycling are illustrated schematically in Fig. 10.

6.1 Upflow Anaerobic Sludge Bed reactors

The UASB process has been successfully applied to a large variety of industrial effluents, originating mainly from the agro-food industry, beverage industry, alcohol distilleries, pulp and paper industry, and the chemical industry.

A simplified flow diagram of the UASB process is presented in Fig. 11. Wastewater flows vertically through the system starting at the bottom. Microbial granules sediment on the reactor floor, forming a sludge bed. Enrichment of the biomass in the reactor is made possible by a three-phase separation system, especially designed to retain sludge flocs and granules and to separate and release the biogas from the system. Apart from granular sludge, a considerable amount of flocculated sludge is formed as well, which in turn constitutes a basis for the formation of new pellets.

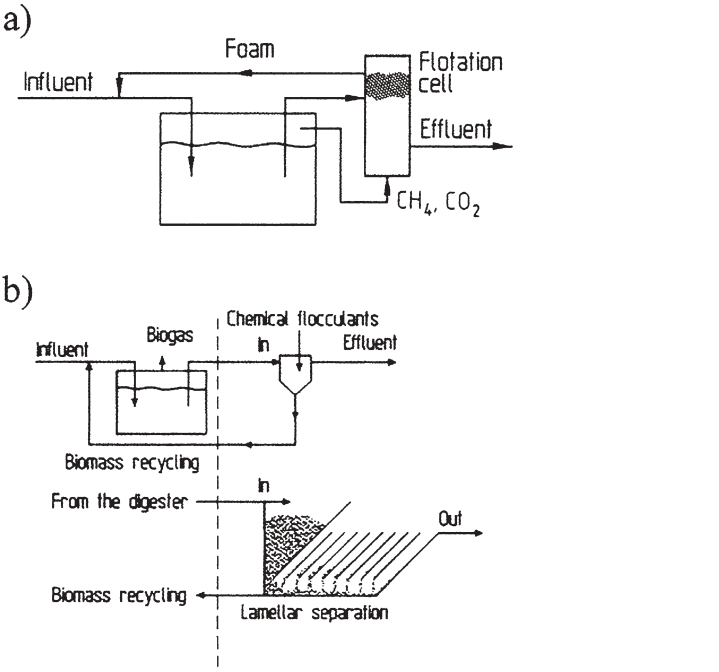

Fig. 10 Schematic representation of methods for biomass recycling in the anaerobic contact process: **a** Foam removal through flotation; **b** Separation by external chemical or physical sedimentation

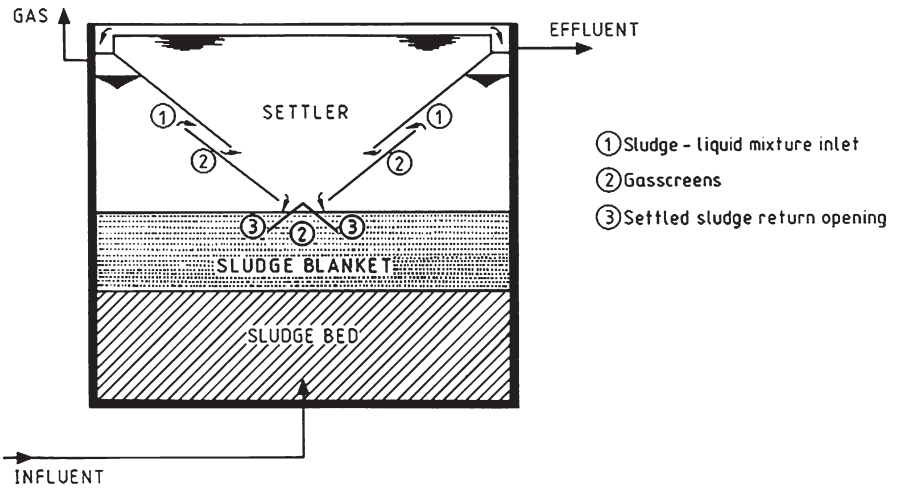

Fig. 11 Schematic representation of the upflow anaerobic sludge bed (UASB) process

A distributor on the floor of the reactor is used for uniform liquid feeding and it must meet special design requirements [52]. In order to achieve an optimal contact between sludge and wastewater, channeling of the wastewater through the sludge-bed, the formation of dead corners in the reactor, and uneven distribution due to clogging of the inlet pipes should be avoided.

For partially and fully soluble wastewaters, the operational upflow velocity in UASB reactors with granular sludge is approximately 1–3 m h^{-1}, while velocities <0.5 m h^{-1} are applied for flocculent types of sludge [52]. Operational results from pilot scale UASB reactors at upflow velocities between 0.01 and 0.65 m h^{-1} reveal that granulation is favored at higher velocities [53, 54]. At even higher superficial velocities (1.0–1.5 m h^{-1}), the granules become more uniform in relation to their settling velocity [55, 56].

Recirculation of partially purified wastewater to the UASB reactor is required only in the case of high COD concentrations in the wastewater in order to avoid pronounced concentration gradients as a function of height. The introduction of recycling can minimize the total operational costs in several cases (savings in alkaline addition), due mainly to the efficient use of the internal buffering capacity [57, 58].

The height of the system is approximately 5–7 m for partially soluble wastewaters, with COD exceeding 3 kg m^{-3}, while for domestic sewage reactor heights are 3–5 m [52]. This in turn generally also entails a considerable amount of surface area. The EGSB reactor is a modification of the UASB reactor in which a higher superficial velocity is applied (5–10 m h^{-1}). Because of the higher upflow velocities, mainly granular sludge is retained in an EGSB system [59]. As a result, the contact between the wastewater and the sludge is higher compared to UASB reactors, resulting in the maximum achievable loading rate.

Wastewater fed into a UASB reactor should be partially but not completely acidified. In the latter case, when complete acidification of the wastewater occurs, flotation and formation of a rather voluminous sludge has been reported [60]. The hydraulic retention time in the acidification tank is between 4–12 h. The corresponding degree of acidification (20–50%) is favorable, both for carbohydrate-rich wastewater as well as for protein- and lipid-rich wastewater [61]. The process chain is generally enhanced by a preceding pre-acidification step that simultaneously ensures hydraulic equilibration. Special care should be given to ensuring that the acidifying biomass is separated prior entering the UASB reactor compartment. Moreover, suspended solids, either poorly degradable or non-degradable, should be prevented from the entering UASB reactors, because an irreversible sharp drop in the specific methanogenic activity occurs, while granule formation is influenced in a negative manner.

Of the large-scale wastewater treatment plants that were designed for anaerobic operation (1215 by 2001 [62]), more than 70% were conceived as UASB and EGSB plants. This speaks well for the idea, but there are also disadvantages to be considered. For example, the process of microbial pellet formation is still very empirical and it is neither applicable to all types of wastewater nor uniformly reproducible. The formation of granular sludge may occasionally

require several months or even years, and sometimes it never takes place; moreover, existing pellets may redissolve and be washed out of the system due to a change in process conditions [60]. For this reason, pellet sludge is extracted from existing plants for the purpose of "seeding" newly commissioned UASB reactors, and material may be transported overseas to this end.

An examination of the utilization efficiency of the existing reactor volume shows that only 25–30% of the space is actually devoted to bioconversion, while the rest functions simply as a phase-separating device. The biosolids concentration approaches 75–85 g L^{-1} in the granular sludge region, but the COD elimination capacity (at maximum space yield) approximates 6–14 kg COD m^{-3} d^{-1} as a result of hindered mass transport. The minimum realizable residence time in a UASB reactor is 2–6 h. However, such short residence times are actually achieved only with lightly contaminated wastewater (1–2 kg COD m^{-3}). A residence time of 8–20 h is required for a moderately concentrated effluent (COD 3–20 kg m^{-3}).

6.2 Fixed-Bed Loop Reactors

The principle underlying this type of reactor combines the advantages of fixed-bed and fluidized-bed reactors, but avoids several of the disadvantages of both (Fig. 12). Most of the liquid responsible for the upward flow in a fixed-bed loop reactor [8, 42–49] leaves the fixed-bed and returns once again through an external loop, where it is mixed with fresh influent. Circulation is gradually increased until concentration gradients no longer play a role. Establishing the correct rate of circulation requires that biomass accumulation in the intergranular volume also be taken into account. This in turn means that the void

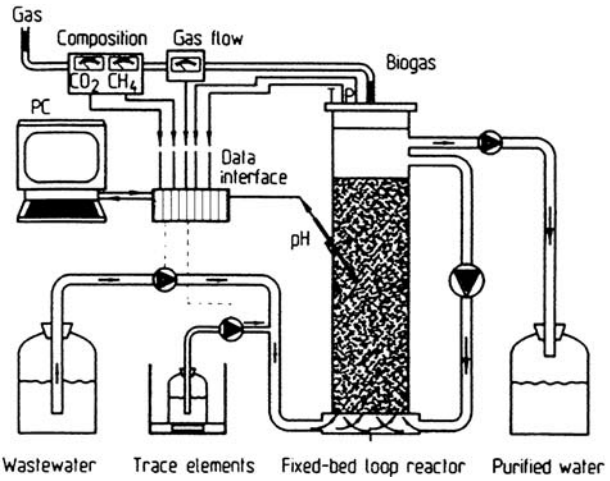

Fig. 12 Schematic illustration of a fixed-bed loop reactor

volume must be neither rinsed entirely free of biomass nor allowed to become clogged. In this way it is possible to establish a very high biomass concentration. Therefore, despite the low propagation rate of anaerobic microorganisms, provision must be made for periodically washing out excess sludge by briefly increasing the circulation rate. Simultaneously, small-suspended solid particles not trapped in the course of physical pretreatment of the wastewater, and which may have accumulated in the fixed-bed loop over time, are also flushed out.

This particular anaerobic-reactor concept has become especially familiar in the literature in conjunction with the use of macroporous carrier materials for microbial immobilization with three-dimensional colonization (Fig. 13). The technique itself results in an increase in particle size as well in the density difference between the particles and the fluid, making it possible to decouple the residence time for the biocatalyst and the fluid in the reactor without the addition of chemicals (for instance for carrier fixation, flocculation, or flotation) or supplementary energy (for example for filtration or centrifugation), and without the need for constructing additional facilities (such as sedimenters or lamellar separators).

Basic process-development work in this area was initiated in the 1980s at the Forschungszentrum Julich (Julich Research Center, Germany), eventually leading to the establishment of the "Biogas High Performance Process" for treating heavily organic-laden wastewaters. This process was successfully commercialized over a period of several years by licensing it to various parties interested in building treatment plants.

The first large-scale plant of this type was for a potato-starch factory, and it took only ten months to build, with operation commencing in September 1987. Figure 14 provides both a flow diagram and a photographic overview of the two-stage facility. It incorporates a pre-acidification tank with a working volume of 1,000 m^3. Four fixed-bed loop reactors (d; 300 m^3 each) for methanization are connected in parallel. These are filled with lava slag that serves as a porous carrier. The plant was designed for a hydraulic load of 2,000 $m^3\ d^{-1}$, resulting in a residence time of 14 h for the methanization reactor (second stage) at a loading rate per unit volume of 30 kg COD $m^{-3}\ d^{-1}$. Operation under full hydraulic load leads to the anaerobic elimination of more than 20 tn of COD per day. At a COD/BOD ratio of 1.7, this corresponds to about 200,000 population equivalents. The process in turn generates ~12,000 m^3 of biogas per day. The exceptional efficiency of microbial colonization in conjunction with a macroporous carrier is apparent from the fact that this plant was able to operate at full capacity within six weeks. Seven large-scale plants of this type are currently active. Apart from the one described above, similar plants have been built for the pulp and paper industry, for baker's yeast fermentation, and for feed manufacture. In the latter application, peak values ≤106 kg COD $m^{-3}\ d^{-1}$ have been achieved without difficulty in facilities with capacities of 20 and 170 m^3 through the use of Siran Rasching rings with a projected space-time yield of 35 kg COD $m^{-3}\ d^{-1}$.

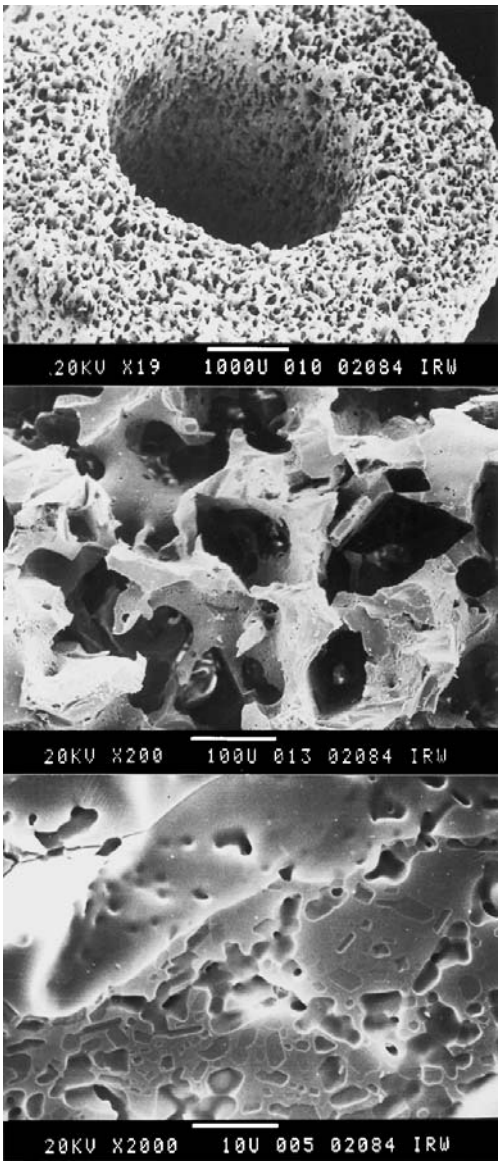

Fig. 13 Scanning electron micrographs at various magnifications showing an open pored sintered glass that has been formed into Rasching rings

a

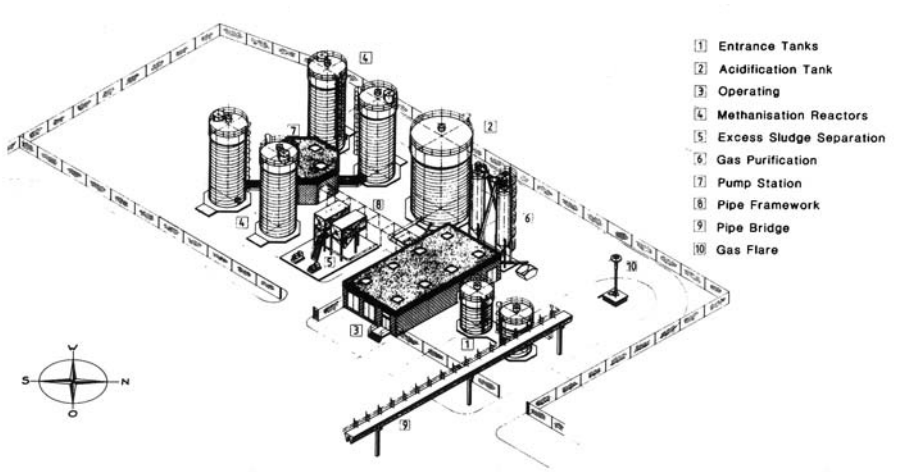

b

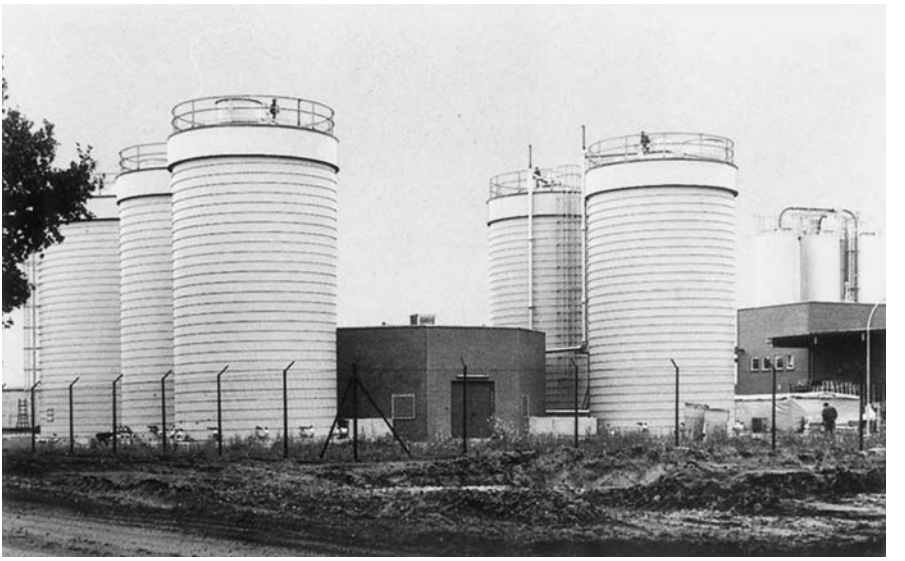

Fig. 14 Flow diagram **a** and photograph **b** of a two stage anaerobic wastewater treatment facility of the fixed-bed loop reactor type, used in the potato starch industry (COD load 35,000 kg/d). Key to diagram **a**: 1, Entrance tanks; 2, Acidification tank; 3, Operations center; 4, Methanization reactors; 5, Excess-sludge separation; 6, Gas purification; 7, Pumping station; 8, Pipe framework; 9, Pipe bridge; 10, Gas flare

7
Comparison of Single-Stage and Two-Stage Process Operation

As a result of stepwise degradation involving various bacterial populations with complex interactions linking fermentative acid formation with methanogenesis, it has been suggested that these two individual steps have to be separated in space by the use of a multistage reactor combination [63–65]. The most widely applied variant is a two-stage mode of operation (Fig. 15), in which acidogenic microorganisms are most active in the first stage and mainly methanogenic microorganisms in the second [66–68]. The latter is usually implemented in the form of an upflow anaerobic sludge blanket or fixed-bed reactor.

Today the trend in anaerobic treatment of highly contaminated wastewater is clearly towards a two-stage process design [69]. The generation time of microorganisms in the first stage is clearly shorter than that in the second stage and therefore, incorporation after the first stage of a sedimenter with partial biomass return is sufficient to maintain stable conditions in the first stage. Nevertheless, in a large-scale operation it is extremely important to ensure effective separation of pre-acidification biomass from the inlet of the second stage to prevent solids loading either in the methanogenic stage or at the outlet of the plant complex as a whole. The presence of acidified biomass in UASB reactors is often responsible for granular sludge floatation and process instability [60, 59].

Taking the anaerobic treatment of distillery residue as an example of dealing with a complex, highly organic-laden effluent from the food industry, it proved possible to define realistic limits for single-stage processing [70, 71]. A fixed-bed loop reactor like the one shown in Fig. 12 was used in this particular study. Very large fluctuations were observed in the fatty-acid spectrum in the reactor effluent, as well as in the hydrogen content of the biogas, despite the unchanging nature of the wastewater and an approximately constant residence

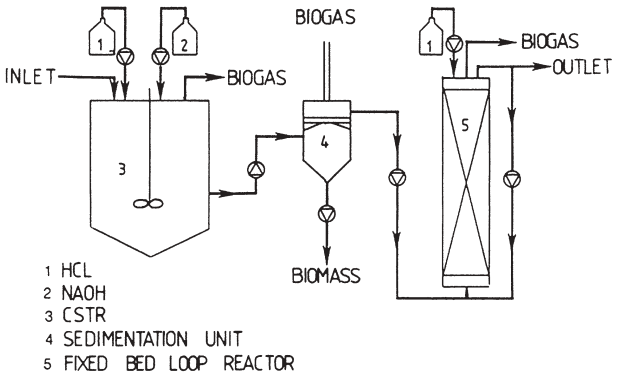

Fig. 15 Schematic representation of a two stage anaerobic bioreactor with acidification followed by methanization

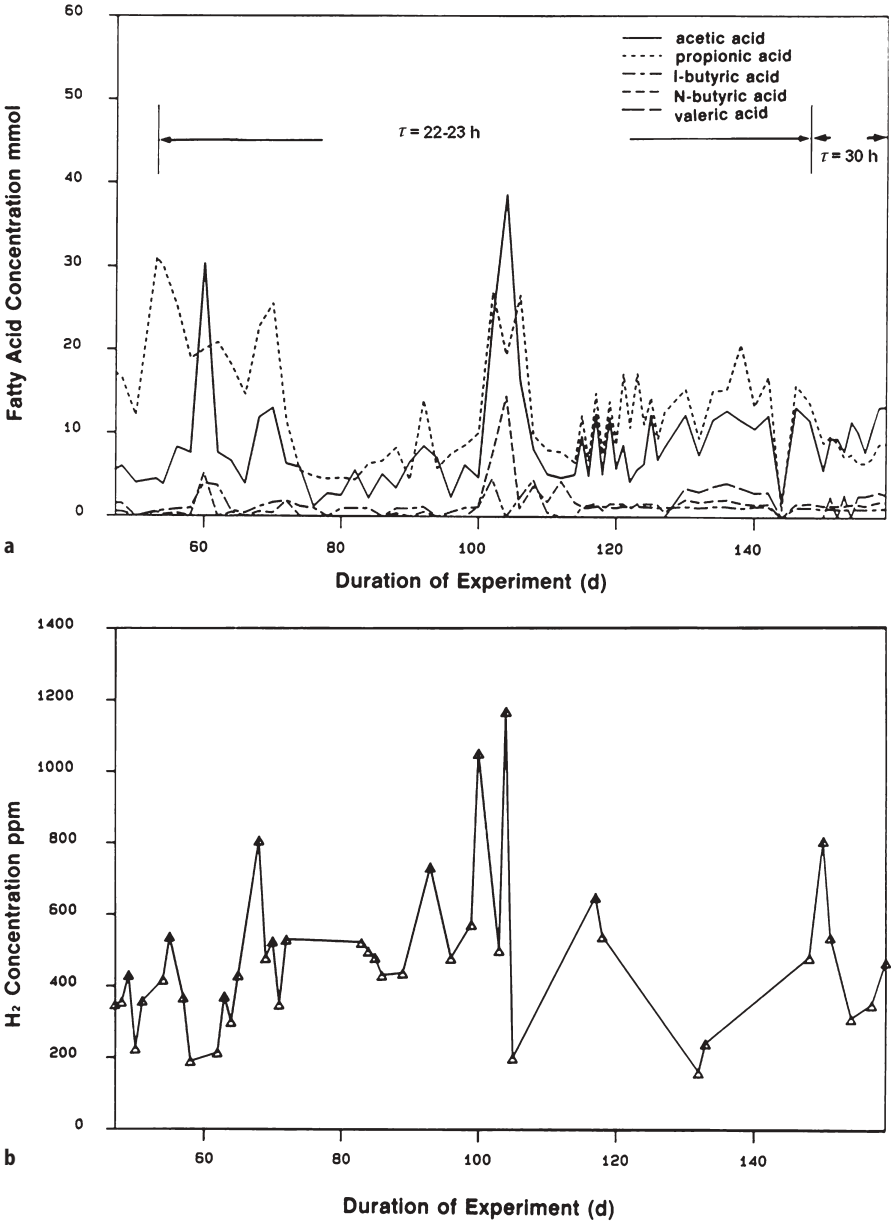

Fig. 16 Fluctuations in **a** fatty acids and **b** hydrogen concentrations in a single fixed-bed loop reactor with a feed consisting of distillery residues

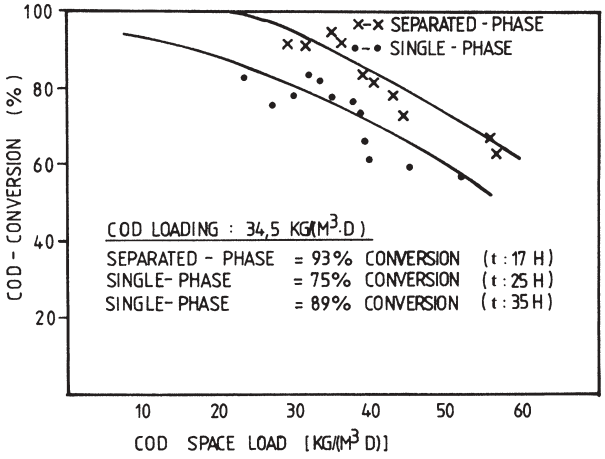

Fig. 17 The effect of COD loading on COD conversion in single stage and two stage configurations for the degradation of distillery residues (COD loading=34.5 kg m^{-3} d^{-1}; single stage configuration: 75% conversion with t=25 h, 89% with t=35 h; two stage configuration: 93% with t=17 h)

time. The observed propionic acid peaks clearly correlate with an increase in the hydrogen concentration (Fig. 16).

In view of these unsatisfactory results (reactor instability and reduced efficiency), a reactor configuration corresponding to that shown in Fig. 15 was installed, along with a fixed-bed loop reactor for methanization. Results for both single-stage and two-stage processes in the anaerobic treatment of distillery residues are presented in Fig. 17. For every space-load tested, the attainable COD conversion was found to be greater in the case of the two-stage process and the process stability was greatly improved as well.

8
Influence of Single-Stage and Two-Stage Methanization Cascade

Wastewaters from the production of sauerkraut and from ethanol distillation were used to compare the two design variations in both single-stage and cascade methanization. Fixed-bed loop reactors were employed in all cases. A preceding stirred tank was used for pre-acidification of the wastewater. The investigation covered residence times of 5–16 h. COD effluent values from the cascade arrangement were in all cases clearly lower than those from the effluent data for single-stage methanization. In fact, the observed differences were more pronounced (by up to 4 kg of COD per cubic meter) in the case of the more contaminated distillery residues compared with the moderately contaminated wastewater from sauerkraut fermentation. The clear superiority of the process involving a two-stage methanization cascade relative to a fixed-bed loop reactor is

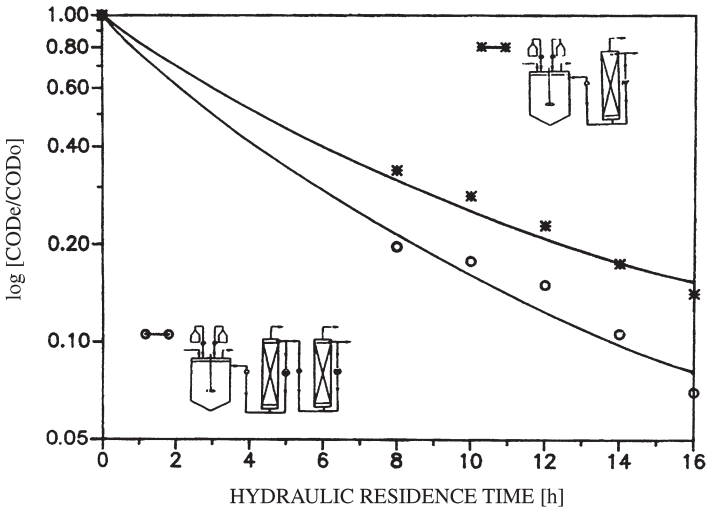

Fig. 18 Change in residual COD as a function of residence time in the anaerobic treatment of distillery residues via a two stage process with and without a cascade arrangement. COD_e=effluent COD; COD_o=initial COD

especially apparent from curves of the residual COD content as a function of residence time (Fig. 18). For a COD reduction of 80% (COD_e/COD_o=0.2), a residence time of ~13 h is required in the case of single-stage methanization. The residual content in the effluent from a two-stage cascade with the same residence time is only 0.1, corresponding to a conversion of 90%. A residence time of as little as 8 h is sufficient to degrade 80% of the COD in the case of the two-stage process. Under these conditions, the observed volume reduction in a methanization cascade compared with the single-stage mode of operation is ~40%.

Results from all of the reaction-engineering investigations reported so far for process design optimization with fixed-bed loop reactors in the anaerobic treatment of highly organic-laden effluents from the food industry are summarized in Fig. 19. The results show the course of the minimum residence time and the associated relative methanization volume for a COD reduction of ~80% at various developmental stages in the corresponding "process evolution". Accordingly, the volume of a two-stage cascade is only 3.5% of that required for a continuously operated stirred-tank reactor (CSTR) lacking provisions for residence time decoupling.

9
Future Prospects

The anaerobic treatment of wastewater represents another example of the fact that innovations may result from the joint application of biological and tech-

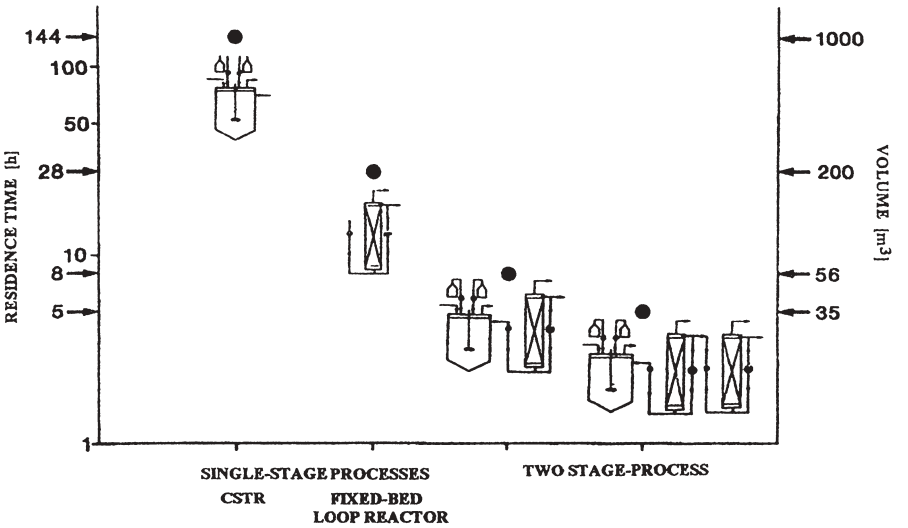

Fig. 19 Decrease in the minimum residence time and relative methanization volume for 85% COD reduction in the treatment of complex residues for the food industry as anaerobic fixed-bed loop technology evolved

nological principles. Despite the sophisticated optimization of the oxygen transfer process, aerobic wastewater treatment becomes less competitive with the anaerobic technique the higher the contamination level of the wastewater. The principle of carrier fixation as a way of preventing the washing-out phenomenon is also derived from a model frequently observed with sessile microorganisms in nature. Additionally, minimizing limitations associated with diffusion problems by increasing the convection current is a typical industrial approach to problem solving. The energy required for the wastewater treatment can in principle be provided directly by gas-driven motors. This approach, even though questionable, is justifiable for the long term. In the case of highly contaminated wastewater, anaerobic treatment is not only energy self-sufficient, but also capable of providing excess energy for use in other applications. In addition, the resulting marked reduction in sludge production should constitute a weighty argument in favor of the anaerobic process.

Concerns related to heavy metal deposition in the wastewater reactor operating under anaerobic conditions have not yet been accorded sufficient attention despite the fact that the distribution of clarification sludge (like that from the activated-sludge process) on agricultural land has been curtailed because of excessive heavy-metal contamination. Wastewater treatment is an industrial process associated with one of the largest levels of mass throughput known, and for this reason it provides a major impetus to further developments in bioprocess technology in general.

Careful experiments in laboratory and pilot-scale experiments can provide sufficient data to design a large-scale system and to predict its performance.

Wastewater treatment plants should in general be regarded as an internal part of the overall production plant and should be designed and handled in an integrated fashion. The upsets and disturbances in the production process should be handled in an optimum fashion so that the total plant (including the wastewater treatment plant) can function productively and optimally.

Due to the multidisciplinary character of the bioprocess engineering required for this successful development, and the operation of the wastewater system, it is essential that the different fields of microbiology, material science, chemical engineering, plant construction, and control engineering should collaborate closely together and carefully consider what is required for a successful operational system.

References

1. Smith MR, Mah RA (1978) Appl Environ Microbiol 36:870
2. Bryant MP, Wolin MJ (1975) Developmental microbiology, mcology, 2nd edn. Verlag T. Hasegawa, Tokyo
3. Hungate RH (1966) The rumen and its microbes. Academic, New York
4. Thauer RK, Jungermann K, Decker K (1977) Bacteriol Rev 41:100
5. Wolin MJ (1976) Microbial formation and utilization of gases. Verlag Goltze, Gottingen
6. Aivasidis A, Wandrey C (1983) Biochemical Eng III 413:489
7. Schurbuscher D, Wandrey C (1991) Anaerobic wastewater process models. In: Rehm HJ, Reed G (eds) Biotechnology 4. VCH Verlag Chemie, Weinheim
8. Aivasidis A (1989) Bioprocess Eng 4:19
9. Cornish-Bowden A, Eisenthal R (1974) Biochemistry J 139:721
10. Hoffmann H, Hofmann U (1971) Einfuhrung in die Optimierung. VCH Verlag Chemie, Weinheim
11. Bergter F (1983) Wachstum von Mikroorganismen. VCH Verlag Chemie, Weinheim
12. Yu HQ, Fang HHP, Tay JH (2001) Chemosphere 44:31
13. Yu HQ, Tay JH, Fang HHP (2001) Water Res 35:1052
14. Liu Y, Xu HL, Show KY, Tay JH (2002) World J Microb Biot 18:99
15. Lettinga G, van Velsen AF, Hobma SW, de Zeeuw W, Klapwijk A (1980) Biotechnol Bioeng 22:699
16. Lettinga G, van Velsen L, de Zeeuw W, Hobma SW (1980) Anaerobic digestion. Applied Science, London
17. Pette KC, Versprille AI (1981) Application of the UASB-concept for wastewater treatment. In: Hughes DE et al (eds) Anaerobic digestion. Elsevier, Amsterdam, p 121
18. Hulshoff Pol LW, Dolfing J, de Zeeuw WJ, Velzeboer CTM, Lettinga G (1983) Water Sci Technol 15:291
19. Dolfing J (1986) Water Sci Technol 18:15
20. Moosbrugger RE, Sam-Soon PALNS, Wentzel MC, Ekama GA, Loewenthal RE, Marais GvR (1993) Contract Report No WRC 249/1/93 of South African Water Research Commission
21. Wentzel MC, Moobrugger RE, Sam-Soon PALNS, Ekama GA, Marais GvR (1994) Water Sci Technol 30:31
22. Schmidt JE, Ahring BK (1996) Biotechnol Bioeng 49:229
23. Yan YG, Tay JH (1997) Water Res 31:1573

24. Britz TJ, Trnovec W, van Schalkwyk C, Roos P (1999) Contract Report No WRC 667/1/99 of South African Water Research Commission
25. Liu Y, Tay JH (2002) Water Res 36:1653
26. Liu Y, Xu HL, Yang SF, Tay JH (2003) Water Res 37:661
27. Strohwald NKH (1991) Contract Report No. WRC 338/1/91 of South African Water Research Commission
28. Nell JH, Kafaar A (1995) Contract Report No. WRC 365/1/95 of South African Water Research Commission
29. Lee S-M, Jung J-Y, Chung Y-C (2001) Water Res 35:471
30. Fuchs W, Binder H, Mavrias G, Braun R (2003) Water Res 37:902
31. Young JC, McCarthy PL (1969) J Water Poll Cont Fed 41:160
32. Frostell B (1979) Vatten 35:169
33. van den Berg L, Lentz CP (1979) Proc 34th Purdue Industrial Waste Conf, West Lafayette, IN, 9 May 1979. Ann Arbor Science, Ann Arbor, MI, p 319
34. Messing RA, Opermann RA (1981) US patent 4 286 061
35. van den Berg L, Kennedy KJ (1981) Biotechnol Lett 3:165
36. Kennedy KJ, van den Berg L (1982) Water Res 16:1391
37. Huysman P, van Meenen P, van Assche P, Verstraete W (1983) Biotechnol Lett 5:643
38. Szendrey LM (1984) Environ Prog 3:222
39. Wulfert K, Weiland P (1985) Chem Ing Tech 57:472
40. Weiland P, Wulfert K (1986) BTF Biotech Forum no 3, 3:151
41. Weiland P, Thomsen H (1990) Water Sci Technol 22:385
42. Aivasidis A, Wandrey C (1985) US Patent 4 532 042
43. Aivasidis A, Wandrey C (1986) DE Patent 3 345 691
44. Aivasidis A, Wandrey C (1987) US Patent 4 670 140
45. Aivasidis A, Wandrey C (1988) Korresp Abwasser 35:216
46. Aivasidis A, Wandrey C (1989) Chem Ing Tech 61:484
47. Aivasidis A, Wandrey C (1990) Ann NY Acad Sci 589:599
48. Aivasidis A, Wandrey C, Kiefer W (1992) US Patent 5 096 814
49. van den Berg L, Lentz CP (1978) Proc 33th Purdue Industrial Waste Conf, West Lafayette, IN, 9–11 May 1978. Ann Arbor Science, Ann Arbor, MI, p 185
50. Schlegel S, Kalbskopf KH (1981) Treatment of liquors from heat-treated sludge using the anaerobic contact process. In: Hughes DE et al (eds) Anaerobic digestion. Elsevier, Amsterdam, p 169
51. Zlokarnik M (1981) Chem Ing Tech 53:600
52. Lettinga G, Pol LWH (1991) Water Sci Tech 24:87
53. Alphenaar PA, Visser A, Lettinga G (1993) Bioresource Technol 43:249
54. O'Flaherty V, Lens PNL, de Beer D, Colleran E (1997) Appl Microbiol Biot 47:102
55. Kosaric N, Blaszczyk R, Orphan L, Lynch C, Maat D (1991) Water Poll Res J Can 26:453
56. Francese A, Cordoba P, Duran J, Sineriz F (1998) World J Microbiol Biot 14:337
57. Romli M, Greenfield PF, Lee PL (1994) Water Res 28:475
58. Imai T, Ukita M, Sekine M, Higuchi T, Fukagawa M (2001) Proc 9th World Congr Anaerobic Digestion 2001, Antwerpen, Belgium
59. Lettinga G (1996) Water Sci Technol 33:85
60. Hickey RF, Wu WM, Veiga MC, Jones R (1991) Water Sci Technol 24:207
61. Jeyaseelan S, Matsuo T (1995) Water Sci Technol 9:153
62. Frankin RJ (2001) Water Sci Technol 44:1
63. Pohland FC, Ghosh S (1971) Environ Lett 1:255
64. Ghosh S, Conrad JR, Klass DL (1975) J Water Poll Control Fed 47:30

65. Massey ML, Pohland FG (1978) J Water Poll Control Fed 50:2204
66. Cohen A, Zoetemeyer RJ, van Deursen A, van Andel JG (1979) Wat Res 13:571
67. Cohen A, Breure AM, van Andel JG, van Deursen A (1980) Wat Res 14:1439
68. Cohen A, Breure AM, van Andel JG, van Deursen A (1982) Wat Res 16:449
69. Demirel B, Yenigün O (2002) J Chem Technol Biot 77:743
70. Aivasidis A (1989) GWF–Wasser/Abwasser 130:163
71. Aivasidis A, Wandrey C, Hilla E (1989) Bioprocess Eng 4:63

Received: March 2004

Adv Biochem Engin/Biotechnol (2005) 92: 77–99
DOI 10.1007/b98918

The Oxygen Mass Transfer, Carbon Dioxide Inhibition, Heat Removal, and the Energy and Cost Efficiencies of High Pressure Fermentation

Arnd Knoll[1] · Bernd Maier[2] · Hermann Tscherrig[3] · Jochen Büchs (✉)[1]

[1] Biochemical Engineering, RWTH Aachen University, Worringer Weg 1, 52056 Aachen, Germany
buechs@biovt.rwth-aachen.de
[2] Merck KGaA, 64293 Darmstadt, Germany
[3] Bioengineering AG, 8636 Wald, Switzerland

Abstract This study focuses on the enhancement of oxygen transfer in aerobic fermentation processes through the use of the reactor headspace pressure as a process variable. Our investigation was performed using an example 5 m^3 fermentor, and by applying the mass transfer (sorption) characteristics obtained from measurements with *Pseudomonas putida* CA-3 in a mineral medium. By applying reactor pressures up to 11 bar (10 bar overpressure)

the oxygen transfer capacities of stirred tank reactors can theoretically be increased to values above 1 kmol m^{-3} h^{-1}, although the problem of heat removal limits that value to levels of 0.7 kmol m^{-3} h^{-1}. However, this is still sufficient for the oxygenation of most aerobic fermentation processes, even at very high cell densities. Possible inhibition by the carbon dioxide partial pressure at elevated total pressures is discussed. It is shown that increasing reactor pressure enhances the energy efficiency, defined as the ratio of the oxygen transfer capacity to the total power consumption of the reactor system. The cost efficiency of the oxygen mass transfer, defined as the ratio of the oxygen transfer capacity to the overall cost of the system (overall purchase cost divided by a project lifetime of ten years, plus total energy cost) also increases with reactor pressure up to 5.6 bar.

Keywords Increased headspace pressure · Pressure fermentation · Process intensification · Heat transfer · Carbon dioxide inhibition · Energy efficiency · Cost efficiency

Abbreviations

A_{HE}	additional heat transfer area [m^2]
C	correlation parameter [–]
$C_{Compressor}$	specific purchase cost of the compressor [Euro h^{-1}]
$C_{Reactor}$	specific purchase cost of the reactor system [Euro h^{-1}]
CE_{OTC}	cost efficiency of the oxygen transfer [kmol $Euro^{-1}$]
c_p	specific heat of the cooling water [J kg^{-1} K^{-1}]
CTR	carbon dioxide transfer rate [kmol m^{-3} h^{-1}]
D	vessel diameter [m]
EE_{OTC}	energy efficiency of oxygen transfer [kmol kWh^{-1}]
H	unaerated liquid height [m]
He_{O2}	Henry-coefficient for oxygen [bar m^3 $kmol^{-1}$]
k_La	volumetric mass transfer coefficient [s^{-1}]
$\dot{m}_W$	mass flow rate of the cooling water [kg h^{-1}]
n	stirrer speed stirrer speed [min^{-1}]
OTC	oxygen transfer capacity [kmol m^{-3} h^{-1}]
OTR	oxygen transfer rate [kmol m^{-3} h^{-1}]
P_c	power consumption of the compressor [kW]
P_s	stirrer power input [kW]
pCO_2	carbon dioxide partial pressure [bar]
p_R	reactor pressure [bar]
Δp	pressure drop in the heat exchanger [bar]
$\dot{Q}$	total heat generation in the reactor [kW m^{-3}]
$\dot{Q}_{met}$	microbial heat generation [kW m^{-3}]
q_{IN}	standard specific gas flow rate of the inlet gas line [N m^3 m^{-3} min^{-1}]
RQ	respiratory quotient [–]
RC	running cost [Euro h^{-1}]
T	temperature [°C]
ΔT	temperature difference between the inlet and outlet of the heat exchanger [K]
ΔT_m	mean temperature gradient between reactor content and cooling water [K]
t_{Plife}	project life time [a]
u_G	superficial gas velocity [m s^{-1}]
UR	average annual utilisation ratio [–]
$\dot{V}_G$	gas flow rate under standard conditions [N m^3 min^{-1}]
V_L	liquid volume [m^3]
V_m	molar gas volume [N m^3 $kmol^{-1}$]
$Y_{Qmet/O2}$	yield coefficient of heat generation related to consumed oxygen [MJ $kmol^{-1}$]

v_1	specific volume [–]
y_i	mole fraction of compound i [kmol kmol^{-1}]
α	correlation parameter [–]
β	correlation parameter [–]
κ	isentropic exponent [–]
η_i	degree of efficiency of the device i [–]
ρ_G	density of compressed gas [kg m^{-3}]
ρ_W	density of cooling water [kg m^{-3}]

1 Introduction

It is still a challenging task in biochemical engineering to oxygenate aerobic fermentation processes sufficiently. Particularly in high density cultures, the oxygen demand by far outstrips the oxygen transfer capacity of conventional bioreactors such as stirred tanks or bubble columns [1], meaning that the dissolved oxygen concentration in the culture medium becomes limiting for microbial growth. This can have detrimental effects on aerobic fermentation processes [2]. In some processes only the growth and production rates diminish, reducing the productivity of the process. However, there are also processes where oxygen limitation has a much greater impact. For example, if the microorganisms are capable of anaerobic metabolism, the metabolic pathway can be shifted in an unfavourable direction [3]. This can result in the formation of by-products, and therefore in declined product yield.

In order to avoid oxygen limitation and anaerobic metabolism, high cell density cultures are often designed as fed-batch processes. This means that a growth restriction is imposed on the process, limiting the nutrients to being fed to the bioreactor one at a time [4]. Initially the cells can be cultivated exponentially using an exponential time schedule for the feeding rate of the limiting nutrient. After reaching the maximum oxygen transfer capacity of the reactor, the feeding rate must be kept constant. Therefore, at higher cell densities only relatively low specific growth rates are obtained and the fermentation time is considerably prolonged [1, 5]. In the case of the production of a protein, the prolonged fermentation time may lead to product losses due to decomposition from enhanced secretion of proteases [6, 7].

Much effort has been made to overcome such limitations by increasing the oxygen transfer capacities of bioreactors. Special aeration systems and aeration using oxygen-enriched air are the most commonly applied enhancements. Over the last decade, the use of oxygen vectors has gained increasing interest, at least in academic research [8, 9]. Among these methods, increased reactor pressure has also been successfully used to enhance the oxygen mass transfer capacity [10, 11]. Despite these promising possibilities, reactor pressure is currently rarely considered to be an important engineering parameter in industrial bioprocess development.

The objective of this study is to demonstrate the improvements in productivity, energy efficiency, and cost efficiency that may be gained by employing the reactor pressure as additional engineering parameter in stirred tank reactors. The financial benefit from using pressurised operation can only be evaluated by considering a specific production process in detail. In this study, an estimate of the benefits of elevated reactor pressure is made for the example of a stirred tank reactor of 5 m^3 working volume via some generally accepted assumptions and equations. A mass transfer (sorption) characteristic was used for these calculations, which was evaluated for a culture of *Pseudomonas putida CA-3* in a 50 L stirred tank reactor of 37 L working volume in mineral media. This estimate should serve to illustrate the effects encountered at elevated pressure.

2 Theory

2.1 Gas-Liquid Mass Transfer

The oxygen transfer rate *OTR* from the gas phase into the culture medium is described by the following equation:

$$OTR = k_L a \cdot \frac{(y_{O2} - y_L) \cdot p_R}{He_{O2}} \tag{1}$$

where $k_L a$ is the specific mass transfer coefficient, y_{O2} is the mole fraction of oxygen at the gas-liquid interface, y_L is the mole fraction of oxygen in the bulk of the culture medium, p_R is the total headspace pressure, and He_{O2} is the Henry coefficient for oxygen. The maximum oxygen transfer capacity *OTC* at a given $k_L a$ value is obtained when the dissolved oxygen concentration in the bulk of the culture medium is close to zero. If the gas phase and the liquid phase is completely mixed and Henry's law is applied, *OTC* can be expressed using Eq. 2.

$$OTC = k_L a \cdot \frac{y_{O2} \cdot p_R}{He_{O2}} \tag{2}$$

For aerated stirred tanks, the mass transfer correlations published so far are mostly of the form:

$$k_L a = C \cdot \left(\frac{P_S}{V_L}\right)^a \cdot u_G^\beta \tag{3}$$

where the superficial gas velocity is:

$$u_G = \frac{\dot{V}_G}{\frac{\pi}{4} D^2} \tag{4}$$

is the gas flow rate under standard conditions, and D is the diameter of the vessel. Equation 3 is generally called the mass transfer or sorption characteristic. In most cases Eq. 3 satisfactorily describes the influence of the specific power input P_S/V_L and the superficial gas velocity u_G on the k_La value, where the correlation parameters C, α and β are specific to a reactor with a given geometry and a given culture medium. Therefore, it is not possible to predict the k_La obtained in liquids of different physico-chemical properties due to different coalescence behaviours, bubble sizes, surface tensions and ionic strengths.

The effect of the reactor pressure on the specific mass transfer coefficient has been investigated by many authors [11–17]. However, the results reported for bubble columns and for aerated stirred tank reactors are inconsistent. Most of the studies conducted in bubble columns reported a pronounced effect of the reactor pressure on k_La [12–14] and this observation has been theoretically explained. According to mechanistically based models, a higher reactor pressure leads to smaller primary gas bubbles resulting in greater interfacial mass transfer area. Since in aerated stirred tank reactors the interfacial area is dominated by the stirrer power input and not by the diameter of the primary gas bubbles, these bubble column models fail to explain the effects that are sometimes observed of the reactor pressure on k_La in stirred tanks. Recently, Maier et al. [15] have shown that some of the contradicting results are artefacts resulting from the inappropriate methods used for the determination of k_La. Furthermore, it was shown that at constant superficial gas velocity the k_La values in a stirred tank reactor remain constant irrespective of pressure. Therefore, mass transfer (sorption) characteristics obtained at ambient pressure can also be used for designing pressurised stirred tank reactors at elevated pressures. By combining Eq. 2 and Eq. 3, the oxygen transfer capacity of a pressurised stirred tank reactor can be calculated as:

$$OTC = C \cdot \left(\frac{P_S}{V_L}\right)^{\alpha} \cdot u_G^{\beta} \cdot \left(\frac{y_{O2} \cdot p_R}{He_{O2}}\right) \tag{5}$$

Assuming a respiratory quotient of RQ=1, the oxygen and carbon dioxide mole fraction in the exhaust gas can be calculated from Eqs. 6 and 7, respectively.

$$y_{O2}^{OUT} = y_{O2}^{IN} - \frac{OTR \cdot V_m}{q_{IN}} \tag{6}$$

$$y_{CO2}^{OUT} = \frac{CTR \cdot V_m}{q_{IN}} - y_{CO2}^{IN} \tag{7}$$

The carbon dioxide partial pressure p_{CO2} in the reactor is calculated by Eq. 8.

$$p_{CO2} = y_{CO2}^{OUT} \cdot p_R \tag{8}$$

To calculate the oxygen transfer capacity from the mass transfer coefficient $k_L a$, the reactor pressure p_R, and the specific gas flow rate q_{IN}, Eqs. 2 and 6 can be rearranged into Eq. 9:

$$OTC = \frac{\frac{k_L a \cdot p_R}{He_{O2}} \cdot y_{O2}^{IN}}{1 + \frac{\frac{k_L a \cdot p_R}{He_{O2}} \cdot V_m}{q_{IN}}} \tag{9}$$

2.2 Heat Generation

The mechanical power input and the microbial metabolism dissipate a specific amount of heat to the culture medium. Based on a consideration of the Gibbs free energy (G), the microbial heat generation can be explained and quantified thermodynamically [18–20]. A reaction is only possible if the change in the Gibbs free energy (ΔG) is negative. Since the biosyntheses of proteins, membranes and other constituents from lower molecular compounds are endergonic processes, energy has to be delivered from elsewhere to carry out these reactions. Therefore, in chemotrophic organisms such reactions are coupled to catabolic reactions that are strongly exergonic. As a result, the ΔG of the overall growth procedure is negative. The change in the Gibbs free energy is caused by a change in enthalpy ΔH and a change in entropy ΔS, as shown in Eq. 10.

$$\Delta G = \Delta H - T\ \Delta S \tag{10}$$

The entropy ΔS produced via catabolic as well as biosynthetic reactions can be neglected in aerobic growth. Therefore, the ΔH that is dissipated to the culture broth (identical to the metabolic heat $\dot{Q}_{met}$) is almost completely represented by ΔH [19]. Since aerobic microorganisms gain energy mainly by the oxidation of carbon sources to carbon dioxide and water, the metabolic heat generation $\dot{Q}_{met}$ is closely related to the oxygen uptake of the microorganisms and, therefore, the oxygen transfer rate. Cooney et al. [21] published the following correlation to estimate the metabolic heat generation $\dot{Q}_{met}$:

$$\dot{Q}_{met} = Y_{\dot{Q}met/O2} \cdot OTR \tag{11}$$

Empirical values for the yield coefficient $Y_{\dot{Q}met/O2}$ are in the range of 450–470 MJ kmol^{-1} [18, 21]. By adding the specific power input to $\dot{Q}_{met}$, the total heat generation within the reactor $\dot{Q}$ can be calculated, following Eq. 12.

$$\dot{Q} = \frac{P_S}{V_L} + \dot{Q}_{met} \tag{12}$$

2.3 Energy Efficiency

The ratio between the oxygen transfer capacity and the total power consumption of a reactor is used for the evaluation of the energy efficiency of the oxygen mass transfer EE_{OTC} [22]. The total power consumption of a stirred tank reactor mainly consists of the stirrer power input, P_S, and the power consumption for the generation of pressurised air, P_C. Since a higher *OTR* leads to increased heat generation, the power requirement of the cooling water pump P_W of the stirred tank reactor must be taken into account. These three contributions to the total energy consumption are related to the reactor volume and the oxygen transfer capacity as specified in Eq. 13.

$$EE_{OTC} = \left(\frac{OTC}{\frac{P_S}{V_L} + \frac{P_C}{V_L} + \frac{P_W}{V_L}} \right) \tag{13}$$

where P_S/V_L is the specific power consumption of the stirrer, P_C/V_L is the specific power consumption of the gas compressor and P_W/V_L is the specific power consumption of the cooling water pump.

2.4 Cost Efficiency

To simplify the estimation of the cost efficiency CE_{OTC} of a designated reactor system operated at elevated pressure in comparison to a normal reactor at ambient pressure, only the reactor (including its specific configuration for the stirrer system and heat removal) and the compressor are taken into account. All of the other installation and peripheral devices, including the electrical measuring and control facilities, are assumed to be constant and are therefore not considered.

2.4.1 Reactor System

The specific purchase cost of the reactor system $C_{Reactor}$ can be regarded as the sum of the reactor cost (a function of the operating pressure), cost of the stirrer drive unit (a function of specific power input), and the cost of the heat exchanger (a function of the heat that has to be removed), divided by the project lifetime t_{Plife} (Eq. 14).

$$C_{Reactor} = \frac{f(p_R) + f\left(\frac{P_S}{V_L}\right) + f(\dot{Q})}{t_{Plife}} \tag{14}$$

2.4.2 Compressor

In this study the specific purchase cost of the compressor is defined as function of the gas flow rate $\dot{V}_G$, divided by the project lifetime (Eq. 15).

$$C_{\text{Compressor}} = \frac{f(\dot{V}_G)}{t_{\text{Plife}}} \tag{15}$$

The influence of pressure on compressor cost was not taken into account, as our survey revealed that for up to 10 bars of overpressure the same type of compressor can be used.

2.4.3 Running Cost

The running cost is defined as the volume specific cost of the power consumption of the stirrer, the compressor and the cooling water pump multiplied by the annual average utilisation ratio *UR* and the energy cost *EC*, as shown in Eq. 16.

$$RC = \left(\frac{P_S}{V_L} + \frac{P_C}{V_L} + \frac{P_W}{V_L}\right) \cdot UR \cdot EC \tag{16}$$

2.4.4 Cost Efficiency

The cost efficiency of the oxygen mass transfer can be calculated from the ratio of the oxygen transfer capacity to the sum of the specific purchase cost of the reactor system, the compressor and the running costs, using Eq. 17.

$$CE_{\text{OTC}} = \frac{OTC}{C_{\text{Reactor}} + C_{\text{Compressor}} + RC} \tag{17}$$

2.5 Power Consumption

To calculate the specific power consumptions of the stirrer P_S/V_L, the compressor P_C/V_L, and the cooling water pump P_W/V_L, the gross power input is considered. Mechanical and electrical losses are taken into account by the respective degrees of efficiency. The specific power consumption of the compressor P_C/V_L can be calculated assuming that the compression of the gas phase takes place in a single stage and under isentropic conditions according to Eq. 18 [23].

$$\frac{P_C}{V_L} = \frac{\dot{V}_G}{\eta_C p V_L} \frac{\kappa}{\kappa - 1} p_1 \cdot \nu_1 \left[\left(\frac{p_2}{p_1} \right)^{\frac{\kappa-1}{\kappa}} - 1 \right] \tag{18}$$

For the compression of gases like nitrogen and oxygen the isentropic exponent κ is about 1.4. The mechanical and electrical losses of the compressor are represented by the degree of efficiency of the compressor η_C.

The flow rate $\dot{m}_W$ of the water that has to be pumped through the heat exchanger to remove the dissipated heat $\dot{Q}$ from the reactor is calculated according to Eq. 19.

$$\dot{m}_W = \frac{\dot{Q}}{C_P \cdot \Delta T} \tag{19}$$

Therefore, the power consumption of the cooling water pump can be estimated by considering the water flow rate $\dot{m}_W$, the energy efficiency of the water pump η_W and the pressure drop Δp in the heat exchanger via Eq. 20 [24].

$$P_W = \frac{\dot{m}_W}{\eta_W \cdot \rho_W} \Delta p \tag{20}$$

3 Materials and Methods

The mass transfer experiments with a culture of *Pseudomonas putida* CA-3 were conducted in a stirred tank bioreactor (LP 351, Bioengineering AG, Wald, Switzerland), especially designed for headspace pressures up to 11 bar. A sketch of the experimental set-up is given in Fig. 1.

The bioreactor is a baffled cylindrical tank with a total volume of 0.05 m^3, a working volume of 0.037 m^3, and a diameter of 0.3 m. The ratio between the unaerated liquid height H and the diameter of the vessel D is 1.75. For agitation the bioreactor is equipped with three six-blade standard Rushton turbines, each with a diameter of 0.12 m. The power consumption of the stirrer is determined by measuring the torque of the stirrer shaft with a hollow shaft torque measurement system (Bioengineering AG, Wald, Switzerland). This design allows the direct measurement of power input into the liquid, avoiding errors caused by friction losses in the bearings and seals. The gas mass flow rate into the bioreactor $\dot{V}_G$ is regulated by a mass flow controller (Bronkhorst F-203AI, The Netherlands). The oxygen concentration of the exhaust gas $y_{O_2}^{OUT}$ was measured by a paramagnetic oxygen analyser (Magos 3, Hartmann und Braun, Germany), and the carbon dioxide concentration of the exhaust gas $y_{O_2}^{OUT}$ was measured by an infrared analyser (UNOR 6 N, Maihak, Germany). The headspace pressure is determined by a pressure probe and controlled by a regulating valve in the exhaust gas line. The dissolved oxygen concentration was measured by a polarographic oxygen probe (Broadley James, USA) mounted at approximately a third of the liquid's height.

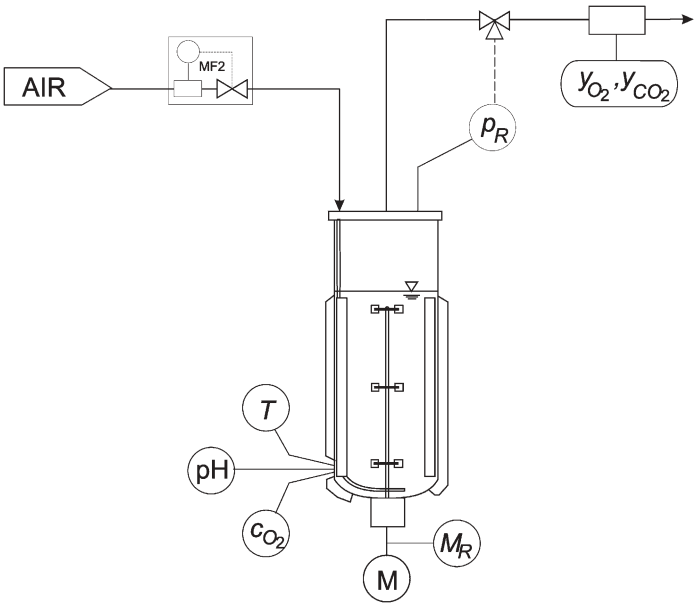

Fig. 1 Experimental set-up

The *OTR* was calculated using an oxygen mass balance between the in- and out-flowing gas, as specified in Eq. 21.

$$OTR = \frac{q_{\mathrm{IN}}}{V_{\mathrm{m}}} \cdot \left[y_{\mathrm{O2}}^{\mathrm{IN}} - \left(\frac{1 - y_{\mathrm{O2}}^{\mathrm{IN}} - y_{\mathrm{CO2}}^{\mathrm{IN}}}{1 - y_{\mathrm{O2}}^{\mathrm{OUT}} - y_{\mathrm{VCO2}}^{\mathrm{OUT}}} \right) \cdot y_{\mathrm{O2}}^{\mathrm{OUT}} \right] \tag{21}$$

where the specific gas flow rate of the inlet gas stream is

$$q_{\mathrm{IN}} = \frac{\dot{V}_{\mathrm{G}}}{V_{\mathrm{L}}} \tag{22}$$

V_{m} is the molar gas volume and V_{L} is the working volume.

Equation 23 was used for the calculation of $k_{\mathrm{L}}a$, assuming a completely mixed gas phase.

$$k_{\mathrm{L}}a = \frac{OTR \cdot He_{\mathrm{O2}}}{(y_{\mathrm{O2}}^{\mathrm{OUT}} - y_{\mathrm{L}}) \cdot p_{\mathrm{R}}} \tag{23}$$

The microorganism *Pseudomonas putida* CA-3 obtained from Dr. W. Duetz, Department of Biotechnology, ETH Zürich, Switzerland was used in fermentations. This microorganism was grown on a defined culture medium with glucose as the sole carbon source. The composition of the culture medium was as follows: glucose 30.0 g L^{-1}, $(NH_4)_2SO_4$ 10.24 g L^{-1}, nitrilotriacetic acid 0.77 g L^{-1}, $MgSO_4 \cdot 7H_2O$ 0.31 g L^{-1}, $CaCl_2$ $2H_2O$ 2.94 mg L^{-1}, $ZnSO_4$ $7H_2O$

7.2 mg L^{-1}, $FeSO_4$ H_2O 39.9 mg L^{-1}, $CuSO_4$ $5H_2O$ 1.2 mg L^{-1}, $CoSO_4$ H_2O 2.8 mg L^{-1}, $MnSO_4$ H_2O 8.5 mg L^{-1}, H_3BO_3 0.31 mg L^{-1}. The Henry coefficient for oxygen for the culture medium was ~830 bar m^3 $kmol^{-1}$. During cultivation the temperature was adjusted to 30 °C and the pH was maintained constant at 7.0 by titration with 0.1 M NH_4OH.

4 Results

In this study, the mass transfer (sorption) characteristic for a culture of *Pseudomonos putida* CA-3 was evaluated in a 50 L stirred tank reactor filled with 37 L of mineral medium. These results were used to theoretically calculate the performance of a geometrically similar reactor of 5 m^3 working volume. This reactor volume was chosen as an example of a typical production scale for heterologous protein expression. The resulting tank diameter and unaerated liquid height of this hypothetical reactor are 1.54 m and 2.68 m, respectively. Without additional heat exchangers the effective heat transfer area is ~10 m^2.

4.1 Gas-Liquid Mass Transfer Characterisation

Values of k_La for fermentations involving the microorganism *Pseudomonas putida* CA-3 were determined for different specific power inputs P_S/V_L in order to obtain the gas-liquid sorption characteristic in the 50 L reactor (Fig. 2). Since it was not our aim to perform an extensive gas-liquid mass transfer characterisation, only one aeration rate was used. More detailed investigations using sodium sulfite as the chemical model system in the same reactor are described in Maier et al. [15]. The log-log plot of our experiments with *Pseudomonas putida* CA-3 shows that the measured specific mass transfer coefficients increase according to the specific power input P_S/V_L to the power of 0.74. By assuming a correlation parameter β of 0.42 [25], and using the results of Fig. 2, the mass transfer correlation can be expressed as:

$$k_La = 0.32 \cdot \left(\frac{P_S}{V_L}\right)^{0.74} \cdot u_G^{0.42} \tag{24}$$

The measured k_La values are typical of microbial culture media, and the obtained correlation is similar to the results found by other authors [25, 26]. The values found in the literature for the correlation parameter α vary over a wide range, from 0.5 to 0.9. The published values for the correlation parameter β have a narrower range, from 0.3 to 0.5. The differences are due to variations in physico-chemical properties (ionic strength, viscosity and surface tension) between the culture broths.

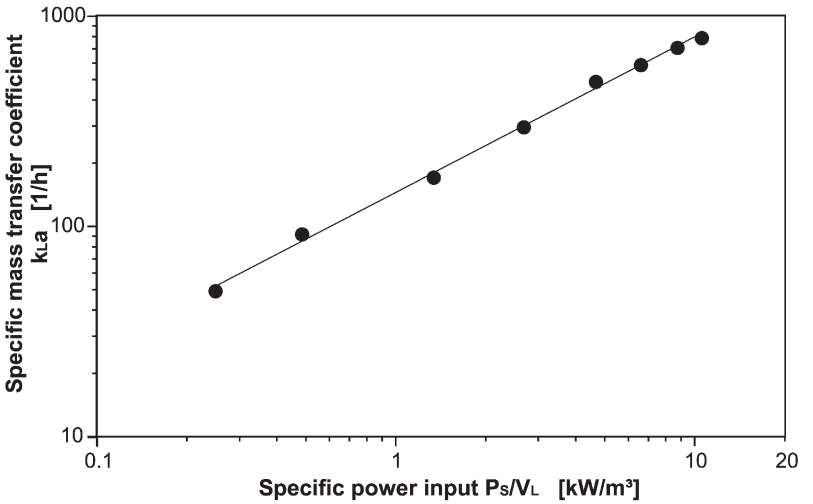

Fig. 2 Specific mass transfer coefficient of a 50 L bioreactor at different specific power inputs at a constant superficial gas velocity of 0.448 m min^{-1} and a reactor pressure of 1.25 bar. A culture of *Pseudomonas putida* CA-3 was grown in mineral medium as the biological model system

4.2 Calculated Oxygen Transfer Capacity

The mass transfer (sorption) characteristic presented above can be used for the theoretical estimate of the oxygen transfer capacity of the geometrically similar reactor system of 5 m^3 working volume under varying operating conditions. Calculations have been carried out using Eqs. 3, 4 and 9, respectively. In the following, the resulting oxygen transfer capacities for two different operation modes are discussed.

Operational mode 1: The standard gas flow rate $\dot{V}_G$ is held constant at 5 N m^3 min^{-1} (1 N m^3 m^{-3} min^{-1}). Hence, the superficial gas velocity decreases from a value of 2.682 m min^{-1} at a reactor pressure of 1 bar to a value of 0.246 m min^{-1} at a reactor pressure of 11 bar.

Operational mode 2: The standard gas flow rate is increased in proportion to the reactor pressure, starting from a value of $\dot{V}_G$=2.5 N m^3 min^{-1} (0.5 N m^3 m^{-3} min^{-1}) at a reactor pressure of 1 bar. Hence, the superficial gas velocity has a constant value of 1.344 m min^{-1} irrespective of the actual reactor pressure. The standard flow rate increases to a maximum value of 27.5 N m^3 min^{-1} (5.5 N m^3 m^{-3} min^{-1}) at 11 bar.

In Fig. 3, the influence of reactor pressure and specific power input on the oxygen transfer capacity is illustrated as a contour plot. Additionally, the theoretical carbon dioxide partial pressures in the gas phase of the reactor are depicted as areas with different grey shades (right y-axis). These carbon dioxide

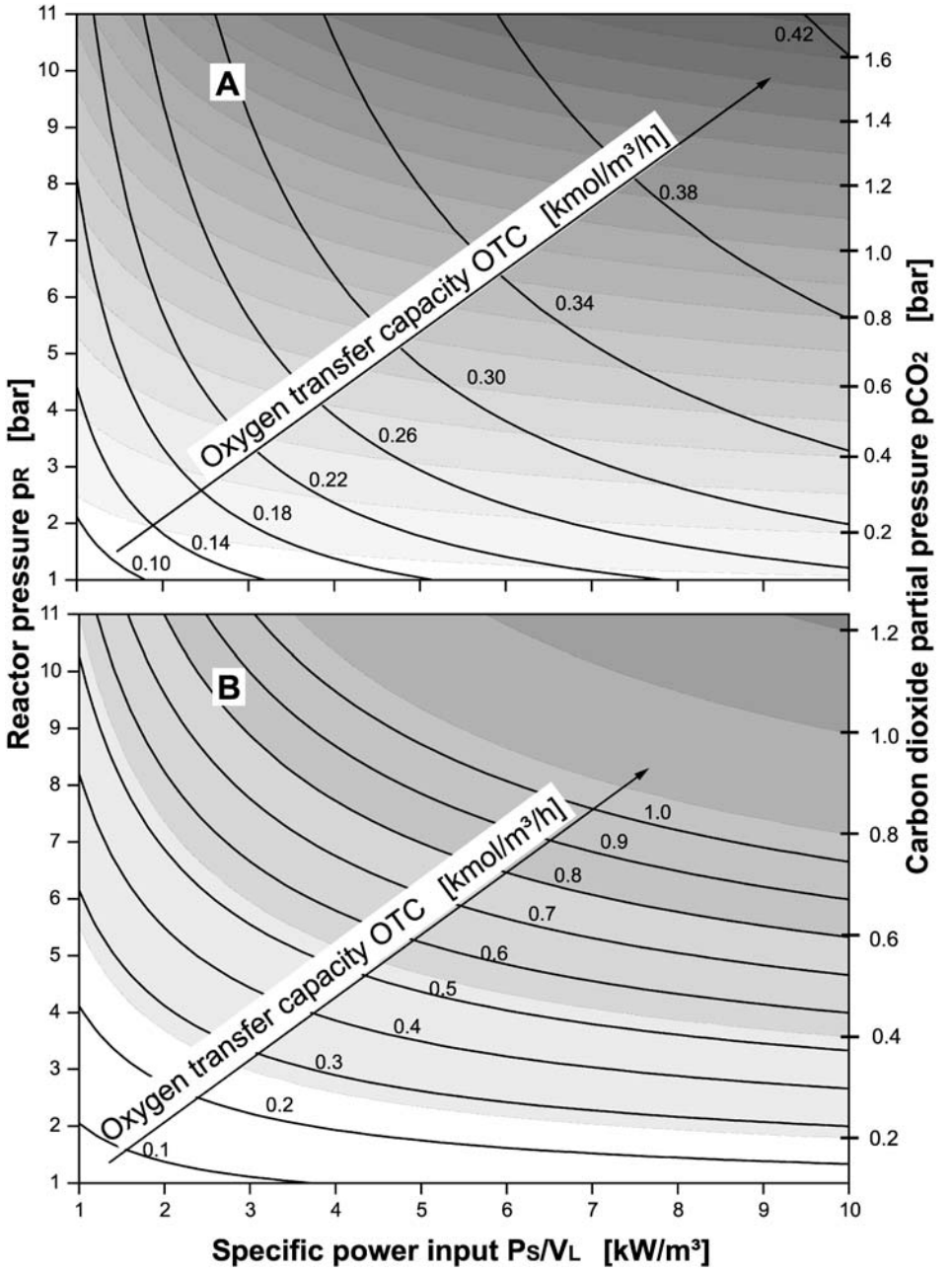

Fig. 3A–B Calculated oxygen transfer capacity (contour plot) and corresponding carbon dioxide partial pressure (right y-axis) for a 5 m^3 bioreactor (**A**) at a constant specific gas flow rate of 1 N m^3 m^{-3} min^{-1} (operational mode 1) and (**B**) at a constant superficial gas velocity of 1.344 m min^{-1} (operational mode 2). Operational mode 2 corresponds to a specific gas flow rate of 0.5 N m^3 m^{-3} min^{-1} at a reactor pressure of 1 bar

pressures may help to estimate the possible inhibition levels, depending on the carbon dioxide sensitivity of the investigated microorganisms. For example, at a carbon dioxide partial pressure of 0.2 bar, the *Pseudomonas putida* CA-3 strain used to obtain the sorption characteristic has a growth rate of only 60% of the growth rate at low carbon dioxide partial pressure (data not shown).

As shown in Fig. 3A for operation mode 1, the oxygen transfer capacity increases with increasing specific power input P_S/V_L and increasing reactor pressure p_R. At the highest possible specific power input and the highest reactor pressure an oxygen transfer capacity above 0.42 kmol m^{-3} h^{-1} is obtained. In this operational mode the superficial gas velocity and, as a consequence, the specific mass transfer coefficient decreases with increasing reactor pressure, while carbon dioxide partial pressure rises to a theoretical maximum of 1.74 bar. This value exceeds by far the carbon dioxide levels of conventional production scale fermentors, even at very high capacities of around 100–200 m^3. Such large fermentors lead to high hydrostatic total pressure values at the bottom, of about 1–1.5 bar.

As shown in Fig. 3B for operational mode 2, the oxygen transfer capacity increases with P_S/V_L and rising p_R. A maximal oxygen transfer capacity greater than 1 kmol m^{-3} h^{-1} is obtained, which is substantial higher than for operational mode 1. For high density cultures of commonly applied microorganisms (such as *S. cerevisiae* or *E. coli*), which reach biomass levels of ~130–180 kg m^{-3} cell dry weight [1], an *OTC* of 1 kmol m^{-3} h^{-1} should be more than sufficient. Oxygen transfer capacities higher than 1 kmol m^{-3} h^{-1} are not depicted in this and the following figures, since these levels are far beyond our experimental results and are not sufficiently covered. Due to higher gas flow rates than in operational mode 1, the carbon dioxide partial pressure rises to lower values. Compared to the carbon dioxide partial pressure corresponding to the maximum *OTC* achieved in operational mode 1, the carbon dioxide partial pressure only reaches values between 0.3 and 0.4 bar. These are values that most microorganisms that are not sensitive to carbon dioxide should be able to tolerate. However, the carbon dioxide sensitivity of the microorganisms studied should be analysed separately.

4.3 Heat Generation

The generation of heat was calculated using Eq. 12 for operational modes 1 and 2, using a metabolic yield coefficient $Y_{Qmet/O2}$ of 470 MJ $kmol^{-1}$ [18]. Figure 4 shows the results. The highest *OTC* in operational mode 1 results in a maximum heat generation of 65.4 kW m^{-3}. At an *OTC* of 1 kmol m^{-3} h^{-1} in operational mode 2, the heat generation reaches 135–140 kW m^{-3}. Such tremendous heat generation can only be removed by introducing additional heat exchangers into the reactor. In this study this additional heat exchanger is

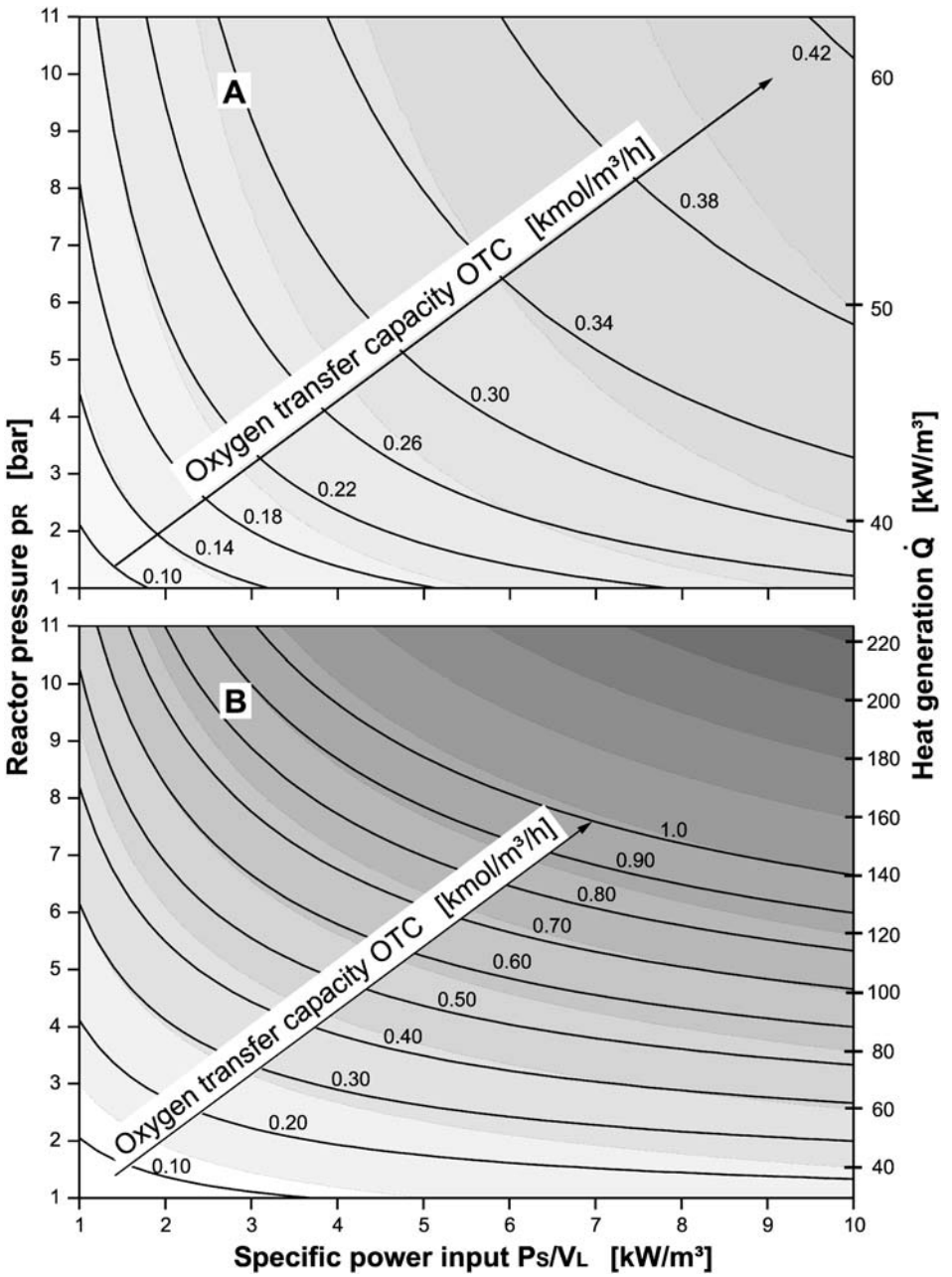

Fig. 4A–B Calculated oxygen transfer capacity (contour plot) and heat generation (right y-axis) for a 5 m^3 bioreactor (**A**) at a constant specific gas flow rate of 1 N m^3 m^{-3} min^{-1} (operational mode 1) and (**B**) at a constant superficial gas velocity of 1.344 m min^{-1} (operational mode 2)

simply considered as an additional heat transfer area A_{HE}, which is estimated using Eq. 25.

$$A_{HE} = \frac{\dot{O}}{k \cdot \Delta T_m} \tag{25}$$

Assuming a constant heat transfer coefficient k of 610 W m^{-2} K^{-1} and a constant mean temperature gradient ΔT_m of 10 K, the removal of 140 kW m^{-3} of heat roughly corresponds to 105 m^2 of additional heat transfer area. To estimate whether such a heat transfer area can be realised practically or not, the application of parallel metal tube bundles with outer tube diameters of 0.035 m was considered. A geometric estimate uncovers that a maximum heat transfer area of 75 m^2 is attainable (data not shown). Hence, only around 94 kW m^{-3} of heat could be removed, corresponding to an *OTC* of around 0.7 kmol m^{-3} h^{-1}. Therefore, heat removal is a limiting parameter in pressure fermentation and must be considered at a very early stage of plant design. Both operational modes clearly show that heat dissipation can be slightly decreased by using reactor pressure instead of specific power input to achieve a particular *OTC*. It may also be possible to apply a larger driving temperature gradient ΔT_m than 10 K to achieve sufficient heat removal. However, this strategy will require a refrigeration unit, resulting in additional costs.

4.4 Energy Efficiency

The energy efficiency of the oxygen transfer is now discussed for the aforementioned operational modes. The value for η_S was averaged from Oosterhuis [27], giving 0.65. The value for η_C, 0.7, was derived from technical data sheets for oil free screw type compressors from Atlas Copco Kompressoren- und Drucklufttechnik GmbH, Germany. The value for η_W of 0.7 was taken from Hölz [24]. Calculated values of EE_{OTC} are presented in Fig. 5. Maximum energy efficiencies of up to 0.023 kmol kWh^{-1} (operational mode 1) can be achieved at a specific power input of ~3 kW m^{-3} and with reactor pressures of up to 11 bar. Remarkably, energy efficiency decreases with increasing specific power input. The maximum value of energy efficiency for a pressure of 5.4 bar and a specific power input of 2.8 kW m^{-3} is 1.7 fold higher than at ambient pressure at the same *OTC* of 0.24 kmol m^{-3} h^{-1}.

In operational mode 2, an optimum relation between the specific power input and the reactor pressure leads to values of energy efficiency of up to 0.025 kmol kWh^{-1}. To achieve an energy efficient operation, the reactor pressure should be increased in proportion to the specific power input. If a pressure is increased more rapidly, the energy efficiency decreases. This is due to the fact that the gas flow rate is also increased with increasing pressure in this operational mode. These elevated gas flow rates are the reason for the decrease in the energy efficiency. However, pressure fermentation enables higher energy efficiencies than for non-pressurised conditions.

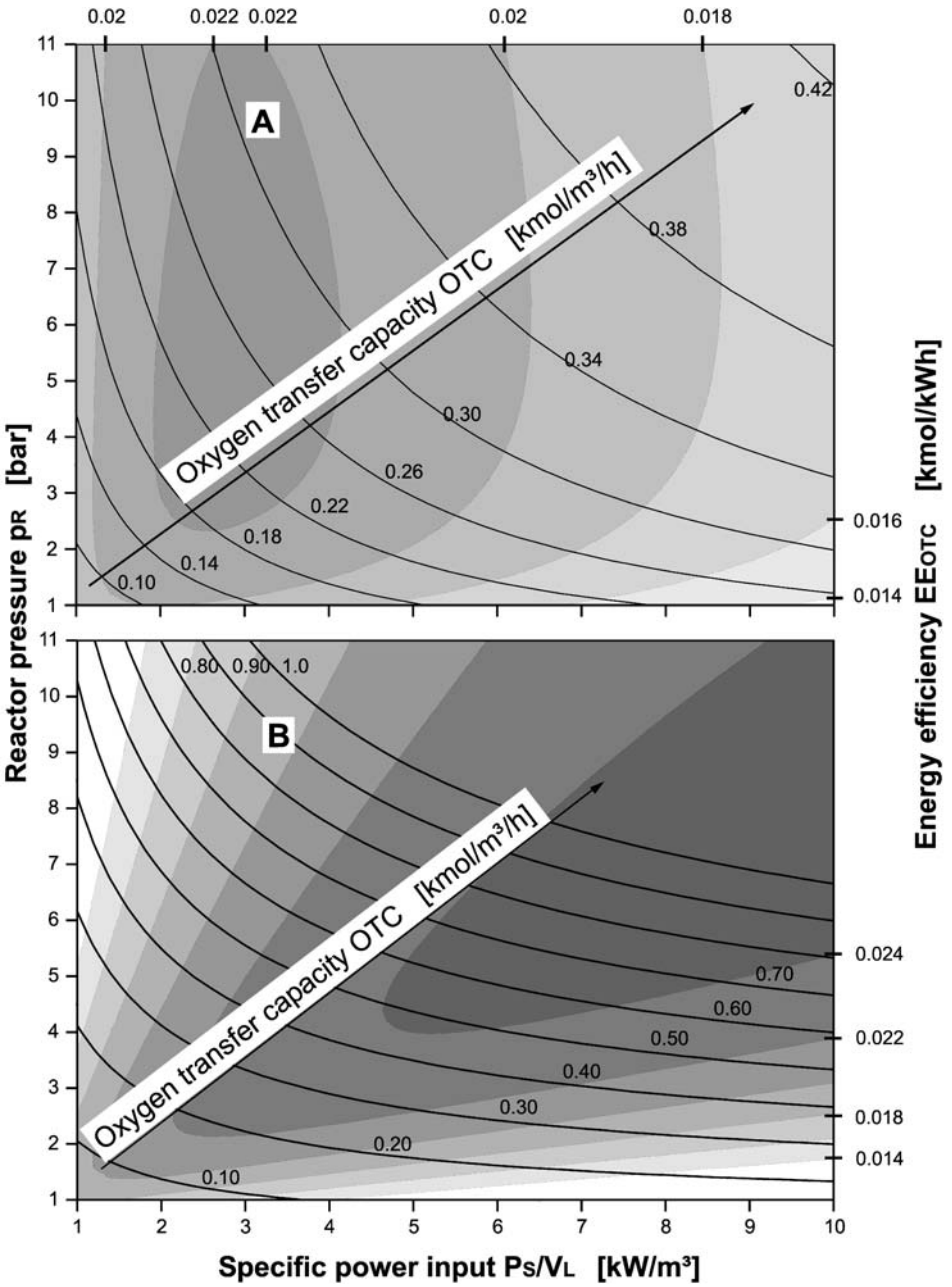

Fig. 5A–B Calculated oxygen transfer capacity (contour plot) and energy efficiency of the oxygen mass transfer (right y-axis) for a 5 m^3 bioreactor (**A**) at a constant specific gas flow rate of 1 N m^3 m^{-3} min^{-1} (operational mode 1) and (**B**) at a constant superficial gas velocity of 1.344 m min^{-1} (operational mode 2)

4.5 Cost Efficiency

For the estimate of the specific purchase cost, a project lifetime of ten years was used.

4.5.1 Reactor System

The purchase cost of the reactor and drive unit of a stirred tank reactor depends on the reactor pressure and the specific power input of the stirrer. For high heat generation at higher *OTC* values the additional costs of heat removal has to be considered. This additional heat transfer area was calculated assuming a constant heat transfer coefficient k of 610 W m^{-2} K^{-1} and a constant mean temperature gradient ΔT_m of 10 K using Eq. 25. The following equation (Eq. 26) for the calculation of the specific purchase cost of a reactor system with a working volume of 5 m^3 was derived from data provided by Bioengineering AG (Wald, Switzerland). This empirical equation takes into account the basic cost of the reactor system and cost contributions stemming from operating pressure, required power input and heat transfer area.

$$C_{\text{Reactor}} = \frac{\left(51944 + 8620 \cdot \ln\left(p_R\right) + 8297 \cdot \ln\left(\frac{P_S}{V_L}\right) + 6000 \cdot A_{HE}\right)}{10 \cdot 8760} \left[\frac{\text{Euro}}{h}\right] \quad (26)$$

(for p_R=1 to 11 bar, P_S/V_L=1 to 10 kW m^{-3}, A_{HE}=0 to 75 m^2).

4.5.2 Compressor

Oil free screw type compressors were considered for the compressor. Since this type of compressor is usually designed to have a working overpressure of 10 bar, the dependence of pressure on compressor cost was neglected in our estimation. Considering a pressure loss from the piping and the aeration system of the reactor of approximately 2 bar, the following calculations should be valid for calculated reactor pressures up to at least 9 bar. Purchase costs of compressors with flow rates of 2.2–28.8 N m^{-3} min^{-1} were kindly calculated and provided by Atlas Copco Kompressoren und Drucklufttechnik GmbH, Germany, according to Eq. 27.

$$C_{\text{Compressor}} = \frac{\left(3524 \cdot \dot{V}_G + 13307\right)}{10 \cdot 8760} \left[\frac{\text{Euro}}{h}\right] \quad (27)$$

(for $\dot{V}_G$=2.2 to 28.8 N m^3 min^{-1}).

4.5.3 Running Costs

An energy cost of 0.15 Euro kWh^{-1} [28] and an annual average utilisation ratio of 0.7 were chosen for our calculations. Compressor power was calculated from Eq. 18 and the power of the cooling water pump from Eq. 20, assuming a pressure drop of 4 bar. The running cost can then be calculated from Eq. 16.

In Fig. 6 the cost efficiency, as estimated using Eq. 17, is shown. In operational mode 1, cost efficiencies can be increased by applying increased headspace pressures. The highest cost efficiencies of up to 0.068 kmol $Euro^{-1}$ are achieved at pressures of 9–11 bar, a specific power input of 2.8 kW m^{-3}, and an *OTC* of 0.3–0.32 kmol m^{-3} h^{-1}. This cost efficiencies are 1.13 fold higher compared to the maximum values of 0.06 kmol $Euro^{-1}$ found at ambient pressure for a specific power input of 2.4 kW m^{-3} and an *OTC* of 0.11 kmol m^{-3} h^{-1}.

In operational mode 2, the cost efficiency reaches values close to 0.076 kmol $Euro^{-1}$ at an *OTC* of 1 kmol m^{-3} h^{-1}. Higher *OTC* values are unrealistic and were not considered in our estimation. This cost efficiency is 1.4-fold higher than the maximum value (0.054 kmol $Euro^{-1}$) obtained at ambient pressure and a specific power input of 2.4 kW m^{-3}.

To determine the maximum cost efficiency at a certain *OTC*, the superficial gas velocity (0–4.02 m min^{-1}), the specific power input (0–10 kW m^{-3}), and the reactor pressure (1–11 bar) were all optimised using Microsoft Excel Solver. Boundary conditions were set for the superficial gas velocity instead of the standard specific gas flow rate, because the first parameter must be limited to prevent possible excessive foam formation. The chosen maximum superficial gas velocity of 4.02 m min^{-1} corresponds to a standard specific gas flow rate of 1.5 N m^3 m^{-3} min^{-1} at ambient pressure. This may be the maximum value that can be realised practically in a fermentor of 5 m^3 working volume. The results of our optimisation as function of the oxygen transfer capacity are presented in Fig. 7.

For non constrained conditions (Fig. 7A), the cost efficiency strongly increases at low *OTC*, and subsequently levels off at an *OTC* of 0.075 kmol m^{-3} h^{-1}. A maximum cost efficiency of 0.067 kmol $Euro^{-1}$ at an *OTC* of 1 kmol m^{-3} h^{-1} is reached. Up to an *OTC* of 0.075 kmol m^{-3} h^{-1} no additional heat transfer area is necessary. Above this value the increase in cost efficiency is impeded by the additional effort needed to remove heat.

Energy efficiency has a very similar trend to cost efficiency. At an oxygen transfer capacity of ~0.1 kmol m^{-3} h^{-1} the increase in operating pressure is most pronounced. Remarkably, reactor pressure is only increased to a maximum value of 4.8 bar. At an *OTC* larger than 0.2–0.3 kmol m^{-3} h^{-1} the pressure even slightly decreases. Specific power input and specific gas flow rate linearly increase up to values of 9.1 kW m^{-3} and about 4.1 N m^3 m^{-3} min^{-1}, respectively.

Carbon dioxide partial pressures of up to only 0.43 bar are observed, which is less than obtained for the conditions presented in Fig. 3. Even if carbon dioxide partial pressures of up to 0.43 bar appear in a bioreactor, microorgan-

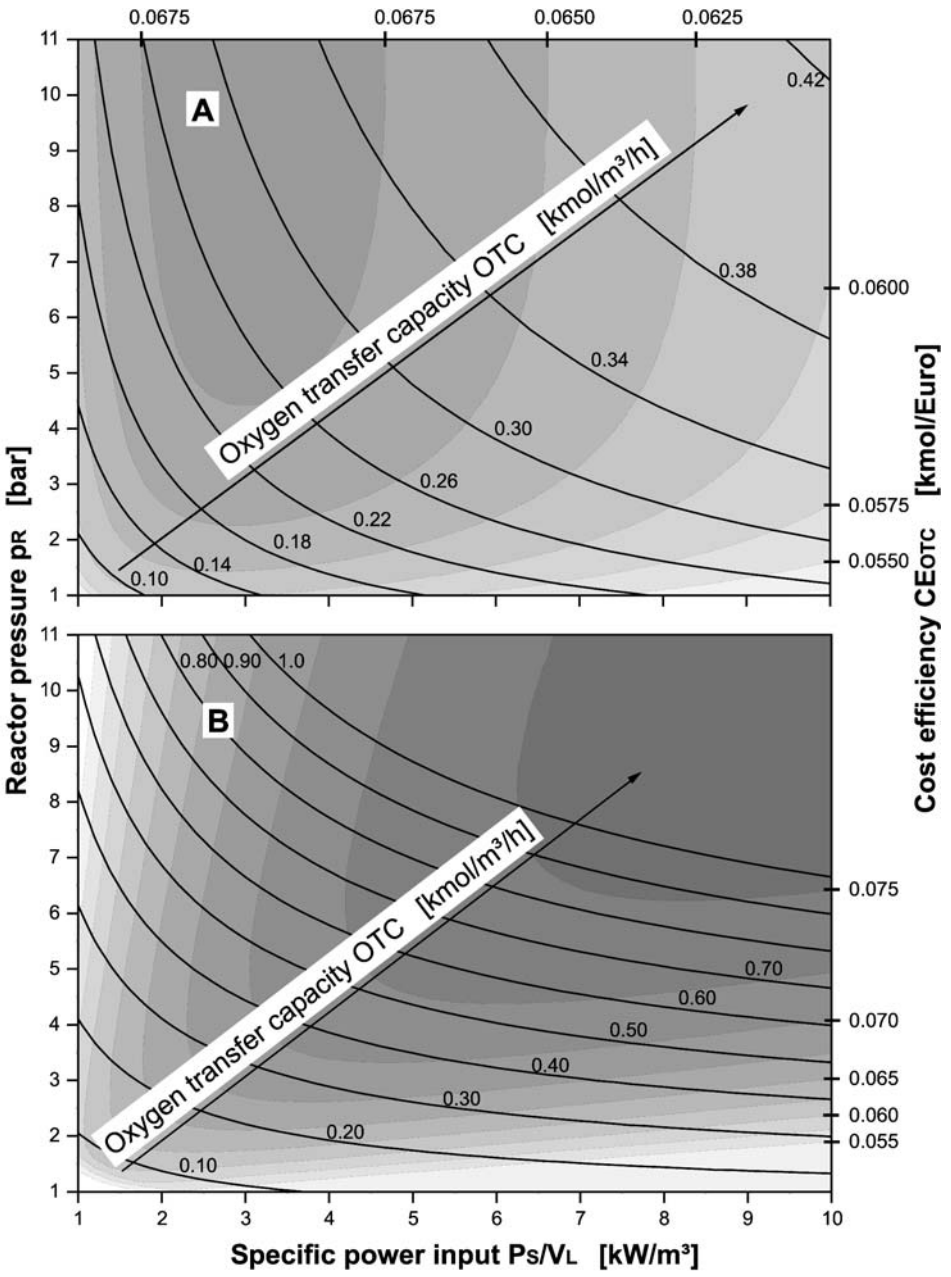

Fig. 6A–B Calculated oxygen transfer capacity (contour plot) and cost efficiency (right y-axis) for a 5 m^3 bioreactor (**A**) at a constant specific gas flow rate of 1 N m^3 m^{-3} min^{-1} (operational mode 1) and (**B**) at a constant superficial gas velocity of 1.344 m min^{-1} (operational mode 2)

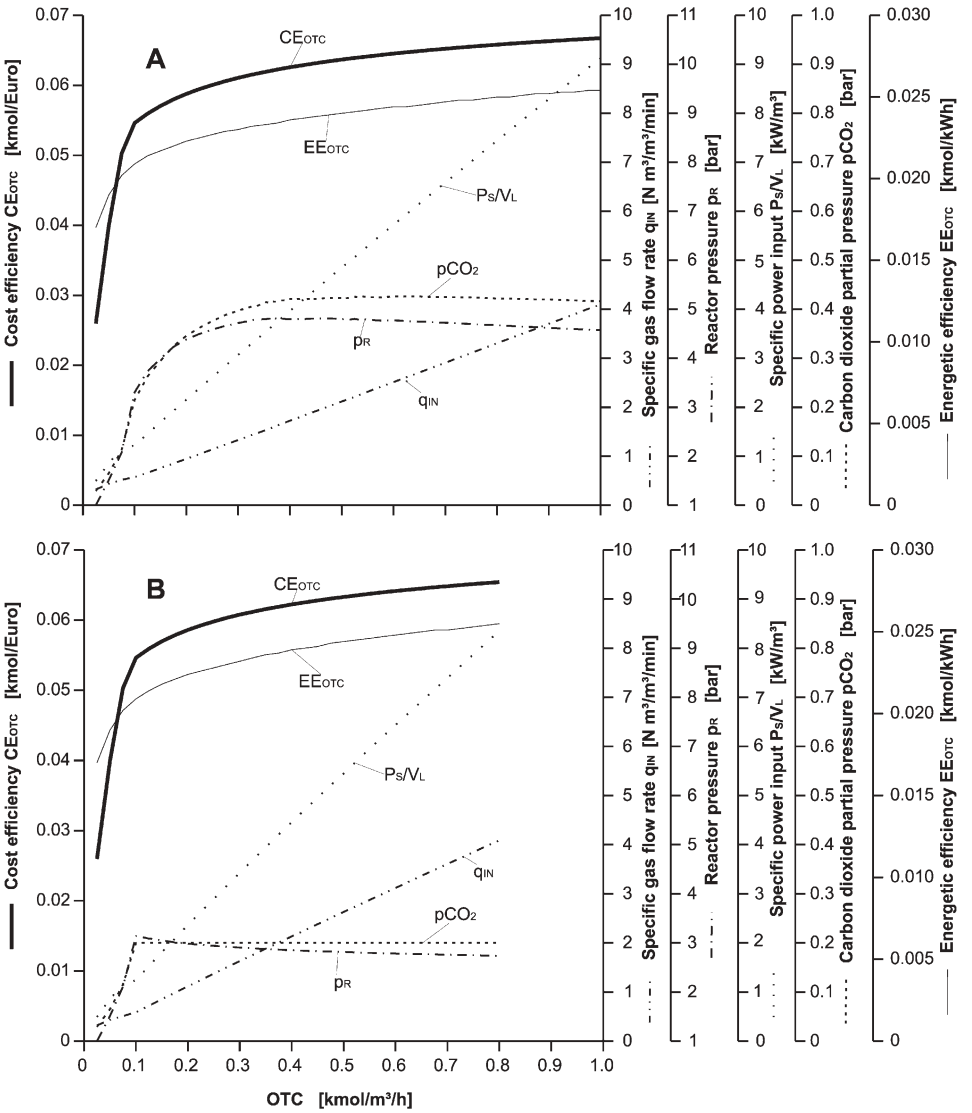

Fig. 7A–B Maximised cost efficiency and related process parameters (**A**) for unconstrained conditions and (**B**) for the boundary condition that the carbon dioxide partial pressure should not exceed 0.2 bar. A maximum superficial gas velocity of 4.02 m min^{-1} was chosen as a second boundary condition. This corresponds to a standard specific gas flow rate of 1.5 N m^3 m^{-3} min^{-1} at ambient pressure

isms such as *Corynebacterium glutamicum* are still able to grow at specific growth rates of more than 0.3 h^{-1} (own unpublished results). If microorganisms are cultured that are relatively sensitive to carbon dioxide, the partial pressure of this gas must be limited to specific levels. In Fig. 7B a calculation is shown, where a maximum carbon dioxide partial pressure of 0.2 bar was chosen as a boundary condition. Under this condition, maximal oxygen transfer capacities of 0.8 kmol m^{-3} h^{-1} are obtained. Maximum admissible carbon dioxide partial pressures lower than 0.2 bar would reduce the maximum obtainable *OTC* to even lower values. The reason for this upper limit in the *OTC* is the fact that the boundary condition of the maximum superficial gas velocity in the reactor (4.02 m min^{-1}) is reached (data not shown).

For the conditions presented in Fig. 7B, the pressure reaches its maximum value at an *OTC* of about 0.1 kmol m^{-3} h^{-1}, as soon as the maximum admissible carbon dioxide partial pressure is reached. From this point, the stirrer power and specific gas flow rate increases with a higher slope than for the unconstrained case (Fig. 7A). The cost efficiency in the constrained case is only slightly smaller than in the unconstrained case.

In the present example the overall specific purchase cost dominates the running costs, especially at high oxygen transfer capacities. This is mainly due to the strong influence of the cost of heat removal (data not shown). The specific purchase and energy costs of the compressor are larger (1.5–2-fold, increasing at higher *OTC*) than the corresponding costs of the stirrer system. The energy cost of the cooling water pump is relatively small (less than 5 %).

5 Conclusions

This study illustrates that the reactor pressure is an important operational parameter of a bioreactor. The oxygen transfer capacity, the energy efficiency, and the cost efficiency of oxygen transfer can be greatly enhanced by employing elevated reactor pressures. However, if reactor pressures up to 11 bar are applied, carbon dioxide partial pressures that are too high may occur. These can have detrimental effects on the growth and production kinetics of the microorganism used. The carbon dioxide sensitivity of the microorganisms should be investigated case by case. The effect can be reduced by an appropriate adjustment in the relevant process parameters. Increasing the specific aeration rate is a suitable measure. An upper limit may be imposed by uncontrollable foam formation inside the reactor at excessive superficial gas velocities. Heat generation within the vessel increases proportionally with oxygen transfer rate and can only be handled by including an additional heat exchanger. However, heat generation can be reduced slightly by using reactor pressure instead of specific power input to achieve a certain *OTC*.

Our estimate was made for the example of a specific microbial system, a culture of *Pseudomonas putida* CA-3 in a mineral medium. If other microbial

systems are employed different sorption characteristics may result. This will lead to different absolute figures than those presented in this study. A different working volume of the bioreactor investigated and different cost parameters will also quantitatively change the results. However, it is believed that the general message of this contribution will still be valid.

Acknowledgement The authors gratefully acknowledge the essential cost information provided by Atlas Copco Kompressoren- und Drucklufttechnik GmbH (Essen, Germany) for the economical evaluation.

References

1. Riesenberg D, Guthke R (1999) Appl Microbiol Biotechnol 51:422
2. Büchs J (2001) Biochem Eng J 7:91
3. Futatsugi M, Ogawa T, Fukuda H (1993) J Ferment Bioeng 76:419
4. Larsson G, Jorgensen SB, Pons MN, Sonnleitner B, Tijsterman A, Titchener-Hooker N (1997) J Biotechnol 59:3
5. van Hoek P, de Hulster E, van Dijken JP, Pronk JT (2000) Biotechnol Bioeng 68:517
6. Ramchuran SO, Nordberg Karlsson E, Velut S, de Maré L, Hagander P, Holst O (2002) Appl Microbiol Biot 60:408
7. Rozkov A (2001) PhD Thesis, Royal Institute of Technology, Stockholm, Sweden
8. Elibol M, Mavituna F (1999) Biochem Eng J 3:1
9. Vanede CJ, Vanhouten R, Beenackers AACM (1995) Chem Eng Sci 50:2911
10. May OE, Herrick, HT, Moyer, AJ, Wells, PA (1934) Ind Eng Chem 26:575
11. Yang JD, Wang NS (1992) Biotechnol Prog 8:244
12. Kojima H, Sawai J, Suzuki H (1997) Chem Eng Sci 52:4111
13. Letzel M, Stankiewicz A (1999) Chem Eng Sci 54:5153
14. Luo XK, Lee DJ, Lau R, Yang GQ, Fan LS (1999) Aiche J 45:665
15. Maier B, Dietrich C, Büchs J (2001) Food Bioprod Process 79:261
16. Oyevaar MH, Delarie T, Vandersluijs CL, Westerterp KR (1989) Chem Eng Process 26:1
17. Oyevaar MH, Zijl, A, Westerterp, R (1988) Chem Eng Technol 11:1
18. Villadsen J, Nielsen, J (1994) Bioreaction engineering principles. Plenum, New York
19. von Stockar U, van der Wielen LA (1997) J Biotechnol 59:25
20. von Stockar U, van der Wielen LA (2003) Adv Biochem Eng Biotechnol 80:1
21. Cooney CL, Wang DIC, Mateles RI (1969) Biotechnol Bioeng 11:269
22. Schügerl K (1991) Bioreaktionstechnik Band 2: Bioreaktoren und ihre Charakterisierung. Salle-Sauerländer Verlag, Frankfurt
23. Hölz H (2000) In: Beitz W, Grote KH (eds) Dubbel Taschenbuch für den Maschinenbau, 20th edn. Springer, Berlin Heidelberg New York, p P27
24. Hölz H (2000) In: Beitz W, Grote KH (eds) Dubbel Taschenbuch für den Maschinenbau, 20th edn. Springer, Berlin Heidelberg New York, p P14
25. Schlüter V (1992) Fortschrittberichte-VDI Reihe 3 Verfahrenstechnik (Nr. 285)
26. Marquez AL, Wild G, Midoux N (1994) Chem Eng Process 33:247
27. Oosterhuis NMG (1983) Adv Ferment Proc Conf 191
28. YelloStrom (2003) Customer information at http://www.yellostrom.de. YelloStrom GmbH, Germany

Received: March 2004

Adv Biochem Engin/Biotechnol (2005) 92: 101–123
DOI 10.1007/b98917

Biochemical Engineering Aspects of Expanded Bed Adsorption

Jürgen Hubbuch (✉)[1] · Jörg Thömmes[2] · Maria-Regina Kula[3]

[1] Institute of Biotechnology, Research Center Jülich GmbH, 52425 Jülich, Germany
j.hubbuch@fz-juelich.de
[2] IDEC Pharmaceuticals Corp., 11011 Torreyana Road, San Diego, CA 92122, USA
[3] Institute of Enzyme Technology, Heinrich-Heine University, Düsseldorf, 52426 Jülich, Germany

Abstract The economic feasibility of a biotechnological production process is directly linked to the number and efficiency of the processes required during purification in order to reach the requested product specifications. Expanded bed adsorption is an integrated process that combines solid-liquid separation and product recovery into a single unit operation. This approach suggests an increased overall yield, lower requirements for capital investments and consumables and most importantly a reduced process time. The success of an integrative process is, however, closely linked to a detailed understanding of the biochemical principles involved and the constraints arising from feedstock complexity. This paper reviews the hydro-

dynamic principles that expanded bed adsorption is based on, discusses current developments in resin and column design, and finally presents a methodology for targeted process development in expanded bed adsorption.

Keywords Expanded Bed Adsorption · Primary capture · Process development · Biomass-Adsorbent interactions

1 Introduction

The rise and success of the biotechnological industry is closely related to the rise and commercial use of recombinant DNA technology, enabling the expression of molecules in industrially exploitable host strains and thus leading to a variety of new products produced on large scales. A direct result of the development of new biologically-produced substances, especially new therapeutic drugs, is that the demands for higher product purity and the requirements from the respective institutional bodies (FDA, ESRA) have increased significantly. The latter especially holds for new antibody-based drugs, which are given at higher dosages and repetitively over long periods of time.

2 Primary Recovery

Given the highly complex nature of the biological feedstocks typically used as sources for the recovery of biotechnological products, for example culture broth or microbial, plant, and tissue homogenates, it is not surprising that downstream processing – combining processes for the isolation, purification and formulation of biological entities – accounts for a major proportion of the production costs for biotechnological products [1, 2]. Fast isolation from particulates such as cells and/or cell debris, gross soluble contaminants and water – leading to a significant concentration of the feedstream – has proven essential to the success of separation processes. The need for several conditioning unit operations to be placed in front of high-resolution steps, and for additional steps to be introduced to ensure the safe removal of viruses, endotoxins or DNA reduces the overall recovery and increases the contribution of recovery operations to the cost of manufactured goods. Since the early conditioning steps – isolation and concentration of the product – traditionally do not contribute much to product purity but account for a high fraction of the overall processing time and significant losses in yield, a change of focus has been observed over the last few years, aiming towards a more selective isolation of the target molecule as early as possible during downstream processing. By combining solid-liquid separation with the ability to isolate the target molecule from a crude feedstream, these integrative primary recovery operations predominantly

target an increased overall yield, lower requirements for capital investments and consumables, and, most importantly, reduced process time. The latter is especially important in the light of increasing process volumes in the biotechnological industry, for instance cell culture bioreactor volumes of 15,000–20,000 L. The following technologies that perform the integration of solid-liquid separation and isolation have already been described in recent literature: membrane filtration [3–5], aqueous two phase extraction [6–8], batch adsorption [9, 10], expanded bed adsorption [11–15], and high gradient magnetic fishing [16, 17]. The most advanced of these industrial integrated primary recovery processes is currently expanded bed adsorption. Comparative studies with other techniques can be found in Hubbuch et al [18], Giovannini and Freitag [19], Blank et al [20] and Gonzalez et al [21].

2.1 Definition of Expanded Bed Adsorption

Fluidised beds have been successfully used in the chemical processing industry since the early 1920s, due to their particle handling, the possibility of reactive interaction between the fluid and solid phase, and the ease of scale-up. Although EBA maintains the fundamental principle of an increased void volume of the stationary phase and its reactive interaction with the fluid stream, it differs significantly from conventional fluidised bed processes used in the chemical processing industries. This resulted in rather confusing terminology in the early days of EBA development. Given the rather short history of expanded bed adsorption – first reports of the use of EBA were published in the early 1990s by Draeger and Chase [22] – a wide variety of terms, such as fluidised bed adsorption [13, 23, 24], expanded bed adsorption [12, 25, 26], classified fluidised bed adsorption [13, 23], and magnetically stabilised fluidised bed adsorption [27, 28] have been used in the literature to describe the application of a bed of chromatographic supports with an overall increased voidage caused by an upward directed liquid flow. The basic reasoning for this arose from the association of the term "fluidised bed" with a perfectly mixed reactor – as used in the chemical processing industry – which provides only a single stage for adsorption, while during the development of expanded bed adsorption a strong emphasis was laid on minimised back mixing of the adsorbent particles leading to enhanced multi-stage chromatographic performance [23, 29]. The terms "classified" or "magnetically stabilised" refer to specific reactor set-ups used to achieve this goal.

While a large number of publications (reviews [11–13, 15] and texts [14, 30]) already exist that deal exhaustively with many different aspects of expanded bed adsorption, it has been only recently that strategies for the systematic development of EBA processes have evolved, combining an understanding of chromatographic processes with tools and theories developed in chemical engineering science [31].

2.2 Process Integration and Operational Principles

Process integration can only be successful if all of the specific requirements of the different unit operations fused into the one single step are accounted for. It is therefore not surprising that in many cases process complexity is increased and process robustness decreased when formerly independent processing steps are compressed into one novel unit operation.

EBA combines solid-liquid separation with adsorptive purification. It is therefore reasonable to assume as a first approximation that the typical transport limitations of an adsorptive process apply; in other words, the kinetics of the adsorption reaction, the internal and external diffusion, as well as the bulk fluid flow through the adsorbent bed all have to be considered as potentially limiting steps. It must also be considered that adsorption takes place in a fluidised bed, where the mobility of the adsorbent particle represents a further resistance to the overall adsorption. Finally, the presence of solids in the feedstock complicates the situation, since it may impact the bulk fluid flow and so the residence time distribution in the adsorbent bed.

The intra-particle processes that occur during EBA are widely independent from the actual process, and our knowledge of established packed bed chromatography is immediately applicable. A difference in process performance when crude feedstreams are processed might, however, arise from the higher complexity and presence of insoluble components in the crude feedstock and the reduction of available adsorbent binding capacity due to blocking of the surface by adsorbed cells or cell components [25, 32]. The success of chromatographic separations is closely linked to a low degree of axial dispersion and so, depending on the separation task at hand, to a certain minimum plate number of the adsorbent bed. This prerequisite – being highly optimised in packed bed chromatography – has been one of the key parameters during the development of EBA as a fluidised bed system, where axial dispersion is reduced by classification (stratification) within the bed. In a simplified form, the settling velocity of an adsorbent particle can be described by the Stokes equation (Eq. 1). For beds containing identical adsorbent particles, the only system parameter leading to classification and therefore to a lower degree of solids mixing is the creation of a voidage gradient within the bed. Al-Dibouni and Garside [33] found an adsorbent size ratio of >2.2 – leading to a gradient in the settling velocities of the adsorbents – to be sufficient for the formation of a stable and "perfectly" classified bed. This stabilised bed is characterised by substantially reduced mobility of the adsorbent particles, and its bulk fluid flow characteristics are close to those of a well packed bed. For modern adsorbents used in expanded bed technology, both the sizes and densities of the adsorbents are varied to ease classification and ensure a low degree of adsorbent movement within the bed. A good overview of various hydrodynamic properties of EBA adsorbents is given by Thömmes [13], Theodossiou et al [34] and Theodossiou and

Table 1 Properties of expanded bed adsorbents, as described in the literature

Adsorbent	Material	Core	Density	Size	Reference
Streamline	Agarose	Quartz	1.2	100–300	[a]
Fastline	Agarose	Tungsten carbide	2.5–3.5	20–200	[b]
HYPERZ	Zirconium oxide (gel matrix)	Zirconium oxide	3.2	75	[c, 39]
CHT	Ceramic hydroxyapatite			20/40/80	[d]
PAA Streamline	Agarose	Quartz	n.d.	n.d.	[40]
Cell-Ti DEAHP	Cellulose	TiO_2	1.21	100–400	[41]
S-HyperD LS	Silica (gel matrix)	Silica	1.4	100–300	[42]
Cellbeads	Cellulose	–	1.6	100–200	[43]
CB-NFBA-L	Agarose	Nd-Fe-B alloy	2.04	140–300	[44]
CN-NFBA-S	Agarose	Nd-Fe-B alloy	1.88	50–165	[44]
Pellicular-L	Agarose	Stainless steel	n.d.	75–180	[45]
Pellicular-S	Agarose	Stainless steel	n.d.	32–75	[45]
ZSA	Agarose	Zirconia-silica	1.75	40	[46]
Zirblast	Agarose	Zirconia	3.85	60–125	[47]
HEG	Hydroxyethyl methacrylate-ethylene dimethyl-acrylate copolymer	–	1.2	105–355	[48]
FmZr	Fluoride-modified zirconia	Zirconia	2.8	38–75	[49]

[a] http://www.amershambisciences.com
[b] http://www.upfront-dk.com
[c] http://www.ciphergen.com
[d] http://www.biorad.com

Thomas [35]. Table 1 shows the range in densities and sizes of the EBA adsorbents described in literature.

This approach is, however, challenged by the properties of the applied feedstock. In contrast to packed bed chromatography, where particulate free buffer solutions with viscosities close to that of water are used, the hydrodynamic properties in expanded beds are influenced by the properties of the crude feedstock. Variations in fluid viscosity between buffer solutions and feedstock might lead to buoyancy induced mixing [36, 37] and changes in the bed expansion, while the adsorption of cell and/or cell debris or the cross-linking of adsorbents by cell debris or DNA might result in a random change in solid phase properties. These effects lead to a higher degree of axial mixing, aggregative fluidisation, channelling, or dead water zones within the bed. Such events may be mitigated by changes in fluid phase properties, such as the adjustment of pH and ionic strength. It has to be considered, however, that such changes directly affect adsorption equilibrium and transport processes – and therefore

the overall chromatographic performance. This underlines the importance of understanding and developing EBA processes in a holistic approach, where the interdependence of fluidisation quality, the adsorption equilibrium, and transport processes is acknowledged and part of the overall design process.

Finally, due to the lower overall degree of backpressure from the expanded bed, optimised fluid distribution is required in order to ensure the fast establishment of plug flow within a column used for EBA. The traditional approach of using horizontal inserts (perforated plates, metal mesh) that produce sufficient backpressure for fluid distribution may be hampered by clogging from cells retained beneath the insert [14, 38, 39].

Provided that the above-mentioned constraints and dependencies are understood and stable process conditions ensured, EBA operation principles mimic those established in packed bed chromatography: equilibration, application of the feed, wash, elution and regeneration. The main operational differences between packed and expanded bed adsorption are related to the differences in the feedstock, where particulate content and changes in density and viscosity require adjustments in volumetric flow, column height, and the adaptation of cleaning procedures to the more challenging feedstock compositions. The biochemical engineering aspects and development of Expanded Bed Adsorption are reviewed in the following sections.

3
The EBA System

3.1
Matrices for Expanded Bed Adsorption

The challenging feedstocks used with EBA systems require new types of adsorbent structures (Fig. 1). Important parameters are size and density, and ligand and physical adsorber design. In order to deal with highly viscous feedstock or higher flow, an increase in size and/or density is desirable (see Eq. 1, Table 1). An increase in specific weight is realised either by using a high-density porous material [40, 51, 52] or by coating a high-density non-porous core with a porous surface [42, 45, 53] (Fig. 1a, b). As the applied flow increases, the utilization of the equilibrium capacity of an adsorbent particle is reduced. A possible solution to this problem might be the use of pellicular adsorbents consisting of small high-density non-porous adsorbents with a thin polymeric ligand layer [35, 46, 47, 53, 54] (Fig. 1c). These adsorbents allow higher fluid velocity, and at the same time exhibit reduced diffusion limitations due to reduced transport length in the adsorbing layer. It has, however, also been shown that highly charged PEI chains used as ligand layers on pellicular media lead to increased cross-linking and compaction within the bed [35]. A further reduction of the adsorbent size to increase the surface volume ratio of the adsorbents is, however, hampered by the commercial flow distributor designs currently avail-

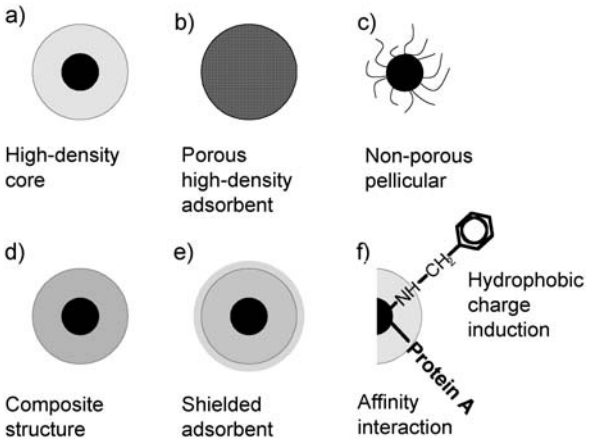

Fig. 1 Schematic overview of matrices used in expanded bed adsorption. **a** Polymeric adsorbent with high density core; **b** porous high density adsorbent; **c** non-porous adsorbent with small polymeric surface grafting. Special design features in order to: **d** enhance uptake rate; **e** and **f** minimize cell adsorption

able. Where perforated plates are used for fluid distribution in EBA columns, it must be considered that the plate or sieve also serves to retain the adsorbent particles within the column. Smaller particles, however, require smaller holes in the flow distribution system, leading to a higher degree of fouling/cell retention beneath the distributor. Only the scalable system (not limited by particle size) currently uses a rotating fluid distribution [16, 55].

A different approach to increasing bed capacity at high fluid velocity is the optimisation of the design of the adsorbent, leading to higher mass transfer rates within the adsorbent. In an exercise comparing Streamline SP and a hyper-diffusive resin S-HyperD LS, Wright et al [43] showed that the distinct structure of the latter resulted in significantly lower intra-particle mass-transfer resistance and faster protein uptake. This behaviour is in accordance with findings by Hubbuch et al. [56, 57] that certain adsorbent architectures might, under optimised conditions, lead to >10-fold faster protein uptake (Fig. 1d).

Adsorbent design has also recently focused upon challenging biomass-adsorbent interactions. Dainiak et al [41, 58] reported polyacrylic acid-coated anion exchanges for cell-resistant expanded bed adsorption (Fig. 1e). When challenging a native and shielded anion exchanger with negatively charged yeast cells, severe binding and clogging has been observed for the native adsorbents, while the shielded adsorbents did not show cell retention. Another approach is based on the use of ligands with highly specific affinities [59] or hydrophobic charge induction ligands that bind proteins under high ionic strength and elute by a shift in pH (Fig. 1f). The high ionic strength used during adsorption shields the long-range electrostatic interactions and so might prevent cell binding [60–62]. A good overview of the impact of physical and topo-

graphical adsorbent characteristics on the recoveries of plasmids, viruses or other nano-particulates is given by Zang et al [63], Thwaites et al [48] and Theodossiou and Thomas [35].

3.2 Hydrodynamic Principles

The hydrodynamic characterization and mathematical description of liquid fluidised beds has been one of the major ways of understanding EBA. Below, a short overview of the principles are given, and some misconceptions about relevant topics in the EBA literature are described. For a more in-depth coverage of this field, an excellent review on the hydrodynamics of liquid fluidisation has been written by Di Felice [64].

3.2.1 Bed Expansion

In a simplistic picture, the fluidisation of a settled bed of adsorbents can be divided into three stages. At very low flow – when the column backpressure is lower than the gravitational force of the adsorbent particles – the settled bed behaves like a packed bed. With increasing flow rate, and so increasing backpressure in the column, a point is reached where the gravitational force of the particles is in equilibrium with the backpressure in the column. This point is characterised by the minimum fluidisation velocity u_{mf} which causes the particles to separate from each other and so form a fluidised bed. With a further increase in the flow, the backpressure in the column remains constant while the degree of bed expansion is increased. The terminal settling velocity of a single adsorbent is determined by its settling velocity u_t. In a simplified approach, the settling velocity is determined by a force balance comprising the gravitational force, the buoyancy, and the flow resistance of the adsorbent particle. In the creeping flow range ($Re_t \leq 0.2$) the terminal settling velocity u_t can be described by the Stokes law:

$$u_t = \frac{(\rho_p - \rho_l)\, d^2 g}{18\,\eta} \tag{1}$$

Here ρ_p and ρ_l are the densities of the adsorbent particle and fluid phase respectively, while d is the adsorbent diameter, η is the fluid viscosity and g is the gravitational force. The true terminal settling velocity is, however, greatly influenced by wall effects, interactions between neighbouring adsorbent particles, and by interactions of the adsorbent particles with particulate components of the feedstock, like cells or cell components. At a given superficial fluid velocity, the bed will equilibrate to a certain expansion reflecting the terminal settling velocities of the adsorbent particles, which are in equilibrium with the interstitial velocity of the fluid in the bed. By increasing the superficial velocity the bed is further expanded, leading to an increase of the cross-sectional area

available for fluid flow – increased voidage – while the range of interstitial fluid velocities in the bed remains constant. At the point where the superficial velocity reaches and exceeds the terminal settling velocity of the single adsorbent particle a "wash out" (hydraulic transport) of the particles by the fluid stream is experienced.

Experimental investigations into the particle size distribution within the EBA systems have confirmed the above picture [65, 66]. It was found that the particle size remained approximately constant in the radial direction, while decreasing with increasing height, leading to a voidage change within the bed from 0.39 to near unity [66].

The degree of bed expansion is generally measured by a bed expansion factor describing the ratio of settled bed height to expanded bed height. Richardson and Zaki [67] developed a simple relationship describing the bed expansion:

$$\frac{u_0}{u_{tc}} = \varepsilon^n \tag{2}$$

Here u_s is the superficial fluid velocity, u_{tc} the corrected Stokes settling velocity, ε the bed voidage, and n is the Richardson-Zaki parameter. It has been further shown by Richardson and Zaki [67] that within the range of particle Reynolds numbers (Re_p) applicable in EBA, n is only a function of the d/D (particle diameter/column diameter) ratio and the respective magnitude of Re_p. Further theoretical approximations for n can be found in Al-Dibouni and Garside [33], Hartman et al [68] or Martin et al [69]. During numerous experimental investigations into EBA systems it has, however, been shown that Eqs. 1 and 2, as well as the theoretical approximations for n mentioned above, are not valid when realistic feedstock is applied to an EBA system (see Fig. 2), and so u_{tc} and n have

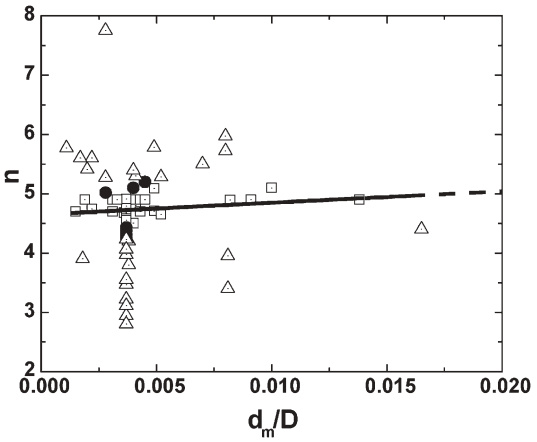

Fig. 2 Literature data on the Richardson-Zaki parameter n determined during EBA processes in comparison to the predicted value derived from the original Richardson-Zaki approach [67]. Squares: 5% deviation; circles: 10% deviation; triangles: 15% deviation; line: predicted value. Data points were taken from [23, 25, 29, 32, 50, 51, 71–77]

to be determined experimentally for each individual system. Given the strong influence of the biomass-adsorbent interaction, in a system comprising crude feedstock u_{tc} does not represent the Stokes settling velocity but an extrapolated value for an average settling velocity of a single adsorbent particle under the given fluid phase conditions and the respective implications arising from biomass/adsorbent interactions.

Furthermore, Lin et al [70] showed that the n value is also a function of the actual adsorbent type – probably related to inter-particle repulsion of the charged adsorbents. The variability of experimentally-determined n values is shown in Fig. 2, where 66 results from 15 literature references are compared to the n values predicted by the Richardson and Zaki [67] approach. From the deviations of experimental values to theoretical predictions it becomes evident that Eq. 2 can only be used for EBA process design when u_{tc} and n are measured experimentally.

3.2.2 Bed Stability/Fluid Mixing

Numerous studies in packed bed chromatographic systems have extensively shown that the performance of a chromatographic separation process can be severely affected by axial dispersion in the liquid phase. The evaluation and quantification of axial mixing is traditionally carried out by performing residence time distribution analysis. Due to the dynamic picture in a fluidised bed when compared to a packed bed – moving adsorbent particles, variation in feedstock viscosity, particulates containing feedstock – the analysis and control of mixing effects is an essential task during process development.

Among many others, four parameters – Bo, D_{ax}, N, and $HETP$ – might be derived from RTD analysis describing liquid mixing in an EBA system. Using this analysis, the system is described for all parts (piping, flow distributor, fluidised bed, column outlet) situated between the inlet of the tracer and its detection. The most common number determined is the Bodenstein number (Bo), which describes mass transfer in flowing fluids. As fluid side mass transfer in EBA systems is closely related to the mixing of the adsorbents and Bo is often used to describe just this, the usage of this number might therefore not be completely correct. It was pointed out by Levenspiel [79] that the correct description of the dimensionless number derived from RTD measurements in EBA systems should be the reciprocal of the vessel dispersion number, and that neither the Peclet number (Pe) for heat transfer nor the Bodenstein number [Bo] for mass transfer gives a correct description. The actual value of the dimensionless number, however, remains the same regardless of its description, and so Bo is used in the following, as in the majority of EBA publications. Another, more common approach in chromatography to express data derived from RTD analysis is the use of the tanks in series model, where the axial mixing is expressed as number of theoretical plates N, or when normalised to the length of the bed as the height equivalent of a theoretical plates $HETP$. As a rule

of thumb, a Bo number >40 describes a sort of plug flow with negligible dispersion.

During the early years of EBA development, numerous studies were performed to evaluate the axial mixing and to characterise the quality and influential parameters for EBA distribution systems (see below), the size distribution and density of adsorbents [77], the fluid velocity [51, 77] and the feedstock viscosity [80]. This allowed a qualified optimisation and understanding of the influential parameters in clear systems. When applying crude feedstock to EBA systems it became apparent, however, that fluidisation might be impaired by the characteristics of the applied feedstock, such as biomass type and concentration, ligand characteristics, ionic strength and pH. This necessitates an analytical technique to describe the influence of these feedstock parameters on the residence time distribution, representing the quality of fluidisation of adsorbents in real biotechnological suspensions. As the presence of biological particulate matter precludes the use of traditional tracers like acetone, initial studies were performed using the fluorescent signal of tryptophane – applicable for up to 7.0–8.0% wet weight biomass concentration – to overcome these limitations [81]. Industrial feedstock contains a higher biomass concentration, compatible with fluorescence detection. In this context, it was shown by Fernandez-Lahore et al [82] that the use of selected ions (Li^+ and Br^-) in combination with ion selective electrodes (ISE) allows RTD analysis in crude feed streams of up to 20% wet weight biomass concentration. This method consequently led to a better understanding of the influence arising from crude feedstock on EBA process performance [31].

3.3 Fluid Distribution

Traditionally, fluid distribution in chromatographic systems is ensured by creating a sufficiently high axial backpressure to evenly distribute the fluid in the radial direction. In conventional chromatography systems, the high backpressure along the packed bed assists significantly in the actual fluid distribution. The most important difference between packed bed and EBA systems, however, is the reduced pressure drop across the bed in EBA and the need for a very even radial fluid distribution at the column inlet to support the formation of the fully classified (expanded) bed. The latter highlights the need for optimal fluid distribution at the inlet of the column. There are currently four different approaches discussed in the literature (Fig. 3).

3.3.1 Distribution Based on the Creation of Back Pressure

Flow distribution based on the creation of backpressure represents the initial approach used in EBA development. Sufficient backpressure is realised by introducing perforated plates (PPD) [26, 53, 83], metal meshes [29], glass frits

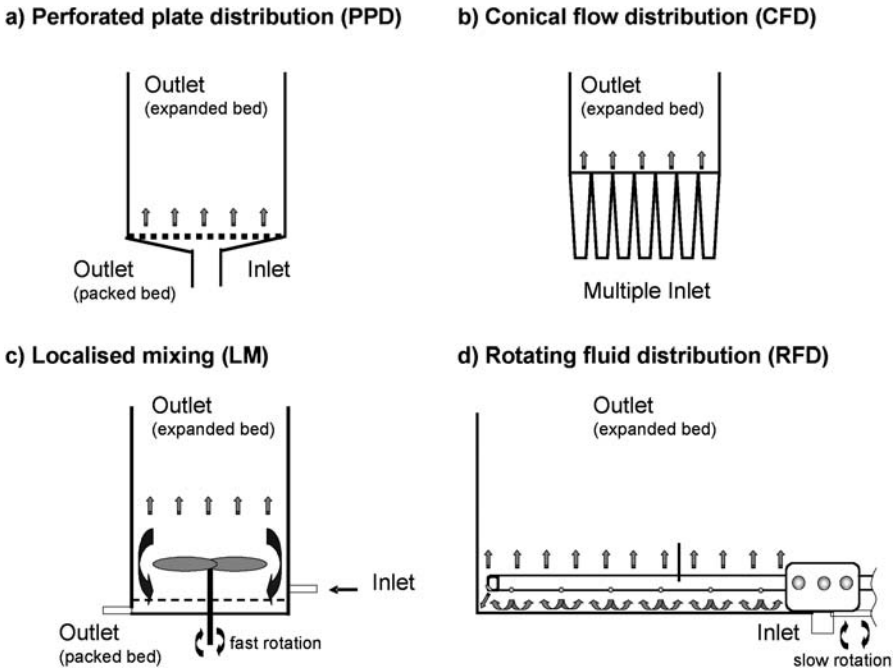

Fig. 3 Schematic overview of different fluid distributor types used in EBA

[84], or a bed of balatoni glass beads at the inlet of the column [51, 76] (Fig. 3a). This technique has been successfully implemented on EBA columns from 2.5 cm to 1 m in diameter [85]. It was, however, shown by Bascoul et al [86] that the actual fluidised bed acted as a fluid distribution system and that an increased bed height might therefore lead to good EBA performance irrespective of the flow distribution system used. This is confirmed by data presented in Fig. 4 showing that all of the investigated flow distribution systems led to an acceptable fluidisation of the bed. The two major drawbacks of these systems are, however, that such a backpressure-related distribution system introduces mechanical strain (creating a filtration effect), and that it is restricted to adsorbent particles of a certain size. It was found for example by Feuser et al [87] and Gehant et al [88] that the cells were mechanically filtered from the feed solution by a distributor net (stainless steel, 70 µm mesh size). PPD systems might therefore restrict fluid flow, cause turbulence [15], leading to a pressure increase [89] and deteriorated flow distribution. To avoid this build up of cells under the distributor plate, Hjorth [14] recommended that the system should be back-flushed intermittently for approximately 5 s (every 10/30 min). Further, it was reported by Bai and Glatz [90, 91] that a major problem in the application of EBA for plant extracts was found in the blockage of the bed support/flow distribution mesh at the column inlet, necessitating centrifugal or filter steps prior to EBA. A more open structure for the various distribution systems,

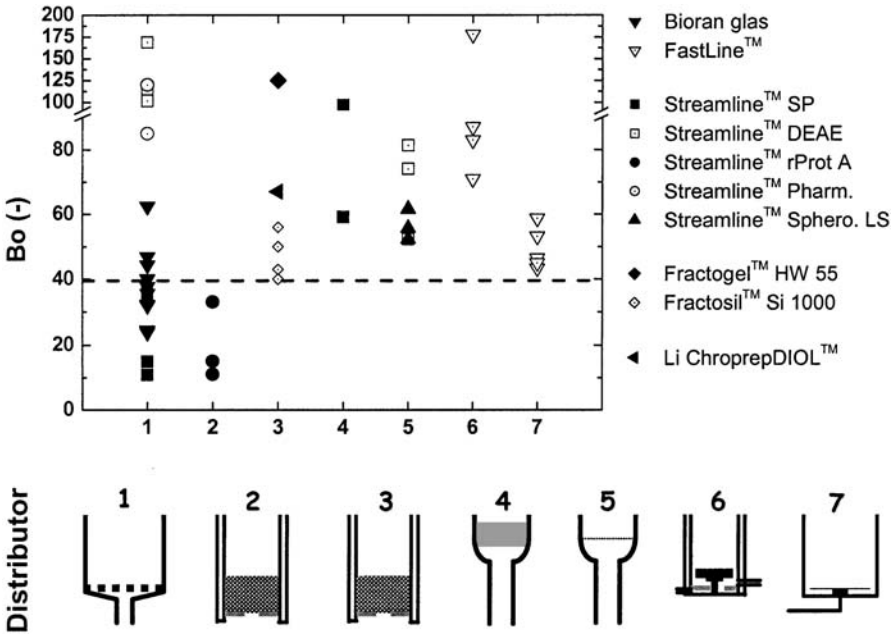

Fig. 4 Literature data on the Bodenstein number (Bo) reported for various adsorbent/fluid distributor systems. Data points were taken from [14, 23, 29, 32, 51, 55, 76, 77, 80, 84, 92]

which would reduce the biomass filtration effect is, however, not feasible, since it would also act as a retention system for the adsorbent particles and restrict the application of smaller adsorbent particles with improved performance.

3.3.2 Distribution Based on Conical Flow Distributors

Conical flow distributors facilitate an increase in the cross-sectional area while simultaneously maintaining plug flow characteristics (Fig. 3b). The latter is, however, restricted to rather steep inlet angles (~5.5°) and so exhibits an unfavourable height to cross sectional-area ratio for large scale applications [92]. The only means of covering a larger area is the use of multiple cones in parallel, and therefore, multiple inlets for the feedstock [39]. Furthermore, a complex sealing system might be necessary to prevent adsorbent particles from falling back into the feeding pipes.

3.3.3 Distribution Using a Localised Mixing Device

An alternative solution, that introduces the processing liquid from side-ports, has been reported for columns up to 40 cm in diameter (Fig. 3c). The distribu-

tion of the fluid is ensured by a mixer positioned at the lower section of the column [93]. The idea of the LM-system is to create a well-mixed region in the lower section of the column, which is required to evenly distribute the fluid entering and to prevent channelling or jetting into the stable section of the bed above. However, the feasibility of this technology has been questioned for large scale applications in particular [15, 94]. Studies with column diameters from 60 cm to 1.5 m confirmed the limited scalability of these systems [95]. Furthermore, a clear reduction in the bed capacity could be observed due to the rather large mixing zone created in the lower section of the bed.

3.3.4 Distribution Using a Rotating Fluid Distributor

The rotating fluid distributor is based on the equal distribution of the feedstock by means of slowly rotating pipes [16, 55]. The feedstock enters the distribution system through one central port and is than distributed into 12 tubular pipes (d_p=20 mm), which are sealed at the end and have fluid outlet holes (d_{out}=3 mm) facing the base of the column. The high fluid velocities through the outlet holes create a turbulent zone beneath the rotating pipes over the cross-sectional area. After rising through this zone, which is mainly defined by the height of the distributor blades above the column base (currently 2–3 cm), a uniform fluid front is developed. The system has been under investigation up to a column diameter of 1.5 m and combines several advantages: fluid distribution without the need for porous nets, compatibility with any size of adsorbent, and good scalability. Modifications of this approach are currently being investigated for commercial use [96].

4 Biomass-Adsorbent Interactions

The interactions between the suspended solids and the fluidised adsorbent particles can be sub-divided into contributions from the transport or collision probability of the two entities and the probability of adsorption onto the adsorbent particle surface. This is analogous to the mechanistic picture describing deep bed filtration processes [97]. The collisions of biomass particulates with adsorbent particles can be described by a number of mechanisms, namely straining, interception, diffusion, hydrodynamic interactions, and electrostatic interactions. Actual system parameters, such as size and density of the biomass, the bed voidage, and the flow regime within the bed may influence the collision probability significantly [98, 99]. The probability of adsorption and retention is clearly influenced by the interplay between electrostatic-, hydrophobic- and van der Waals interactions and the hydrodynamic shear stress acting on the adsorbed particulates. In order to design and operate robust EBA processes, it is of utmost importance to minimise biomass-adsorbent interactions.

4.1 Methods for the Evaluation of Biomass-Adsorbent Interactions

Various methods have been developed to analyse the extent of biomass-adsorbent interactions. These can be divided into tools that examine the amount of cell adsorption on the adsorbent particle under various fluid phase conditions, analysis of the physical characteristics (size and surface charge) of the particulates, and investigations into the influence of feedstock composition on the stability of the expanded bed under realistic process conditions (Fig. 5).

Finite bath experiments are carried out in small well-mixed batch reactors where a dilute suspension of biomass is incubated with the adsorbent particle under defined fluid phase conditions. The cell concentration in solution is then monitored by measuring the evolution of the turbidity over time [31, 100]. Experiments with increasing ionic strength buffer clearly confirmed the influence of electrostatic attraction on the diffusion-controlled adsorption process of the cells on the adsorbent surface. From a great number of experiments it could be concluded that – as a rule of thumb – a decrease of less than 10% of the cell concentration after 10 min could act as a threshold parameter indicating systems with critical biomass adsorbent interaction. A more quantitative analysis can be obtained using a kinetic expression proposed by Daniels [101]. This

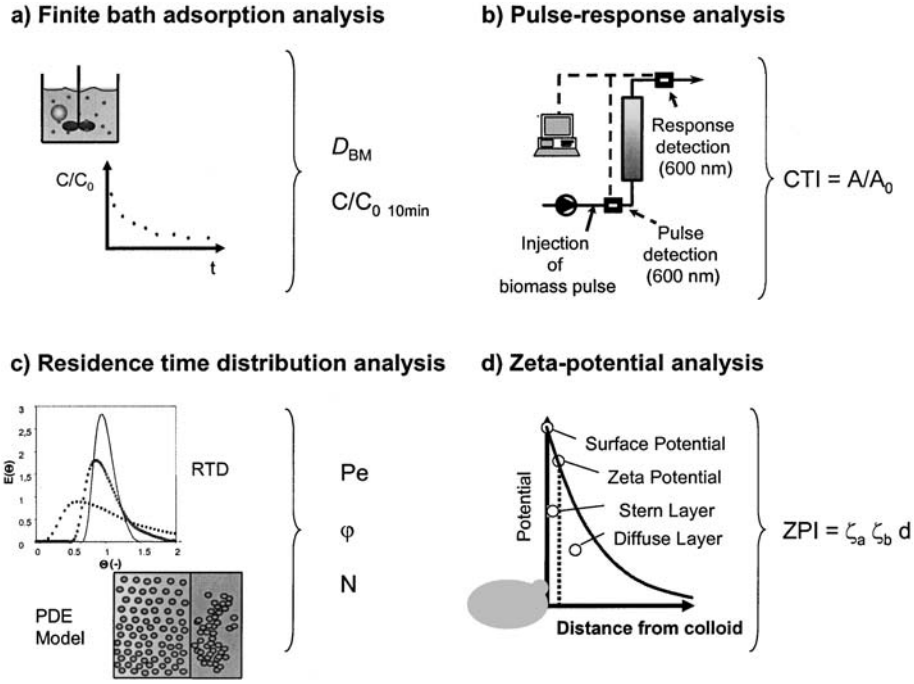

Fig. 5 Methods and obtained parameters for the evaluation of biomass-adsorbent interactions

method can be used for the initial screening of possible adsorbents and reaction conditions for a given capture step due to the ease of operation and small scale.

A more realistic and therefore sensitive method is the pulse-response method [38, 87]. This analysis is based on the retention of a dilute pulse of biomass by an equilibrated and expanded adsorbent bed. The cell transmission index (CTI) describing the extent of biomass adsorption interactions is defined as the fraction of biomass leaving the column for a given system. It has been reported that a CTI value greater than 0.9 might act as a threshold indicating suitable operating conditions for EBA, while systems with considerably lower CTI values indicate problematic systems, which should not be considered for further development [31].

A direct link between the CTI and the physical parameters of the system has only recently been established. It was shown by Lin et al [102] that by combining the interactions resulting from the effective surface charge of the adsorbent (represented by the zeta-potential of the adsorbent ζ_a), the effective surface charge of the biomass (ζ_b), and the size (d) of the biomass under investigation, a parameter ($-\zeta_a\,\zeta_b\,d$) can be derived which is directly related to findings from CTI analysis. By investigating cells and homogenates of *S. cerevisiae* and *E. coli*, a parameter value of ($-\zeta_a\,\zeta_b\,d$)~120 (under the given experimental conditions) was found to correspond to a CTI value of 0.9. This approach offers not only a fast screening method but might also be applied to the in-process control of new fermentation batches prior to their application to an EBA system.

The fourth analytical technique allows the transition from diluted cell suspension to the real process feedstock. Using this transition, the effect of the biomass concentration on the extent of biomass/adsorbent interactions is captured. The method is based on an RTD analysis in a system challenged with a real feedstock under the exact operating conditions of the EBA process [81, 100]. Applying a pulse of a non-interacting tracer facilitates analysis using an advanced RTD model originally introduced by Villermaux and Swaaij [103]. In this model, the bed is virtually divided into a stable fraction φ characterised by a Pe number and a region with non-ideal fluidisation behaviour ($1-\varphi$). Systems exhibiting φ values of greater than 0.8 were reported to result in successful EBA processes [31].

4.2 Phenomenological Picture of Biomass-Adsorbent Interactions

The phenomenological picture of biomass-adsorbent interactions can be envisaged in several ways. The retention of small debris on the adsorbent surface – either reversible or irreversible – might lead to a reduced capacity of the adsorbent as well as to a reduction in the expansion factor during the loading. The latter might, however, also be connected to an increasing protein load on the adsorbent.

The bed expansion can be seen as a first indicator of biomass adsorbent interactions. It is for example well known that DNA in solution might act as a

bridging agent leading to agglomerates of adsorbent particles. Theodossiou et al. [34] showed that a clear correlation between the adsorbent structure, the amount of bound DNA, and the respective expansion of the bed existed. From a characteristic decline followed by an incline of the bed porosity with an increasing amount of DNA applied in the feedstock they concluded that a rearrangement of the DNA strands on the adsorbent surface leads to a repulsion of the loaded adsorbents. Lin et al [70] showed that with increasing biomass concentration a sudden and significant increase of u_{tc} and n is obtained, indicating a strongly interacting system.

The aggregation of adsorbents due to bound cells/cell debris or bridging DNA might lead to a significantly reduced capacity, increased mixing within the bed and/or channelling effects [81]. The latter picture might, however, also arise from an uneven flow distribution due to fouling and clogging of the flow distributor [39].

The expansion behaviour described above was correlated by Lin et al [70] to the PDE data describing the fraction of aggregation within the bed. A clear correlation existed identifying three sections – non-interacting, intermediate, and aggregative – within the studied system. The affiliation of a system to one of these groups was clearly influenced by the susceptibility towards biomass/adsorbent interactions (represented by the CTI) as well as biomass concentration and adsorbent type. At an extreme case of biomass-adsorbent interactions the expanded bed collapsed.

5 Process Development

EBA process development requires a detailed understanding of the influencing parameters and their interrelation, given the complex feedstock and the reduced parameter flexibility due to the integration of two formerly independent unit operations. One of the most important pre-requisites for successful process development is the characterisation of feedstock properties, the evaluation of possible influences on EBA performance arising from the feedstock composition, and the influence of changes occurring during cultivation and/or homogenisation steps prior to feedstock application (Fig. 6). Calado et al [104] reported for example that the media composition for the cultivation of *S. cerevisiae* played a significant role in the achieved bed capacity during the recovery of cutinase. By reducing the amount of yeast extract, a 6.7-fold higher usable bed capacity could be reached. Batch to batch variations – pH, ionic strength, biomass concentration and surface characteristics, product concentration – during cultivation might further pose a severe impact on EBA performance. Brixius et al [98, 99] showed that the actual homogenisation conditions that impact on characteristic homogenate properties such as debris size and surface charge play a major role when optimising EBA performance. A decrease in debris size was generally accompanied by a reduction in the effective surface

charge, leading to a reduction in both the collision probability between the cell debris and the adsorbent and the probability of retention on the surface. It was therefore concluded that homogenisation should be optimised not only for high product release but also for low biomass-adsorbent interactions in the subsequent purification step. Further, Gehant et al [88] showed that buffer conditioning prior to the homogenisation step – in contrast to post-homogenisation conditioning – led to a significant decrease in screen fouling at the column inlet. A methodological design approach for efficient EBA process development has been provided by Lin et al [31] and Sonnenfeld and Thömmes [105]. This approach is shown schematically in Fig. 6. Initially, promising systems are identified based on a simultaneous analysis of adsorbent capacity for the respective product – isothermal characterisation – and their susceptibility for biomass adsorbent interaction – batch adsorption studies of cells/cell debris and pulse-response analysis. To further evaluate the influence of realistic feedstock conditions on the respective adsorbent bed, RTD analysis of the system is performed during the application of the feedstock. Only systems showing a low degree of axial dispersion or channelling and therefore stable expansion are further investigated for expansion characteristics and chromatographic breakthrough performance. The experimental effort of the latter can be minimised by the use of appropriate model descriptions. In this context, the model of Hall et al [106] was proven to be a good and robust approximation for the prediction of sorption efficiency in EBA. It is based on the simulation of breakthrough behaviour of molecules exhibiting an irreversible or very favourable isotherm under the precondition that internal and external transport are the only limiting parameters determining sorption efficiency. For the application of this model, an equilibrium capacity Q_{eq} and the apparent particle-side transport coefficient D_e must be determined, while the fluid side transport coefficient k_f is estimated from literature correlations [107, 108]. The feasibility of this strategy has been shown in case studies for the isolation of formate dehydrogenase from an *E. coli* homogenate [109], the isolation of recombinant human insulin from whole broth of *S. cerevisiae* [99], as well as the recovery of an antibody from a high cell density CHO culture [105].

Further – economical – optimisation of existing EBA processes can be performed by reducing buffer consumption and avoiding mixing within the column due to density differences of subsequent feed streams. Bai and Glatz [90] reported reduced bed capacities due to an increased dispersion of in the bed after applying viscous plant extracts. Furthermore, it was shown by Fee and Liten [36] and Fee [37] that buoyancy induced mixing results in increased buffer consumption. The authors reported an optimised strategy that used a short plug of density-enhanced buffers for efficient washing procedures. Finally, Walter and Feuser [110] showed that bed capacity, regeneration and therefore the life cycle of the adsorbent represented one of the most important parameters during the economical evaluation of EBA processes, and that EBA technology might lead to an economic advantage, reducing the cost of manufactured goods on a single unit operation basis by about 50%. It was, however, also

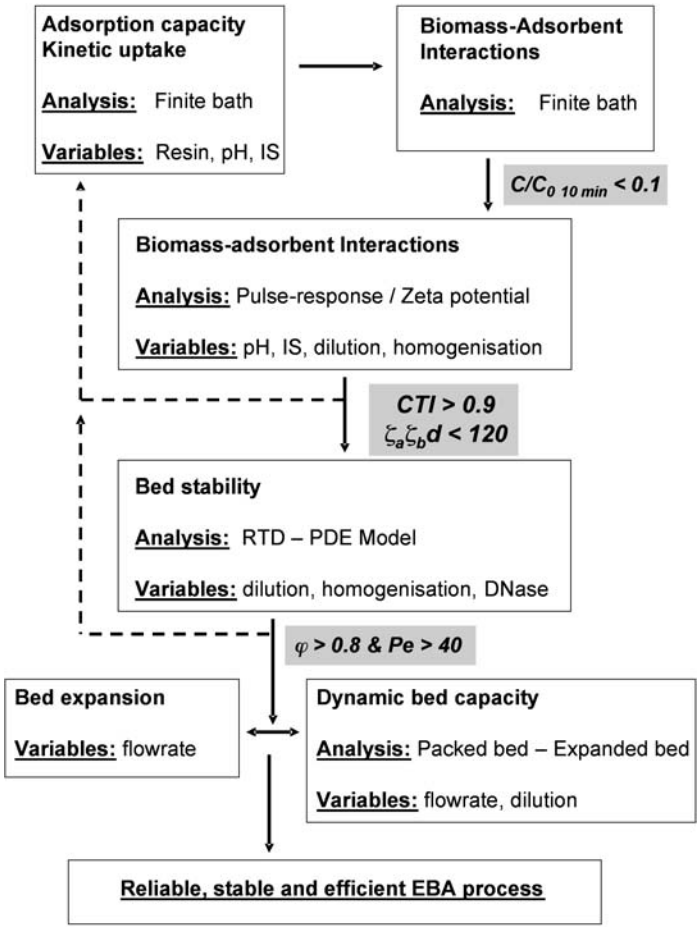

Fig. 6 Strategy for a directed process development in EBA

pointed out that the use of preexisting conventional large-scale equipment may reduce this margin in favour of conventional steps.

6 Concluding Remarks

The understanding and predictability of EBA processes has advanced considerably over the last few years, paving the way toward rational process design. A prerequisite for successful EBA design is, however, a good understanding of the interrelated parameters arising from the fusion of fluidised bed hydrodynamics, mechanisms of cell-surface interactions, and chromatographic principles. In order to evaluate this complex interplay, a variety of tools are now

available to derive technical and economic data for a sound evaluation of process options. A reliable and robust EBA process might therefore lead to increased overall yield combined with reduced operational time.

References

1. Blanch HW, Clark DS (1996) Biochemical engineering. Marcel Dekker, New York
2. Asenjo JA, Leser EW (1996) Process integration in biotechnology. In: Verrall M (ed) Downstream processing of natural products. Wiley, New York, p 123
3. Davies JL, Bbaganz F, Ison AP, Lye GJ (2000) Biotechnol Bioeng 69:429
4. Kendall D, Lye GJ, Levy MS (2002) Biotechnol Bioeng 79:816
5. Castilho LR, Anspach FB, Deckwer WD (2002) Biotechnol Prog 18:776
6. Kula MR (1990) Bioseparation 1:181
7. Hustedt H, Kroner KH, Kula MR (1985) Application of phase partitioning in biotechnology. In: Walter H, Brooks D, Fisher D (eds) Partitioning in aqueous two-phase systems: theory, methods, uses and application to biotechnology. Academic, New York, p 529
8. Kula MR (1985) Liquid/liquid extraction of biopolymers. In: Humphrey A, Cooney CL (eds) Comprehensive biotechnology, vol II. Pergamon, New York, p 451
9. O'Shannessy K, Scoble J, Scopes RK (1996) Bioseparation 6:77
10. Scoble J, O'Shannessy K, Scopes RK (1996) Bioseparation 6:243
11. Chase HA (1994) TIBTECH 12:296
12. Hjorth R (1997) TIBTECH 15:230
13. Thömmes J (1997) Adv Biochem Eng Biot 58:185
14. Hjorth R, Leijon P, Barnfield Frei AK, Jägersten C (1998) Expanded bed adsorption chromatography. In: Subramanian G (ed) Bioseparation and bioprocessing. Wiley VCH, Weinheim, p 199
15. Anspach FB, Curbelo D, Hartmann R, Garke G, Deckwer WD (1999) J Chromatogr A 865:129
16. Hubbuch JJ (2001) Development of adsorptive separation systems for recovery of proteins from crude bioprocess liquors. PhD thesis, Technical University of Denmark, Lyngby, Denmark
17. Hubbuch JJ, Thomas ORT (2002) Biotechnol Bioeng 79:302
18. Hubbuch JJ, Matthiesen DB, Hobley TJ, Thomas ORT (2001) Bioseparation 10:99
19. Giovannini R, Freitag R (2001) Biotechnol Bioeng 73:522
20. Blank GS, Zapata G, Fahrner R, Milton M, Yedinak C, Knudsen H, Schmelzer C (2001) Bioseparation 10:65
21. Gonzalez Y, Ibarra N, Gomez H, Gonzalez M, Dorta L, Padilla S, Valdez R (2002) J Chromatogr B 784:183
22. Draeger NM, Chase HA (1990) I Chem E Symp Series 118:161
23. Thömmes J, Weiher M, Karau A, Kula MR (1995) Biotechnol Bioeng 48:367
24. Voute N, Bataille D, Girot P, Boschetti E (1999) Bioseparation 8:121
25. Chase HA, Draegger NM (1992) J Chromatogr 597:129
26. Barnfield Frei AK, Johansson HJ, Johansson S, Leijon P (1997) Bioprocess Eng 16:57
27. Burns MA, Graves DJ (1985) Biotechnol Prog 1:95
28. Chetty AS, Burns MA (1991) Biotechnol Bioeng 38:963
29. Lan JCW, Hamilton GE, Lyddiatt A (1999) Bioseparation 8:43
30. Janson J-C, Rydén L (1998) Protein purification, 2nd edn. Wiley, New York
31. Lin DQ, Fernandez-Lahore HM, Kula MR, Thömmes J (2001) Bioseparation 10:7

32. Draeger NM, Chase HA (1991) T I Chem E 69:45
33. Al-Dibouni MR, Garside J (1979) T I Chem E 57:94
34. Theodossiou I, Elsner HD, Thomas ORT, Holey TJ (2002) J Chromatogr A 964:77
35. Theodossiou I, Thomas ORT (2002) J Chromatogr A 971:73
36. Fee C, Liten A (2000) Bioseparation 10:21
37. Fee C (2001) Chem Eng Process 40:329
38. Feuser J, Walter J, Kula MR, Thömmes J (1999) Bioseparation 8:99
39. Feuser J, Striffler U, Walter J, Barnfield Frej AK, Tarnström A (2000) EBA processing of mammalian cell culture fluid – design studies on column hardware. EBA 2000 3rd Int Conf on Expanded Bed Adsorption. Garmisch-Partenkirchen, Germany, 14–17 May 2000
40. Santambien P, Shiloach J, Trinh L, Schapman A, Boschetti E (2002) Extended reports from the 4th Int Conf on Expanded Bed Adsorption. St. Petersburg, FL, USA, 8–11 Sept 2002, p 13
41. Dainiak MB, Galaev IY, Mattiasson B (2002) Biotechnol Prog 18:815
42. Lei YL, Lin DQ, Yao SJ, Zhu ZQ (2003) J Appl Polym Sci 90:2848
43. Wright PR, Muzzio FJ, Glasser BJ (1999) Biotechnol Prog 15:932
44. Pai A, Gondkar S, Lali, A (2000) J Chromatogr A 867:113
45. Tong XD, Sun Y (2001) J Chromatogr A 943:63
46. Pålsson E, Gustavsson PE, Larsson PO (2000) J Chromatogr A 912:235
47. Jahanshahi M, Sun Y, Santos E, Pacek A, Franco TT, Nieniow A, Lyddiatt A (2002) Biotechnol Bioeng 80:201
48. Thwaites E, Burton SC, Lyddiatt A (2001) J Chromatogr A 943:77
49. Nayak DP, Ponrathnam S, Rajan CR (2001) J Chromatogr A 922:63
50. Mullick A, Flickinger MC (1999) Biotechnol Bioeng 65:282
51. Finette GMS, Mao QM, Hearn MTW (1996) J Chromatogr A 743:57
52. Griffith CM, Morris, J, Robichaud M, Annen MJ, McCormick AV, Flickinger MC (1997) J Chromatogr A 776:179
53. Amersham Pharmacia Biotech (1997) Expanded bed adsorption, principles and methods. Amersham Pharmacia Biotech, Uppsala, Sweden
54. Theodossiou I, Søndergaard M, Thomas ORT (2001) Bioseparation 10:31
55. Hubbuch JJ, Heeboll-Nielsen A, Hobley TJ, Thomas ORT (2002) Biotechnol Bioeng 78:35
56. Hubbuch J, Linden T, Knieps E, Ljunglöf A, Thömmes J, Kula M-R (2003) J Chromatogr A (in press)
57. Hubbuch J, Linden T, Knieps E, Thömmes J, Kula M-R (2003) J Chromatogr A (in press)
58. Dainiak MB, Galaev IY, Mattiasson B (2002) J Chromatogr A 942:123
59. Chase HA (1998) J Mol Recognit 11:217
60. Hamilton GE, Luechau F, Burton SC, Lyddiatt A (2000) J Biotechnol 79:103
61. Burton SC, Harding DRK (2001) J Biochem Biophys Methods 49:275
62. Smith MP, Bulmer MA, Hjorth R, Titchener-Hooker NJ (2002) J Chromatogr A 968:121
63. Zhang Z, Burton S, Williams S, Thwaites E, Lyddiatt A (2001) Bioseparation 10:113
64. Di Felice R (1995) Chem Eng Sci 50:1213
65. Bruce LJ, Chase HA (2001) Chem Eng Sci 56:3149
66. Willoughby NA, Hjorth R, Titchener-Hooker NJ (2000) Biotechnol Bioeng 69:648
67. Richardson JF, Zaki WN (1954) T I Chem Eng 32:35
68. Hartman M, Trnka D, Havlin V (1992) Chem Eng Sci 47:3162
69. Martin BLA, Kolar Z, Wesselingh JA (1981) Trans Instn Chem Engrs 59:100
70. Lin DQ, Thömmes J, Kula M-R, Hubbuch JJ (2003) The influence of biomass on the hydrodynamic behaviour and stability of expanded beds. Biotechnol Bioeng (in press)
71. Dasari G, Prince I, Hearn MTW (1993) J Chromatogr A 631:115

72. Chang, YK, Chase, HA (1994) Expanded bed adsorption for the direct extraction of proteins. In Pyle DL (ed) Separations for biotechnology, vol 3. The Royal Society of Chemistry, London, p 106
73. de Luca L, Hellenbroich D, Titchener-Hooker NJ, Chase HA (1994) Bioseparation 4:311
74. Morton P, Lyddiatt A (1994) J Chem Technol Biot 59:106
75. Hjorth R, Kämpe S, Carlsson M (1995) Bioseparation 5:217
76. Thömmes J, Bader A, Halfar M, Karau A, Kula MR (1996) J Chromatogr A 752:111
77. Karau A, Benken C, Thömmes J, Kula MR (1997) Biotechnol Bioeng 55:54
78. Chang YK, Mc Creath GE, Chase HA (1995) Biotechnol Bioeng 48:355
79. Levenspiel O (1999) Chemical reaction engineering, 3rd edn. Wiley, New York
80. Chang YK, Chase HA (1996) Biotechnol Bioeng 49:512
81. Fernandez-Lahore HM, Kleef R, Kula MR, Thömmes J (1999) Biotechnol Bioeng 64:484
82. Fernandez-Lahore HM, Lin DQ, Hubbuch JJ, Kula M-R, Thömmes J (2001) Biotechnol Prog 17:1128
83. Kazumasa Y, Munehiro N, Takao O, Akinori S (1996) Process for purifying recombinant human serum albumin. European patent EP0699687
84. Ghoose S, Chase H (2000) Bioseparation 9:21
85. Amersham Pharmacia Biotech (1999) Downstream 28:3
86. Bascoul A, Delmas H, Couderc JP (1988) Chem Eng J 37:11
87. Feuser J, Halfar M, Lütkemeyer D, Ameskamp N, Kula MR, Thömmes J (1999) Process Biochem 34:159
88. Gehant RL, Brown AM, Arroyo AY, Heinsohn HG, Kahn DW (2002) Extended reports from the 4th Int Conf on Expanded Bed Adsorption. St. Petersburg, FL, USA, 8–11 Sept 2002, p 19
89. Brobjer M (1999) Bioseparation 8:219
90. Bai Y, Glatz CE (2003) Biotechnol Bioeng 81:775
91. Bai Y, Glatz CE (2003) Biotechnol Bioeng 81:855
92. Zafirakos E, Lihme A (1999) Bioseparation 8:85
93. Blevins RD (1984) Applied fluid dynamics handbook. Van-Nostrand Reinhold, New York
94. Diehl P (1998) Genetic Engineering News, October, p 14
95. Hobley TF, Hubbuch JJ, Heebøll-Nielsen, Thomas ORT (2002) Extended reports from the 4th Int Conf on Expanded Bed Adsorption. St. Petersburg, FL, USA, 8–11 Sept 2002, p 27
96. Feuser J, Barnfield-Frej KAK, Lundkvist M, Walter JK (2002) EBA columns at technical scale. Extended reports from the 4th Int Conf on Expanded Bed Adsorption. St. Petersburg, FL, USA, 8–11 Sept 2002, p 30
97. Herzig JP, Leclerc DM, LeGoff P (1970) Ind Eng Chem 62:8
98. Brixius P, Lin DQ, Mollerup I, Hubbuch J, Kula MR (2002) Extended reports from the 4th Int Conf on Expanded Bed Adsorption. St. Petersburg, FL, USA, 8–11 Sept 2002, p 6
99. Brixius P (2003) On the influence of feedstock properties and composition on process development of expanded bed adsorption. PhD thesis, Heinrich-Heine University, Düsseldorf
100. Fernandez-Lahore HM, Geilenkirchen S, Boldt K, Nagel A, Kula MR, Thömmes J (2000) J Chromatogr A 873:195
101. Daniels SL (1980) Mechanisms involved in sorption of microorganisms to solid surfaces. In: Bitton G, Marshall KC (eds) Adsorption of microorganisms to surfaces. Wiley, New York, p 7
102. Lin DQ, Brixius PJ, Hubbuch JJ, Thömmes J, Kula M-R (2003) Biotechnol Bioeng 83:149
103. Villermaux J, van Swaaij WPM (1969) Chem Eng Sci 24:1097

104. Calado CRC, Cabral JMS, Fonseca LP (2002) J Chem Technol Biot 77:1231
105. Sonnenfeld A, Thömmes J (2002) Extended reports from the 4th Int Conf on Expanded Bed Adsorption. St. Petersburg, FL, USA, 8–11 Sept 2002, p 22
106. Hall KR, Eagelton LC, Acrivos A, Vermeulen T (1966) I&EC Fundamentals 5:212
107. Nelson PA, Galloway TR (1975) AIChE J 10:605
108. Nagel A (2000) Fließbettadsorption: Stofftransportmechanismen in der Proteinaufarbeitung. PhD Thesis, RWTH, Aachen
109. Reichert U, Knieps E, Slusarczyk H, Kula MR, Thömmes J (2001) J Biochem Biophys Meth 49:533
110. Walter J, Feuser J (2002) Extended reports from the 4th Int Conf on Expanded Bed Adsorption. St. Petersburg, FL, USA, 8–11 Sept 2002, p 37

Received: March 2004

Adv Biochem Engin/Biotechnol (2005) 92: 125 – 143
DOI 10.1007/b98916

Parallel Reactor Systems for Bioprocess Development

Dirk Weuster-Botz (✉)

Lehrstuhl für Bioverfahrenstechnik, Technische Universität München,
Boltzmannstrasse 15, 85748 Garching, Germany
d.weuster-botz@lrz.tum.de

Abstract Controlled parallel bioreactor systems allow fed-batch operation at early stages of process development. The characteristics of shaken bioreactors operated in parallel (shake flask, microtiter plate), sparged bioreactors (small-scale bubble column) and stirred bioreactors (stirred-tank, stirred column) are briefly summarized. Parallel fed-batch operation is achieved with an intermittent feeding and pH-control system for up to 16 bioreactors operated in parallel on a scale of 100 ml. Examples of the scale-up and scale-down of pH-controlled microbial fed-batch processes demonstrate that controlled parallel reactor systems can result in more effective bioprocess development. Future developments are also outlined, including units of 48 parallel stirred-tank reactors with individual pH- and pO_2-controls and automation as well as liquid handling system, operated on a scale of ml.

Keywords Bioprocess development · Parallel bioreactors · Intermittent feeding · Parallel control · Scale-up/scale-down

1 Introduction

Three intermeshing operational steps are usually necessary for the development of biotechnological production processes: the manufacture of the biocatalyst (biocatalyst design), optimization of the reaction conditions (medium design), and bioprocess development up to the technical scale (bioprocess design). While the first two operational steps are carried out with the aid of simple batch reactors (shaken microtiter plates and/or shake flasks) operated in parallel, the development of the production process is implemented in the controlled laboratory stirred-tank reactor. Converting process results achieved in uncontrolled batch reactors into a high-performance, controlled fed-batch process corresponding to the present state of the art is generally an extremely labor-intensive and time-consuming task. A significant reason for this is the difficulties encountered in extracting process information, as well as the often problematic scale-up from the shake flask reaction system into the sequentially-operated laboratory stirred-tank reactor. The challenge is to transfer progress in molecular biotechnology (sequence analysis, metabolic design, protein design, …) into economical production processes as quickly as possible. Even today, a decade or more is still required to realize biotechnological processes industrially. On the basis of this industrial experience, it has been stated that [1]:

"Time-scale has now become possibly the most critical aspect in meeting the needs of the pharmaceutical industry … The key determining factor now is not the identification of an appropriate enzyme but the speed of scale-up …The importance of integrated process development is the key lesson."

Controlled parallel reactor systems (see Fig. 1) could increase the speed of scale-up. They allow the development of fed-batch processes at early stages of the process development, and so contribute to the integration of biocatalyst design, medium design and bioprocess design.

2 Parallel Bioreactors

2.1 Shake Flask

The classical parallel reactor used for biotechnology is the shake flask. Here, Erlenmeyer flasks with a total volume of 100–5000 ml are used, which are provided with a sterile closure. With the aid of autoclave-capable, deep-bed filters, convective gas exchange between the headspace of the shake flask and the environment (and therefore contamination from external microbes after steril-

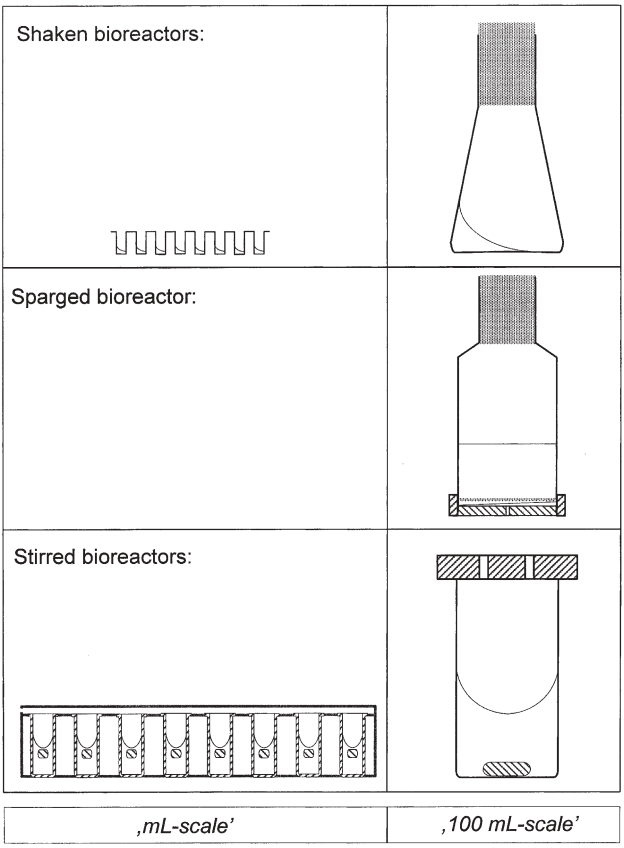

Fig. 1 Scheme for parallel bioreactor systems. Shaken bioreactors: microtiter plate, shake flask. Sparged bioreactor: small-scale bubble column. Stirred bioreactors: stirred-tank reactor unit, stirred-tank (stirred column is not indicated). The parallel bioreactors on the right (shake flask, small-scale bubble column, stirred-tank) can be used with an intermittent feeding and pH-control device (see Fig. 2). The parallel bioreactors on the left can be operated with a liquid handling system (see Fig. 10)

ization) is prevented. Up to several hundred shake flasks can be attached to a base tray for the cultivation of microorganisms in temperature-controlled incubators. The base tray with the shake flasks is moved in a circular motion with an equipment-specific eccentricity (2.5–5 cm) at rotational speeds that may reach >300 rpm. The power input from the rotary motion passed to the flask system via the walls of the shake flasks causes the reaction mixture to mix and for heat and mass to be transferred [2].

The most important reaction-engineering differences between the simple shake flask without baffles and the stirred-tank reactor are: (i) the small ratio of the maximum local energy dissipation in the shake flask to the mean power input – the power consumption in the shake flask is much more evenly dis-

tributed than in the stirred-tank reactor [3, 4]; (ii) the lack of control of important process variables (such as pH and pO_2), and; (iii) smaller maximum oxygen mass transfer coefficients, due to the surface aeration in the shake flask: $<0.1\ s^{-1}$ compared to $<0.35\ s^{-1}$ [6].

Most ways of modifying the reaction-engineering properties of shake flasks relate to an improvement in the mass transfer between the gas phase outside the shake flask and the liquid phase inside the shake flask. To this end, in one investigation a convective gas exchange between shake flask and environment was implemented, instead of the usual diffusive gas exchange. In the simplest case, the Erlenmeyer flask was replaced by a cylindrical or quadratic reaction vessel, which had a thin sterile membrane that enabled gas exchange with the environment, and that covered the whole capacity at the top of the vessel [7]. As a result of the larger exchange surface than the shake flask, and the abridged diffusion path, the diffusive gas exchange between the reaction vessel and the environment was improved. By shaking these reaction vessels in the incubator, convective mass transfer was achieved through the thin sterile membrane, in addition to improved diffusive mass transfer. Using this arrangement, an overall oxygen mass transfer coefficient of $0.07\ s^{-1}$ was measured at a rotation speed of 200 rpm (an increase of a factor of four compared to a 1000 ml shake flask).

Although the direct convective gas exchange requires more complex apparatus in every shake flask (the injection of sterile gas via a needle into the head space of the shake flask [8, 9]), the significant advantage of this direct convective gas exchange is the possibility of influencing the oxygen transfer rate in the liquid phase, by adjusting the oxygen content in the added gas. In this way, the same oxygen transfer rates can, in principle, be achieved in the shake flask as in a stirred-tank reactor with air sparging.

2.2 Shaken Microtiter Plates

Microtiter plates are plastic (polystyrene or polypropylene) or glass plates with stamped cylindrical indents ("wells"). The usual microtiter plates applied for the cultivation of microorganisms have up to 96 wells with working volumes of up to several 100 µl per well. Microtiter plates are used, along with microtiter plate spectrometers and liquid handling systems (lab-robots), for the automation of wet-chemical analyses and for automated measurements of the growth of cells and microorganisms (turbidimetric analysis). As well as the automation of toxicological investigations, the parallel cultivation of microorganisms enables time-effective screening of strains or reaction conditions in shaken microtiter plates [10].

For batch cultivation of microorganisms in wells, microtiter plates must be moved in circular paths, analogous to shake flasks, with rotation speeds of up to 300 rpm and an eccentricity of 50 mm or with rotation speeds of up to 900 rpm and an eccentricity of 6 mm, in order to produce both sufficient mixing and sufficient oxygen transfer rate by means of surface aeration [11].

Oxygen transfer capacities analogous to shake flasks are possible in microtiter plate reactors. Higher oxygen mass transfer rates (up to 0.1 s^{-1}) can be achieved in deep-well microtiter plates at high rotation speeds, if the liquid volume is small. In this case most of the liquid forms a thin film on the wall of each well. It should be noted that the operating conditions commonly used for shaking machines will not produce the same oxygen mass transfer capacities in microtiter plates as in shake flasks.

Microbial growth can only be monitored in microtiter plate reactors, however, up to cell densities of 0.2–0.3 g l^{-1}, if the cell density is recorded directly with a microtiter plate spectrometer, using turbidimetric analysis.

2.3 Parallel Stirred-Tank Reactors

In order to be able to operate as many as possible stirred-tank reactors in parallel, small stirred-tank reactors have been combined into units of 4–6 reactors. With a working volume of 300–500 ml, all important process variables (temperature, stirrer speed, pH and pO_2) can be individually controlled in each stirred-tank reactor operated in parallel. The power is generally fed in using magnetically-coupled stirring bodies. In most cases, the oxygen mass transfer coefficient is as lower, as in stirred-tank reactors individually operated on a semi-technical scale, especially if the stirrer bar is operated at the bottom of the vessel. The expenditure on apparatus is considerable: 18 pumps are needed for 6 miniaturized stirred-tank reactors if an individual substrate feeding should also be enabled, as well as the acid and base addition for the pH control.

2.4 Parallel Bubble Columns

Bubble columns represent mass transfer and reaction equipment in which a gas phase and a liquid phase are brought into contact. The gas phase is dispersed in the liquid phase in the form of bubbles. Bubble column reactors are characterized by their simple construction and the absolute absence of any mechanical moving equipment. Small-scale bubble columns with a diameter of 6 cm and a working volume of 100–300 ml are employed simply as "shake flasks without shaker" [12–14]. In contrast to the shake flask, a decrease in the liquid volume is not required to achieve high oxygen transfer rates, and an interruption of the gas supply through off-line sampling is avoided.

The choice of the gas distributor and its design are critical for mass transfer in bubble columns. The simplest possibility for gas dispersion is provided by static spargers, such as perforated plates or sintered plates. The latter are particularly well suited for obtaining small gas bubbles and homogeneous bubble distributions across the entire column cross-section. The oxygen mass transfer coefficient is a function of the superficial gas velocity and the average pore diameter of the sparger [15]. The increase in the mass transfer coefficient

is particularly pronounced for small pore diameters and high superficial gas velocities. An oxygen mass transfer coefficient of 0.2 s^{-1} has been theoretically and experimentally estimated for a superficial gas velocity of 0.7 cm s^{-1} and a pore diameter of 10 µm (non-coalescing Newtonian fluids with low viscosities). Consequently, significantly higher oxygen mass transfer coefficients than in the shake flask can be achieved under optimum conditions for pore diameters below 20 µm and superficial gas velocities above 0.4 cm s^{-1}.

The power input in small-scale bubble columns increases with rising superficial gas velocity, and slightly increases with decreasing average pore diameter of the static sparger [15]. At a fluid column height of 7 cm, for example, a power input of 100 W m^{-3} is achieved at a superficial gas velocity of 0.4 cm s^{-1} with an average pore diameter of 10 µm. This is rather low compared to the power inputs of stirred-tank reactors, which are generally above 1000 W m^{-3}.

A reaction-engineering comparison of the shaken microtiter plate, the shake flask, the small-scale bubble column, and a stirred-tank reactor indicates that the small-scale bubble columns should be classified between shake flasks and stirred-tank reactors with respect to the number of parallel reactors, working volume, and oxygen transfer (see Table 1). Only with respect to the maximum power input is this classification incorrect: the maximum power input of a small-scale bubble column amounts to 200 W m^{-3} and is therefore more than one magnitude below the maximum possible power input to shake flasks (4500 W m^{-3}), which is of the same order of magnitude as in stirred-tank reactors [3]. As a consequence, biological systems in which the (local) energy dissipation influences the reaction may show a different process performance in small-scale bubble columns. Examples are microorganisms whose morphology depends on the energy dissipation in the reactor: in the case of low energy dissipation, pellets may be formed with diameters of several millimeters. The morphology and the resultant mass transfer limitations in the pellet may often influence the biological reaction.

Another consequence of the low power input in small-scale bubble columns is that the parameters that characterize the mass transfer may be sensitive to changes in physical properties during the reaction. In particular, the

Table 1 Reaction engineering comparison of shaken microtiter plates, shake flasks, small-scale bubble columns and parallel stirred-tank reactors used in the parallel cultivation of microbial cells

	Microtiter plate	Shake flask	Bubble column	Stirred-tank
Number of parallel reactors	~1000	~100	<16	<6
Working volume (mL)	<1	<100	<300	~500
Power input, (W L^{-1})	?	<4.4	<0.2	<8
Oxygen mass transfer coefficient (s^{-1})	<0.1	<0.1	<0.2	<0.35

surface tension of the reaction medium has a greater influence on small-scale bubble columns than on the shaking flask or the stirred-tank reactor. The surface tension in small-scale bubble columns essentially determines the primary bubble diameter at the static sparger, and therefore the average bubble diameter, the bubble rising velocity and the gas hold-up in the reaction medium. All of these parameters influence the oxygen mass transfer coefficient.

One possible way to overcome any problems that arise that may be related to a lower power input is to use magnetic stirrers, which can easily be used in small-scale bubble columns [16].

3
Parallel Feeding Technology

3.1
Early Approaches

Initial approaches to parallel fed-batch process control in shake flasks were published as early as the beginning of the 1950s [17]. With the aid of an "increment-fed shaker system", one substrate could be fed simultaneously to up to 40 shake flasks. In this case, every shake flask was connected to an system that could inject 50 ml of substrate. The pistons in all injection systems were moved with the aid of a stepping motor, where the mechanical piston stroke was transmitted via correspondingly shaped feeding disks to 8 injection systems arranged in a line in each case. The shape of the feeding disks and the speed of the stepping motor determined the feeding profile. Over 24 hours, up to 50 ml of substrate can be fed into a shake flask.

Simple diffusive processes were also employed as an alternative to the convective feeding of substrates to shake flasks [18]. Pellets of concentrated substrates were formed and coated with a polymer, which allowed the diffusive transport of the enclosed substrate. With the aid of this diffusive substrate feeding, it was also possible to realize the smallest feeding quantities. However, scale-up of the "optimum" number of substrate pellets in the shake flasks into a substrate feeding profile in the stirred-tank reactor proved difficult.

A modernized variant of the increment-fed shaker system was realized with the aid of multi-channel injection pumps [19]. The shake flasks were connected with substrate filled injection systems, which were inserted into multi-channel injection pumps. With the aid of this parallel proportioning technology, continuous substrate volume flows of a minimum of 160 µl h^{-1} could be realized. Also, different substrate quantities could be fed in with a multi-channel injection pump, through the selection of different injection diameters.

Requirements for a feeding technology for a maximum high number of parallel small-scale reactors are: (i) small feeding volumes; (ii) feeding accuracy that is adapted to the small reaction volume; (iii) sterile feeding, and; (iv) pH

control of the individual small-scale reactors. It is necessary to maintain a physiological pH value in individual parallel small-scale reactors in many cases in the single batch approach. Additional feeding of substrates (and therefore the subsequent increases in cell density and product and secondary product concentrations) generally makes individual pH control mandatory. The possibility of maintaining physiological pH values through the integration of suitable buffer systems is very unlikely. This means that the parallel feeding of a substrate in small-scale reactors is generally only appropriate if a parallel pH control is also available.

3.2 Intermittent Feeding and Parallel pH Control

A valve distributor enables the fed-batch operation of parallel reactors using only one high-precision piston pump (see Fig. 2). If a pre-determined substrate quantity should be dosed into a reactor with the aid of the precision pump, the corresponding 2/2-way valve is opened, the necessary substrate quantity is dosed, and, after releasing the discharge pressure built up during the feeding procedure, the previously-opened 2/2-way valve is closed. This ensures that the quantity supported by the pump is also fed exactly into the respective small-scale reactor [20]. Parallel feeding into small-scale reactors is implemented intermittently, and every individual feeding is linked to the minimum feeding quantity of the equipment employed. This means that the required feeding quantity time-profile is approximated in the form of a step function (see Fig. 2).

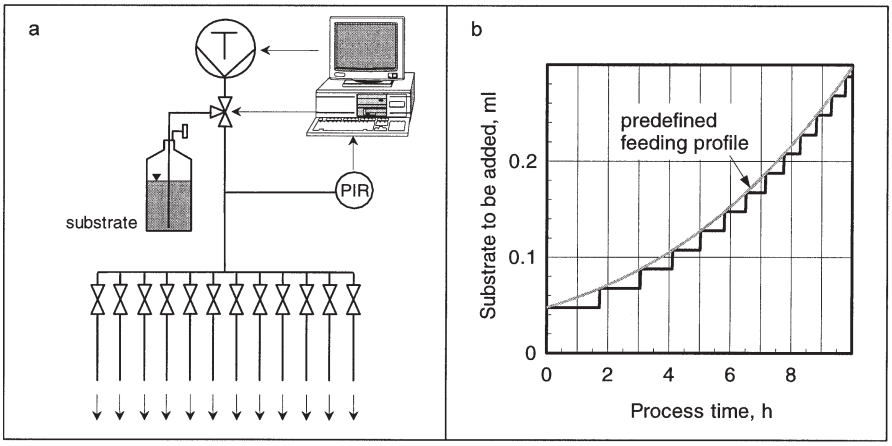

Fig. 2 **a** Scheme for the intermittent feeding assembly for individual substrate or base/acid addition into up to 16 small-scale bioreactors. **b** Scheme for the approximation of a predefined feeding profile with the intermittent feeding assembly

The accuracy of this intermittent feeding is dependent on: (i) the minimum feeding quantity; (ii) the maximum feeding speed; (iii) the necessary delay after a feeding procedure, and; (iv) the number of parallel reactors.

The minimum feeding quantity depends on the "step resolution" of the piston pump and the way the feeding lines are connected to the small-scale reactors. The minimum possible liquid drop that can detach from the point of the needle generally represents the minimum feeding quantity. Therefore, the minimum feeding quantity is a function of the surface tension, the density, and the viscosity of the liquid to be dosed. The maximum feeding speed is basically determined by the viscosity of the liquid to be fed and the pressure characteristics of the piston pump.

The necessary delay to reduce the pressure after a feeding procedure is dependent on the feeding speed (and/or the built-up feeding pressure), the stiffness of the feeding tube material employed, and also the viscosity of the liquid to be fed.

The possible number of parallel reactors is dependent on the permissible deviation from the feeding quantity time-profile, the minimum feeding quantity, the realizable feeding speed, and the necessary delay after a feeding procedure.

For example, if a glucose solution of 500 g l^{-1} is to be fed, a minimum feeding quantity of 50 µl, a maximum feeding speed of 3 ml min^{-1}, and a minimum delay period after a feeding procedure of 20 s can be achieved (for Teflon tubes with a inner diameter of 0.8 mm and an overall length of 1.7 m at 22 °C). Therefore, feed-flows of 9.4–1800 µl min^{-1} can be realized in 16 small-scale reactors operated in parallel, if the maximum interval between two feedings into a reaction vessel should be less than 15 minutes.

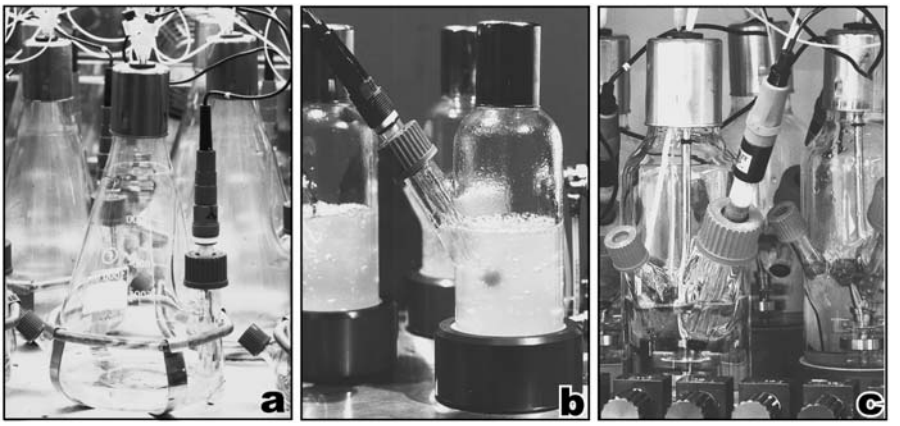

Fig. 3a–c Photographs of parallel bioreactors with autoclavable pH probes in an incubator chamber. **a** 1000 ml shake flask (working volume 100 ml). **b** 500 ml small-scale bubble column (working volume 200 ml. **c** 500 ml stirred column (working volume 200 ml)

This intermittent feeding technology that uses a piston pump and a valve distributor is also capable of being used with parallel pH control. In this case, the quantities of base/acid to be fed are not specified over feeding quantity-time profiles before the beginning of the parallel investigations, but need to be generated online by pH controllers. Each of the parallel small-scale reactors is provided with an autoclave-capable pH probe (see Fig. 3a). Using parallel amplifiers, the data are made available to a process computer. With the aid of parallel-implemented single PI controllers with "anti-wind-up" mechanisms, a functional parallel pH control is enabled.

The performance of this parallel pH control has been demonstrated with the parallel cultivation of the bacterium *Escherichia coli* in shake flasks [21]. After inoculating the 500 ml shake flasks each equipped with pH probe, and in each case filled with 100 ml buffered mineral salt medium and glucose, they were operated for 4.5 h in batch cultivation at 37 °C with 200 rpm and an eccentricity of 3.3 cm, and the pH in the individual shake flasks was recorded (see Fig. 4). After consumption of the initial 6 g l^{-1} glucose, a glucose solution with 500 g l^{-1} glucose was fed into all nine parallel shake flasks, where a linearly increasing feed flow was realized (8.7 µl min^{-1} to 42.85 µl min^{-1} from 5.5 to 9.5 h).

The pH fell from 7.0 at the beginning to values around 6.5 (see Fig. 4). After activating the parallel pH control, and using 10% NH_4OH for titration, the pH was controlled in all parallel shake flasks with a deviation of ±0.1 pH units maximum to the specified set-point of pH 7.0.

The concentrations of *E. coli* cells in the individual shake flasks indicated deviations commonplace in biological systems (see Fig. 4). After 12 h, a cell density of an average 5.1 g l^{-1} dry cell weight was reached. In the shake flasks with uncontrolled pH cell densities of a maximum of 2.5 g l^{-1} dry cell weight were be achieved (with addition of 20 g l^{-1} glucose), due to the pH drop, up to pH 5.0. The relative standard deviation in the cell densities reached in the parallel approach was 12.6% with a process time of 12 h.

4 Application Examples

In this section, the performances of parallel reactor systems in bioprocess development will be characterized via 3 examples: (i) *Escherichia coli* BL21 (DE3)pLysS, with the gene *rbf*M of *Salmonella enterica* under the control of the *lac*-promotor for the production of the enzyme GDP-α-D-mannose-pyrophosphorylase [12, 21]; (ii) *Staphylococcus carnosus* pXPhCT2 for the expression of synthetic human calcitonin precursors under the control of a xylose inducible promoter [22], and; (iii) recombinant *Bacillus subtilis* for the manufacture of riboflavin, which was made available by Roche Vitamins, Kaiseraugst, Switzerland.

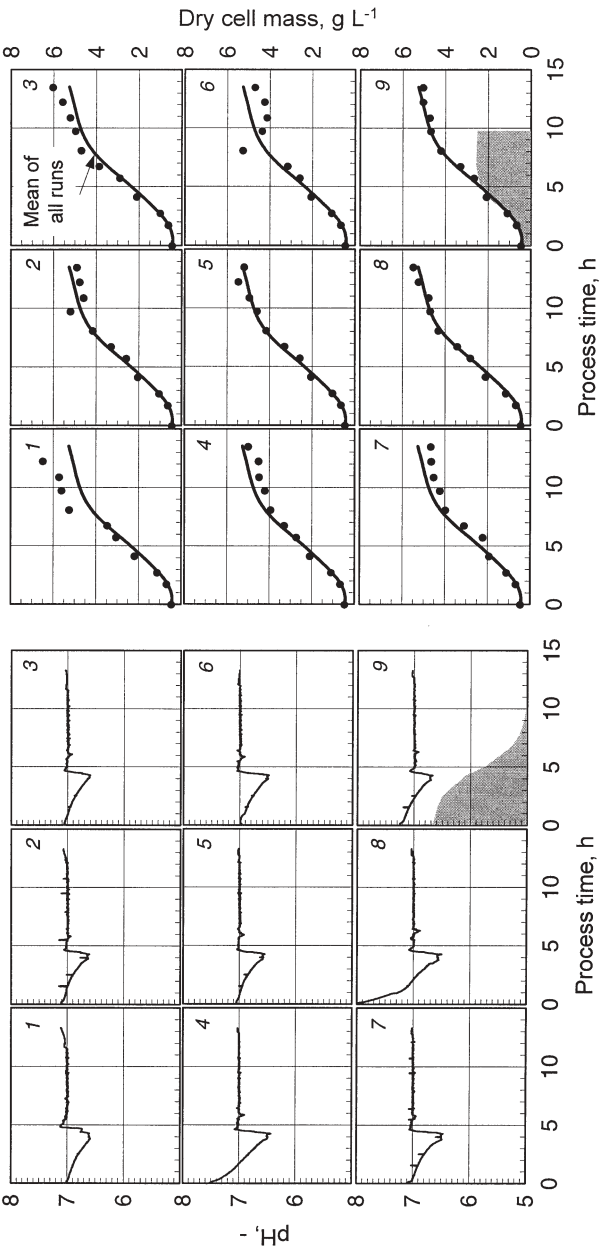

Fig. 4 Parallel fed-batch cultivation of *E. coli* in pH controlled shake flasks. On-line measured pH compared to the pH uncontrolled shake flask (shaded area), off-line measured optical density expressed as dry cell mass concentrations (filled circles), and mean of all pH controlled parallel runs (lines) compared to the pH uncontrolled shake flask (shaded area) at the same operaing conditions: 500 ml shake flasks with 100 ml of mineral medium, operated at 200 rpm (with an eccentricity of 3.3 cm), at 37 °C, with a linear gradient intermittent feeding of 8.7 up to 42.85 µl min^{-1} with 500 g l^{-1} sterile glucose (process time 5.5–9.5 h); base addition was performed with 10% NH_4OH at a pH set-point of 7.0

In the following, parallel feeding assemblies (fedbatch-pro, DASGIP, Germany) were used for individual feeding of substrates and for individual base addition for pH-control [12, 21, 23]. Up to 16 small-scale bubble columns, with a working volume of 200–400 ml (see Fig. 3b), were operated in parallel in an incubator chamber (PROFORS, Infors, Switzerland). First prototypes of stirred columns were applied in a few experiments (see Fig. 3c). A stirred column was constructed by modifying a standard small-scale bubble column. A bottom bearing was installed for the stirrer shaft in the middle of the static sparger. The permanent magnets and the stirrers (both equipment from Sixfors, Infors AG, Switzerland) were fixed to the stirrer shaft, which was held in a vertical position by a top bearing. A flat-bladed disc turbine with six blades and an outer diameter of 28 mm was used [16].

4.1 Parallel pH Control

Individual pH control is a primary prerequisite for higher cell concentrations in parallel reactors, particularly when utilizing defined media. This is investigated via the two expression systems *Escherichia coli* and *Staphylococcus carnosus* (see Fig. 5). Cell densities of 0.6 g l^{-1} (*S. carnosus*) and 2.5 g l^{-1} (*E. coli*) can usually be achieved in uncontrolled shake flasks at sufficiently high rotation speed. One reason for this limitated cell density in the shake flasks is the missing pH control. Below pH 6.0 (*S. carnosus*) and pH 5.5 (*E. coli*) growth stops. If, on the other hand, the parallel reactor is coupled to a parallel pH control, higher cell densities are made possible: the cell density of *S. carnosus* can be increased by a factor of five or more to 3.2 g l^{-1}. Far higher cell densities are possible with pH control in the case of *E. coli* too. However, where glucose is used as a carbon source, the substrate must be added simultaneously in the parallel approach, in order to limit the growth rate of *E. coli* and to suppress acetate formation.

4.2 Oxygen Transfer

The oxygen transfer capacity of the parallel reactor system can represent the limiting process variable in aerobic processes. This especially applies to the case where high cell densities are enabled by parallel pH control and intermittent substrate feeding. In principle, the highest oxygen transfer rates can be achieved in stirred columns (see Fig. 6). Even with relatively small superficial gas velocities, similar oxygen mass transfer coefficients to those obtained in technical stirred-tank reactors (>0.15 s^{-1}) become possible. This oxygen transfer rate is only achieved in bubble columns with high superficial gas velocities (0.5–0.6 cm s^{-1}), as shown by experimental investigations and mass transfer modeling. The maximum mass transfer rate in shake flasks (OTR_{max}<80 mM h^{-1}) is possible only at high rotation speed and for very small filling volumes [2].

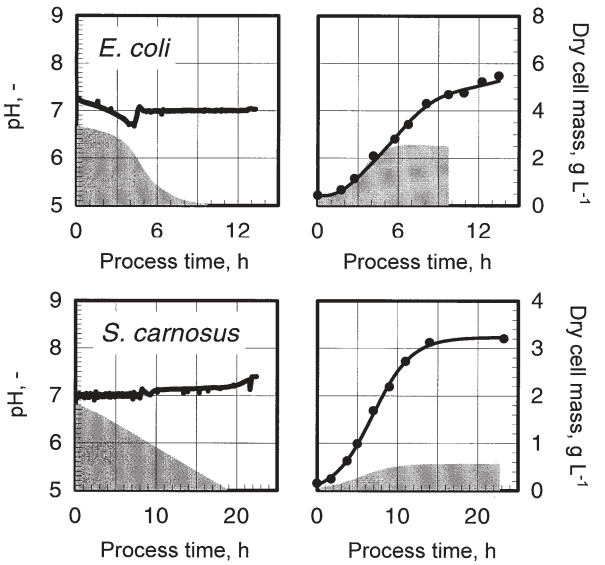

Fig. 5 Fed-batch cultivation of *E. coli* and *Staphylococcus carnosus* in small-scale bioreactors (shake flask, bubble column) with pH control (the line is the mean of all parallel runs) and without pH control (shaded area)

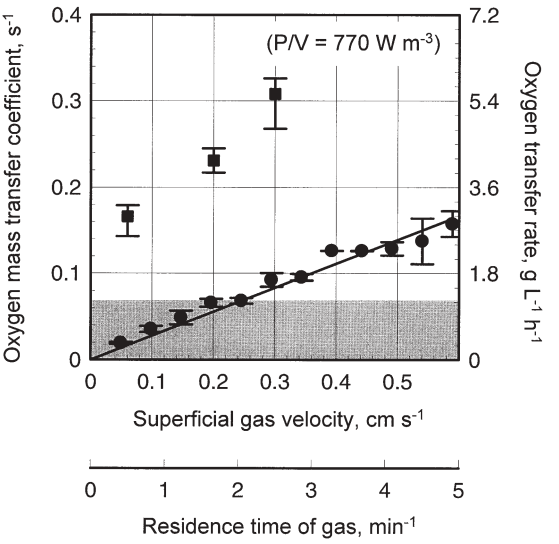

Fig. 6 Oxygen mass transfer coefficient and maximum of the oxygen transfer rate at Δc_{O2}= 5 mg O_2 l^{-1} in parallel bioreactors with a mineral *E. coli* medium for shake flask (shaded area), bubble column (filled circles), stirred column (filled squares), as function of the superficial gas velocity (aeration with air) measured via the dynamic nitrogen desorption method

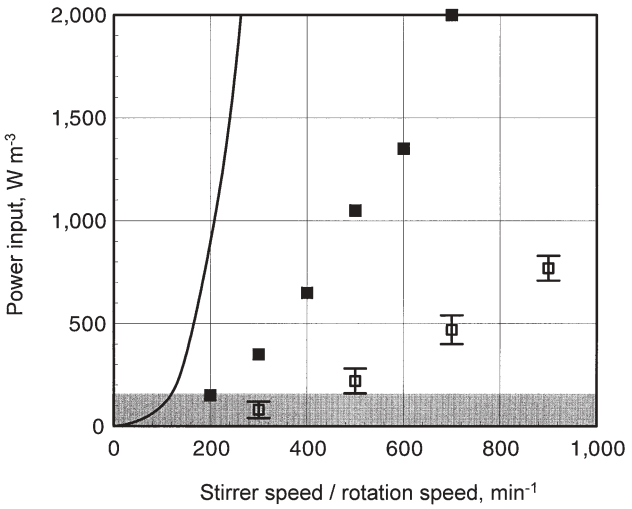

Fig. 7 Power input in parallel bioreactors with a mineral *E. coli* medium for 1000 ml shake flask with a working volume of 100 ml (line), bubble column (shaded area), stirred columns without (empty squares) and with (filled squares) baffles

4.3 Power Input

The volume-related power input represents a further important process variable, in particular in the case where the power input co-determines the morphology and/or aggregate structure and therefore the synthesis capacity of the biocatalysts. Here again, the parallel reactor systems considered have significant differences (see Fig. 7): while the power input in parallel bubble columns does not exceed 100 W m^{-3} and therefore is more than an order of magnitude below that of the stirred-tank reactor, high power inputs are already being achieved in shake flasks with small rotation speeds. The volume-related power input of the stirred column (with baffle plates) is comparable to shake flasks, since both reaction systems are operated over different speed ranges (shake flask <400 min^{-1}, stirred column <1200 min^{-1}) but with comparable Newton numbers.

4.4 Scale-Up and Scale-Down

Controlled parallel reactor systems enable the development of fed-batch processes, in particular during bioprocess development, as well as optimization of the reaction conditions under controlled process conditions in the parallel approach. An example of this is the development of an induction process for the effective expression of a heterologous protein (GDP-α-D-man-

nose-pyrophosphorylase) in *E. coli* under the control of the *lac*-Promotor [12]. The induction profile was formulated as a double-sigmoid function, and the resulting six model variables were experimentally determined with the aid of a stochastic search strategy. The fed-batch process, optimized in the parallel approach, can be transferred directly from the 200 ml scale into the 4 L laboratory stirred-tank reactor, and so the enzyme activity was increased by a factor of 3.5 to more than 700 U l^{-1}. For substrate-limited processes, as in this case, this means that the substrate must be also added intermittently, as in the parallel approach.

A further application of this controlled parallel technology is the optimization of current commercial production processes. Further development of production strains, in parallel with on-going production, requires an evaluation of new strain variants under process conditions. For this, controlled stirred-tank reactors on a laboratory scale have been employed up to now in a sequential manner, so this evaluation is generally the rate-determining step of the process improvement.

The performance of the parallel reactor system was studied for the example of the scale-down of the industrial production process to the manufacture of riboflavin with *Bacillus subtilis*. Initially, only small-scale bubble columns with high superficial gas velocity and stirred columns were taken into consideration as controlled parallel reactors, due to the required oxygen transfer capacity. A scale-down can succeed only if all process variables are transferred as exactly as possible to the 200 ml scale. The boundary conditions, specific to each reaction system, must be considered. For example, the higher vaporization rate at higher superficial gas velocity in the small-scale bubble column must be balanced by lower substrate concentrations during the feeding. In the parallel approach, the reaction conditions must be adjusted as far as possible to the reference system on the technical scale. Fig. 8 shows some selected state variables (pH, temperature, oxygen mass transfer coefficient, pO_2) achieved in the small-scale bubble columns, as compared to those from a laboratory-scale stirred-tank reactor.

One difference between stirred-tank reactors and small-scale parallel bubble columns, in regards to the characteristics of the oxygen partial pressure, is especially clear: due to the intermittent substrate feeding, the pO_2 decreases rapidly each time a substrate pulse is added. After consumption of the added glucose by the microorganisms, the pO_2 increases until glucose is added again. The minimum pO_2 is decisive for the scale-down. As far as possible, it should not fall significantly below the pO_2 of the reference process.

In spite of the careful transfer of all process variables from the laboratory-scale stirred-tank reactor to the small-scale bubble columns, it was, initially, not possible to achieve the same process performance at the small scale: the state variables (biomass and riboflavin concentrations as well as yields) were reduced in the parallel approach throughout the whole process to an average of 65% of the state variables of the fed-batch process in the stirred-tank reactor. Finally, increasing the power input through the use of stirred columns in the

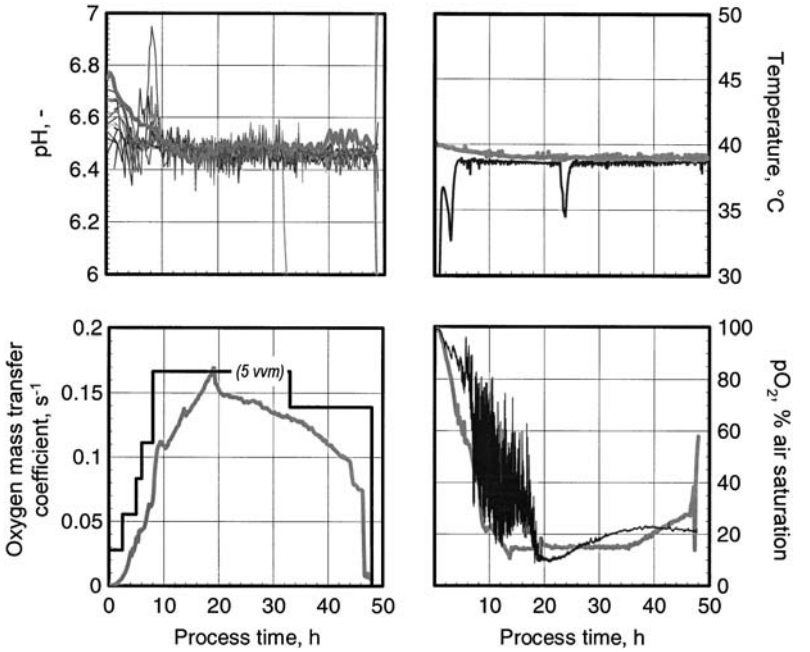

Fig. 8 Scale-down of the riboflavin fed-batch production process with *Bacillus subtilis*: pH, temperature, oxygen mass transfer coefficient and pO_2 as functions of the process time in pH controlled parallel operated small-scale bubble columns and in the 20 l stirred-tank reactor (gray lines) used as reference

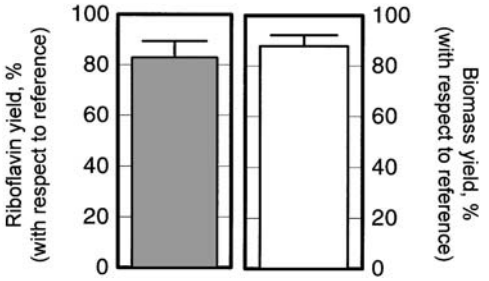

Fig. 9 Scale-down of the riboflavin fed-batch production process with *Bacillus subtilis*: yields in pH-controlled stirred columns after 48 h (with respect to the reference fed-batch process in a stirred-tank reactor on a 20 l scale)

parallel approach enabled an almost complete scale-down of the industrial production process (see Fig. 9). Microscopic investigations indicated reinforced agglomerations of product crystals and cells in small-scale bubble columns due to the low power input, so that mass transfer limitations were probably responsible for the smaller product and biomass concentrations.

5 Discussion and Outlook

Parallel reactor systems, with intermittent substrate feeding and pH control, can enable a more effective process development, since up to 16 times the data can be gained at the same time. However, the selection of a suitable parallel reactor system requires a particular degree of bioprocess knowledge, in particular of the oxygen consumption and the power input. Also, the scale transfer (scale-up and/or scale-down) must be implemented carefully. In particular, the limits of the parallel reaction systems must be known and taken into consideration. Online respiration activity measurement, which is now available for shake flasks, can help to evaluate the physiological state of an aerobic culture at small scales [24].

The estimated errors in the process variables in parallel reactor systems with intermittent substrate feeding and pH control (including biomass concentration, product concentration, and yields), in particular for end point determinations, can be greater than in a simple batch investigation in a shake flask, since all process interventions have associated inherent imprecisions (intermittent feeding, pH control, temperature control, superficial gas velocity, …). Generally, with end point determinations, standard deviations of 10–15% are observed.

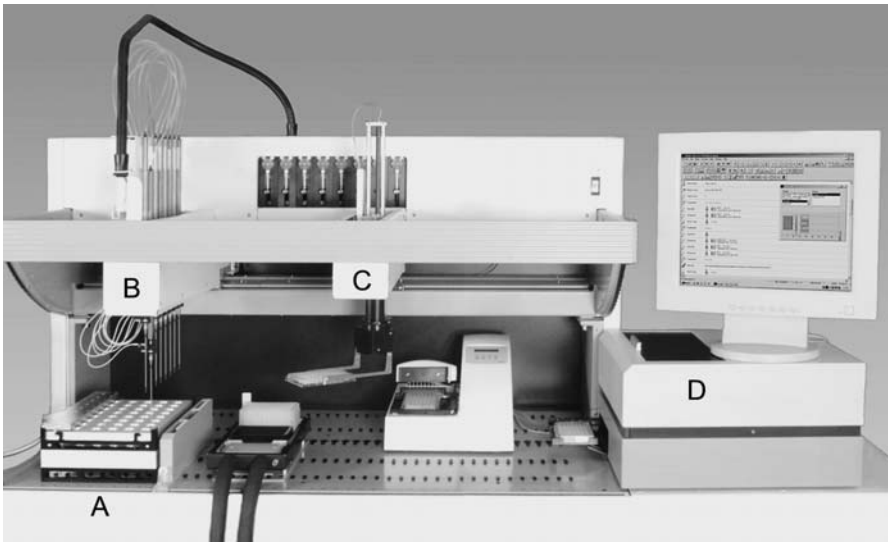

Fig. 10 Photograph of the prototype of a unit of 48 parallel ml-scale stirred-tank reactors (A) controlled by a liquid handling system (B, C) and equipped with a microtiter plate reader (D) for automation of at-line analytics (optical density, metabolite concentrations)

As well as a parallel cultivation technology, parallel optimization strategies are required for effective bioprocess development. Stochastic search strategies, for example Genetic Algorithms, appear especially suitable for this, particularly if many variables have to be considered and several objectives need to be pursued simultaneously [25].

In the future, far more than 16 parallel bioreactors will be necessary for a whole series of applications; for example, if parallel reactor systems are used with screening procedures. With the technologies described above, there are limits on further paralleling, and the automation cannot be increased much more. To overcome these limitations, units of 48 parallel stirred-tank reactors at the ml scale are being developed with temperature control, individual pH control and pO_2 monitoring, which can be fully automated and operated sterile with a liquid handling system (see Fig. 10). The liquid handling system allows intermittent substrate addition, base or acid addition for individual pH control, and automated at-line analysis (optical density, metabolite concentrations and other state variables) [26–28].

References

1. OECD (2001) The application of biotechnology to industrial sustainability. OECD Publications Service, Paris, p 69
2. Maier U, Losen M, Büchs J (2004) Biochem Eng J 17:155–167
3. Büchs J, Zoels B (2001) J Chem Eng Jpn 34:647
4. Büchs J, Maier U, Milbradt C, Zoels B (2000) Biotech Bioeng 68:594
5. Büchs J, Lotter S, Milbradt C (2001) Biochem Eng J 7:135
6. Maier U, Büchs J (2001) Biochem Eng J 7:99
7. Kato I, Tanaka H (1998) J Ferment Bioeng 85:404
8. Tanaka H, Ishikawa H, Nobayashi H, Tagaki Y (1991) J Ferment Bioeng 72:204
9. Kamoshita Y, Ohashi R, Suzuki T (1998) J Ferment Bioeng 85:218
10. Duetz WA, Ruedi L, Hermann R, O'Connor K, Büchs J, Witholt B (2000) Appl Environ Microbiol 66:2641
11. Hermann R, Lehmann M, Büchs J (2003) Biotech Bioeng 81:178
12. Altenbach-Rehm J, Nell C, Arnold M, Weuster-Botz D (1999) Chem Eng Technol 22:1051
13. Weuster-Botz D, Altenbach-Rehm J (2000) US patent US6,063,618
14. Weuster-Botz D, Altenbach-Rehm J (2002) European patent EP0845029
15. Weuster-Botz D, Altenbach-Rehm J, Hawrylenko A (2001) Bioproc Biosys Eng 24:3
16. Weuster-Botz D, Stevens S, Hawrylenko A (2002) Biochem Eng J 11:69
17. Dale RF, Amsz J, Shu P, Peppler HJ, Rudert FJ (1953) J Biotech 43:213
18. Pirt SJ (1975) Principles of microbe and cell cultivation. Blackwell, Oxford, UK
19. Westgate PJ, Curtis WR, Emery AH, Hasegawa PM, Heinstein PF (1991) Biotech Bioeng 38:241
20. Drescher T, Altenbach-Rehm J, Weuster-Botz D (2001) US patent US6,202,713
21. Weuster-Botz D, Altenbach-Rehm J, Arnold M (2001) Biochem Eng J 7:163
22. Elling K, Ritter J, Verseck S (1996) Glycobiol 6:591
23. Dilsen S, Paul W, Herforth D, Sandgathe A, Altenbach-Rehm J, Freudl R, Wandrey C, Weuster-Botz D (2001) J Biotechnol 88:77
24. Anderlei T, Zang W, Papaspyro M, Büchs J (2004) Biochem Eng J 17:187–194

25. Weuster-Botz D (2000) J Biosci Bioeng 90:473
26. Puskeiler R, Zacher KH, Weuster-Botz D (2002) German patent application DE10260691.9
27. Puskeiler R, Zacher KH, Ducret A, Weuster-Botz D (2003) Stirred-tank bioreactors at ml-scale. In: Book of abstracts 21. DECHEMA-Jahrestagung der Biotechnologen, DECHEMA, Frankfurt, p V13
28. Institute of Biochemical Engineering, Technische Universität München (2004) Homepage. http://www.mw.tum.de/biovt/

Received: March 2004

Adv Biochem Engin/Biotechnol (2005) 92: 145–172
DOI 10.1007/b98921

From Stationary to Instationary Metabolic Flux Analysis

Wolfgang Wiechert (✉) · Katharina Nöh

Department of Simulation, Institute of Systems Engineering, University of Siegen, Paul-Bonatz-Strasse 9–11, 57068 Siegen, Germany
{wiechert,noeh}@simtec.mb.uni-siegen.de, WWW: www.simtec.mb.uni-siegen.de

Abstract Metabolic flux analysis using ^{13}C labeled substrates is an important tool for metabolic engineering. Although it has now been evolving for more than ten years, metabolic flux analysis has still not reached the limits of its application. Current developments aim at extending to instationary industrial production conditions like batch and fed-batch fermentations on the one hand, and at miniaturization and high throughput flux analysis on the other. In both cases, reducing the duration of the labeling experiment is of major interest. For that reason, there is now interest in the instationary transient of the ^{13}C enrichment during a labeling experiment. This paper presents some recent developments in the field of instationary metabolic flux analysis and discusses some critical aspects and limitations using some simulation examples.

Keywords Instationary metabolic flux analysis · Carbon labeling experiments · Repeated sampling · High throughput flux analysis · Network simulation

Abbreviations and Symbols

MFA	metabolic flux analysis
CLE	carbon labeling experiment
A	amplitude of ppp_1 flux fluctuation
$^{i}\mathbf{A}$	linear cumomer transition matrix
B,C,D,E	pool names in the simple example network
B,C,D,E	pool sizes in the simple example network
$^{i}\mathbf{b}$	bimolecular cumomer transition function
M	metabolite pool name
M#ijk	isotopomer or cumomer of M
m_{ijk}	isotopomer or cumomer fraction of M
$\mathbf{N}$	stoichiometric matrix
p	fraction of old biomass at stopping time
ppp_1	oxidative pentose phosphate pathway flux
q^{net}, q^{xch}	net and exchange flux of q
T	experiment stopping time
u,v,w,p,q,r	fluxes in the simple example network
v_{upt}	substrate uptake rate
v_{effl}	biomass efflux rate
$\mathbf{v}$	metabolic flux vector
$\mathbf{X}$	intracellular pool size vector
$x^{\star}$	stationary labeling fraction
$\mathbf{x}$	intracellular labeling state vector
$\mathbf{x}^{inp}$	input labeling state vector
$^{i}\mathbf{x}$	cumomer labeling state vector of weight i
X_{IM}	pool size of an intermediate metabolite pool
X_{BM}	pool size of a biomass pool
x_{IM}	labeling fraction of an intermediate metabolite pool
x_{BM}	labeling fraction of a biomass pool
$x_{WC}{}^{\star}$	washout corrected labeling fraction
σ	specific substrate uptake rate
μ	specific growth rate
α	ratio between intermediate and biomass pool size
γ	specific protein turnover

1 Introduction

1.1 Metabolic Flux Analysis

Metabolic Flux Analysis (MFA) has become a standard and widely used tool in metabolic engineering. It has been successfully applied to different classes of microorganisms like bacteria, eucaryotic cells and higher cells, as illustrated by [1–5]. The purpose of a MFA experiment is to determine all fluxes in a certain part of the metabolic network of a microorganism in vivo. Typically, the pathways of interest are the central metabolic pathways (including glycolysis, pentose phosphate pathway, citric acid cycle) but also parts of the biosynthesis pathways (like amino acid production).

In the course of the metabolic engineering cycle [6] of an organism under investigation, MFA serves as a tool to characterize its metabolic capabilities, to diagnose the effect of genetic manipulations, and to find possible targets for further genetic engineering. After more than a decade of development MFA has matured into a useful tool, that is not only restricted to academic use but – due to standardized experimental protocols, widely available measurement instrumentation and publicly available software systems – is now also widely used in industry.

More details about the historical development of MFA, the experimental procedures, required measurement equipment and the various applications can be taken from several review papers [7–11]. The focus of this contribution is on future perspectives of MFA, where we use simulation studies to illustrate some new concepts. Certainly, some of these methods will also find their way into industrial applications in the future.

In this contribution, MFA always refers to a ^{13}C MFA based on a carbon labeling experiment (CLE). This method has replaced the classical stoichiometric MFA which is generally less powerful but also much less complicated [12, 13]. On the other hand, stoichiometry is still an essential part of ^{13}C MFA which in fact extends stoichiometric MFA. An important difference is that the balance of metabolites related to energy metabolism (ATP, NADH, NADPH) are usually not included in ^{13}C MFA because they are susceptible to producing erroneous results [8]. In the following, the reader is assumed to be familiar with the basic procedure and terminology of CLEs [14]. Roughly, the following three steps have to be carried out (see Figs. 1, 2):

1. *Experiment*: A microbial culture is fed with a ^{13}C labeled substrate whose chemical composition is known precisely. Popular substrates are specifically labeled glucose (for example [1-^{13}C]), uniformly labeled glucose ([U-^{13}C]) or a mixture of both, but other substrates, like labeled lactate [15], are also used. The substrate molecules are then metabolized by the microorganisms. The labeled molecules are chemically rearranged, split into pieces and recombined in the metabolic pathways and cycles. Finally, ^{13}C isotopes can be

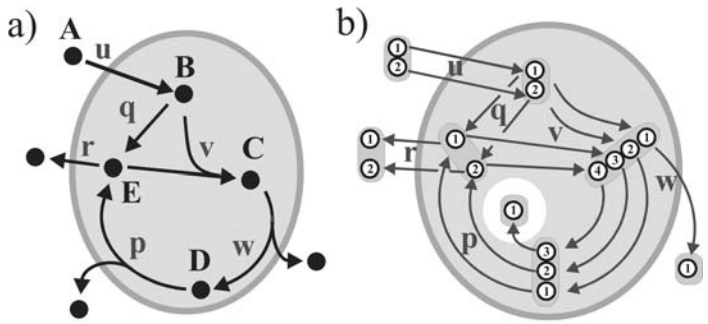

Fig. 1 Simple example networks used to illustrate a carbon labeling experiment. Left: metabolic network; right: carbon atom transition network. The input substrate is taken up by the cell and labeled carbon atoms are distributed over the complete network. The reaction step q takes place in both directions and is described by net and exchange fluxes q^{net}, q^{xch}. A set of free fluxes is given by u, q^{net}, q^{xch}

found in all intracellular intermediates and biomass components. A simulated CLE is shown in Fig. 2a for the simple example network shown in Fig. 1. While the metabolic fluxes remain constant during the whole experiment, the labeling enrichment in all intracellular pools shows a transient behavior starting with natural labeling and approaches a stationary state at the end.

2. *Measurement*: After a certain time for equilibrating the carbon labeling all over the network, the cells are disrupted, some preparative steps are carried out, and finally the labeling information is measured by various kinds of NMR or MS instruments [16–19]. Additionally, the extracellular fluxes that connect the observed metabolic network with its environment (including the substrate uptake, product formation, CO_2 production, biomass formation) are determined by standard mass balancing methods.
3. *Evaluation*: The intracellular fluxes that cannot be directly measured have to be estimated from the measurement data set. Essentially, this is a parameter fitting procedure based on a complex mathematical model describing the relation between the unknown fluxes and the measurements [20, 21]. A system analysis follows that is used to judge the identifiability and statistical quality of the estimated fluxes [22, 23]. These steps are supported by some software systems currently available [24].

1.2 Experiments under Instationary Conditions

A basic precondition of all currently established MFA procedures is *metabolic stationarity*, which means that all metabolic fluxes are constant during the complete duration of the CLE. Because all currently established MFA methods also rely on the assumption of an equilibrated labeling state, the experiment should take as long as possible to reach an *isotopic stationarity*, at least

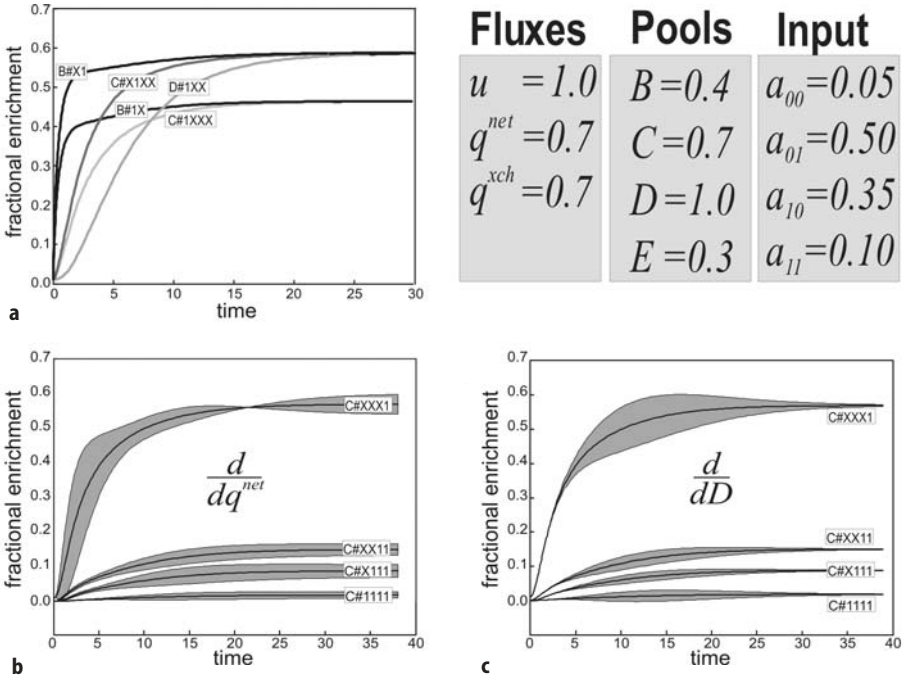

Fig. 2 Simulated time course of a ^{13}C labeling experiment with the simple example system from Fig. 1. Top: positional labeling fractions in some chosen carbon atom pools of B, C and D. Bottom left: (scaled) sensitivities of some chosen C cumomer fractions of weights 1–4 with respect to the flux q^{net}. Bottom right: (scaled) sensitivities of the same fractions with respect to pool size D. See also Fig. 3

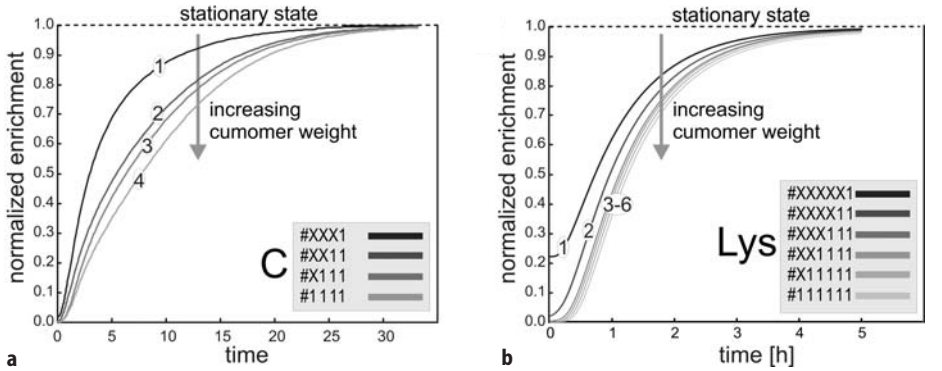

Fig. 3 Delayed convergence of cumomer fractions with increasing weight for: (left) some C cumomers in the simple example from Fig. 1 with the parameters from Fig. 2; (right) for some lysine cumomers in a complex *Corynebacterium* network with parameters given in the text

approximately (see Figs. 2a, 3). In practice a CLE is always prematurely terminated for several reasons:

1. A metabolically stationary state can be best established and monitored in a *continuous culture* where, in principle, arbitrarily long durations could be realized if the substrate costs were not limiting. This is also the reason why a labeling experiment has to be stopped after several biomass residences.
2. Experiments with a continuous culture do not always make sense because many recombinant microorganisms turn out to be instable. Moreover, the predominating industrial process conditions are *batch* and *fed-batch*. Therefore, one of the greatest challenges of MFA with respect to industrial applications is the extension of established methods to the case of metabolic instationarity with *slowly* changing fluxes. This condition for example is approximately fulfilled in the exponential or stationary growth phase of a batch culture or a fed-batch culture with non-limiting substrate and an approximately exponential feed strategy without rapid changes.
3. The other great challenge for the development of future MFA methods is the application to *high throughput screening* in order to characterize a large number of microorganisms in parallel experiments. This requires miniaturized bioreactors ranging from mini reactors to microtiter plates. Consequently, the sensitivity of the measurement equipment has to be strongly improved, because sample volumes have to be extremely small. Clearly, high throughput screening will predominantly be performed in batch culture to keep the process equipment as simple as possible. Moreover, microreactors cannot be precisely controlled over a long time span. Therefore, if labeling experiments are carried out at small scales the time duration of the labeling experiment – aside from many other problems – will again be an important issue.
4. In all experiments (especially with eucaryotic and higher cells) *population inhomogeneity*, *adaptation* and *synchronization* of microorganisms may play a role. It is well known that metabolism can be different in young and old cells due to ageing of microorganisms. For this reason, the experimental duration must be chosen to be as short as possible. As a consequence, the measured labeling information must be taken from the dynamic isotopic transient phase of the CLE. This transient starts with the initially unlabeled state of the system and proceeds to the stationary labeling state.

In each case it should be pointed out that at least approximately constant fluxes must be assumed. If this precondition is not sufficiently well satisfied, the currently available mathematical methods for data evaluation cannot be applied.

Summarizing, there are currently good reasons to strive to shorten the duration of CLEs. However, one drawback of such a premature termination is that the labeling state of the measured compounds is not equilibrated at stopping time, which leads to biased flux estimates with the currently available evaluation algorithms (see Sect. 3.4).

1.3 Different Kinds of Instationarity

1.3.1 Metabolic Instationarity

It has become clear that the word "instationary" has different meanings for a CLE. On the one hand, it can be used for metabolic fluxes, where basically four different situations can be encountered:

1. Metabolism is *completely stationary* during the labeling experiment. This is an ideal, but nevertheless it will be the standard assumption in the following text (except for in Sect. 5).
2. The fluxes are *almost stationary*, which means that they may be slowly changing, or fluctuating with small amplitudes and so they can be assumed to be approximately constant. Certainly, this case is much closer to reality. However, it is treated like the first case in practice.
3. If there are *macroscopically instationary* metabolic fluxes there is a significant change during the labeling experiment, which can be the case, for example, in a batch experiment where the experimental duration chosen is too large, in a fed-batch experiment where the feed is changing too quickly (for instance a substrate-limited bakers yeast production), in a continuous culture with mutation or contaminations, or in a synchronized oscillating culture (see Sect. 5).
4. Finally, *microscopically instationary fluxes* can be the case when every single cell has oscillating fluxes corresponding to the cell cycle, or when there is a population inhomogeneity. This situation is in general not visible in the population mean (see Sect. 5) but it will have the same effect as macroscopically instationary fluxes because a CLE is essentially modeled on the basis of a single cell model.

In general, if the fluctuations are too large, the fluxes must be considered to be macro- or microscopically instationary, and MFA becomes impossible. In Sect. 5.2 we investigate the extent to which fluctuations can be tolerated.

1.3.2 Isotopic Instationarity

On the other hand, the word "instationary" can be used with respect to the labeling state of the system. Here the following can be the case (see Figs. 2, 3):

1. The labeling state is *completely stationary*, which means that the isotopes have been completely equilibrated all over the intermediate metabolism and biomass components. In a strict sense it will take an infinite time to reach this state.
2. The labeling state is *almost stationary*, which means that its deviation from the stationary state can be neglected in flux analysis. Precisely, the difference

must be below the measurement precision of the NMR or MS instruments. In fact, no labeling experiment has ever been driven to this state, because this would be much too expensive (see Sect. 3.2).
3. The labeling state has reached *stationarity in intermediate metabolism* but not in the biomass compounds. In this case the asymptotic behavior of the system can be extrapolated from a washout correction (see Sect. 3.2) that makes use of the timescale separation between intracellular intermediates and biomass compounds. This correction is now common practice in MFA.
4. The time duration of the experiment is even shorter, which means that the labeling state of all cell compounds is still in the *early transient state* when the CLE is stopped. A future goal of MFA development is to carry out and evaluate such early-terminated experiments.

1.4 Classifying CLEs

It is now possible to classify carbon labeling experiments from the viewpoint of the experimental conditions. Depending on these conditions, it can be decided whether the experimental data can already be evaluated with the currently available computational methods or whether the development of new methods will become necessary. The "fact sheet" of a CLE has the following items:

1. *Process operation mode*: Experiments can be done in a batch, fed-batch or continuous culture. The essential difference with respect to data evaluation is that different kinds of data correction have to be applied in each case (see Sect. 3.3).
2. *Measurement equipment*: Although there are strong differences between NMR and MS instruments with respect to flux analysis, a detailed discussion of modern NMR and MS methods exceeds the scope of this contribution. Essentially, we can distinguish between ^{1}H NMR, ^{13}C NMR, 2D-NMR [7, 17] on the one hand and GC-MS, LC-MS [18, 19] on the other. In general, MS is much more sensitive than NMR and only very small sample amounts are necessary. This makes MS the more promising candidate for high throughput MFA.
3. *Measured substances*: Labeling information can be obtained from cell compounds like hydrolyzed protein, or directly from cellular intermediates. In many cases it is also possible to measure the labeling state of excreted products from the supernatant. With respect to the labeling dynamics, these products behave in a similar way as the intermediates because they are directly coupled to central metabolic pathways.
4. *Sampling times*: Sampling can be done, as in all classical CLEs, once at the end of the labeling phase or repeatedly over the time course of the experiment. The latter will be important if we do not wait for the stationary labeling state in the intermediate metabolites (see Sect. 4).

5. *Total pool sizes*: For the evaluation of isotopically instationary experiments from the transient labeling information of intracellular intermediates it is necessary to know at least a few of the total pool sizes of intermediary metabolites. The reason is that these pool sizes determine the time constants of the system (see Sect. 3.1). In contrast to labeling measurements, the problem with pool size measurements is that the loss of material in each preparation step must be precisely known. Nevertheless, due to the tremendous progress in MS technology in recent years, powerful analytical methods for quantitative metabolomics are now available.

1.5 Recent Progress

1.5.1 Experimental Progress

Some recent developments illustrate that instationary conditions are now well within the reach of experimental methods. Some new types of experiments have been developed very recently:

1. Several experiments have been reported where batch conditions have been used for the CLE. In [3, 25, 26] a small volume bioreactor is used to grow a *Streptomyces* strain. In [27, 28] a higher experimental throughput is achieved with shake flasks in order to characterize several mutants of a microorganism. Cell harvesting typically takes place in the mid-exponential phase.
2. The sensor reactor described in [29, 30] was designed to do CLEs along with an industrial fed batch or batch process. To this end, a sample is moved from a production bioreactor to the sensor reactor. Here, the process is driven synchronously to the large reactor by using a controller. Several fed-batch experiments have been done in the sensor reactor to achieve a serial flux mapping in the metabolically instationary time course of the production process [31].
3. Miniaturized reactors have been developed in several research teams. Mixing in a microplate system is characterized in [32]. Stoichiometric MFA is used for metabolic screening with Well-Plates in [33] on a sub-mililiter scale. In [34] parallel minireactor systems with integrated process measurement and control are described.
4. Rapid sampling techniques have been developed to draw samples at high frequencies while the intracellular metabolism is simultaneously stopped by methanol quenching [35–37].

1.5.2 Analytical Progress

Along with the experimental progress, analytical methods have also strongly improved:

1. In recent years MS technology has improved and it now outperforms NMR with respect to sensitivity. Some major developments with respect to labeling measurements have been described in [38–41].
2. Measurements of metabolic products in the culture supernatant have been repeatedly reported [42]. Although this typically gives direct information about intracellular precursors it is difficult to correct this data properly (see Sect. 3.3). In the case of multiple cosubstrate uptake, reciprocal ^{13}C labeling [43] then helps to distinguish biosynthetically produced intermediates from external cosubstrates.
3. Direct measurement of labeling in free intracellular amino acids by MS methods was demonstrated in [39]. A broader spectrum of intracellular intermediates has been observed by another MS technique in [41]. In particular, these measurements have been combined with a sampling procedure during the transient state of the experiment. The isotopic instationarity was clearly shown by this experiment, and the labeling time constants were estimated for the first time.
4. The precise direct measurement of intracellular pool sizes is also important for the evaluation of rapid sampling experiments. Current MS instruments facilitate the measurement of the majority of central metabolic pools with high precisions and detection limits [44, 45]. A special GC/MS technique to measure intracellular free amino acid pool sizes has been developed in [39]. An impressive application of this was a culture of *Saccharomyces cerevisiae* showing autonomous oscillations [46] where a strong oscillation of some free amino acid pool sizes was demonstrated.

For the future development of MFA, this means that the time duration of labeling experiments will be significantly reduced because intracellular intermediates are directly observed. The potential of the new types of experiments will be investigated in more detail in the following.

1.5.3 Computational Progress

Finally, the following computational developments will contribute towards the evaluations of the new type of experiments:

1. Several methods have been developed to reduce the computational effort of flux estimation [47, 48]. For experiments with fully labeled substrates, specialized methods are available [49, 50].
2. The evaluation of NMR and MS spectra has been improved by better correction methods and semi-automatic evaluation tools [40, 51–53].
3. The simulation and computation of instationary sensitivities is possible with the recent developments described in [54].

However, the computational cost of instationary data evaluation is still extremely high because a large set of differential equations has to be repeatedly solved in a parameter fitting procedure (see Sect. 2.2).

2
Simulation of Instationary Labeling Experiments

2.1
Mathematical Modeling

In order to simulate the transient course of a CLE state, variables have to be introduced that characterize the complete labeling state of the system. Different representations of the labeling state by fractions of isotopomers, cumomers, bondomers or cumulative bondomers have been proposed in the literature for different experimental configurations [20, 50]. Because all of these representations are essentially equivalent from a mathematical viewpoint, isotopomers and cumomers are used in the following. More details on the mathematical formalism can be taken from [11, 21].

An isotopomer of a certain metabolite M with n carbon atoms is one of the 2^n different $^{12}C/^{13}C$ labeling configurations in which the molecule can be encountered. If for example n=3, the molecule M has the eight configurations M#000, M#001, M#010, M#011, M#100, M#101, M#110, M#111, where an Index 0 denotes a ^{12}C atom and an index 1 denotes a ^{13}C atom. The corresponding fractions m_{000}, m_{001}, m_{010}, m_{011}, m_{100}, m_{101}, m_{110}, m_{111} of M are the isotopomer fractions which together completely characterize the labeling state of M. Clearly, they must add up to 1, corresponding to 100%.

A cumomer can be interpreted as a certain labeled fragment of a molecule. A cumomer fraction is the sum of all isotopomer fractions where the labeled fragment is contained in the isotopomer. For example, if the labeled fragment consists of the first and second carbon atom of M, the corresponding cumomer is denoted by M#11X, and the corresponding cumomer fraction is m_{11X}= m_{110}+m_{111}. In this notation, those carbon atoms that belong to the labeled fragment are indicated by a 1. The others may be labeled or unlabeled and are therefore denoted by the letter X. As another example, when the considered fragment is only the first carbon atom of M, the cumomer is denoted by M#1XX and it holds that m_{1XX}=m_{100}+m_{101}+m_{110}+m_{111}.

Notice that a given isotopomer can fit into different cumomer patterns and it therefore contributes to different cumomer fractions. For example, the isotopomer M#111 contains fragments M#X11 and M#1XX. Consequently, the sum of all 2^n cumomer fractions belonging to one metabolite is not 1. Nevertheless, cumomer fractions can be easily transformed into isotopomer fractions and vice versa [20]. Finally, the weight of a cumomer is defined to be the number of carbon atoms in its labeled fragment. For example, M#X11 has weight 2 and M#1XX has weight 1.

The system can now be described with both isotopomer and cumomer fractions. In each case the labeling state vector **x** which combines all isotopomer or cumomer fractions of all metabolites in the network has a very high dimension in practice. For example, a typical network including all amino acid synthesis pathways has several thousand isotopomers. On the other hand the input

labeling vector $\mathbf{x}^{inp}$ of the isotopomer or cumomer fractions of labeled substrates has a much smaller dimension because only one or two substances are typically fed. Moreover, this vector is completely known. In order to describe the labeling dynamics, the constant vector $\mathbf{X}$ of all metabolite pool sizes must also be known. By inserting multiple copies of the pool size values, $\mathbf{X}$ is sized in such a way that one pool size value is associated with each cumomer fraction. Consequently, $\mathbf{x}$ and $\mathbf{X}$ have the same dimensions, which simplifies the following notation. Finally, the vector of all intracellular (constant) fluxes that must be determined by the experiment is denoted by the vector $\mathbf{v}$.

Writing balance equations for all pools, the complete mathematical model for an isotopically (but not metabolically) instationary labeling experiment has the same general form for both isotopomer or cumomer fractions:

$$\operatorname{diag}(\mathbf{X}) \cdot \dot{\mathbf{x}} = \mathbf{f}(\mathbf{v}, \mathbf{x}^{inp}, \mathbf{x}). \tag{1}$$

Notice that the stoichiometric balances $\mathbf{N} \cdot \mathbf{v} = 0$ with the stoichiometric matrix $\mathbf{N}$ are already implied by the equations.

2.2 Cascaded Equations

The major advantage of the cumomer representation (like for the cumulative bondomer representation [50]) in contrast to isotopomers is that the general equation system (1) has a convenient mathematical structure that can be exploited for the numerical solution of the equations. Precisely, the vector $\mathbf{x}$ can be partitioned into a series of subvectors

$$\mathbf{x} = ({}^0\mathbf{x}, {}^1\mathbf{x}, {}^2\mathbf{x} \ldots)^T \tag{2}$$

in such a way that the vector ${}^i\mathbf{x}$ collects the fractions of all cumomers of weight *i*. Then the equations can be rewritten in the general form [21]

$$\begin{aligned} &{}^0\mathbf{x} = \mathbf{1} \\ &\operatorname{diag}({}^i\mathbf{X}) \cdot {}^i\dot{\mathbf{x}} = {}^i\mathbf{A}(\mathbf{v}) \cdot {}^i\mathbf{x} + {}^i\mathbf{b}(\mathbf{v}, \mathbf{x}^{inp}, {}^0\mathbf{x}, {}^1\mathbf{x}, \mathrm{K}, {}^{i-1}\mathbf{x}), \; i = 1, 2, \ldots \end{aligned} \tag{3}$$

where the nonlinear functions ${}^i\mathbf{b}$ represent the bimolecular reaction steps in the reaction network. These functions contain products of cumomer fractions.

Additionally, the sensitivity of the labeling state with respect to the fluxes and pool sizes is required for parameter fitting and the statistical evaluation of labeling experiments. By implicit differentiation of (1) this leads to the following set of sensitivity equations in the instationary case:

$$\begin{aligned} \operatorname{diag}(\mathbf{X}) \cdot \frac{\mathrm{d}\dot{\mathbf{x}}}{\mathrm{d}\mathbf{v}} &= \frac{\mathrm{d}\mathbf{f}}{\mathrm{d}\mathbf{v}} + \frac{\mathrm{d}\mathbf{f}}{\mathrm{d}\mathbf{x}} \cdot \frac{\mathrm{d}\mathbf{x}}{\mathrm{d}\mathbf{v}} \\ \frac{\mathrm{d}\operatorname{diag}(\mathbf{X})}{\mathrm{d}\mathbf{X}} \cdot \dot{\mathbf{x}} + \operatorname{diag}(\mathbf{X}) \cdot \frac{\mathrm{d}\dot{\mathbf{x}}}{\mathrm{d}\mathbf{X}} &= \frac{\mathrm{d}\mathbf{f}}{\mathrm{d}\mathbf{x}} \cdot \frac{\mathrm{d}\mathbf{f}}{\mathrm{d}\mathbf{X}} \end{aligned} \tag{4}$$

Here $d\mathbf{x}/d\mathbf{v}$ and $d\mathbf{x}/d\mathbf{X}$ are matrices of scalar sensitivities $d\mathbf{x}_i/d\mathbf{v}_j$ and $d\mathbf{x}_i/d\mathbf{X}_k$. For this reason, the sensitivity equation systems have an extremely high dimension and it is generally a time-consuming procedure to solve them. A simulation algorithm that exploits the cascaded structure of Eqs. 3 and 4 to compute the sensitivities on a computer network was developed in [54]. This simulator is also used for the simulations in this text.

2.3 A Simple Example

The concepts introduced above are now illustrated for a very simple example network shown in Fig. 1 that nevertheless exhibits some of the most important peculiarities of metabolic networks. Due to the bimolecular reaction step v, the system has a nonlinear structure. Moreover, a reversible reaction q occurs in the system. This network has already been investigated in [23], and for that reason it is well understood in the stationary case.

A set of free fluxes for the system is given by the substrate uptake u, and by the net and exchange fluxes q^{net}, q^{xch} of the bidirectional reaction step q. Given the values of these fluxes, all remaining fluxes are determined by stoichiometry. Figure 2 shows a simulated time course of a CLE done with the example system. Notice that cumomer fractions are shown and for that reason the sum of the stationary values need not be 1. The cumomers of weight 1 directly correspond to the carbon atom network of the system, and the corresponding fractions are also called positional labeling fractions [20]. As can be seen, the labeled material first appears in the two carbon atom positions of pool B and then (with a time delay) also in the corresponding pools of C and D. The connected carbon atom pools of B, C and D asymptotically show the same labeling fractions because they form a unidirectional linear chain.

Figure 2b also shows some selected labeling sensitivities of pool C with respect to the flux q^{net}. In the sensitivity plot, the (appropriately scaled) absolute value of the sensitivity is visualized by a tube around the time course. Clearly, the flux sensitivities asymptotically tend to the sensitivities of the isotopically stationary CLE. Interestingly, the sensitivity can change its sign, as can be seen for the C#XXX1 sensitivity.

Some sensitivities of the C labeling fractions with respect to the pool size of D are shown in Fig. 2c. As expected, the pool size sensitivities tend to zero with increasing time. This corresponds to the fact that the pool sizes have no influence on the stationary state of the system. Notice that sensitivity maxima occur in the isotopically transient phase. This gives a first hint that the sampling times play an important role in gathering a great deal of information about the fluxes.

Cumomers of higher weight are only formed when two cumomers of lower weight join in the bimolecular reaction step v, and consequently they occur later in time (Fig. 3a). This indicates that the right time to measure labeling fractions does not only depend on the metabolite pool but also on their weight.

3
Short-Time Labeling Experiments

3.1
Time Constants of Labeling Dynamics

It was pointed out in Sect. 1.3.2 that the biomass labeling state at the end of a CLE is never really stationary. However, it may come very close to the stationary state so that the error due to this approximation might be neglected or corrected. For this reason, it is quite important to know what the time constants of the ^{13}C labeling dynamics in a given experiment are. There are basically two such time constants that govern the system behavior (see Fig. 4).

First, the ratio

$$\frac{X_{\mathrm{IM}}}{v_{\mathrm{upt}}} = \frac{\text{average intermediary pool size}}{\text{substrate uptake rate}} = \frac{1}{\sigma} \tag{5}$$

determines the dynamics of labeling in the intermediary pools of metabolism. Here σ is a kind of specific substrate uptake rate.

Second, the ratio

$$\frac{X_{\mathrm{BM}}}{v_{\mathrm{effi}}} = \frac{\text{average biomass pool size}}{\text{biomass efflux rate}} = \frac{1}{\mu} \tag{6}$$

determines the labeling dynamics of a certain species of labeled molecules incorporated in the biomass. It turns out to be equal to the reciprocal growth rate μ of the microorganism (the residence time of a continuous culture).

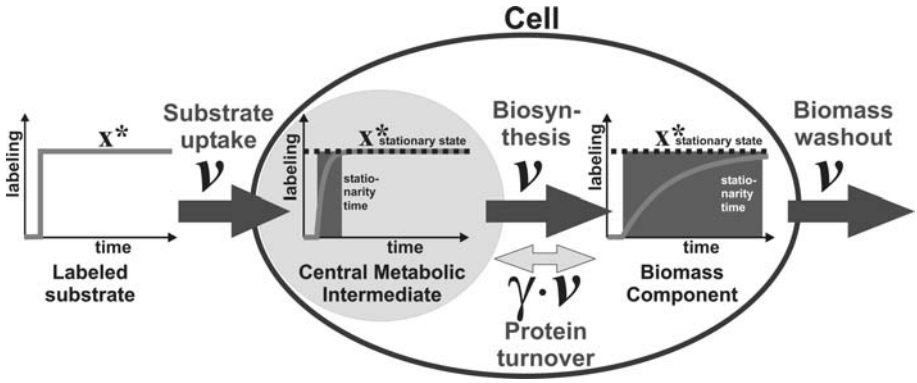

Fig. 4 Heavily simplified model for intermediary metabolism, biomass formation and protein turnover in a growing cell. A typical time course for labeling enrichment in the intermediates and the biomass is shown (see also Fig. 6). A critical assumption is that protein turnover can be neglected (γ=0)

Recent measurements of intracellular intermediate concentrations can be taken from [44, 45, 55, 56]. The concentrations of protein bound amino acids can be precisely estimated from the cellular protein content and the distribution of the amino acids in the protein [55, 57]. Some typical values are X_{IM}= 1 mM (with large variations), X_{BM}=100 mM, v_{upt}=100 mM/h (for growing cells), v_{effl}=10 mM/h and typical time constants in the literature are $1/\sigma$=0.01 h and $1/\mu$=10 h. Therefore, the time needed to saturate the first intermediary pool after substrate uptake is about 1000 times shorter than the time it takes to equilibrate the labeling state in the biomass. However, this does not mean that the complete intermediary metabolism is equilibrated after such a short time.

In the established MFA procedures, labeling information is taken from biomass compounds as, for example, hydrolyzed proteins. Only in this way can a sufficiently large amount of labeled material be gathered to obtain meaningful signals with the measurement instruments (NMR, MS). However, as discussed in Sect. 1.5.2, the intracellular intermediate labeling state will be completely available to measurements in the near future.

An important precondition for separating the time scales between intracellular intermediates and biomass compounds is the absence of protein turnover (γ=0 in Fig. 4). This means that all fluxes from intermediary metabolism to biomass are "one track roads" and so metabolites incorporated into biomass will never return. This has been the standard assumption for labeling experiments so far. However, it is known that proteolysis can take place in the case of cell starvation or when cells are adapting to changing external conditions [58, 59].

Unfortunately, little is currently known about the quantity and significance of this effect. In general, protein turnover is a rather complicated process [59]. Because genetic regulation and adaptation processes influence the turnover rate it can be expected to play a more significant role in eucaryotic cells than in bacteria. As a quantitative result, a turnover rate of 1% per hour for *Saccharomyces cerevisiae* is given in [58]. By measuring the labeling states of both free amino acids and the cell protein, it might be possible to quantify the turnover with a CLE in the future. However, in the following section protein turnover will be neglected, except for in Sect. 3.6.

3.2 Washout Correction

The concept of "washout correction" was originally introduced for continuous cultures where biomass is washed out from the bioreactor volume due to dilution. The correction can be used for experiments where the intermediary labeling state is equilibrated but not the biomass labeling state.

Based on the assumption of absent protein turnover (γ=0) the complete cellular system can be abstracted as a linear chain from intermediary metabolism to biomass, as shown in Fig. 4. Here, only one single isotopomer or cumomer pool is drawn representatively for all pools. The labeling fraction of

the substrate is denoted by x^*, v is the flux through the system, and X_{IM}, X_{BM} are the pool sizes of the intermediate metabolite and the corresponding biomass metabolite. In this case, the labeling dynamics described by the fractional labeling variables x_{IM}, x_{BM} are given by the equation

$$\begin{aligned} X_{IM} \cdot \dot{x}_{IM} &= x^* \cdot v - x_{IM} \cdot v,\ x_{IM}(0) = 0 \\ X_{BM} \cdot \dot{x}_{BM} &= x_{IM} \cdot v - x_{BM} \cdot v,\ x_{BM}(0) = 0 \end{aligned} \tag{7}$$

As explained before, the growth rate $\mu = v/X_{BM}$ of the microorganisms and the pool size ratio $\alpha = X_{IM}/X_{BM}$ will play important roles in the solution of this equation system. Dividing by the pool sizes on both sides produces:

$$\begin{aligned} \dot{x}_{IM} &= (x^* - x_{IM}) \cdot \mu/\alpha \\ \dot{x}_{BM} &= (x_{IM} - x_{BM}) \cdot \mu \end{aligned} \tag{8}$$

The explicit solution of Eq. 8 can be easily computed as:

$$\begin{aligned} \frac{x_{IM}(t)}{x^*} &= 1 - \exp\left(-\frac{\mu}{\alpha t}\right) \\ \frac{x_{BM}(t)}{x^*} &= 1 + \frac{\alpha}{1-\alpha}\exp\left(-\frac{\mu}{\alpha t}\right) - \frac{1}{1-\alpha}\exp(-\mu t) \end{aligned} \tag{9}$$

Here the ratio between transient and asymptotic fractional labeling is taken as a relative measure of stationarity (see Fig. 5). The solution is a superposition of a fast process with time constant α/μ and a much slower process with time constant $1/\mu$. Clearly the fast subsystem directly corresponds to intermediary metabolism while the slow subsystem corresponds to the cell growth (see Fig. 4). The clue to washout correction now is to assume that the small time

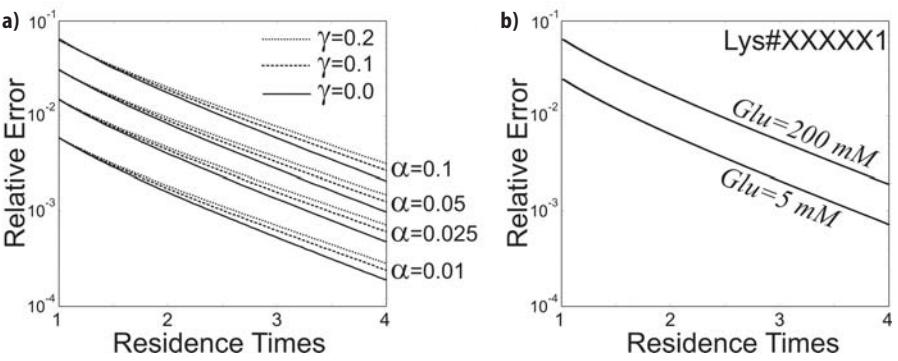

Fig. 5 Relative extrapolation error of washout correction for: (left) the simplified example from Fig. 4 (the ratio α between intermediate and biomass pool sizes and the specific protein turnover rate γ are varied); (right) the complex *Corynebacterium* network with two different glutamate pool sizes

constant α/μ can be neglected compared to the large one, so $\alpha \ll 1$. In this case it is admissible to set

$$x_{\mathrm{IM}}(t) \approx x^{*} \tag{10}$$

from the very beginning of the CLE. With this approximation, the slow subsystem has the solution:

$$\frac{x_{\mathrm{IM}}(t)}{x^{*}} \approx 1 - \exp(-\mu t) \tag{11}$$

From this approximation, the stationary state of the CLE can be extrapolated using the washout correction formula [14, 51]

$$x^{*}_{\mathrm{WC}} = \frac{x_{\mathrm{BM}}}{1 - \exp(-\mu t)} \tag{12}$$

if the stopping time T of the experiment is chosen to be sufficiently large. Incorporating this formula into the measurement prediction of flux analysis software allows us to evaluate prematurely terminated experiments. In certain cases (uniformly labeled substrates) the correction can also be done directly for the measurements [51].

3.3 Correction for Batch and Fed-Batch Processes

The concept of washout correction can be easily extended to batch and fed-batch cultures. In general, there is an "old" biomass which is present when the experiment is started, and a labeled "young" biomass which is formed during the CLE. The basic idea of washout correction is to correct the influence of the old biomass on the measured signals. Because the young biomass – like the old one – also contains ^{12}C atoms, both types cannot be distinguished from the measurements. However, if the approximation from Eq. 10 holds, and the fraction of old biomass at the stopping time of the experiment is calculated as p, then washout correction can be generalized. In this case, the measured cumomer fraction x_{BM}, corresponding to a certain cumomer fraction $x = x(T)$ in biomass will be

$$x_{\mathrm{BM}} = (1-p)\cdot x \Rightarrow x^{*}_{\mathrm{WC}} = \frac{x_{\mathrm{BM}}}{1-p} \tag{13}$$

In the case of the continuous culture it obviously holds that $p = \exp(-\mu T)$. To be precise, the natural ^{13}C enrichment of unlabeled molecules, which is 1.13%, should also be taken into account in the correction [60]. However, this has been left out here for simplicity.

3.4
How Early Can a Labeling Experiment be Stopped?

The question now is: how early can a CLE can be stopped before the approximation (10) becomes invalid? Applying the washout correction to the true solution of the system given by Eq. 9 the extrapolation error relative to the stationary state is given by:

$$\left|\frac{x^*_{WC} - x^*}{x^*}\right| = \frac{\alpha}{1-\alpha} \cdot \left|\frac{\exp(-\mu T/\alpha) - \exp(-\mu T)}{1-\exp(-\mu t)}\right| \tag{14}$$

Obviously, the error tends to zero for large stopping times (when the influence of the transient labeling phase vanishes asymptotically). It can be seen that the washout correction error depends critically on the ratio α between the free metabolite pool size and the corresponding metabolite pool size in biomass, and on the scaled time μt which is the number of biomass residence times in the reactor. Figure 5a (with γ=0) shows a plot of the error for different ratios.

In order to obtain a first guess for the error for a real cell we must take into account that the intracellular pool represents the complete lumped intermediary metabolism instead of a single pool in the simple model shown in Fig. 4. Taking an average concentration of proteinogenic amino acid of 100 mM, ten intermediate pools with a concentration of 1 mM, and neglecting all others, the ratio will be α=0.1, which is a surprisingly large value.

To find out a suitable stopping time, the requirements for the measurement precision must also be known. From our experiences of past experiments, it can be said that the measurement precision should be between ~0.1% and ~1.0% to obtain statistically well determined flux estimates [61]. Taking this precision requirement, it follows from Fig. 5a with α=0.1 that the experiment should take at least 3–4 biomass residence times. However, this is only a first guess for the time constants.

3.5
A More Realistic System

A more detailed estimate for the time constants can only be obtained from a real metabolic network, because the topology of the network also plays an important role [62]. For example, cyclic pathways will have different time constants compared to linear pathways, even if the number and size of the pools are the same in each case.

To present a more realistic example, the complete network of *Corynebacterium glutamicum* from [15] is now investigated and the corresponding CLE is simulated. For the sake of brevity, all pools are assumed to have the same concentration of 5 mM. This is a rather large value for most pools and will produce some kind of worst case estimate for the admissible stopping time. The biomass effluxes v_{effl} are calculated from the biomass composition as usual [12].

The cell is fed with a mixture of 30% [1-^{13}C] glucose and 70% naturally labeled glucose with v_{upt}=60 mM/h, and the growth rate is assumed to be μ=0.1 h^{-1}.

As a representative pool, lysine is chosen to check the validity of the washout correction for this example. Lysine is synthesized from pyruvate and oxalo acetate and is therefore linked both to sugar metabolism and the citric acid cycle. As was already shown for the simple example from Fig. 1, there is a time delay between cumomer pools of weight 1 and higher weighted pools (Fig. 3b). The practical consequence of this is that the required CLE duration also depends on the measurement instruments used. The higher the weight of the measured cumomers, the longer must the CLE duration be chosen. For example, ^{1}H NMR measures only cumomers of weight 1, as is the case with summed fractional labeling from MS data [2]. On the other hand, ^{13}C NMR also relates to cumomers of weight 2 and 3 [23] and MS data contains information about all cumomer weights. However, in this example the lysine cumomer fractions of higher weight turn out to be below the detection limit and so only the positional labeling fraction of the sixth lysine carbon atoms is considered here.

A washout correction is now performed according to Eq. 12, and the result is compared with the true stationary state at infinity (Fig. 5b). The picture changes if there is an extremely large metabolite pool in the metabolic network. This is the case for example in *C. glutamicum*, where glutamate concentrations can reach values of more than 100 mM. When the size of the glutamate pool is switched from 5 mM to 200 mM in the simulation, the total capacity of the intracellular intermediates is dramatically raised and the time constants increase by about one residence time (Fig. 5b).

In general, the results for the correction error correspond perfectly to the result obtained from the rough estimation in Fig. 5a with the ratio α=0.1. However, as pointed out before, the chosen pool sizes of 5 mM in the large example are unrealistically large. The simple model from Fig. 5a overestimates the admissible stopping time by approximately one residence time.

It must be pointed out that the transient dynamics of the system are also influenced by the labeling of the substrate. A different outcome results if a mixture of unlabeled and fully labeled substrate is used (not shown here) because larger amounts of higher weighted cumomers will then be present. Moreover, these cumomers will appear much earlier because they are formed as fragments of the fully labeled substrate. Consequently, their correction errors will also be more significant.

Summarizing, it becomes clear that the question of how long the experiment should take cannot be generally answered. The answer critically depends on:

1. the required measurement precision for flux estimation
2. the substrate mixture chosen
3. the measurement equipment (measured cumomer weights)

In general, it turns out that the stopping time required has been underestimated in many past experiments. In fact, stationarity times in intermediary metabolism of the order of $1/\mu$ or more must be expected for realistic systems.

This also coincides with the experimental evidence given in [41] where the intermediate labeling was not stationary after one hour for μ=0.1 h^{-1}.

3.6 Influence of Protein Turnover

To complete the picture, the influence of protein turnover is studied for the simplified system in Fig. 4 at least. A small backward flux of magnitude γv from biomass to the intermediary pool is assumed, while the flux from intermediary metabolism to biomass is increased to $(1+\gamma)\cdot v$ to maintain the stoichiometry. Here γ can be interpreted as a specific protein turnover rate. The system equations are now:

$$\begin{aligned} X_{IM}\cdot\dot{x}_{IM} &= x^{*}\cdot v - x_{IM}\cdot(1+\gamma)\cdot v + x_{BM}\cdot\gamma\cdot v, \quad x_{IM}(0)=0 \\ X_{BM}\cdot\dot{x}_{IM} &= x_{IM}\cdot(1+\gamma)\cdot v + x_{BM}\cdot(1+\gamma)\cdot v, \qquad x_{BM}(0)=0 \end{aligned} \tag{15}$$

The two time constants of this modified system can be computed to a first order approximation by:

$$\frac{1}{\mu}\left(1-\frac{\alpha\gamma}{1-\alpha}\right)^{-1} \quad \text{and} \quad \frac{\alpha}{\mu}\left(1+\frac{\gamma}{1-\alpha}\right)^{-1} \tag{16}$$

This shows that the slow process is almost unchanged, because $\alpha\gamma\approx 0$ but the fast process is accelerated by a factor ~$1+\gamma$. However, because intermediate and biomass labeling is not decoupled anymore in the case of protein turnover, the large time constant influences both intermediates and biomass. A typical time course for a system with and without protein turnover is shown in Fig. 6. Here the dynamics of biomass labeling remains almost unchanged, and consequently the washout correction still works well (see Fig. 5a). On the other hand, the intermediate labeling takes a much longer time to equilibrate if there is a protein turnover. This effect has some consequences for new types of experiments, and will be discussed in Sect. 4.2.

4 Labeling Experiments with Repeated Sampling

4.1 A New Type of Experiment

It was shown in Section 3.4 that washout correction will fail when the CLE is stopped too early. This represents a principal limitation to the application of the classical flux estimation procedure based on stationary labeling. A promising way out of this trap is the direct measurement of the intracellular metabolites. The experiment duration can then be cut down to a small multiple of the time

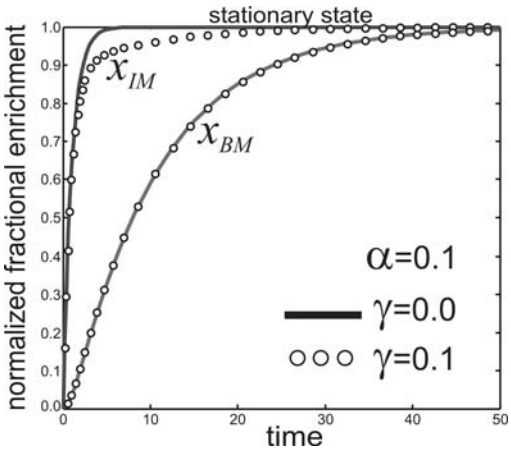

Fig. 6 Labeling time course of the intracellular intermediates and the biomass for the simplified example from Fig. 4 with and without a protein turnover γ

constant α/μ (see Sect. 3.4). However, as was shown in Fig. 6, this time can still be of the order of $1/\mu$ if there is significant protein turnover.

A step further would be to stop the experiment before the intermediary labeling state becomes stationary. In this case, the pool sizes of the intermediates must also be known, because they determine the time constants in detail. This will provide the opportunity to carry out even very short experiments with a duration well below the generation time of the microorganism.

One drawback of this approach is that no simple extrapolation procedure for the stationary state of the intermediate labeling enrichment is available because there is no irreversible barrier between compartments as in the case of intermediates and biomass components. Moreover, even modern MS instruments are unable to quantify the pool sizes and labeling states of all intracellular pools with reasonably small measurement errors. In this case, the measurement information might not be sufficient for flux analysis.

Therefore, the missing information about the time constants in intermediate metabolism can only be obtained by taking repeated samples. In [41] the intracellular labeling state is observed at times 0, 40 and 60 min in the transient of a CLE with μ=0.1 h^{-1}. Clearly, to have measurements of as many intracellular pool sizes as possible is invaluable information. On the other hand, this might not be necessary when it is possible to estimate the pool sizes from the labeling data too.

4.2 A Simple Example

To get a first impression of how much flux information can be obtained from a CLE with repeated sampling, a simulation study has been performed with the simple example from Fig. 1. Repeated samples are drawn from the simulated transient data shown in Fig. 2a and statistically evaluated afterwards using the

computed sensitivity data. To keep the description of the example simple, it is assumed here that the eight isotopomer fractions of the pools B and E can be measured directly with a precision of 0.01. This is not a critical assumption, because isotopomer fractions of metabolite pools with up to three carbon atoms can usually be resolved from NMR or MS measurements [63]. Moreover, all pool sizes in the network are assumed to be measurable to 10% precision. From the fluxes, only the substrate uptake is assumed to be directly measurable.

The intracellular free fluxes q^{net} and q^{xch} must now be estimated from the available measurements. Several virtual flux determination experiments with different amounts of available information are now carried out:

1. In order to obtain a reference for the achievable precision of the flux estimates the stationary experiment is carried out first. It is already known from the investigation in [23] that the system is identifiable in this case. Because no knowledge about pool sizes is required in the stationary case, the uncertainties in pool size measurements do not influence the results. It turns out that q^{net} can be estimated with a standard deviation of 0.019 and q^{xch} with a standard deviation of 0.045. In general, exchange fluxes cannot be estimated as well as net fluxes [22, 61].
2. In a second scenario the system is sampled at one single time T in the transient phase. Additionally, all pool sizes are assumed to be known exactly. Figure 7a shows the effect on the determinacy of the free fluxes for different sampling times. As may be expected, the standard deviations tend asymptotically to their stationary values ($T=\infty$). Surprisingly, the exchange fluxes can be even better determined if an early sample is taken. This is intuitively correct, because the influence of the reaction q on the pool E is then undisturbed by the influence of the reaction sequence v, w, p.
3. If the pool sizes are measured, the net flux uncertainty is slightly worse than before (Fig. 7a). However, this is only the case for early sampling times, because the pool size sensitivities then are low (see Fig. 2c). Interestingly, the standard deviations of the exchange fluxes remain almost unchanged.
4. In a third simulation, the pool size measurements are completely left out. Clearly, it cannot be expected that the missing information can be obtained from a single transient sample. For that reason, repeated samples at times 5, 10, 15 and 20 are taken. Figure 7b shows that the fluxes are still identifiable. The estimated standard deviations can be very small if all of the available measurement information from four samples is cumulated. Additionally, the missing pool size information can be reconstructed from the data (not shown here).

In summary, it turns out that experiments with repeated sampling are very promising for flux estimation. Even with one single very early sample and approximately known pool sizes, it was possible to obtain standard deviations that are comparable to their asymptotic values. Moreover, exchange fluxes can be determined more accurately with the instationary than with the stationary experiment.

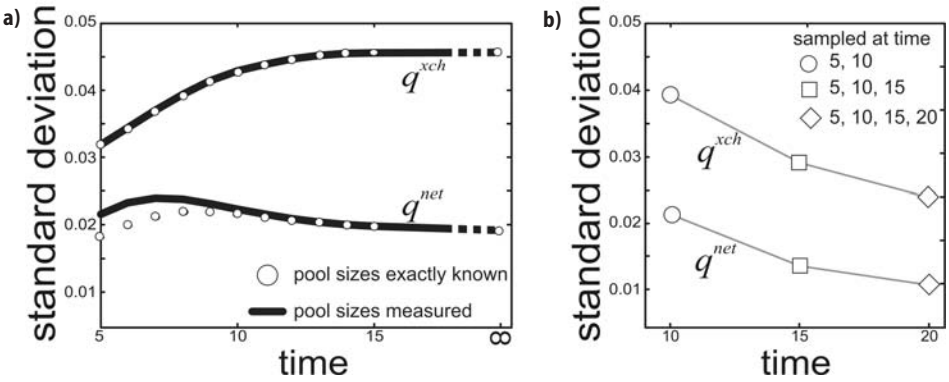

Fig. 7 Statistical determinacy of the free fluxes as estimated from an instationary labeling experiment with the example network from Fig. 1. Standard deviations are shown for the cases that: (left) one single labeling measurement at time T is taken and all pool sizes are either known or measured; (right) no pool sizes are measured but a repeated labeling measurement is available

5
When Fluxes Become Instationary

5.1
Possible Pitfalls

As was mentioned in Sect. 1.3.1, metabolic stationarity is only approximately the case even in a continuous culture. However, whether they can be tolerated in MFA depends on the magnitude of the population inhomogeneity or the instationarity oscillations or fluctuations. An experiment with autonomous oscillations of *S. cerevisiae* has been reported in [46] where the amino acid pool sizes (and presumably also the fluxes) showed a strong oscillation. Clearly, the established mathematical tools for CLE data evaluation based on the model from Sect. 2.1 cannot be applied in this situation. However, metabolic instationarity need not be that pronounced in practice.

Here an important difference between the classical stoichiometric MFA method and the ^{13}C MFA method emerges. Stoichiometric MFA is a linear method, which means that the estimated fluxes are linearly dependent on the measurements. In contrast, ^{13}C MFA has a complex nonlinear dependency between measurements and fluxes. Figure 8 shows the essential difference between a linear and nonlinear input-output behavior of a system. Basically, the CLE is carried out with each single cell that might have instationary fluxes (microscopic instationarity). On the other hand, a measurement is always taken from a population which need not be synchronized and so only a mean value is observed. However, the following arguments hold both for mean values with respect to time and mean values with respect to a population.

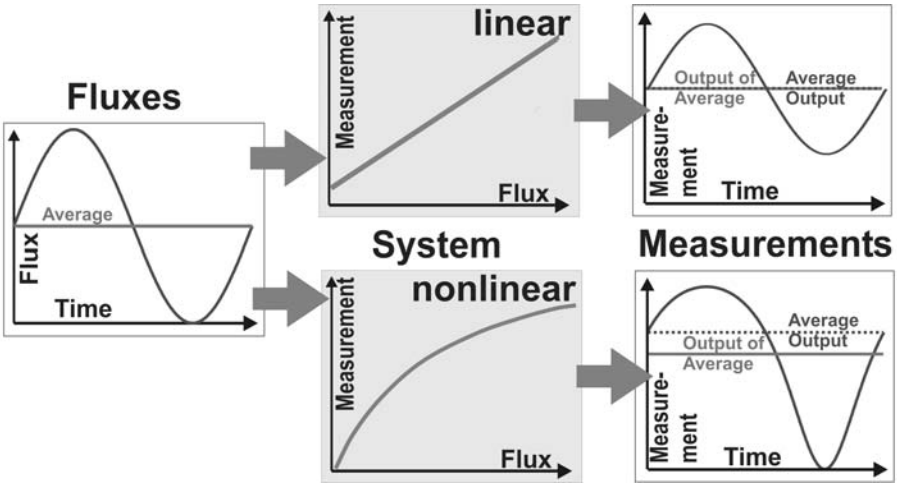

Fig. 8 Different behaviors of linear and nonlinear systems with respect to mean value operations. A linear system transduces the mean value of a fluctuating signal to the corresponding mean value of the output signal. This is not the case for a nonlinear system

For any linear system, the mean output (with respect to time or population) is always the same as the output of the mean fluxes (Fig. 8). This means that, although only a mean value is measured, the corresponding flux estimates have a meaningful interpretation in terms of the mean flux pattern of the population. This is not true for a nonlinear procedure. Fig. 8 shows that in the nonlinear case the mean value of the measurements can be significantly different from the measurements corresponding to a mean flux pattern. Therefore, an important pitfall of ^{13}C MFA in the case of (micro- and macroscopically) instationary metabolic fluxes is that the estimated fluxes generally cannot be interpreted as a mean flux pattern with respect to population or time.

5.2 An Example with Fluctuating Fluxes

A conceptual simulation study has been performed to quantify the significance of these nonlinear effects for a realistic example. For the *Corynebacterium* network already discussed in Sect. 3.5 (with all intermediate concentrations set to 5 mM), a fluctuation of the intracellular fluxes is investigated. To illustrate the effects that occur, it was assumed that only one free flux fluctuates around a stationary value. Because DNA synthesis might have changing demands over time, the oxidative pentose phosphate pathway flux ppp_1, which determines the precursor supply for DNA synthesis, was chosen.

It should be pointed out that in an oscillating culture, not only the fluxes but also pool sizes can change [46]. However, this effect was not taken into account

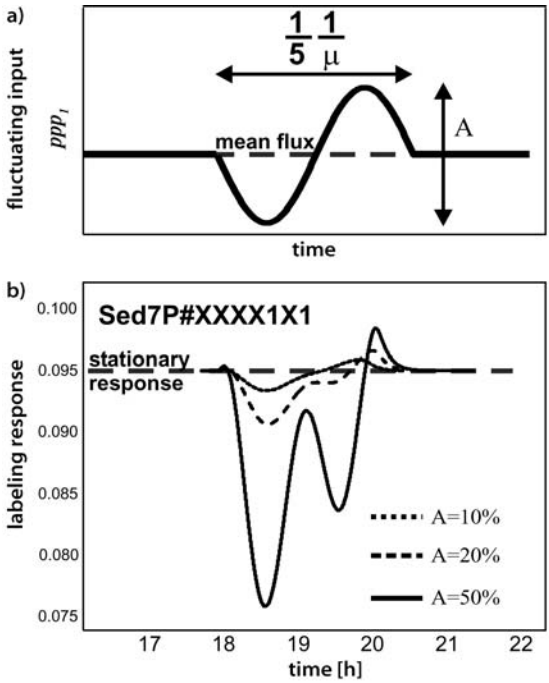

Fig. 9 Effect of fluctuating metabolic fluxes on metabolic flux analysis. Top: the flux ppp_1 in a *Corynebacterium* network is assumed to fluctuate with a cyclic pattern. Bottom: the response of the Sed7P#XXXX1X1 pool for different amplitudes A of the disturbance

and quasi-stationarity of the metabolic regulation was assumed. This means that the stoichiometric equations are assumed to hold all of the time and so all fluxes that depend on the free flux ppp_1 also change with a similar pattern. As shown in Fig. 9a, the flux disturbance takes place for 20% of the residence time $1/\mu$ while the fluxes are constant for the remaining 80% of the time. Therefore, the system can relax to its stationary state after each disturbance. The corresponding cyclic labeling time course is shown in Fig. 9b.

The amplitude A of the ppp_1 fluctuation, given as a percentage of ppp_1, is now taken as a parameter to investigate the behavior of the nonlinear system (see Fig. 9a). A labeling experiment was simulated for different values of A. The simulation was then driven for several cell cycles until the transient labeling phase damped out and the system output showed a regular cyclic pattern. The results are shown in Fig. 9b, where the response of the seduheptulose-7-phosphate cumomer pool Sed7P#XXXX1X1 is chosen as an example that showed the most pronounced nonlinear effect (worst case). It turns out that for increasing amplitudes A of the input signal, the output signal differs more and more in shape from the input signal. Much more important is the fact that the *mean* output signal becomes more and more different from the *mean* input signal.

This effect can be quantified by computing the mean deviation between the stationary signal and the disturbed signal over time. It turns out that there is almost no measurement bias if $\alpha<15\%$. For medium values of $15\%<\alpha<30\%$, the bias is still below the typical measurement precision. Only for large values of $\alpha>30\%$ can the bias be higher than 1% and will therefore certainly influence the flux estimation.

Surprisingly, this labeling system is relatively robust with respect to flux fluctuations, which means that the measured time or population mean is not too different from the ideal stationary case. However, it should be pointed out that this conceptual study is based on rather vague assumptions, so the picture may change if the pool sizes are fluctuating too.

6 Conclusions

Several promising candidates for instationary MFA have been identified in this contribution, which will further broaden the scope of this method in the near future:

1. Batch experiments in small reactor volumes are best suited for high throughput flux analysis in screening applications. The labeling information should then be taken from the intermediate pools. Because repeated sampling is not possible in this configuration, the experiment should not be terminated before the intermediary labeling state is approximately stationary. Fortunately, a high measurement precision is typically not the goal in a screening application.
2. The improvement in preexisting industrial batch and fed batch production processes requires high precision methods because small changes must be detected. In this situation, flux analysis can be achieved with the sensor reactor concept, which is tailored to produce highly reliable data. In this reactor, all kinds of labeling experiments are possible including repeated sampling.
3. The investigation of metabolic transients in microorganisms for research purposes is always challenging. If high precision equipment is available, repeated sampling experiments promise to provide information about even short time changes in the metabolic fluxes. On the other hand, the example study from Sect. 3.5 shows that such an experiment might even help to determine new fluxes or to significantly improve the precision of estimated exchange fluxes.

In each case, strong requirements for their precision and reliability must be fulfilled by the measuring instruments. Moreover, data evaluation becomes computationally very expensive when isotopically instationary data must be fitted to the model.

On the other hand, it becomes clear that MFA is currently reaching the biological limits of its applicability. If population inhomogeneities and flux

oscillations are significant, it is not possible to obtain any meaningful result. Hopefully, these processes still provide a statement about the average flux distribution in the population. Otherwise, only single cell methods have the potential to provide an insight into an individual cell.

Acknowledgements This work was partially funded by DFG grant WI 1705/4.

References

1. Dauner M, Sonderegger M, Szyperski T, Wüthrich K, Hohmann H-P, Sauer U, Bailey JE (2001) Appl Env Microbiol 68:1760
2. Christensen B, Nielsen J (2000) Biotechn Bioeng 68:652
3. Yang C, Hua Q, Shimizu K (2002) Metab Eng 4:202
4. Puccetti C, Aureli T, Manetti C, Conti F (2002) NMR Biomed 15:404
5. Matsuda F, Morino K, Miyashita M (2003) Plant Cell Physiol 44:510
6. Stephanopoulos GN, Aristidou AA, Nielsen J (1998) Metabolic engineering. Academic, San Diego
7. Szyperski T (1998) Q Rev Biophys 31:41
8. Wiechert W (2001) Metab Eng 3:195
9. Christensen B, Nielsen J (2000) Adv Biochem Eng Biot 66:209
10. Klapa MI, Stephanopoulos G (2000) In: Schügerl K, Bellgardt K-H (eds) Bioreaction engineering, modeling and control, vol 3. Springer, Berlin Heidelberg New York, p 106
11. Wiechert W (2002) In: Setlow J, Hollaender A (eds) Genetic engineering: principles and methods, vol 24. Kluwer, Dordrecht, p 215
12. Vallino JJ, Stephanopoulos G (1993) Biotechn Bioeng 41:633
13. Varma A, Palsson BO (1994) Bio-Technol 12:994
14. Marx A, de Graaf AA, Wiechert W, Eggeling L, Sahm H (1996) Biotechn Bioeng 49:111
15. Petersen S, de Graaf AA, Eggeling L, Möllney M, Wiechert W, Sahm H (2000) J Biol Chem 275:35932
16. Sauer U, Hatzimanitakis V, Bailey JE, Hochuli M, Szyperski T, Wüthrich K (1997) Nat Biotechnol 15:448
17. de Graaf AA (2000) In: Barbotin J-N, Portais J-C (eds) NMR in biotechnology: theory and applications. Horizon, Bountiful, UT, chap 4
18. Christensen B, Nielsen J (1999) Metab Eng 1:282
19. Wittmann C (2001) Adv Biochem Eng Biotechn 74:39
20. Wiechert W, Möllney M, Isermann N, Wurzel M, de Graaf AA (1999) Biotechn Bioeng 66:69
21. Wiechert W, Wurzel M (2001) Math Biosci 169:173
22. Möllney M, Wiechert W, Kownatzki D, de Graaf AA (1999) Biotechn Bioeng 66:86
23. Isermann N, Wiechert W (2003) Math Biosci 183:175
24. Wiechert W, Möllney M, Petersen S, de Graaf AA (2001) Metab Eng 3:265
25. Jonsbu E, Christensen B, Nielsen J (2001) Appl Microbiol Biot 56:93
26. Gombert AK, Santos MMd, Christensen B, Nielsen J (2001) J Bacteriol 183:1441
27. Canonaco F, Hess TA, Heri S, Wang T, Szyperski T, Sauer U (2001) Fems Microbiol Lett 204:247
28. Wittmann C, Heinzle E (2002) Appl Env Microbiol 68:5843
29. Massaoudi ME, Spelthahn J, Drysch A, Takors R (2003) Metab Eng 5:86
30. Drysch A, Massaoudi ME, Mack C, Takors R (2003) Metab Eng 5:96
31. Drysch A, Massaoudi ME, Wiechert W, de Graaf AA, Takors R (2003) Biotechn Bioeng

32. Weiss S, John GT, Klimant I, Heinzle E (2002) Biotechn Progr 18:821
33. Balcarcel RR, Clark LM (2003) Biotechnol Progr 19:98
34. Weuster-Botz D (2005) Adv Biochem Eng Biotechnol 92:125
35. Theobald U, Mailinger W, Baltes M, Rizzi M, Reuss M (1997) Biotechn Bioeng 55:305
36. Schäfer U, Boos V, Takors R, Weuster-Botz D (1999) Anal Biochem 270:88
37. Lange HC, Emam M, van Zuijlen G, Visser D, van Dam JC, Frank J, de Mattos MJT, Heijnen JJ (2001) Biotechn Bioeng 75:334
38. Dauner M, Sauer U (2000) Biotechnol Progr 16:642
39. Wittmann C, Hans MA, Heinzle E (2002) Anal Biochem 307:379
40. Rantanen A, Rousu J, Kokkonen JT, Tarkiainen V, Ketola RA (2002) Metab Eng 4:285
41. van Winden W (2002)^{13}C labeling technique for metabolic network and flux analysis. PhD thesis, TU Delft, The Netherlands
42. Zupke C, Stephanopoulos G (1995) Biotechnol Bioeng 45:292
43. Christensen B, Nielsen J (2002) Biotechnol Progr 18:163
44. Buchholz A, Takors R, Wandrey C (2001) Anal Biochem 295:129
45. van Dam JC, Eman MR, Frank J, Lange HC, van Dedem GWK, Heijnen SJ (2002) Anal Chim Acta 460:209
46. Heinzle E, Wittmann C (2003) Biotechnol Bioeng 82:143
47. Christensen B, Nielsen J (2000) Biotechnol Bioeng 68:652
48. Rousu J, Rantanen A, Maaheimo H, Pitkänen E, Saarela K, Ukkonen E (2003) Lecture notes in computer science, vol 2602. Springer, Berlin Heidelberg New York, p 88
49. Szyperski T (1995) Eur J Biochem 232:433
50. van Winden W, Heijnen JJ, Verheijen PJT (2002) Biotechnol Bioeng 80:731
51. van Winden W, Schipper D, Verheijen PJT, Heijnen S (2001) Metab Eng 3:322
52. van Winden W, Wittmann C, Heinzle E, Heijnen JJ (2002) Biotechnol Bioeng 80:477
53. Wahl A, Dauner M, Wiechert W (2003) Biotechnol Bioeng 85:259
54. Nöh K, Wiechert W (2003) In: Hohmann R (ed) Frontiers in simulation: 17. Symposium simulation. SCS, Erlangen, p 427
55. Chassagnole C, Noisommit-Rizzi N, Schmid JW, Mauch K, Reuss M (2002) Biotechnol Bioeng 79:53
56. Hans MA, Heinzle E, Wittmann C (2001) Appl Microbiol Biot 56:776
57. Neidhardt FC, Ingraham JL, Schaechter M (1990) Physiology of the bacterial cell. Sinauer Associates, Sunderland, MA
58. Lopez S, Gancedo JM (1979) Biochem J 178:769
59. Rivett AJ (1986) Curr Top Cell Regul 28:291
60. Fischer E, Sauer U (2003) Eur J Biochem 270:880–891
61. Wiechert W, Siefke C, de Graaf AA, Marx A (1997) Biotechnol Bioeng 55:118
62. Anderson DH (1983) Compartmental modelling and tracer kinetics. Springer, Berlin Heidelberg New York
63. de Graaf AA, Mahle M, Möllney M, Wiechert W, Stahmann P, Sahm H (2000) J Biotechnol 77:25

Received: October 2003

Adv Biochem Engin/Biotechnol (2005) 92: 173–196
DOI 10.1007/b98913

Applying *Metabolic Profiling* Techniques for Stimulus-Response Experiments: Chances and Pitfalls

M. Oldiges · Ralf Takors (✉)

Institute of Biotechnology, Forschungszentrum Jülich GmbH, 52425 Jülich, Germany
r.takors@fz-juelich.de

Abstract So far it is mainly transcriptome and proteome analysis that has been applied to elucidate the correlation between genotype and phenotype although thorough metabolome studies can provide substantial information on the control of the metabolism at the biochemical level. Stimulus-response experiments, i.e. the investigation of metabolism dynamics after a glucose pulse (pulse experiment), can be used to study the in vivo enzyme kinetics offering insight into underlying reaction mechanisms. Usually, this requires rapid cell quenching combined with cell inactivation to 'freeze' the microbial metabolism response at a definite time-lag after pulse stimulation. To access the 'frozen' metabolic reply, adequate analytical methods are needed to measure intracellular metabolite concentrations in the cell extract. As shown in the introductory review part, stimulus-response experiments were usually applied to study central metabolism dynamics in wildtype strains. Our own results, presented in the second part of the contribution, indicate that stimulus-response experiments should also be applied to analyse pathway dynamics in anabolic routes. Using the example of the aromatic amino acid pathway, an LC-MS/MS technique is presented that allows the quantification of intracellular pools of central metabolism as well as of the aromatic amino acid pathway. Based on the analytical approach *metabolic profiling* is performed to monitor the metabolism dynamics after a glucose pulse experiment allowing the conclusion that pulse stimulation is transmitted to the anabolic pathway of interest.

Keywords *Escherichia coli* · Metabolic profiling · LC-MS/MS · Intracellular metabolites · *Saccharomyces cerevisiae*

Abbreviations and Symbols

DAHP	3-deoxy-arabino-heptulosonate 7-phosphate
DAH	3-deoxy-arabino-heptulosonate
3-DHQ	3-dehydroquinate
3-DHS	3-dehydroshikimate
SHIK/SHI	shikimate
S3P	shikimate 3-phosphate
PP	phenylpyruvate
L-phe	L-phenylalanine
L-trp	L-tryptophan
L-tyr	L-tyrosine
PEP	phosphoenolpyruvate
DHAP	dihydroxyacetonphosphat
GAP	glyceraldehyde 3-phosphate
2PG	2-phospho-D-glycerate
3PG	3-phospho-D-glycerate
P5P	pentose 5-phosphates
G6P	glucose 6-phosphate
F6P	fructose 6-phosphate
6PG	6-phosphogluconate
FBP	fructose 1,6-bisphosphate
AMP	adenosine 5-monophosphate
ADP	adenosine 5-diphosphate
ATP	adenosine 5-triphosphate
MMT	Metabolic Modelling Tool
NAD	nicotinamide adenine dinucleotide
NADH	reduced nicotinamide adenine dinucleotide
NADP	nicotinamide adenine dinucleotide phosphate
NADPH	reduced nicotinamide adenine dinucleotide phosphate
PTS	phosphoenolpyruvate:phosphotransferasesystem
GC	gas chromatography
NMR	nuclear magnetic resonance
LC	liquid chromatography
HPLC	high performance liquid chromatography
UV	ultraviolet detection
HPAE	high performance anion exchange chromatography
PAD	pulsed amperometric detection
CE	capillary electrophoresis
SPE	solid-phase extraction
MCA	metabolic control analysis
E4P	erythrose-4-phosphate
amu	atomic mass unit
SRM	selected reaction monitoring
MRM	multiple reaction monitoring
MS	mass spectrometry/mass spectrometer
m/z	mass to charge ratio
θ_{90}	mixing time

E. coli	*Escherichia coli*
Z. mobilis	*Zymomonas mobilis*
S. cerevisiae	*Saccharomyces cerevisiae*
tkt	transketolase
$AroF^{fbr}$	L-tyrosine feedback-resistant DAHP synthase
$AroF^{wt}$	L-tyrosine feedback-sensitive wildtype DAHP synthase

1 Introduction

In the past much effort has been put into the investigation of the gene sequence of (micro-) organisms (genomics), the gene transcription (transcriptomics) and the translation (proteomics) of the coded information. The metabolome (metabolomics) only played a minor role in the field of the 'omics' research, but it is currently gaining more and more interest because the metabolome is downstream of gene regulation and thus contains valuable information about biochemical interactions defining the phenotype of the organism [1].

According to Fiehn [2], metabolome analysis is multifunctional making use of different analytical approaches depending on the topic of the study. Metabolome analysis can thus be subdivided into (i) *target analysis*, aiming at measuring distinct substrates or products e.g. to distinguish differences after genetic modification, (ii) *metabolic profiling*, focusing on a complete pathway or linked pathways and (iii) *metabolomics*, striving for an unbiased, semi-quantitative overview of whole-cell metabolic patterns. For a more rapid analysis, *metabolic fingerprinting* [3] can be used, which reduces the analytical effort to the analysis of these metabolites with biochemical relevance. Quite recently, another variant of high-throughput classification was presented, it is called *metabolic footprinting* [1], which differs from the aforementioned methods by analysing extracellular metabolites instead of intracellular pools.

In *target analysis*, the bulk of metabolome information is usually ignored, because of the narrow focus on a specific compound. However, beneficially, selective sample preparation steps can be applied and optimized to improve the data quality leading to precise pool quantification. On the other hand, following the unbiased *metabolomics* approach, sample preparation must not be compound specific to prevent any exclusion of potentially interesting metabolite signals. Hence, *metabolomics* provide a comprehensive semi-quantitative overview of the biological system, however quantitative information about intracellular pool sizes, for instance, is usually not accessible or are less accurate.

Metabolic profiling aims at the quantification of pre-selected metabolic pathways or groups of metabolites in a metabolic segment and promises to be an effective method for investigating microbial metabolism in a quantitative manner. Knowledge about the changes of the intracellular metabolite concentrations offers a direct access to the identification of metabolism kinetics especially to the in vivo kinetics of the underlying enzymatic reactions. Even

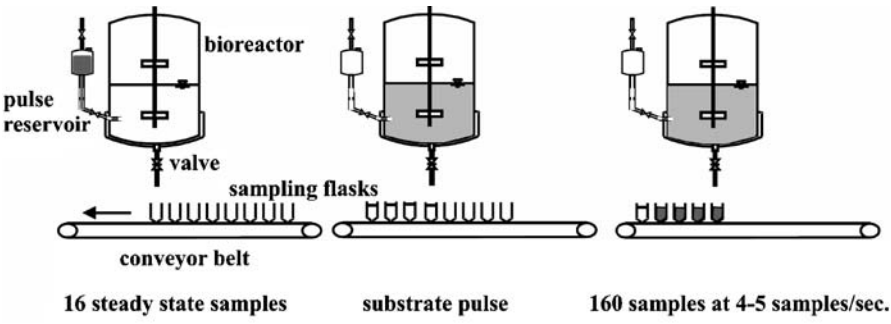

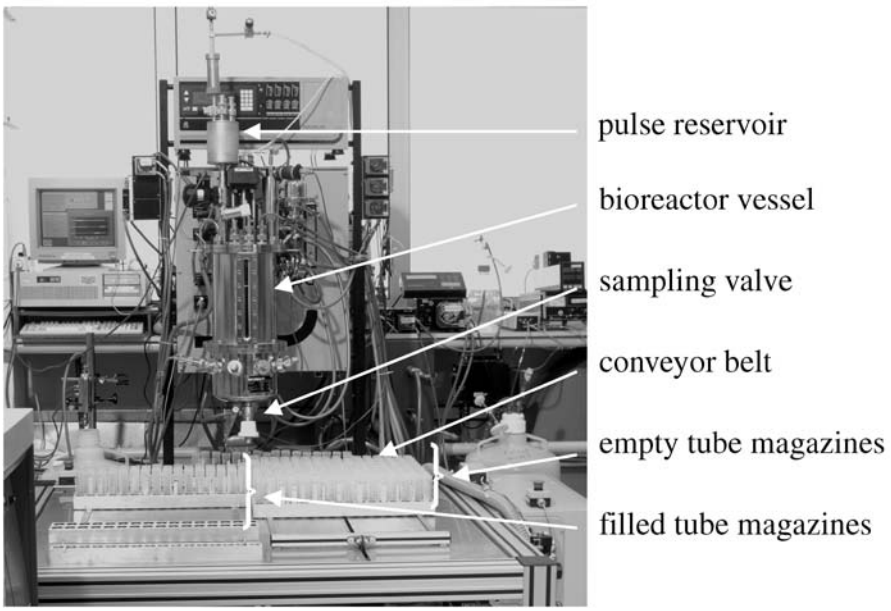

Fig. 1 Experimental setup for stimulus-response experiments used by Schäfer et al. [5]. Automated rapid sampling unit in the lower foreground

with a low sample frequency of one or two samples per fermentation, *metabolic profiling* may elucidate long-term limiting or inhibiting steps in metabolism, which can be used for iterative strain optimisation.

However, short-term dynamics of enzymatic reactions which typically appear on a subsecond time-scale after stimulus-response experiments obviously cannot be detected with such low sample frequencies. Hence, specialized rapid sampling devices must be developed and applied. As an example, Fig. 1 shows the coupled experimental setup of a bioreactor and a rapid sampling unit [4] which was used by Schäfer et al. [5]. A glucose solution is added from a pulse reservoir to the (usually) glucose-limited culture and subsequently mixed in the bioreactor (mixing time θ_{90}: about 700 ms). Samples are taken shortly before

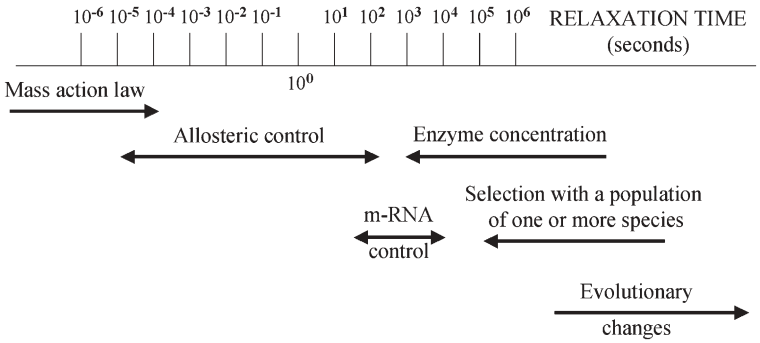

Fig. 2 Adaptational mechanisms in organisms and order of magnitude of their relaxation times [6]

and immediately after the glucose addition and are sprayed into sample tubes containing –50 °C cold methanol solution to rapidly stop metabolism during the sampling process and to preserve the metabolic answer inside the cells.

The high turnover rates of metabolites after the stimulus necessitate a rapid sampling approach with frequencies of 4–5 Hz to resolve the highly dynamic, fast metabolic answers. After cell extraction, this answer is accessible by sophisticated analytics aiming at the quantification of low assay concentrations which represent the temporarily changing pool sizes as a consequence of the initial stimulus. These data are the basis for qualitative system characterization as well as for quantitative system modelling. Both aim at a mechanistic understanding of the biological system which should provide the basis for efficient *metabolic engineering*. Because of the complexity of the data obtained, especially mathematical modelling is applied for further analysis.

Roels [6] ranked the relaxation times after a stimulation for several cellular responses according to their time scale (Fig. 2). Mass action law kinetics clearly presents the fastest response followed by the allosteric processes, controlling the activity of enzymes. Changes on the genetic or the proteomic level are slower and the enzyme concentrations can be assumed to be constant for a few minutes after stimulation. Keeping this in mind, a stimulus response experiment, e.g. using a substrate pulse (glucose), will show no effect for the genetic or proteomic properties of metabolism within an observation window of one or two minutes. Hence, the recorded response will only contain information about the enzyme kinetics and at the same time avoiding the superimposing effect of gene regulation, protein inactivation etc.

However, as a consequence, the obtained data or derived metabolic models are only valid for the conditions chosen. The choice of the experimental scenario may limit the prediction of the metabolic behaviour for different conditions. For instance, metabolism in a wild-type organism does not necessarily show identical properties compared to a recombinant production organism in a production process. Hence, if the metabolism in a production strain under

production conditions has to be studied, the experimental conditions for the stimulus response experiment should be as similar as possible compared to the production process.

This paper intends to give an overview of the chances and pitfalls of *metabolic profiling* to study dynamics in microbial central metabolism after stimulus-response fermentation experiments (pulse experiments). Furthermore, if the experimental focus switches from the investigation of catabolic to anabolic pathways – which is also motivated by their commercial importance – some additional restrictions must be considered. Respectively, typical problems are also outlined using the aromatic amino acid pathway as an example.

2
Tools and Techniques for Stimulus-Response Experiments

2.1
Stimulus of Metabolism

To perform stimulus-response experiments, the microbial stimulation must be chosen with care. On the one hand, the stimulus should be strong enough to initiate detectable signals (i.e. measurable changes of intracellular pool sizes) in the metabolites of interest. On the other hand, the system stimulation should not cause any damage of cell function. Furthermore, if a microbial production strain is analysed, cell stimulation should preferably obey basic characteristics of the usually realized production conditions of the strain in order to enable the transfer of the results obtained to the 'real' production process.

As a consequence, microbial systems such as *Escherichia coli*, *Zymomonas mobilis* or *Saccharomyces cerevisiae* are often stimulated by a rapid, one-step increase of the sole carbon source (for instance glucose). Before the pulse, a limiting amount of substrate is fed and metabolism should be at (pseudo) steady-state. Due to the stimulus, metabolism will be shifted-away from steady-state and metabolite concentrations show dynamic changes. To prevent any time delay of the external stimulation, the one-step increase of the extracellular carbon source should rapidly be transmitted into the cell. In general, this can be achieved by profiting of highly affine carbon uptake systems such as the carbohydrate phosphoenolpyruvate:phosphotransferase system (PTS) or (fast) facilitated diffusion mechanisms which are often the basis for substrate uptake in bacteria. It is noteworthy that other substrates which are not quickly consumed by the cell are consequently not suited to stimulate the biological system. This is especially remarkable if co-substrates or auxotrophic substances are intended to be used in pulse experiments. For this reason glucose is commonly used as the pulse substrate for various microorganisms, although pulse experiments with e.g. glycerol in *E. coli* are also described [7].

The first pioneering investigations using glucose pulse experiments were conducted with *S. cerevisiae* [8,9]. They stimulated a glucose limited chemostat

culture with a glucose pulse and by the sequential procedure of pulsing, rapid sampling at the same time inactivating the metabolism, extraction of the intracellular metabolites and their enzymatic measurement they were able to follow the intracellular dynamics. The concentration time courses obtained were used for detailed modelling using structured, mechanistic metabolism models [10]. These results encouraged the accomplishment of similar studies using *S. cerevisiae* [11–14], *Z. mobilis* [15, 16] and *E. coli* [5, 17–20]. Besides the invaluable results which were deduced from these experiments glucose pulse experiments have been limited to the investigation of central metabolism namely glucose uptake, glycolysis, pentose phosphate pathway and citric acid cycle in wildtype microorganism.

2.2 Rapid Sampling

After pulsing, rapid sampling is necessary to store the fast and dynamic metabolic answer in a sequence of samples. To prevent unwanted, post-pulse metabolism activity, the sampling process must include the immediate quenching of cellular metabolism.

Theobald et al. [8, 9] was the first who presented and applied an appropriate rapid sampling approach after glucose-pulse stimulation of *S. cerevisiae* grown under glucose-limited conditions. Together with his co-workers he manually sampled about 15–20 samples per minute. Later on, Weuster-Botz [16] presented a sampling tube device to perform sampling, inactivation and extraction continuously in a tube connected to the bioreactor thus monitoring central metabolism intermediates of *Zymomonas mobilis* on a sub-second time-scale.

Thereupon, an automated sampling device [4] coupled to a bioreactor was developed by Schäfer et al. [5] which is characterized by an automatic step-wise transport of the sampling tubes via a conveyor belt installed below the sampling valve of the bioreactor. Sampling rates of 4–5 Hz have been achieved while the total device including the bioreactor valves for glucose addition and sampling has been computer-controlled.

As an alternative, Buziol et al. [25] developed an apparatus consisting of a cascade of sampling valves, closely connected to the outlet of the bioreactor where the substrate pulse is added into a separate mixing chamber. Because the residence time of each liquid flow volume element is defined by the distance between the mixing chamber and the sampling valve, very fast metabolism responses can be continuously monitored by taking samples close to the mixing chamber. However, this beneficial quality also causes significant problems if metabolism dynamics are to be monitored a couple of seconds (or even minutes) after stimulation, because of the formation of concentration, pH- and dissolved oxygen-gradients inside the sampling tube (valve-cascade).

At the same time, Visser et al. [26] developed the BioScope-approach, making use of the idea of allowing continuous sampling via a stopped-flow technique. As a difference to Buziol et al. [25] they circumvented the potential

problem of dissolved-oxygen gradients in the sampling tube by using oxygen-permeable silicon membranes of up to several meters in length.

The approaches of Buziol et al. [25] and Visser et al. [26] are advantageous with respect to the relatively low amount of substrate that is necessary to stimulate the biological system, especially if one intends to 'stimulate' using for instance ^{13}C labelled glucose. However, one should take into account that two qualities are necessary to monitor metabolism dynamics after stimulus-response – namely high data frequency and an observation window of up to a couple of minutes. Especially the latter might cause problems in the sampling devices based on sampling tubes.

2.3 Quenching of Metabolism

Quenching of metabolism means that all metabolic activity inside the cell is stopped thus preventing any further conversions of metabolites by enzymatic reactions. The quenching should be realized within a subsecond time-scale because, depending on the metabolite of interest, the first intracellular effects related to the substrate pulse may occur within the first second (e.g. conversion of cytosolic glucose at 1 mM s^{-1} and cytosolic ATP at 1,5 mM s^{-1} [8, 21]).

One way to achieve this, is the immediate cell disruption (via extraction) at the same time denaturating all cellular enzymes using extreme pH conditions [9]. A disadvantage of this procedure is that the concentration of the intracellular metabolites is diluted in the fermentation supernatant of the sample and that the fermentation medium cannot be separated from the cells. Hence, such a procedure is only useful for the investigation of metabolites which are likely to occur only inside the cells.

The separation of the quenching and the cell extraction step offers the advantage that the cells in the sample can be concentrated by a centrifugation or filtration step at low temperature, thereby removing the fermentation medium. Saez and Lagunas [22] suggested washing the sampled cells after filtration with 50% methanol at –40 °C and de Koning and van Dam [21] finally sprayed the sample into the cold methanol solution. They showed that the temperature shift during the spraying process effectively blocked further metabolic activity. Additionally, it was observed that cells like *Saccharomyces cerevisiae* are resistant to leakage of metabolites when suspended in the cold methanol quenching solution. However, this resistance might not be a general characteristic of all microorganisms, because cell leakage strongly depends on the cell membrane composition. For instance, metabolite leaking was reported for glycolytic intermediates of *Lactococcus lactis* [23]. Maharjan [24] describes the detection of ^{14}C-labelled compounds after methanol quenching of *E. coli,* but no metabolites from glycolysis or pentose-phosphate pathway or cofactors, e.g. the adenosine phosphates (ATP, ADP, AMP) were identified in this study, so that *E. coli* may also be attributed as tolerant with respect to metabolite leakage during methanol quenching at –40 °C.

2.4 Extraction of Metabolites

The extraction reagent should disrupt the cells to release the intracellular metabolites and to denaturate the enzymes to prevent further conversions. Usually, the extraction agent is added after cold methanol quenching and centrifugation or it has already been used during a combined quenching and extraction step. Different extraction methods have been described for the extraction of the intracellular metabolites in various microorganisms [27]. For extraction of *Saccharomyces cerevisiae* several procedures have been published. Among them are chloroform [21], perchloric acid and alkalic ethanol solution [9] and buffered hot ethanol [28]. Additionally freeze/thaw cycles were applied to complete disruption of the cells [8].

For extraction of *E. coli*, similar methods were studied based on perchloric acid [5, 18, 29], potassium hydroxide solution [18] or a hot Tris-H_2SO_4/EDTA solution [18]. In contrast to *Saccharomyces cerevisiae*, freeze/thaw cycles showed no effect on the extraction of adenosine phosphates in *E. coli* [30].

In general, the choice of the right extraction method strongly depends on the metabolites of interest. Reduced nucleotides such as NADH or NADPH are instable during acid extractions, but stable under alkaline conditions. On the other hand, the oxidized nucleotides NAD and NADP are rapidly degraded under alkaline conditions, requiring acid extraction [31]. This representative example shows that it is essential to study the stability of the metabolites of interest under extraction conditions and that the optimal extraction conditions may be specific for different organisms. So, care must be taken to find the optimal extraction conditions concerning stability of the metabolites and extraction efficiency. In a comparative study adenosine triphosphate (ATP) was chosen as an indicator for the extraction efficiency during acid and alkaline extraction [30–32]. For *Thermoanaerobacter finnii* both methods resulted in quite similar levels, whereas perchloric acid extraction yielded a higher ATP value for *E. coli* compared to the alkaline procedure. Again, this result underlines the necessity of identifying optimal extraction conditions with respect to the biological system and the pools that should be analysed. Recently it was noted that analysis protocols developed for *S. cerevisiae* could not be directly transferred to *Penicillium* samples [58].

2.5 Analytical Access to Intracellular Metabolites

For the quantitative measurement of intracellular metabolites a variety of different analytical methods have been investigated, using enzymatic assays [33], GC-MS [34, 35], NMR [36–38], HPLC-UV [30], HPAE-PAD [39], HPLC-MS [29], HPAE-MS/MS [40] and CE-MS [41].

The measurement of intracellular metabolites with the aid of enzymatic assays is a prevalent method that benefits from the enzyme's substrate speci-

ficity allowing the quantification of distinct metabolite pools in the complex biological matrix. Hence, this approach was applied for the metabolite analysis of the first stimulus-response experiments with *Saccharomyces cerevisiae* [9, 21] and it was also considered in subsequent studies focussing on *S. cerevisiae* [11, 13] and *E. coli* [5, 18].

Despite the invaluable results obtained by enzymatic analysis, some potential drawbacks should be specified:

1. Enzymatic assays need a relatively large sample volume of about 100–300 µL for each metabolite measurement. Considering a typical sample size of 1 to 2 mL, this represents about 10–30% of the totally available sample volume. As a consequence, only a limited number of metabolites can be measured thus reducing the data density representing the metabolic dynamics after pulse stimulation.
2. The high enzyme specificity also represents an inherent disadvantage because each metabolite needs separate, time consuming, measurements. Of course, (expensive) measurement automation can be installed, however this cannot overcome the constraints outlined in (1.).
3. Enzymatic metabolite assays are always coupled to NAD(H) or NADP(H) consuming or generating reactions to allow UV based detection. Hence reaction cascades are usually necessary to achieve final concentration measurements of the metabolites of interest. Unfortunately, these are rather error-prone due to the sequential analytical procedure.
4. The selectivity of the enzymatic assays can be strongly influenced by the sample matrix (e.g. the cytoplasm composition), as found by our own studies. As an example, Fig. 3 is given showing the courses of the enzymatically measured, intracellular glucose-6-phophate (G6P) concentration [33] as a function of the assay incubation time considering two different cell extracts of *E. coli* K12 (Fig. 3A) and *E. coli* 4pF49 (Fig. 3B), respectively. For genotype details of *E. coli* 4pF49 see Appendix. Both cell extracts were prepared identically, e.g. metabolism inactivation at –50 °C cold methanol solution (60% v/v), cell extraction with perchloric acid (43% v/v) and subsequent neutralisation. Regarding the strong acidic extraction conditions, one would assume that no measurable enzyme activity would be left after cell disruption. However, Fig. 3A reveals that enzymatic G6P measurements in *E. coli* K12 extracts strongly interfered with the sample matrix, causing a steady increase of the measured fictive G6P concentration over time, whereas measurement results of *E. coli* 4pF49 (Fig. 3B) were unaffected by the matrix. Apparently, the varying extract composition of different *E. coli* strains had a significant influence on the enzymatic measurements.

To elucidate the phenomenon, cell extract samples of another glucose pulse experiment using a similar strain, called *E. coli* 4pF20 (see Appendix) were further subjected to ultrafiltration (molecular cut-off: 5000 Da) before the application of enzymatic fructose-1,6-bisphosphate (FBP) measurements. As indicated in Fig. 4, the 'FBP dynamics' were thus revealed as measurement arte-

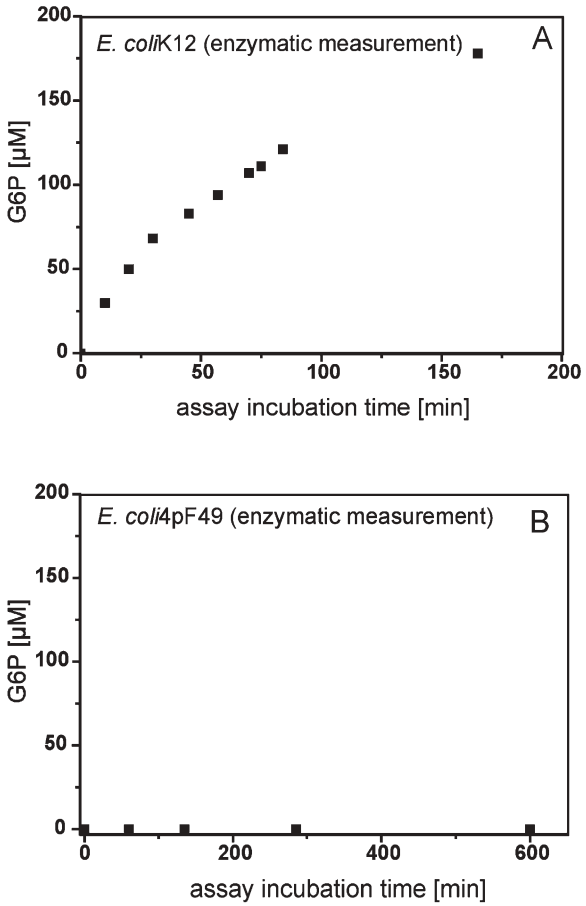

Fig. 3 Enzymatic G6P measurement (assay concentration) for *E. coli* K12 (**A**) and *E. coli* 4pF49 (**B**)

facts allowing the conclusion that – apparently – a significant, superimposing enzyme activity was left in the extract, even after perchloric acid treatment. Please note that extract 'rest activity' is not constant in the samples and that it overlays the 'true' FBP content (see Fig. 4B) by far. Hence, cell extract samples must be additionally treated by ultrafiltration making the application of enzymatic tests very time intensive.

Compared to the enzymatic approach, the NMR approach suffers from the relatively low sensitivity of this technique requiring a biomass content of several grams cell-dry weight for a quantitative cell content analysis. The application of alternative HPLC based methods with UV detection is also limited, because only nucleotides are well detectable (e.g. via HPLC-UV) while central metabolism intermediates, such as sugar phosphates from glycolysis and pentose phosphate pathway, only show a very low UV activity. However, it is

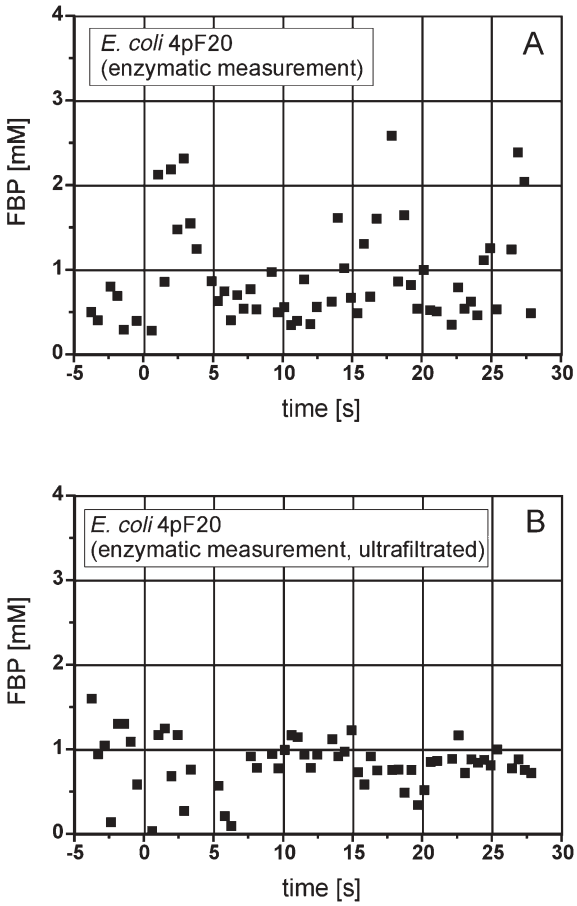

Fig. 4 Enzymatic FBP measurements (intracellular concentration) in glucose pulse experiment with *E. coli* 4pF20 before (**A**) and after an additional ultrafiltration step (**B**)

noteworthy that the biological matrix can still cause detection problems because of the complexity of the sample content.

To overcome problems in the detection of compounds with low UV activity, pulsed amperometric detection (PAD) coupled to a high-performance anion exchange (HPAE) chromatography was used instead. Because most of the metabolites can be deprotonated and thus negatively charged, anion exchange chromatography is a suitable separation method, but the salt and buffer content of the matrix can also hamper PAD [39]. In addition, this method is only useful for the measurement of metabolites which are stable under extremely high pH-values, because of a sodium hydroxide gradient used for column elution. Smits et al. [42] improved the HPAE-PAD method by applying solid-phase extraction (SPE) to clean up the sugar phosphates in extracts of *Saccharomyces cerevisiae* prior to injection.

The coupling of chromatographic separation with mass spectrometrical identification was a logical consequence of the analytical problems described in the preceding. First, GC-MS approaches were published focussing on the isotopomer analysis of proteinogenic amino acids in biomass hydrolysates [43, 44]. However, this approach needs a complicated sample preparation for metabolite derivatization to increase their volatility. Thus thermolabile or large molecules are difficult to detect – apart from the problems that might occur during the derivatization procedure – which favours their detection by liquid chromatography.

Therefore, the coupling of MS to liquid chromatography seemed to be a much more universal approach for metabolic profiling. After reliable sources with electrospray ionisation were commercially available, it was shown that this technique is well suited for intracellular analysis in extracts of *E. coli* with LC-MS [29] and *Saccharomyces cerevisiae* with HPAE-MS/MS [40]. Both methods were successfully applied to analyse intracellular metabolite courses after stimulus-response experiments. Compared to the LC-MS approach, much lower detection limits were achieved using the HPAE-MS/MS technique, presumably due to the 'delicate' ion trap used in the LC-MS. However, the applicability of HPAE may be limited due to the sodium hydroxide gradient necessary for elution which is usually not encountered using HPLC-MS.

2.6 Data Modelling

Monitoring intracellular metabolism dynamics after stimulus-response experiments during observation windows of several seconds up to minutes, usually provides several thousand pool data per experiment. Obviously, these data should not be analysed purely intuitively and qualitatively. Because the dynamic metabolic patterns resemble in vivo enzyme kinetics, the underlying mechanistic information should be uncovered with the aid of structured reaction models using the measurements for their identification. These in vivo enzyme kinetic models can be the basis for the application of detailed metabolic control analysis (MCA), thus enabling the identification of reactions that exert significant flux control for instance in the biosynthetic pathways of interest [12]. Considering the experimental procedures of the stimulus-response experiments some modelling constraints should be specified as well as necessary, simplifying assumptions:

1. Because *metabolic profiling* usually cannot distinguish between different cell-types, and cell age, only non-segregated models can be used.
2. An averaged metabolite concentration is measured in the sample thus forcing the models to assume homogenous metabolite dilution in the cells at the same time excluding potential metabolite channelling effects. However, cell compartments can be considered, if additional measurement information is available or homogenous concentrations in the compartments is fully simulated.

3. Because of the relatively short observation window, active enzyme concentrations can be assumed to be (more or less) constant thus neglecting any influence of superimposing gene regulation.

Following these constraints some structured models were already identified focusing on the central metabolism of *S. cerevisiae* [10, 11] and *E. coli* [18]. However, it should be noted that the identification of structured metabolism models based on stimulus-response data is not necessarily unequivocal. Because of lacking measurement and biological system information, different model solutions are possible that need to be discriminated carefully [20, 45]. Therefore, special software tools such as the Metabolic Modelling Tool (MMT) [19, 46] are necessary that allow the identification and validation of a set of competing approaches for the modelling of metabolism dynamics.

3
Short Example: Response-Stimulus Monitoring – Not Limited to Central Metabolism Alone

So far, stimulus-response experiments were performed using wild-type bacteria and yeasts restricting *metabolic profiling* analysis on central metabolism – namely glucose uptake, glycolysis, tricarboxylic acid cycle and pentose-phosphate pathway. This focus might be surprising because especially anabolic pathway products such as amino acids, vitamins, antibiotics etc. are of outstanding commercial interest and are thus in the focus of metabolic engineering.

Obviously some challenging problems exist that significantly hamper the application of the state-of-the-art glucose pulse approach to analyse anabolic pathways. Using the example of the aromatic amino acid pathway (Fig. 5) in a L-phenylalanine (L-phe) producing recombinant *E. coli* strain, the following section will exemplarily address some of the potential problems one is faced with if an anabolic biosynthetic route were to be analysed in addition to the 'state-of-the-art' central metabolism analysis.

3.1
Analytical Access

The analytical access to the metabolites of the aromatic amino acid pathway is an essential problem. While almost all metabolites of central metabolism are commercially available and may be measured enzymatically [33] or, most promisingly, with the aid of LC-MS technology [29, 40] similar analytical approaches for the intracellular measurement of intermediates of the aromatic amino acid pathway are lacking. Mousdale and Coggins [47] described an HPLC-UV method, but this is only applicable for the measurement of culture supernatants. Although tools such as LC-MS provide a universal analytical approach for quantifying intracellular metabolite concentrations, nevertheless,

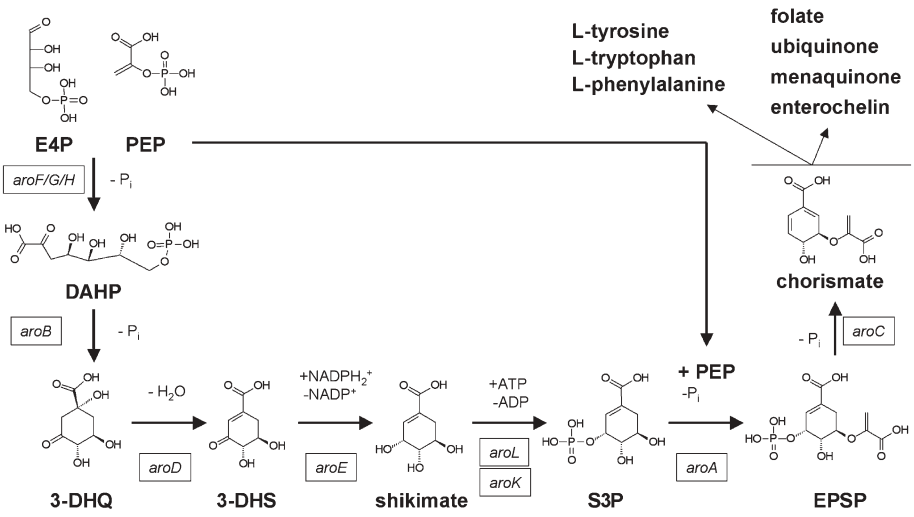

Fig. 5 Aromatic amino acid pathway leading to the three aromatic amino acids and other compounds derived from chorismate

at least purified standards of the intermediates are necessary, which are usually not available commercially. Hence, time-consuming chemical synthesis or the isolation and purification of the substances from fermentation supernatant using special 'knock-out' mutants is the consequence. Concerning the first five pathway intermediates of the aromatic amino acid pathway shikimate is the only one which is commercially available. The other metabolites, namely 3-deoxy-D-arabino-heptulosonate-7-phosphate (DAHP) and its dephosphorylated derivative DAH [48], 3-dehydroshikimate (3-DHS) [49] and shikimate-3-phosphate (S3P) [50] were isolated from culture supernatant of *E. coli* mutant strains and 3-dehydroquinate (3-DHQ) was obtained using a chemical approach [51].

Based on these standards, an LC-MS/MS method was developed using a triple stage quadrupole MS with an electrospray ionisation source (ESI) for detection (TSQ Quantum, ThermoFinnigan). Additionally, metabolites of the central metabolism were also integrated in the method to enable parallel measurement of catabolic and anabolic pathways. The optimized MS specific and compound specific MS/MS parameters are shown in Table 1 and Table 2, respectively. The LC separation is performed using the previously described cyclodextrin method [29], with the exception of using a LC split flow of 100 µL/min into the MS detector. To correct for matrix effects, e.g. ion suppression during the ionisation process [52], the standard addition method [53] was used for quantification in the cell extract samples. Peak detection and integration was based upon the signal-to-noise ratio in the compound specific MS/MS traces. To ensure stability of the metabolites, the recovery was measured with the developed LC-MS/MS method after cell extraction using perchloric

Table 1 MS specific parameters

mass spectrometer	TSQ Quantum (ThermoFinnigan)
LC split flow	100 µL/min
Ionisation	ESI
Sheath gas	50 units (nitrogen)
Auxiliary gas	15 units (nitrogen)
Capillary voltage	4.0 kV
Capillary temperature	375°C
MS scan modus	Multiple reaction monitoring (MRM)
Polarity	Negative (–)
Data type	Centroid
Q2 collision gas	Argon (1.5 mTorr)
Isolation width	1.5 amu
Scan time	150 ms per SRM
Q1+Q3 peak width	0.7 amu

Table 2 Compound specific MS/MS parameters

compound	precursor ion (*m*/*z*)	product ion (*m*/*z*)	collision energy [eV]
3-Deoxy-arabino-heptulosonate 7-phosphate (DAHP)	287.1	79.0	45
3-Deoxy-arabino-heptulosonate (DAH)	207.2	87.0	12
3-Dehydroquinate (3-DHQ)	189.1	170.8	12
3-Dehydroshikimate (3-DHS)	171.1	127.0	12
Shikimate (SHIK)	173.1	93.0	17
Shikimate 3-phosphate (S3P)	253.1	97.0	17
L-Phenylalanine (L-phe)	164.2	147.0	12
Phosphoenolpyruvate (PEP)	167.0	79.0	13
Dihydroxyacetonphosphat (DHAP), Glyceraldehyde 3-phosphate (GAP)[a]	169.1	97.0	10
2-Phospho-D-glycerate (2PG),3-Phospho-D-glycerate (3PG)[a]	185.1	79.0	35
Pentose 5-phosphates (P5P)[a]	229.1	97.0	15
Glucose 6-phosphate (G6P), Fructose 6-phosphate (F6P)[a]	259.1	97.0	17
6-Phosphogluconate (6PG)	275.1	97.0	17
Fructose 1,6-bisphosphate (FBP)	339.1	97.0	20
Adenosine 5-monophosphate (AMP)	346.2	79.0	35
Adenosine 5-diphosphate (ADP)	426.2	134.0	25
Adenosine 5-triphosphate (ATP)	506.2	158.9	33
Nicotinamide adenine dinucleotide (NAD)	662.4	540.1	17
Nicotinamide adenine dinucleotide phosphate (NADP)	742.4	620.0	17

[a] isobaric compounds with identical fragmentation pattern which are not separated by chromatography and are taken as lumped pool.

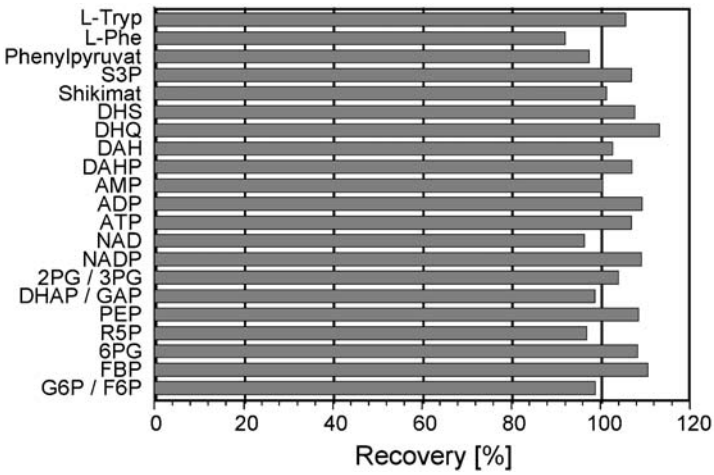

Fig. 6 Recovery of metabolites measured with LC-MS/MS after cell extraction using perchloric acid

acid. Metabolite recoveries were found to be in the range of 95–110% (Fig. 6). It is noteworthy that the presented analytical approach allows both – the analysis of central metabolism intermediates and the monitoring of aromatic amino acid pathway intermediates representing the first five reaction steps.

3.2 Experimental Set-Up

So far, the investigation of the central metabolism dynamics after glucose pulses was performed using glucose-limited chemostat cultures as described in the preceding section. However, this procedure should not be followed if recombinant microbial production strains (e.g. L-phenylalanine producing *E. coli*) are used, because of the potential loss of plasmid-encoded gene information during the glucose-limited, steady-state cultivation before the pulse. Instead, short-term, glucose-limited fed-batch approaches should be favoured [54], which resemble the 'real' production conditions, presented by Gerigk et al. [57], as much as possible. Hence, the experiment was performed with a non-growing tyrosine (L-tyr) limited culture in the production phase of a fed-batch experiment.

3.3 Signal Dilution

The analysis of metabolite concentration profiles of the central metabolism benefits from the relatively short reaction sequence from the signal input (glucose pulse) to its output (metabolite of interest). However, the signal cascade to intermediates of anabolic pathways is significantly longer, meaning that

concentration dynamics may be strongly diluted in the network before they reach the desired target. The choice of the aromatic amino acid pathway as an anabolic pathway example was also motivated by the fact, that both precursors, phosphoenolpyruvate (PEP) and erythrose-4-phosphate (E4P), are closely connected to the signal input (glucose pulse) via the PTS, glycolysis and pentose-phosphate pathway, respectively. Hence, a sufficiently strong signal transmission from the signal input (glucose uptake) to the aromatic amino acid pathway via PEP and E4P should be assumed.

3.4 Experiments with L-Phenylalanine Producing *E. coli* strains

Following the fed-batch process strategy described elsewhere [54], a glucose pulse experiment was conducted during the L-tyrosine limited L-phenylalanine production phase with non-growing *E. coli* 4pF49. After the cell extraction with perchloric acid, the neutralized samples were measured using the aforementioned LC-MS/MS method.

Results of the intracellular metabolic response are given in Fig. 7 and Fig. 8. Attention should be paid to the relatively low intracellular µM pool sizes that are still detectable using LC-MS/MS. The observed pool dynamics indicate that glucose pulse experiments can be applied to recombinant production strains during realistic fed-batch production conditions. While almost unchanged metabolite concentrations were measured during the pre-pulse period, significant dynamics can be observed during the post-pulse period of 27 seconds, not only in the intermediates of glycolysis and pentose-phosphate pathway but also in the nucleotides. For instance, a significant increase of the lumped G6P/F6P pool immediately after the pulse is identifiable, which is further transmitted to FBP and also transferred into the pentose-phosphate pathway, indicated by the lumped pentose-phosphate pool P5P.

To elucidate the signal-to-noise ratio in the experimental data, the mean value and standard deviation of the pre-pulse concentrations (steady-state) were calculated. These data were added to each diagram in Figs. 7 and 8 as horizontal lines. Most of the steady-state data are within the standard deviation range and significant changes in the pool concentrations after the pulse can be observed. Only for NAD and NADP the changes are not very significant and close to the standard deviation limit, as it could also be deduced from the concentration time courses of both metabolites. For the aromatic amino acid pathway the glucose pulse dependent increase of the DAHP pool is a factor of 26 higher than the calculated pre-pulse standard deviation which stresses the flux stimulation into this pathway.

Please note that the PEP pool did not rapidly diminish as one could assume according to the underlying PTS system that needs PEP for glucose uptake. On the other hand, similar experiments with other *E. coli* strains (data not shown) did reveal declining PEP pools after the glucose pulse thus outlining the importance of a (complex) model-based analysis of the metabolism dynamics

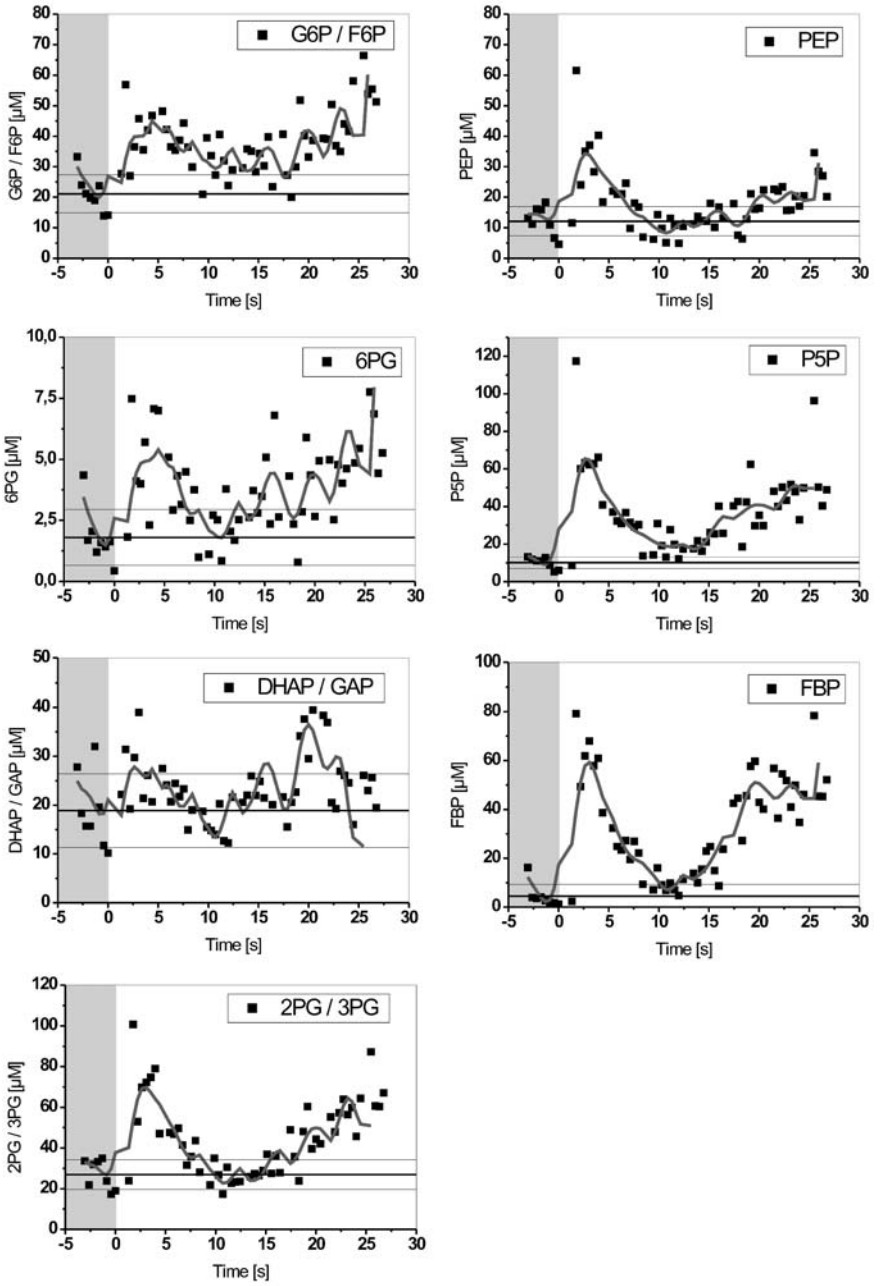

Fig. 7 Glucose pulse experiment with L-phenylalanine producing strain *E. coli* 4pF49, intracellular concentration of metabolites from central metabolism, time of pulse addition t=0 s, line graph represents smoothed data (FFT filter, 5 points) to enhance the visualisation. The three horizontal lines in each diagram display the mean steady-state concentration (*middle bold line*) ± standard deviation (*upper and lower thin line*)

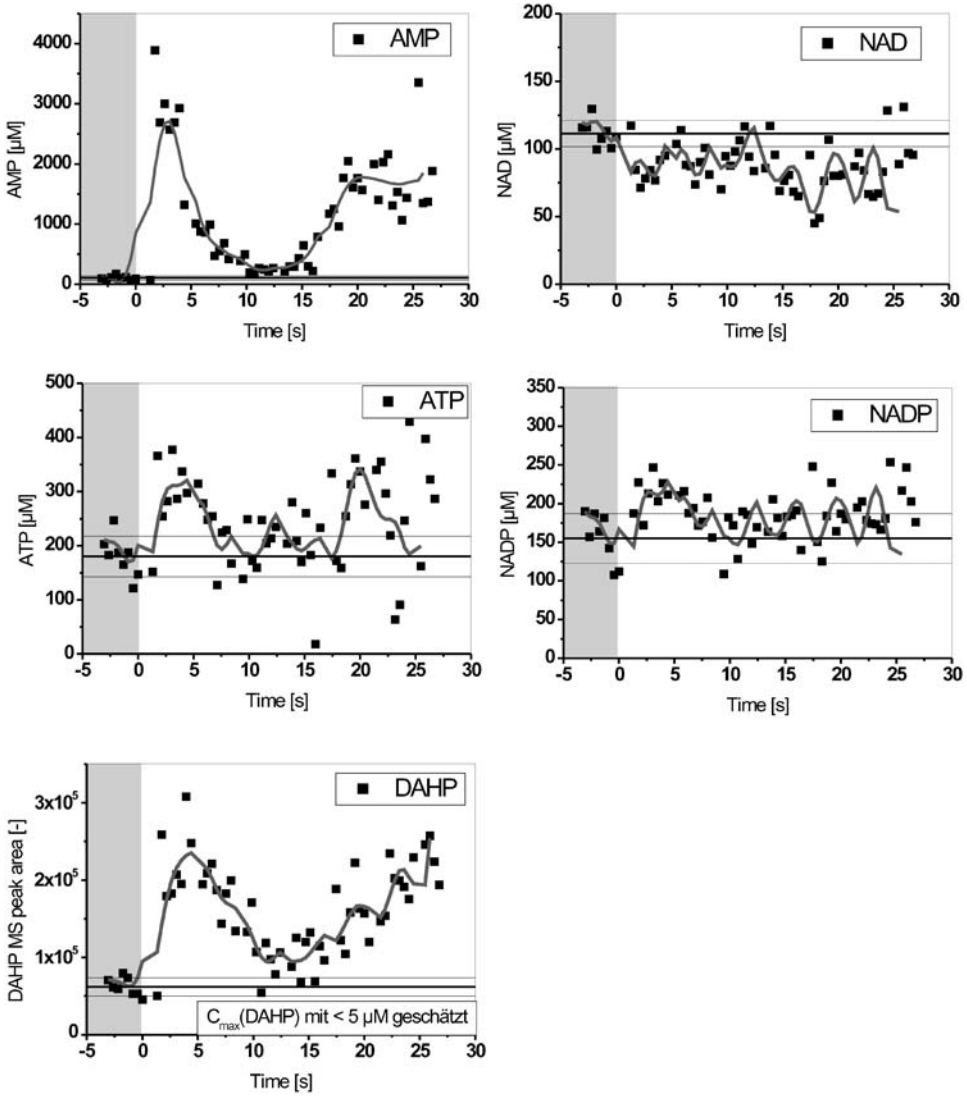

Fig. 8 Glucose pulse experiment with L-phenylalanine producing strain *E. coli* 4pF49, intracellular concentration of nucleotides and DAHP, time of pulse addition t=0 s, line graph represents smoothed data (FFT filter, 5 points) to enhance the visualisation. DAHP is displayed by the measured MS peak area because only a qualitative reference standard was available. Nevertheless, an MS/concentration relation has been estimated as shown. The three horizontal lines in each diagram display the mean steady-state concentration (*middle bold line*) ± standard deviation (*upper and lower thin line*)

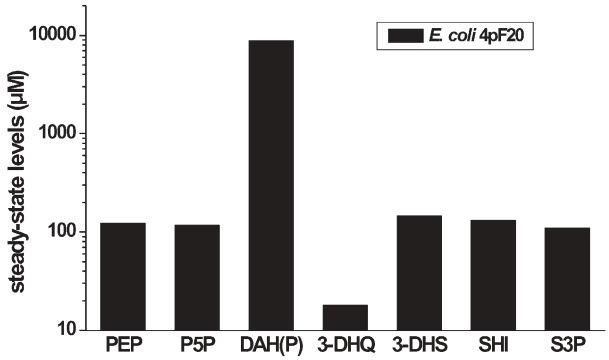

Fig. 9 Intracellular steady-state metabolite levels in *E. coli* 4pF20, possessing an *aroF*^{fbr} overexpression. The precursors phosphoenolpyruvate (PEP), the lumped pentose-phosphate pool (P5P), DAH(P), 3-dehydroquinate (3-DHQ), 3-dehydroshikimate (3-DHS), shikimate (SHI) and shikimate 3-phosphate (S3P) are shown. DAH(P) corresponds to the pool of the dephosphorylated derivative DAH, because there was only a qualitative standard available for DAHP, so the quantitative DAH result is shown instead. This is justified by a constant DAH/DAHP ratio measured in the study

to identify the underlying mechanistic interactions. E4P was not detectable, which is in agreement with previous observations of Williams et al. [59] and Ruijter and Visser [60]. In their critical review of in-vivo measured E4P levels they concluded that only very low E4P pools should be expected in vivo (if at all), because of E4P's tendency to react into dimeric forms [59]. Considering that even AroF fortified strains were used in this study, no significant E4P pool should be expected. To allow at least some speculation about the E4P supply via transketolase reaction (tkt), the lumped pentose-phosphate pool P5P can be used as reference instead.

With respect to the aromatic amino acid pathway a rapid increase of the DAHP pool, the first metabolite in that pathway, was measured directly after the pulse addition (Fig. 8). After decline to a minimum at 12 s the DAHP pool rises again, reaching the almost similar pool size at 25 s compared to the first maximum. Both pool rises coincided with increasing precursor pools, namely PEP and P5P, thus allowing the assumption that the carbon flux via DAHP-synthase is fortified by the increased precursor supply from central metabolism, due to the glucose pulse. However, effluxes of the DAHP pool (via 3-dehydroquinate synthase, AroB) leading to 3-dehydroquinate, may be limiting. Hence, no pool sizes of the subsequent metabolites of the aromatic amino acid pathway were detected.

To detect the metabolite pools downstream of DAHP after glucose pulse a further fortification of the flux into the aromatic amino acid pathway is apparently necessary. This can be achieved by genetic modification of the current *E. coli* strain, i.e. by replacing the wild-type DAHP-synthase (encoded by *aroF*^{wt}) by a tyrosine feedback resistant mutant *aroF*^{fbr}. Consequently, elevated

L-Tyr concentrations in the fermentation experiment can be used without lowering the DAHP synthase activity which finally results in amplified aromatic amino acid pathway fluxes together with increased glucose uptake rates [61].

Using the 'novel' strain *E. coli* 4pF20 under respectively changed pulse conditions lead to detectable pool sizes of DHQ, DHS, shikimate and S3P, metabolites downstream of DAHP, as shown by the measured steady-state concentrations in *E. coli* 4pF20 (Fig. 9).

Summarizing, one can conclude that anabolic pathways such as the aromatic amino acid pathway can be induced by glucose pulse experiments and that analysis, e.g. using LC-MS/MS is also promising for quantifying pathway pools. Please note that further *metabolic profiling* studies focusing on pathway dynamics in the aromatic amino acid biosynthesis are described elsewhere [55].

4 Conclusions and Outlook

During the last decade, remarkable analytical improvements were achieved enabling the thorough quantitative analysis of central metabolism and/or metabolic pathways by *metabolic profiling*. Among those, chromatographic separation combined with mass spectrometry seems to be the method of choice to quantify intracellular pool sizes at µM level using for instance LC-MS/MS techniques.

The concerted application of these *metabolic profiling* approaches in 'classical' stimulus-response experiments with rapid sampling, metabolism inactivation, modelling etc. can provide very valuable insights into the biochemical reaction network of living cells. Preferably, these experiments should also aim at the analysis of anabolic pathways leading to commercially interesting products to use the derived information for further *metabolic engineering*.

This contribution primarily represents, a short example of a stimulus-response experiment which also considers an anabolic pathway, namely aromatic amino acid synthesis, following the *metabolic profiling* approach. It was shown that the LC-MS/MS approach can be applied for metabolites of central metabolism as well as for intermediates of the aromatic amino acid pathway. Considering the dynamics of the "entrance" metabolite DAHP, it can be assumed that glucose pulses are transmitted to the anabolic pathway of interest, which is certainly important with respect to further *metabolic profiling* studies.

Referring to the recently published definition of *modern metabolic engineering* [56], the experimental procedure described previously allows one to derive the in vivo enzyme kinetic information needed to "… enter the living cell…". Hence the concerted approach of stimulus-response experiments, *metabolic profiling* and metabolic modelling may represent a powerful tool to start *modern metabolic engineering*.

Acknowledgements The authors are indebted to Prof. Wandrey for his generous support and the excellent working conditions provided at the Institute of Biotechnology at the Forschungszentrum Jülich GmbH. We would also like to thank S. Zaja, M. Kunze and U. Degner

for their analytical and experimental support and of course, for the preparation of L-phe producing strains without those the study presented would not have been possible. The work was partially financed by Deutsche Forschungsgemeinschaft DFG (grant number GR 1711/1–1).

Appendix The L-phenylalanine production strains with the names *E. coli* 4pF20 (coding for the genotype Δ(*pheA tyrA aroF*)/pJF119EH $aroF^{fbr}$ $pheA^{fbr}$ *amp*) and *E. coli* 4pF49 (coding for the genotype Δ(*pheA tyrA aroF*)/pJF119EH $aroF^{wt}$ $pheA^{fbr}$ *amp*) were used for the glucose pulse experiments. Details of *E. coli* 4pF20 are presented in Gerigk et al. [57], *E. coli* 4pF49 was constructed by Degner and Sprenger (unpublished results).

References

1. Allen J, Davey HM, Broadhurst D, Heald JK, Rowland JJ, Oliver SG, Kell DB (2003) Nature Biotechnology 21:692
2. Fiehn O (2002) Plant Molecular Biology 48:155
3. Fiehn O (2001) Comparative and Functional Genomics 2:155
4. Paschold H, Weuster-Botz D, Schäfer U, Boos W (1998) German Patent DE 197 05 289 C1
5. Schaefer U, Boos W, Takors R, Weuster-Botz D (1999) Analytical Biochemistry 270:88
6. Roels JA (1983) Energetics and kinetics in biotechnology. Elsevier Biomedical Press, Amsterdam New York Oxford
7. Buchholz A, Hurlebaus J, Wandrey C, Takors R (2002) Biomolecular Engineering 19:5
8. Theobald U, Mailinger W, Reuss M, Rizzi M (1993) Analytical Biochemistry 214:31
9. Theobald U, Mailinger W, Baltes M, Rizzi M, Reuss M (1997) Biotechnology and Bioengineering 55:305
10. Rizzi M, Baltes M, Theobald U, Reuss M (1997) Biotechnology and Bioengineering 55:592
11. Vaseghi S, Baumeister A, Rizzi M, Reuss M (1999) Metabolic Engineering 1:128
12. Mauch K, Vaseghi S, Reuss M (2000) In: Schügerl K, Bellgardt KH (eds) Bioreaction Engineering. Springer, Heidelberg Berlin New York
13. Lange HC, Eman M, van Zuijlen G, Visser D, van Dam JC, Frank J, de Mattos MJT, Heijnen JJ (2001) Biotechnology and Bioengineering 75:406
14. Ostergaard S, Olsson L, Nielsen J (2001) Biotechnology and Bioengineering 73:412
15. Weuster-Botz D, deGraaf AA (1996) Advances in Biochemical Engineering and Biotechnology, vol 54, p 76
16. WeusterBotz D (1997) Analytical Biochemistry 246:225
17. Sauter T, Kremling A, Bettenbrock K, Fischer S, Gilles ED (2002) Proceedings of the 5th German Workshop on Artificial Life. IOS Press
18. Chassagnole C, Noisommit-Rizzi N, Schmid JW, Mauch K, Reuss M (2002) Biotechnology and Bioengineering 79:53
19. Hurlebaus J, Buchholz A, Alt W, Wiechert W, Takors R (2002) In Silico Biology 2:1
20. Degenring D, Froemel C, Dikta G, Takors R (2003) Journal of Process Control (in press)
21. Dekoning W, Vandam K (1992) Analytical Biochemistry 204:118
22. Saez MJ, Lagunas R (1976) Molecular and Cellular Biochemistry 13:73
23. Jensen NBS, Jokumsen KV, Villadsen J (1999) Biotechnology and Bioengineering 63:356
24. Maharjan RP, Ferenci T (2003) Analytical Biochemistry 313:145
25. Buziol S, Bashir I, Baumeister A, Claassen W, Noisommit-Rizzi N, Mailinger W, Reuss M (2002) Biotechnology and Bioengineering 80:632
26. Visser D, van Zuylen GA, van Dam JC, Oudshoorn A, Eman MR, Ras C, van Gulik WM, Frank J, van Dedem GWK, Heijnen JJ (2002) Biotechnology and Bioengineering 79:674

27. Karl DM (1980) Microbiological Reviews 44:739
28. Gonzalez B, Francois J, Renaud M (1997) Yeast 13:1347
29. Buchholz A, Takors R, Wandrey C (2001) Analytical Biochemistry 295:129
30. Meyer S, Noisommit-Rizzi N, Reuss M, Neubauer P (1999) Analytical Biochemistry 271:43
31. Schmid U, Schimz KL, Sahm H (1989) Analytical Biochemistry 180:17
32. Bagnara AS, Finch LR (1972) Analytical Biochemistry 45:24
33. Bergmeyer H (1984) Methods of Enzymatic Analysis. Verlag Chemie, Weinheim
34. Harvey DJ, Horning MG (1973) Journal of Chromatography 76:51
35. Katona ZF, Sass P, Molnar-Perl I (1999) Journal of Chromatography A 847:91
36. Ogino H (1982) Proc Natl Acad Sci, vol 79, USA p 5828
37. Teleman A, Richard P, Toivari M, Penttilla M (1999) Analytical Biochemistry 272:71
38. De Graaf AA, Striegel K, Wittig RM, Laufer B, Schmitz G, Wiechert W, Sprenger GA, Sahm H (1999) Archives of Microbiology 171:371
39. Bhattacharya M, Fuhrman L, Ingram A, Nickerson KW, Conway T (1995) Analytical Biochemistry 232:98
40. van Dam JC, Eman MR, Frank J, Lange HC, van Dedem GWK, Heijnen SJ (2002) Analytica Chimica Acta 460:209
41. Soga T, Ueno Y, Naraoka H, Ohashi Y, Tomita M, Nishioka T (2002) Analytical Chemistry 74:2233
42. Smits HP, Cohen A, Buttler T, Nielsen J, Olsson L (1998) Analytical Biochemistry 261:36
43. Christensen B, Nielsen J (1999) Metabolic Engineering 1:282
44. Dauner M, Sauer U (2000) Biotechnology Progress 16:642
45. Wiechert W, Takors R (2003) In: Westerhoff HV, Kholodenko BN (eds) Metabolic Engineering in a Post Genomic Era (in press)
46. Haunschild MD, Freisleben B, Wiechert W, Takors R (2002) 16th European Simulation Multiconference ESM'2002, vol Modelling and Simulation 2002. SCS Europe, Darmstadt, 03.–05.06. p 436
47. Mousdale DM, Coggins JR (1985) Journal of Chromatography 329:268
48. Mehdi S, Frost JW, Knowles J (1987) Metabolism of the Aromatic Amino Acids (Methods in Enzymology), vol 142, p 306
49. Dell KA, Frost JW (1993) Journal of the American Chemical Society 115:11581
50. Coggins JR, Boocock MR, Chaudhuri S, Lambert JM, Lumsden J, Nimmo GA, Smith DDS (1987) Metabolism of the Aromatic Amino Acids (Methods in Eynzmology), vol 142, p 325
51. Grewe R, Jeschke JP (1956) Chemische Berichte-Recueil 89:2080
52. Zimmer D (2003) Chromatographia 57:S325
53. Bader M (1980) Journal of Chemical Education 57:703
54. Schmitz M, Hirsch E, Bongaerts J, Takors R (2002) Biotechnology Progress 18:935
55. Oldiges M, Kunze M, Degenring D, Takors R (2003) (submitted)
56. Westerhoff HV (2001) Metabolic Engineering 3:207
57. Gerigk MR, Maass D, Kreutzer A, Sprenger G, Bongaerts J, Wubbolts M, Takors R (2002) Bioprocess and Biosystems Engineering 25:43
58. Mashego MR, Wu L, Van Dam JC, Ras C, Vinke JL, Van Winden WA, Van Gulik WM, Heijnen JJ (2004) Biotechnology and Bioengineering 85:620
59. Williams JF, Blackmore PF, Duke CC, Macleod JK (1980) International Journal of Biochemistry 12:339
60. Ruijter GJG, Visser J (1999) Biochimie 81:267
61. Takagi M, Nishio Y, Oh G, Yoshida T (1996) Biotechnology and Bioengineering 52:653

Received: April 2004

Adv Biochem Engin/Biotechnol (2005) 92: 197–224
DOI 10.1007/b98912

Technical Application of Biological Principles in Asymmetric Catalysis

Andreas Liese (✉)

Institut für Biochemie, Westfälische Wilhelms-Universität Münster,
Wilhelm-Klemm-Strasse 2, 48149 Münster, Germany
aliese@uni-muenster.de

Abstract The production of enantiopure compounds is becoming increasingly important to the chemical and biotechnological industries. Bioorganic transformations look set to meet this demand due to their inherently regio- and stereoselective natures. In this sense, biosynthesis needs to be viewed as "chemistry by nature". Biological principles that have been optimized over thousands of years experience a new renaissance when used for technical asymmetric catalysis; however, to be able to use them, we need an appropriate technology: reaction engineering. Indeed, various biological principles are already being applied in technical asymmetric synthesis without the scientific community at large being aware of this.

1 Biological Principles

The American Heritage Dictionary defines a *principle* as "a rule or law concerning the functioning of natural phenomena or mechanical processes" [1]. In other words, a principle is a statement of fact that has wide general applicability and has already been tested by many workers over long periods of time. *Biological principles* are those principles that have been developed and applied by nature over thousands of years. Over the course of time they are even optimized by evolution. Some examples are:

1. Living systems obey physical and chemical laws.
2. All organisms capture, store and transmit energy.
3. All organisms are adapted to their habitat.
4. Evolution is irreversible.
5. Growth is a fundamental characteristic of life.
6. Energy fixation in plants is carried out via photosynthesis.

The transfer of biological principles and concepts to technical applications leads to astonishingly successful results. Often, even if no transfer was planned in the first place, the solutions developed for a given problem look surprisingly similar. One example is the development of highly specialized tools for drilling hard materials. The drill of the yellow-headed giant wasp of North America uses the same structure/principle as a drill that was developed by engineers to drill holes into hard materials [2]. Leonardo da Vinci (1452–1519) used nature as a source of inspiration. Based on his observations of how birds fly, he planned the first machines that would enable men to fly too. Both examples demonstrate that bio-inspired design and development has consistently has provided and will continue to point to solutions to technological problems. But what other principles from nature can be transferred to chemical synthesis and chemical technology besides these engineering-based examples? We will explore this question in the following sections.

The word "biotechnology" implies that different disciplines of natural sciences are united in this field. Aside from biology and the discipline-specific technology, chemistry, physics, and engineering are also of fundamental importance. This fact becomes especially obvious if one considers a whole cell as a microfabrication unit (Fig. 1): Anton from DuPont has pointed out before: "You are looking at living organisms as tiny chemical factories in their own right–multiple 2-micron-sized reactors" [3].

Nature had to find ways to synthesize complex compounds, often in a highly stereoselective manner, from primitive starting materials, such as CO_2 or glucose. Initiating multi-step reactions in sequences or cycles solves this task. Enantio- or regioselectivity is introduced via highly selective catalysts: enzymes. These biological catalysts are generally of high molecular weight and are either homogeneously solubilized within the cells, or alternatively they are bound to membranes. Nature had to solve the problem that different reaction steps have to occur spatially separated in order to prevent cross-reactions or inhibitions. Therefore, different compartments in the cell exist, forming independent reaction volumes. The macromolecular biocatalysts are either retained inside membranes (if they are solubilized), or alternatively, they are coupled to membranes. Starting materials need to be transported into the cell, and products out of the cell. Besides this, intermediates need to be transported between different compartments of the cell. Therefore, different procedures are established, such as diffusive and active transport. Side products are removed by separation or even by reactive work-up, whereby they become integrated as starting materials into subsequent reaction sequences. To keep these little

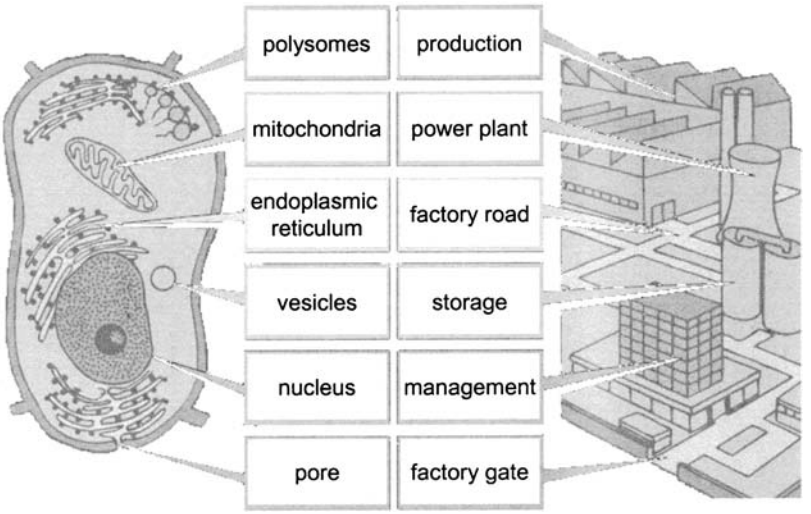

Fig. 1 The whole cell as a microfabrication unit [190]

micron-sized factories running, energy needs to be supplied, either by photosynthesis or respiration. Energy is stored in chemical compounds, for instance as adenosine triphosphate (ATP), and is transported coupled to a mass-transfer action. These biological factories are very well adapted to their function and to their surroundings. A two foot long neuron, a two pound ostrich egg, and a 0.2 µm bacterium all represent a single cell. Bacteria can be found in the Antarctica surviving significantly below 0 °C, as well as in boiling fountains in the Yellowstone National Park in the USA. In other words, a cell is nothing more than a biological factory producing chemicals (Fig. 1), that is optimized for its special task. Nevertheless, as different as the shape and the functions of different cells are, they all follow the same biological principles as far as biosynthesis is concerned. These basic biological principles are:

1. Complex chemicals are synthesized in reaction sequences.
2. Biological catalysts are macromolecular and in general homogeneously soluble.
3. Membranes retain macromolecular, homogeneously solubilized catalysts.
4. Coupling to membranes heterogenizes catalysts.
5. Key steps of reaction sequences are catalyzed.
6. Energy and mass transport are most often coupled.
7. Mass transport over gas/liquid barriers is facilitated by membranes.

There are undoubtedly other biological principles of biosynthesis beyond these, but the ones listed above seem to be the fundamental ones. In this chapter we will start by focusing on technical asymmetric catalysis. Then we will investigate the transfer and applicability of biological principles to technical asymmetric chemistry.

2
Technical Asymmetric Catalysis

The term "catalysis" was first coined by Berzelius in 1836 and stems from the Greek meaning "down" or "loosen" [4]. Up until then, only affinity, as a chemical driving force, was known. Berzelius stated that reactions occur by "catalytic contact". Ostwald developed a more detailed understanding of catalysis in 1883 [5]. He described catalysis as the phenomenon in which a small quantity of a certain substance, the catalyst, increases the rate of a chemical reaction or the rate of approaching the equilibrium of a chemical reaction, without itself being substantially consumed. Only thermodynamically feasible reactions can be accelerated by catalysts [6].

Biological catalysts were already being used by man long before Berzelius and Ostwald conducted their investigations, without anybody even being aware of their existence in the production of food and beverages. Sumerians and Babylonians practiced beer brewing before 6000 B.C., references to wine making can be found in the Book of Genesis, and Egyptians used yeast for baking bread. However, the knowledge of the production of chemicals such as alcohols and organic acids by fermentation is relatively recent, and the first reports in the literature appeared only in the second half of the nineteenth century. In 1921, Chapman reviewed a number of early industrial fermentation processes for the production of organic chemicals [7]. Gradually, it was discovered that microorganisms could modify certain compounds by simple, chemically well-defined reactions, which are further catalyzed by enzymes. Nowadays, these processes are called "biotransformations". The essential difference between fermentation and biotransformation is that there are several catalytic steps between substrate and product in fermentation while there is only one or two in biotransformation. Also, the chemical structures of the substrate and the product resemble one another in a biotransformation, but this is not necessarily so in fermentation.

Early industrial catalytic processes used inorganic compounds as catalysts. An example is the so-called "Deacon process", the oxidation of HCl into Cl_2, as well as the production of sulfuric acid (Table 1). The production of sulfuric acid had already been commercialized by the mid-eighteenth century [4]. It is worth noting that a homogeneous catalyst was used in the first industrially applied catalytic process.

Asymmetric catalysis is a special discipline in the field of catalysis that enables the selective synthesis of just one single enantiomer of a racemate [8]. In the chemical industry, this field of research has become more and more important over the past 20–30 years. This is due to the fact that many compounds associated with living organisms are chiral, including DNA, enzymes, antibodies, and hormones. Typically, different enantiomers of a particular compound have different biological activities. Prominent examples are limonene and propanolol. (*S*)-Limonene smells like lemons and the enantio-complementary (*R*)-enantiomer smells like oranges. (*S*)-Propanolol is used as a drug against high blood pressure, whereas the (*R*)-enantiomer is contraceptive.

Table 1 The first industrial chemically catalyzed processes [4]

Year	Process	Catalyst
1750	H_2SO_4 lead chamber process (*homogeneous catalyst system*)	NO/NO_2
1870	SO_2 oxidation	Pt
1880	Deacon process (Cl_2 from HCl)	$ZnCl_2/CuCl_2$
1885	Claus Process (H_2S and SO_2 to S)	Bauxite
1900	Methane from synthesis gas	Ni
1910	Haber-Bosch ammonia synthesis	Fe/K
1920	Methanol synthesis (high pressure process)	Zn, Cr oxide
	Fischer-Tropsch synthesis	Promoted Fe, Co
	Acetaldehyde from acetylene (*homogeneous catalyst system*)	Hg^{2+}/H_2SO_4

In the past, almost all drugs were marketed as racemic 1:1 mixtures of both enantiomers (this still applies to some drugs today too). This has sometimes lead to severe complications, such as in the sad case of thalidomide, an anti-inflammatory and sedative drug. In the 1990s, the American Food and Drug Administration (FDA) decided that a racemic drug could be patented again in its enantiopure form, if it can be proved unequivocally that the enantiomer to be patented is solely responsible for the origin of the pharmaceutical effect [9]. Besides this, there is also an economical (and environmental) consideration: if 50% of the mixture yields no effect, 50% of the production costs are spent on waste.

As one can see from these points, there is also huge financial potential hidden in the so-called "chiral switches", compounds that were formerly introduced to the market as racemates, but which can now be reregistered with the FDA in single enantiomer forms; Fig. 2 illustrates the predicted exponential growth of the world market for chiral technology.

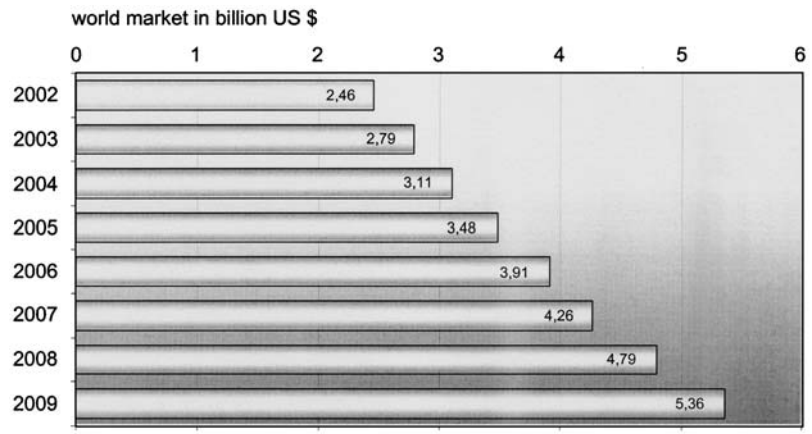

Fig. 2 World market for chiral technologies in billions of US$ [191]

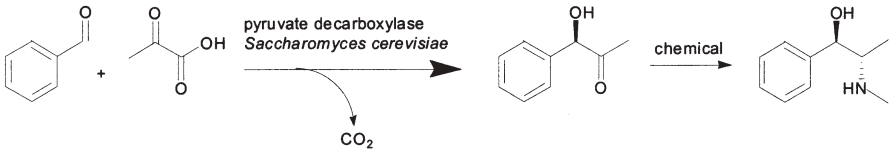

Fig. 3 Synthesis of L-ephedrine

Once again however, here as well, nature is first. It has been practicing asymmetric catalysis since thousands of years in its micron-sized reactors, namely cells. In 1858, Pasteur [10] was first to demonstrate the microbial resolution of tartaric acid. He performed fermentation of the ammonium salt of racemic tartaric acid, mediated by the mold *Penicillium glaucum*. The fermentation yielded (–)-tartrate. Even if this is a resolution process and not asymmetric synthesis, it was the first time that nature's enantioselectivity has been demonstrated. L-Lactic acid was probably the first optically active compound to be produced industrially by fermentation. Its asymmetric synthesis via biochemistry was first accomplished in the USA in 1880 [11]. Neuberg and Hirsch [12] discovered in 1921 that the condensation of benzaldehyde with acetaldehyde in the presence of yeast results in optically active (1*R*)-hydroxy-1-phenyl-2-propanone. This compound was then further chemically processed into L-(–)-ephedrine (Fig. 3) by Knoll A.G., Ludwigshafen, in Germany (1930) [13].

Numerous authors have given overviews of biotransformations used in industry [11, 14–25]. The use of biocatalysis from the viewpoint of a chemist in the lab is summarized in several books as well. Recent ones are [26–31]. Some selected examples of technical asymmetric biotransformations as applied in industry are given in Table 2. Late in 2002, M.-R. Kula and M. Pohl received the German Future Prize 2002 – awarded by the President of the Federal Republic of Germany for Technology and Innovation – for their project: "Soft Chemistry with Biological Catalysts".

Like nature, man has also been – and still is – developing chiral catalysts. These achievements have been acknowledged by several Nobel Prizes in the field of chirality (Table 3). The latest one in this field has been awarded to W. Knowles, R. Noyori, and K. Sharpless in 2001 for their work on asymmetric catalysis.

The first asymmetric synthesis developed by man was the cyanohydrin synthesis, which was the focus of E. Fischer's seminal work on asymmetric induction [11]. Subsequently, following Bredig's results that quinine catalyzes the enantioselective hydrocyanation of aldehydes [32], several cinchona alkaloid bases were investigated in enantioselective processes [33]. Today, most of the synthetic chiral catalysts are based on transition metals, modified by optically active additives, or by transition metal complexes, containing optically active ligands [6]. The milestones of man-made asymmetric catalysis are summarized in Table 4.

Table 2 Examples of technical asymmetric biosyntheses applied in industry [4, 21]

Year	Process	Catalyst
1880	L-lactic acid formation by fermentation of glucose or lactose	Lactobacillus
1930	L-ephedrine intermediate through asymmetric C–C bond formation	Yeast
	sorbitol to L-sorbose oxidation in vitamin C production	*Gluconobacter suboxydans*
1950	L-amino acids through fermentation	Brevi-, Corynebacterium species
1970	L-aspartic acid by the addition of ammonia to fumaric acid	aspartase (*E. coli*)
1980	L-dopa from ammonia, pyruvate and catechol	bacterial enzymes
	L-malic acid by the addition of water to fumaric acid	fumarase (Brevibacterium)
2000	(1*S*)-hydroxy-(3-phenoxy-phenyl)-acetonitrile by hydrocyanation	oxynitrilase

Table 3 Nobel Prizes in the field of chirality

Year	Awarded to	Nobel Prize in chemistry for
1902	Hermann E. Fischer	recognition of the extraordinary services he has rendered by his work on sugar and purine syntheses
1975	John W. Cornforth	work on the stereochemistry of enzyme-catalyzed reactions
	Vladimir Prelog	research into the stereochemistry of organic molecules and reactions
1990	Elias J. Corey	development of the theory and methodology of organic synthesis
2001	William S. Knowles, Ryoji Noyori	work on chirally catalyzed hydrogenation reactions
	K. Barry Sharpless	work on chirally catalyzed oxidation reactions

Table 4 Milestones in chemical asymmetric catalysis

Year	Process	Literature
1912	enantioselective hydrocyanation	[32]
1932	support of metallic catalysts in asymmetric (de)hydrogenations on quartz	[175]
1939	modification of a *heterogeneous* Pt hydrogenation catalyst by a chinchona alkaloid	[176]
1966	homogeneous asymmetric (cyclopropanation of styrene) catalysis by a soluble chiral metal complex 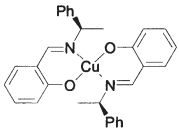	[177]
1968	hydrogenation of olefines with modified *Wilkinson* catalyst	[178, 179]
1971	synthesis of L-dopa catalyzed by Rh-DIPAMP complex 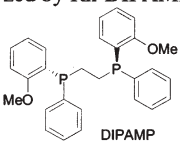 DIPAMP	[180, 181]
1980	asymmetric epoxidation of allylic alcohols with Ti^{IV}-tartrate complex	[182]
1981	reduction of ketones catalyzed by oxazaborolidines 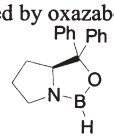	[183, 184]
1984	$ZnEt_2$ addition to aldehydes catalyzed by β-amino alcohols 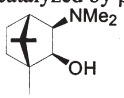	[185]
1988	asymmetric dihydroxylation via ligand-accelerated catalysis with chinchona alkaloid 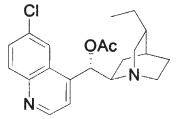	[186]
1991	epoxidation of unfunctionalized olefines catalzed by Mn^{III} salene complex 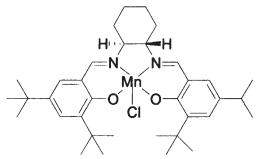	[187]
1993	L-menthol synthesis with (*S*)-BINAP 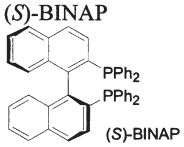	[188, 189]

3
Transfer of Biological Principles to Technical Asymmetric Catalysis

As we have seen, nature is already applying highly advanced technologies in its own micro fabrication units, the whole cells. Indeed, nature's asymmetric catalysis has been slowly perfected to the highest degree. It uses enantio- and regioselective catalysts, the enzymes; an approach that means that there is no need to introduce and later cleave off protecting groups, a concept that is still common in general chemistry. We also noted that the first asymmetric compounds to be produced industrially were done so using biotransformations.

3.1
In vitro Biological Reaction Sequences

Biological catalysts have been optimized by evolution over the course of time. Since their reaction conditions are generally compatible with natural processes, biocatalysts have been applied by nature in reaction sequences and cycles [34], for example in the citric acid cycle. This represents the first biological principle: *complex chemicals are synthesized in reaction sequences.* The intermediate separation and purification approach common to *classical* organic syntheses, used due to incompatibilities between reaction steps, is generally not needed if biocatalysts are used (Fig. 4). In *modern* organic synthesis, however, these additional separation and purification steps are frequently not needed anymore.

In the chemical literature, several names are used to describe reaction sequences: cascade, consecutive, domino, iterative, one-pot (one-flask), sequential, tandem, and zipper reactions [35]. Listed below are two main reaction types to be differentiated. One is the so-called domino (or "cascade") reaction, where the reaction sequence is initiated (or "triggered") by the first step. The other one is the tandem (or "sequence") reaction, which consists of a two-step reaction performed in a consecutive fashion [36]. The first type is especially important if the intermediates are unstable. For a recent review on enzyme-initiated domino reactions, see [36]. In the last decade, more and more biocatalyzed reaction sequences have been investigated. A comprehensive review on this

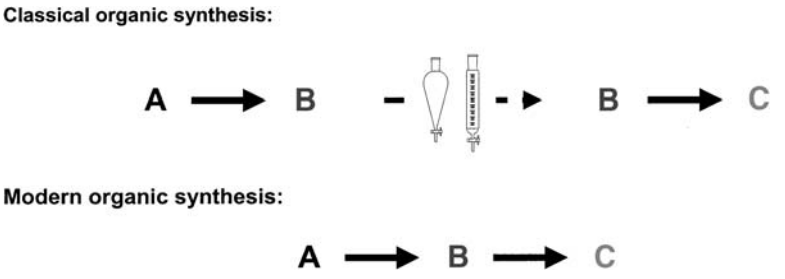

Fig. 4 Comparison of classical and modern organic synthesis

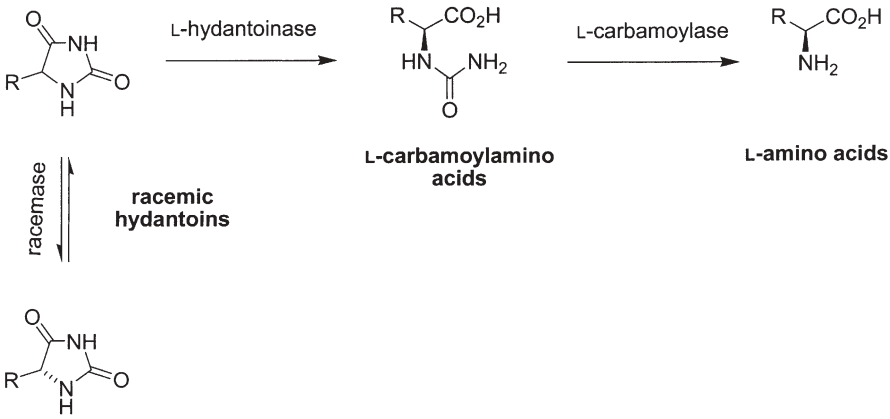

Fig. 5 Synthesis of L-amino acids by the sequential usage of a hydantoinase and a carbamoylase [38, 39]

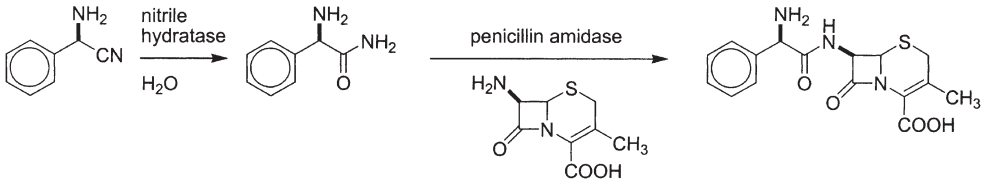

Fig. 6 Two-step enzymatic synthesis of cephalexin from D-phenylglycine nitrile [40]

topic has been published by Bruggink et al. [37]. Examples are the synthesis of L-amino acids through the sequential usage of a hydantoinase and a carbamoylase [38, 39] even integrating an additional racemase (Fig. 5), the two-step enzymatic synthesis of cephalexin from D-phenylglycine nitrile [40] (Fig. 6), the two-step enzymatic synthesis of L-lactic acid from acetaldehyde [41], and the four-step enzymatic synthesis of non-natural carbohydrates from glycerol [42, 43] (Fig. 7). In the latter example, the different enzymes are activated stepwise by switching the pH.

In a 12-step enzymatic conversion in one-pot, the corrin moiety of vitamin B_{12} was transformed on a milligram scale [37, 44, 45].

Multicatalyst systems have been established for in situ cofactor regeneration for several decades. Examples are the regeneration of the precious nicotinamide cofactors [46–50] or the regeneration of the expensive nucleotide sugars [51–55]. Besides this, there are also several examples of reaction sequences to transform sugars and synthesize oligosaccharides in one-pot [55–60]. The performance of such reaction sequences have even been optimized by means of mathematical methods, as in the case of the synthesis of the *O*-glycan core 2 structure [61].

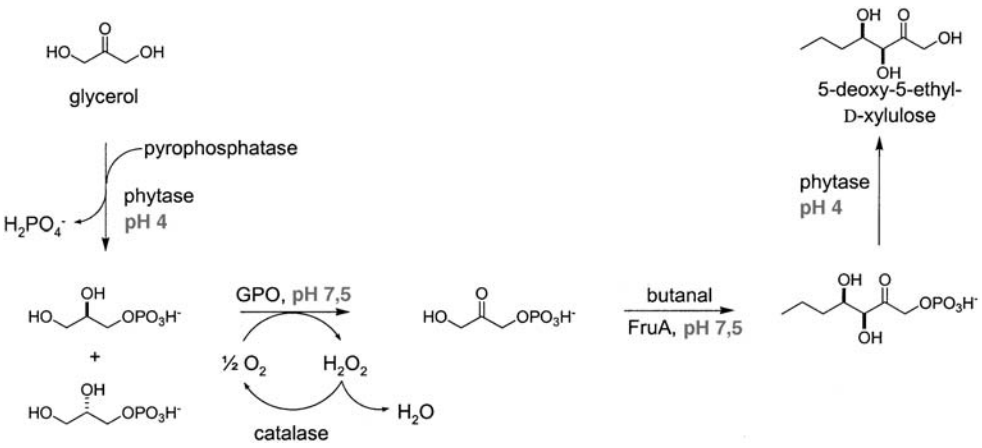

Fig. 7 Four-step enzymatic synthesis of non-natural carbohydrates from glycerol [42, 43]

3.2
In vivo Biological Reaction Sequences

Besides the application of isolated enzymes, whole cells have also been applied in order to utilize their in vivo reaction sequences for the synthesis of fine chemicals. The most popular microorganism for biocatalysis is baker's yeast (*Saccharomyces cerevisiae*) [62]. However, utilizing whole cells as "bags of enzymes" has some drawbacks: 1) low enzymatic activities; 2) often low permeability for substrate and product; 3) inhibition of cell growth by reactants; 4) degradation of substrate or product by cellular activity, and; 5) difficulties with isolation and purification from the reaction mixture [63]. Nevertheless, many approaches for whole cell conversions have been investigated and are applied on an industrial scale [21]. These limitations can partly be overcome by reaction engineering. Furthermore, new strains are constructed by means of recent genetic engineering technologies where the desired enzymes are cloned and overexpressed [64, 65]. A very prominent example is the asymmetric reduction of ethyl 4-chloro-3-oxobutanoate to ethyl (*S*)-4-chloro-3-hydroxy-butanoate. In this case *Escherichia coli* cells expressing both the carbonyl reductase gene from *Candida magnoliae* and the glucose dehydrogenase gene from *Bacillus megaterium* are used as the catalyst. In a two-phase system consisting of an organic solvent and an aqueous phase, ethyl (*S*)-4-chloro-3-hydroxy-butanoate is formed in the aqueous phase and reextracted into the organic phase (Fig. 8). Reportedly, the final concentration of the product amounted to 2.58 M (430 g L^{-1}), the molar yield being 85% [66–70]. By applying wild-type cells of *Lactobacillus kefir*, the two-step enantio- and diastereoselective reduction of 2,5-hexandione was carried out in a continuously operated process, yielding a space-time yield of 64 g L^{-1} d^{-1} [71, 72] (Fig. 9).

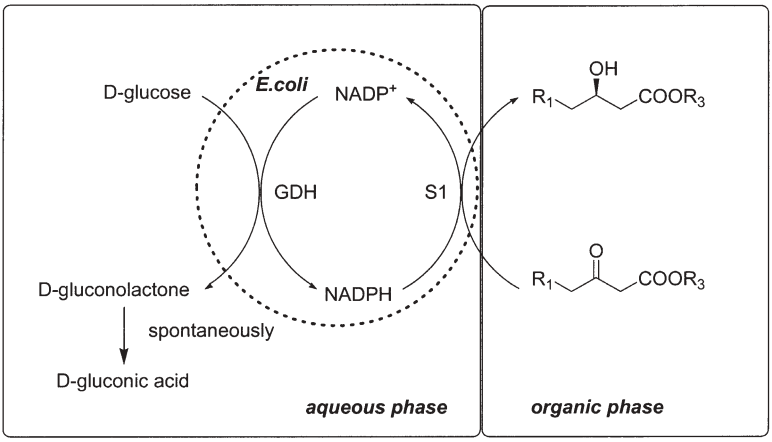

Fig. 8 *Escherichia coli* cells expressing both the carbonyl reductase gene from *Candida magnoliae* (S1) and the glucose dehydrogenase (GDH) gene from *Bacillus megaterium* being used as a catalyst [69, 70]

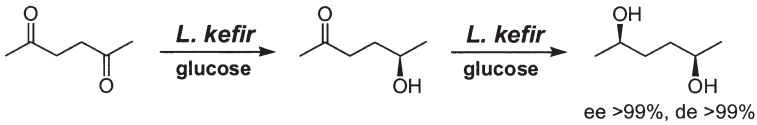

Fig. 9 Synthesis of (2*R*,5*R*)-hexandiol with resting cells from *Lactobacillus kefir* [71, 72]

A new way to carry out a reaction sequence was introduced by the *Kyowa Hakko* company. Recombinant *E. coli* and *C. ammoniagenes* is used for the industrial manufacture of oligosaccharides; for instance Lewis X [63, 73–77]. Here, different enzyme activities are located in different recombinant *E. coli* cells that are added to the batch process as a function of time, thereby circumventing feedback inhibitions. This highlights the importance of reaction engineering and technical chemistry if biological principles are to be transferred to technically useful forms of asymmetric catalysis. If different catalysts are combined in a one-pot synthesis, problems with feedback inhibition and concurring reactions often occur. Therefore, it is often important to separate individual reaction chambers. Nature too had to solve this problem, and it also uses the separation of reaction chambers, like in the Golgi apparatus. Therefore, separation of reaction chambers is a further biological principle.

3.3 Chemoenzymatic Reaction Sequences

A newly arising and very promising field is the combination of chemo- and biocatalysis (see Bruggink et al. [37]). The first combined one-pot synthesis utilizing a bio- and chemocatalyst seems to be the conversion of D-glucose into

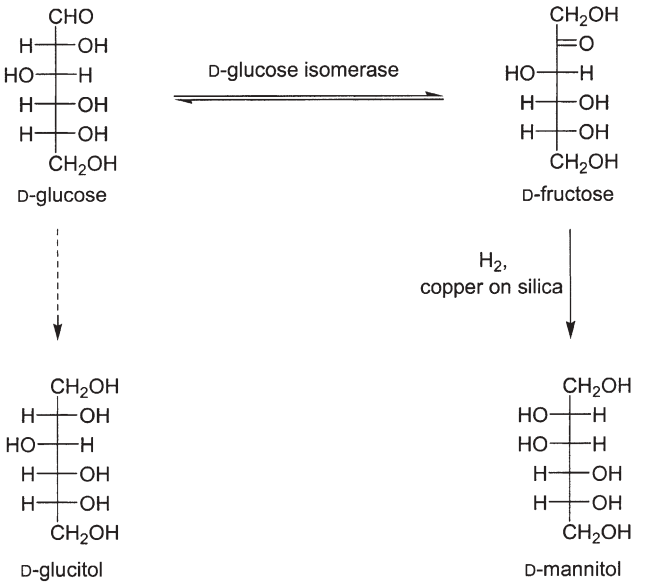

Fig. 10 Chemoenzymatic Synthesis of D-mannitol [78]

D-mannitol, published in 1980 [78]. Glucose isomerase transforms glucose into fructose, resulting in a 1:1 mixture. A copper catalyst added at the same time hydrogenates fructose to mannitol (Fig. 10). The yield of D-mannitol is twice as high as by the traditional process. These combinations are especially useful if dynamic kinetic resolutions need to be established (for a recent comprehensive review, see [79]). In the dynamic kinetic resolution of β-hydroxy nitriles, yields of up to 81%, and an ee of up to 99% for the acylated alcohol are reached [80] (Fig. 11). The non-acylated starting material (hydroxyl nitrile) is isomerized *in situ* by a ruthenium catalyst.

Using this approach, it is possible to transfer a classical kinetic resolution ideally to a 100% ee/100% yield synthesis. DSM Fine Chemicals has recently

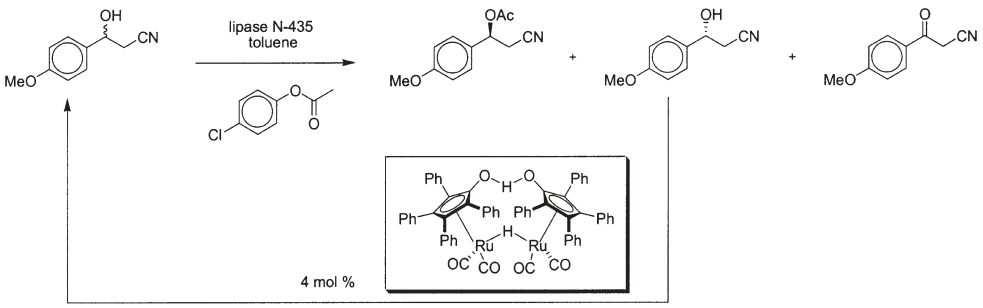

Fig. 11 Dynamic kinetic resolution of β-hydroxy nitriles [80]

scaled up such a dynamic kinetic resolution to a multiton per year scale. A lipase catalyzes the esterification of the (*R*)-secondary alcohol from a racemic mixture, while at the same time the remaining (*S*)-enantiomer is racemized by a homogeneous metal catalyst [81]. The ester is inert to the metal complex and does not racemize. As result, a nearly quantitative yield of the enantiopure ester is yielded (ee>99%).

3.4 Electroenzymatic Reaction Sequences

Chemical asymmetric catalysis and enantioselective biocatalysis are often complementary; sometimes they are even competitive, as in the production of fine chemicals. From the perspective of atom- and energy-efficiency, the combination of both fields is becoming more and more important. Electroenzymatic synthesis utilizes electrons as cheap redox equivalents. The advantages of using enzymes as enantioselective catalysts are combined here with the waste-free electrochemical in situ generation or regeneration of reagents. In contrast to whole cells in nature, where by necessity energy and mass transport are almost always coupled – as for example in the respiratory chain or in photosynthesis – it is possible to separate both processes in vitro. This is a very stimulating, positive difference, however, to the sixth biological principle: *energy and mass transport are coupled*. In electroenzymatic synthesis, electrons can be directly transferred from an electrode to enzymes or mediators. The feasibility of supplying redox equivalents directly via an electrode has been demonstrated on some selected examples (for reviews see [82–84]). This enables new possibilities in setting up reaction sequences according to the first biological principle: *complex chemicals are synthesized in reaction sequences*. Here electrochemical and biocatalytical steps are combined favorably in sequences or cycles, and result in a method that has been named "electroenzymatic synthesis".

Furthermore, utilization of almost mass-free electrons as redox equivalents allows us to set up redox reactions without side products. Both components of the electroenzymatic synthesis concept are intrinsically environmentally friendly [85]. In addition, electrons are the cheapest redox equivalents available besides oxygen and hydrogen, especially on an industrial scale (Fig. 12).

Three different methods for carrying out redox reactions can be differentiated, and those used for the oxidation of a substrate are outlined in Fig. 13. The simplest method is to apply stoichiometric amounts of an oxidation reagent (Fig. 13, top). The disadvantage of this method is that stoichiometric amounts of waste are created in the form of the spent oxidation reagent, which is also unattractive from an economical point of view. Alternatively, two electrochemical methods can be applied: electrochemical regeneration of catalytic amounts of the oxidation reagent (indirect electrolysis, Fig. 13, bottom left), or the direct electrochemical oxidation of the substrate, omitting the oxidation reagent altogether (Fig. 13, bottom right).

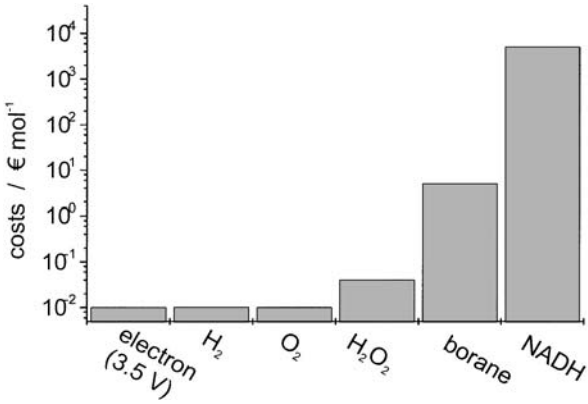

Fig. 12 Costs of redox reagents, per mole (logarithmic scale)

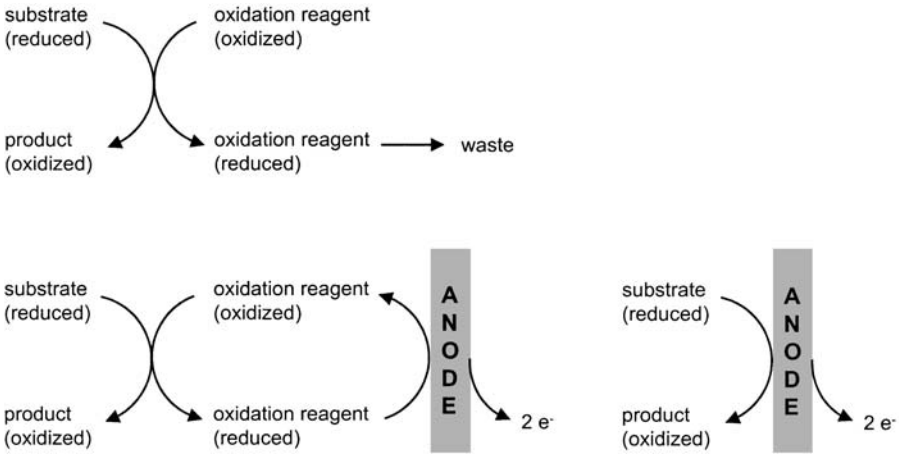

Fig. 13 Comparison of requirements of oxidation reactions with those of stoichiometric oxidant equivalents. Top: stoichiometric oxidant with waste production. Bottom left: electrochemical regeneration of catalytic amounts of oxidant. Bottom right: direct electrochemical regeneration [84]

Obviously, oxidoreductases are ideally suited for combining with electrochemical steps. For all of the reactions they catalyze, stoichiometric amounts of redox equivalents in relation to the starting material are needed. Since natural redox equivalents are often very expensive (see NADH in Fig. 12), they need to be regenerated if applied in asymmetric catalysis on a technical or even industrial scale. At this point, electrochemistry comes into play. In contrast to enzymatic regeneration methods of, say, nicotinamide cofactors, no side products are produced electrochemically from the regeneration [86–88]. In electroenzymatic synthesis, as seen in Fig. 14, the enzymatic regeneration of NAD^+

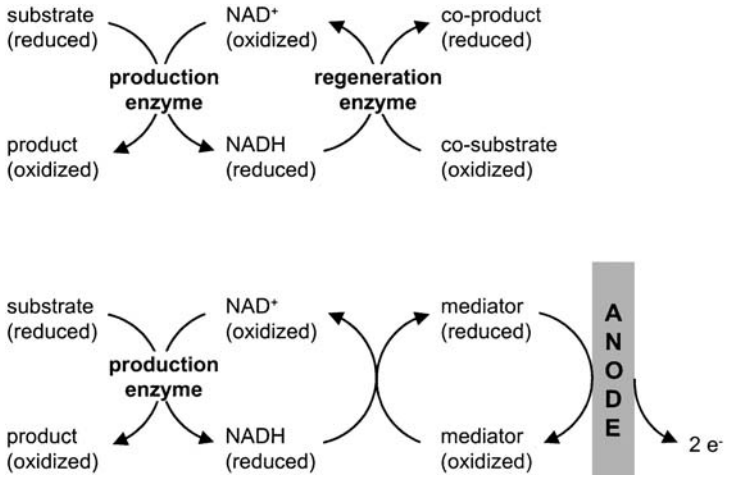

Fig. 14 Substitution of a regeneration enzyme, its co-substrate, and formed co-product, for free-electrochemical cofactor regeneration with catalytic amounts of mediator [84]

is replaced by either indirect cofactor regeneration via a mediator or by direct electrochemical regeneration (not shown), sparing the mediator. The reverse procedure can also be applied for the regeneration of the reduced nicotinamide cofactor.

In the literature, several examples of electroenzymatic synthesis have been reported. So far, the major application of it is the regeneration of cofactors, where mainly indirect electrolyses are applied. The FAD prosthetic group in ethylphenolmethylene hydroxylase is regenerated indirectly with the water-soluble 1,ω-bisferrocenyl-polyethyleneglycol [89, 90]. NAD(P)H is reported to be efficiently regenerated with water-soluble polyethyleneglycol-bound Cp*Rh(bipyridyl)-complexes as mediators in continuously operated membrane reactors [82, 87, 88, 91–94]. Likewise, methyl viologen and several other mediators are used for the regeneration of reduced cofactors [83, 95]. The aforementioned rhodium-complex acts as a selective redox catalyst, only transferring a hydride to the 4-position of NAD^+ and $NADP^+$. For the regeneration of the oxidized cofactors, $ABTS^{2-}$ (2,2′-azinobis(3-ethylbenzothiazoline-6-sulfonate), 1,10-phenanthrolin-5,6-dione or the respective *N*-methylated compound can be successfully applied [96–100]. Turnover frequencies $tof = 35\ h^{-1}$ were reached.

Besides the regeneration of cofactors and direct activation of enzymes, electrochemistry can also be used to generate reactants in situ. A promising target is the in situ generation of H_2O_2 as a redox equivalent for peroxidases. Peroxidases catalyze a broad spectrum of reactions. Their applications as biocatalysts for selective reactions in oxidations of non-activated carbons, epoxidations, hydroxylations, and sulfoxidations have been extensively reviewed [83, 101–104]. Nevertheless, technical application of peroxidases is hampered by their

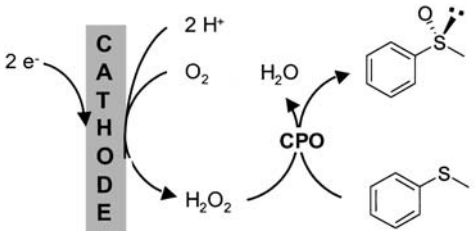

Fig. 15 In situ generation of hydrogen peroxide by cathodic reduction of oxygen coupled to the subsequent chloroperoxidase (CPO)-catalyzed sulfoxidation of thioanisole [192]

instability at high concentrations of the co-substrate hydrogen peroxide. For example, the heme peroxidase chloroperoxidase (CPO, EC 1.11.1.10) from the mold *Caldariomyces fumago*, catalyzing the enantioselective sulfoxidation of thioanisole to (*R*)-methylphenylsulfoxide (*ee* > 98.5%, Fig. 15) [105–107], is rapidly deactivated at 50 μM H_2O_2 (half-life $\tau_{1/2}$ = 38 min) [108, 109].

Generating H_2O_2 in situ by the reduction of oxygen prevents it from accumulating in high concentrations. This can be carried out either using a chemical reducing agent like ascorbic acid, or using glucose oxidase, which oxidizes glucose to gluconic acid while hydrogen peroxide is formed as coproduct [110, 111]. The disadvantage of this method is obvious: a second starting material needs to be introduced stoichiometrically into the reaction system, and consequently a side-product is also synthesized and accumulates stoichiometrically.

An alternative approach was published by Laane et al. [112]. For the CPO-catalyzed chlorination of barbituric acid, Laane produced the required H_2O_2 by cathodic reduction of oxygen. The advantage of this approach is that no side products are formed whatsoever and that electrons are used as cheap redox equivalents. This procedure has been transferred to the utilization of chloroperoxidase to catalyze enantioselective sulfoxidations (Fig. 15).

An elegant electrochemical approach was published by Biade et al. for the de-racemization of racemic lactate [113]; see Fig. 16. The L-selective lactate de-

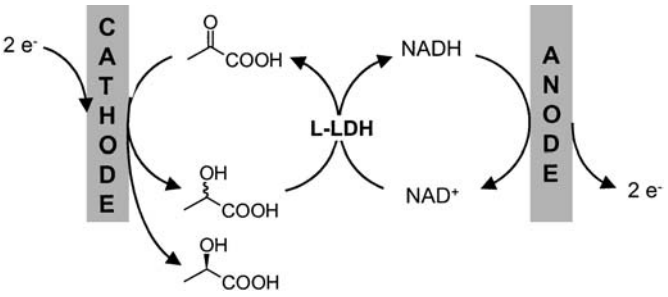

Fig. 16 Direct anodic regeneration of NAD^+ coupled to the racemic cathodic reduction of pyruvate (LDH = lactate dehydrogenase) [113]

hydrogenase only oxidizes L-lactate to pyruvate, which is subsequently electrochemically reduced to racemic lactate. Here D-lactate is left over. Besides the regeneration of cofactors, direct electron transfer to enzymes at electrodes has also been described. Prominent examples are hydrogenases [114–118].

Despite the success of electroenzymatic synthesis on a laboratory scale, no electroenzymatic synthesis has yet been scaled up to an industrial process. The reason for this might be that the process engineering optimization of these electroenzymatic syntheses is still a subject that is rarely treated [95, 119, 120].

3.5 Chemzymes

The biological catalysts, the enzymes, inspire this area of research. Enzymes are ideal catalysts, optimized by nature over several generations. They are homogeneously soluble, highly selective biocatalysts of high molecular weight. This allows their retention by, say, ultrafiltration membranes due to their size [121, 122]: typically 20,000–200,000 g mol^{-1}. Therefore, the recycling of such catalysts is possible, for example, through the use of a continuously operated enzyme membrane reactor (EMR) [123]. The second biological principle, namely that *biological catalysts are macromolecular and in general homogeneously soluble*, has motivated the field of classical chemical catalysis. Metal ligands have been covalently bound via linkers to polymeric backbones of high molecular weight. For this purpose, the polymeric backbone and the linkers are chosen in such a way that the resulting macromolecular catalyst is (in contrast to biocatalysts) homogeneously soluble in the solvent of choice – not restricted to water – and can be retained using membranes. This is the application of the third biological principle: *membranes retain macromolecular, homogeneously solubilized catalysts.* In this fashion, the major restriction to using biocatalysts has been overcome, namely that enzymes are typically limited to water as the solvent [124]. In this way, the high solubility of hydrophobic reactants in organic solvents increases the chance of reaching a high *space-time yield* (*sty*). This synthetic version of an enzyme is called a chemzyme (*chem*ical en*zyme*, Fig. 17) or also sometimes a synzyme (*syn*thetic en*zyme*). In contrast to enzymes, which generally possess one active site, it is possible to couple a number of active sites – often via a spacer unit – to a polymeric backbone.

The advantages of combining the chemical and the enzymatic approaches have been demonstrated on different examples. Prominent chemzymes synthesized have been made out of rhodium (diphenylphosphinomethyl) ligands for hydrogenation and hydroformylation of mono alkenes [125, 126], amino alcohols as ligands for diethylzinc reduction [127], oxazaborolidine ligands for borane reductions [128–131], polyleucine derivative ligands for the Julia-Colonna asymmetric epoxidation of chalcone [132], ligands catalyzing the Sharpless dihydroxylation [133], and those using the Gao-Noyori catalyst for transfer hydrogenation [134] that were bound to homogeneously soluble polymers (such as polystyrene, polymethacrylate, polysiloxane). The resulting

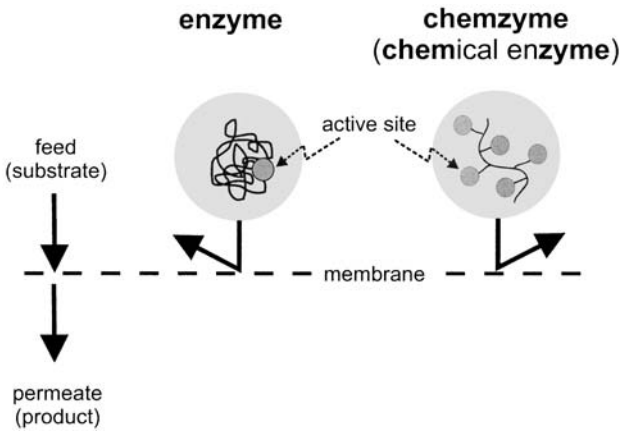

Fig. 17 Comparison between an enzyme and a chemzyme

soluble polymer-bound catalysts, chemzymes, can now be retained by ultrafiltration or nanofiltration membranes like enzymes; therefore, they can now be applied in a *chemzyme membrane reactor* (CMR) [130, 132, 134–138]. Similar approaches have been developed for other classes of catalysts attached to polymers [133, 139–141], dendrimers [142–144], or hyperbranched polyglycerols [145]. Even the direct retention of non-polymer enlarged ligands by a nanofiltration membrane has been described in the literature [146, 147].

One crucial factor for the successful application of chemzymes is the *retention* (*R*). As can be seen from Fig. 18, a retention of $R > 0.999$ is required to render the application of the chemzyme feasible in a continuously operated process. If, for example, a retention of $R = 0.98$ is given, then this means that 2% of the catalyst is lost per residence time; in other words, after 37 residence times, half of the catalyst is gone. This is the case with a BINAP-ruthenium hydrogenation catalyst, as outlined in the literature [146].

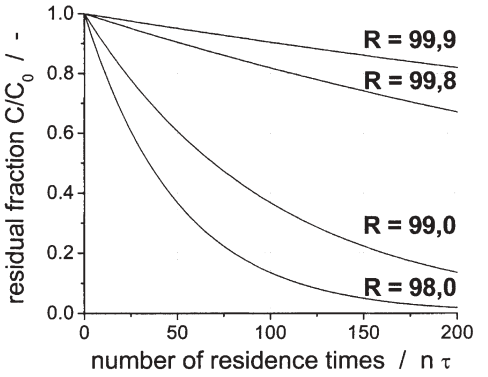

Fig. 18 Retention as a function of the number of residence times n_τ

The field of the synthesis and application of chemzymes is very new, having only been initiated in the last decade. New reactors had to be developed to use the newly synthesized chemzymes. The transfer of the second biological principle, namely that of a soluble, macromolecular catalyst to technical asymmetric catalysis, offers a very high potential for the chemical industry. Therefore, many different reviews have been published on this topic within the last two years [131, 137, 138, 141]. Beyond the aspects discussed so far, transferring the biological principles to technical asymmetric synthesis also allows for the development of new methods that could not be established by nature. For example, ruthenium or rhodium are usually the central atoms in homogeneous hydrogenation catalysts, whereas in natural enzymes zinc, copper, iron, nickel, and magnesium are most common. This might be due to the lack of availability of precious metals in nature. However, this opens up a huge potential for modifying enzymes accordingly and applying the resulting chemzymes for enantioselective reductions. In nature, reduction equivalents are generally supplied via nicotinamide cofactors, acting as mediators that need to be recycled. When utilizing chemzymes, it is possible to carry out enantioselective reductions directly with either formate, 2-propanol, or even molecular hydrogen as a low cost supply of the reduction equivalents.

3.6 Reaction Engineering

Since nature found the syntheses of enzymes to be complex, laborious tasks, it needed to develop methods for recycling enzymes. Therefore, nature either couples its catalysts to heterogeneous supports or it retains them using membranes. Still, in contrast to the majority of chemical catalysts, enzymes are macromolecular and (in general) homogeneously soluble. This is the previously named second biological principle: *biological catalysts are macromolecular and in general homogeneously soluble*. Therefore, it is easy for nature to recycle its catalysts by either retaining them by coupling them to membranes (third and fourth biological principles). The industrial application of the enzyme membrane reactor is based on work by Wandrey et al. [148–150]. In 1981, Degussa introduced a continuous acylase process that employed an enzyme-membrane reactor (EMR). The bench top reactor consisted of a flat sheet membrane that was replaced by a hollow-fiber module for large-scale operation [130, 131].

Heterogenization of catalysts is one of the oldest technologies used to retain and to recycle catalysts in technical asymmetric catalysis [146, 151, 152]. Such heterogenized catalysts are then applied in slurry or plug flow reactors. However, heterogenized or immobilized enantioselective homogeneous catalysts often perform rather disappointingly. Their reduced enantioselectivity may be caused by the heterogeneous support itself [152, 153], or – and perhaps additionally – mass transport limitations may be the reason. An alternative approach is the application of homogeneously soluble catalysts in two-phase systems,

where the catalyst is only soluble in one phase and is recycled in this way. An example is the hydroformylation process of the former Ruhrchemie/Rhone-Poulenc companies [154]. The water-soluble homogeneous catalyst is separated from the reactants in the organic phase. However, it is sometimes very difficult to transfer this very interesting concept to asymmetric synthesis, since the different polarities of the two-phase system might disturb the stereochemical processes at the catalyst [154].

In the case of the application of enzymes there is a clear trend towards aqueous/organic two-phase systems, even if this is a rather old technology, especially in regard to the application of hydrolases [155–157]. This technique is currently experiencing a renaissance for the application of oxidoreductases and lyases [158–164]. New solvent systems like ionic liquids also play an increasing role [165–167].

One major problem in designing processes involving a gas phase is the efficient contact and transfer of compounds between the gas phase and the liquid phase. In nature, membranes are used to establish a large interfacial area for phase transfer, such as oxygen in the lungs. This is represented by the seventh biological principle: *mass transport over gas/liquid barriers is facilitated by membranes*. Because of the low solubility of, say, hydrogen in the liquid phase, hydrogenations show the characteristics of a "fed-batch" reaction regarding hydrogen. H_2 is fed into the reacting solution from the gaseous reservoir according to the coupled equilibrium between the gas and the liquid phase. Henry's law describes this equilibrium. The solubility of hydrogen at equilibrium in the liquid phase $[H_2]_{eq}$ is proportional to the partial pressure of H_2 in the gas phase, p_{H_2}, and is correlated by the specific Henry coefficient H_{H_2}, which is uniquely different for each individual system.

$$p_{H_2} = H_{H_2} \cdot [H_2]_{eq}$$

with p_{H_2} (bar) is the hydrogen pressure in the gas phase, H_{H_2} (bar mM^{-1}) is the specific Henry coefficient for H_2, and $[H_2]_{eq}$ (mM) is the equilibrium solubility.

For the reaction to occur, hydrogen has to move from the gas into the liquid phase, so its diffusion determines the maximum rate of the overall reaction.

The area of the interface A and the mass transport coefficient k_l determine the rate of hydrogen solvation. In various literature references it is documented that the rate of solvation is the rate-limiting factor [168, 169]. Increasing the area of the interface and reduction of the diameter of the liquid film leads to an increased overall reaction rate.

A new methodology for hydrogenation has been developed [170] that has been applied to hydrogenations using chemzymes or enzymes [171]. If a dense membrane replaces the gas/liquid interface, the two parameters A and k_l become decoupled (Fig. 19). Also, the overall pressure p is now separated into the two partial pressures p_g and p_l for the gas and the liquid phases, respectively. In this way, it was possible to establish a pressure difference between the gas and the liquid phase. This method has also been successfully established and

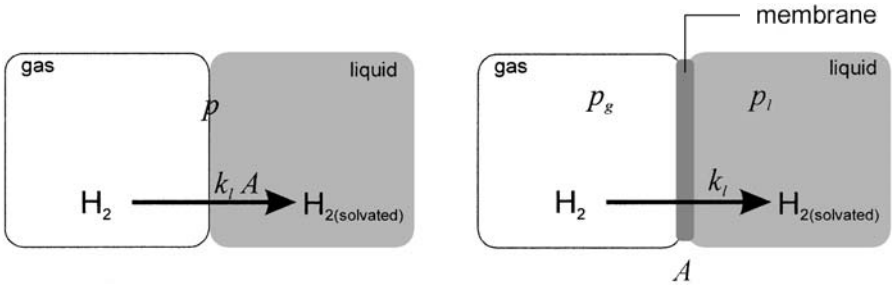

Fig. 19 Decoupling A and k_l by replacing the interface with a dense membrane (left: classical gas/liquid interface, right: membrane-separated gas and liquid phase)

applied for two different gases, oxygen and hydrogen. The advantageous application of nature's method for supplying gas to a liquid phase has been demonstrated in fermentations of mammalian cells, which are sensitive to direct contact with a gas/liquid interface [172]. Here oxygen is supplied to the liquid phase via dense silicon membranes (silicon tubing). The same method was later applied *in vitro* to oxidations catalyzed by monooxygenases [173, 174].

When using continuously operated membrane reactors, as with chemzymes and enzymes, additional advantages arise. On the retentate side of the membrane reactor, which corresponds to the actual reaction volume, no gas phase is involved, so it is simpler to control the residence time. In comparison to classical autoclaves, where the gas volume accounts for one third to one half of the reactor volume, the effective gas volume in the reactor is reduced drastically in the approach chosen here. Aside from these practical aspects, it also minimizes the risks introduced by using gaseous hydrogen.

4 Conclusion

Various biological principles are already being applied in current technical asymmetric syntheses without the scientific community at large being aware of this. Very efficient production processes have been designed in cases where reaction engineering has been integrated into the process. These successes suggest that we may expect that sustainable, technical asymmetric catalysis will be widely used in industry in the future.

It is not unusual for strikingly new concepts to require "incubation periods" of a decade or more to become accepted and successful. The transistor, the laser, and conducting organic polymers are cases in point: for all of them, their most attractive applications did not become commonplace until decades after their initial discoveries (by which time the original patents had long expired).

In summary, an understanding of biological principles and processes in terms of both chemistry and physics is a prerequisite for the development of

novel engineered systems that utilize these biological principles. To implement these concepts we require engineers that can integrate knowledge of such diverse fields as biocatalysis, physical organic chemistry, and biochemical engineering.

References

1. Houghton Mifflin Co. (1992) The American Heritage dictionary of the english language. Houghton Mifflin Co., Boston, MA
2. Nachtigall W (1991) In: Witt R, Lieckfeld C-P (eds) Bionik–patente der natur. Pro Futura Verlag GmbH, München, p 7
3. Anton DL (1998) Chem Eng News 15
4. Kieboom AP, Moulijn J, Leeuwen PWNM, Santen RAv (1999) In: Santen RAv, Moulijn J, Leeuwen PWNM, Averill BA (eds) Catalysis: an integrated approach. Elsevier, Amsterdam, p 3
5. Engels S, Stolz R, Göbel W, Nawrocki F, Nowak A (1989) ABC geschichte der chemie. VEB Deutscher Verlag für Grundstoffindustrie, Leipzig
6. Cornils B, Herrmann WA, Schlögl R, Wong C-H (1999) Catalysis from A to Z: a concise encyclopedia. Wiley-VCH, Weinheim
7. Turner MK (1998) In: Kelly DR (ed) Biotransformations I (Biotechnology), vol 8. Wiley-VCH, Weinheim, p 9ff
8. Enders D, Hoffmann R (1985) Chem Unserer Zeit 19:177
9. Stinson SC (1999) Chem Eng News (22nd of November) 57
10. Pasteur L (1858) CR Acad Sci (Paris) 46:615
11. Sheldon RA (1993) Chirotechnology. Marcel Dekker, New York
12. Neuberg C, Ohle H (1921) Biochem Z 127:326
13. Hildebrandt G, Klavehn W (1932) Deutsches Reichspatent Nr. 584 459
14. Bornscheuer U (2000) In: Rehm H, Reed G, Pühler A, Stadler P (eds) Biotechnology-serie, vol 8b. Wiley-VCH, Weinheim, p 277
15. Peters J (1998) In: Rehm H-J, Reed G, Pühler A, Stadler P (eds) Biotechnology, vol 8a. Wiley-VCH, Weinheim, p 393
16. Liese A, Villela Filho M (1999) Curr Opin Biotech 10:595
17. Patel RN (2001) Adv Synth Catal 343:527
18. Patel RN (2000) Stereoselective biocatalysis. Marcel Dekker, New York
19. Tanaka A, Tosa T, Kobayashi T (1993) Industrial application of immobilized biocatalysts. Marcel Decker, New York
20. Collins AN, Sheldrake GN, Crosby J (1992) Chirality in industry. Wiley, New York
21. Liese A, Seelbach K, Wandrey C (2000) Industrial biotransformations. VCH-Wiley, Weinheim
22. Schmid A, Dordick JS, Hauer B, Kiener A, Wubbolts M, Witholt B (2001) Nature 409:258
23. Straathof A, Panke S, Schmidt A (2002) Curr Opin Biotech 13:538
24. Thomas SM, DiCosimo R, Nagarajan V (2002) Trend Biotech 20:238
25. Breuer M, Ditrich K, Habicher T, Hauer B, Kesseler M, Stuermer R, Zelinski T (2004) Angew Chem Int Edit 43:788
26. Faber K (2000) Biotransformations in organic synthesis. Springer, Berlin Heidelberg New York
27. Griengl H (2000) Biocatalysis. Springer, Berlin Heidelberg New York
28. Liese A (2002) In: Drauz K, HW (eds) Enzyme catalysis in organic synthesis, 2nd edn, vol 3. VCH-Wiley, Weinheim, p 1419

29. Drauz K, Waldmann H (2002) Enzyme catalysis in organic synthesis. Wiley-VCH, Weinheim
30. Silverman RB (2002) The organic chemistry of enzyme-catalyzed reactions. Academic, San Diego, CA
31. Bommarius A, Riebel B (2004) Biocatalysis: fundamentals and applications. Wiley-VCH, Weinheim
32. Bredig G, Fiske PS (1912) Biochem Z 46:7
33. Wynberg H (1986) Top Stereochem 16:87
34. Cane DE (1990) Chem Rev 90:1089
35. Bunce RA (1995) Tetrahedron 51:13103
36. Mayer SF, Kroutil W, Faber K (2001) Chem Soc Rev 30:332
37. Bruggink A, Schoevaart R, Kieboom T (2003) Org Process Res Dev 7:622
38. Wiese A, Wilms B, Syldatk C, Mattes R, Altenbuchner J (2001) Appl Microbiol Biot 55:750
39. Ragnitz K, Syldatk C, Pietzsch M (2001) Enzyme Microb Tech 28:713
40. Wegman MA, van Langen LM, van Rantwijk F, Sheldon RA (2002) Biotechnol Bioeng 79:356
41. Miyazaki M, Ogino K, Shibue M, Nakamura H, Maeda H (2002) Chem Lett 758
42. Schoevaart R, van Rantwijk F, Sheldon RA (2001) J Org Chem 66:351
43. Schoevaart R, van Rantwijk F, Sheldon RA (2000) J Org Chem 65:6940
44. Scott AI (1994) Synlett 871
45. Roessner CA, Scott AI (1996) Annu Rev Microbiol 50:467
46. Jones JB, Sneddon DW, Higgins W, Lewis AJ (1972) J Chem Soc Chem Commun 856
47. Wichmann R, Wandrey C, Bückmann AF, Kula M-R (1981) Biotechnol Bioeng 23:2789
48. Wong C-H, Whitesides GM (1982) J Org Chem 47:2816
49. Kruse W, Hummel W, Kragl U (1996) Recl Trav Chim Pay B 115:239
50. Mertens R, Greiner L, van den Ban ECD, Haaker HBCM, Liese A (2003) J Mol Catal B–Enzym 24–25:39
51. Zervosen A, Elling L (1996) J Am Chem Soc 118:1836
52. Herrmann G, Ichikawa Y, Wandrey C, Gaeta F, Paulson JC, Wong C-H (1993) Tetrahedron Lett 4:1193
53. Wong C-H, Halcomb RL, Ichikawa Y, Kajimoto T (1995) Angew Chem 107:453
54. Wong C-H, Halcomb RL, Ichikawa Y, Kajimoto T (1995) Angew Chem 107:569
55. Brinkmann N, Malissard M, Ramuz M, Römer U, Schumacher T, Berger EG, Elling L, Wandrey C, Liese A (2001) Bioorg Med Chem Lett 11:2503
56. Rentmeister A, Hoh C, Weidner S, Dräger G, Elling L, Liese A, Wandrey C (2004) Biocatal Biotransfor 22:49
57. Blixt O, Paulson JC (2003) Adv Synth Catal 345:687
58. Dudziak G, Zeng S, Berger EG, Gellego RG, Kamerling JP, Kragl U, Wandrey C (1998) Bioorg Med Chem 8:2595
59. Petersen M, Zannetti MT, Fessner W-D (1997) Top Curr Chem 186:87
60. Bulter T, Schumacher T, Namdjou D-J, Gallego RG, Clausen H, Elling L (2001) Chembiochem 2:884
61. Hoh C, Dudziak G, Liese A (2001) Bioorg Med Chem Lett 12:1031
62. Hoffmann N (1996) Chem Unserer Zeit 30:201
63. Endo T, Koizumi S (2001) Adv Synth Catal 343:521
64. Stewart JD (2000) Curr Opin Biotechnol 11:363
65. Rodriguez S, Schroeder KT, Kayser MM, Stewart JD (2000) J Org Chem 65:2586
66. Kataoka M, Rohani LPS, Yamamoto K, Wada M, Kawabata H, Kita K, Yanase H, Shimizu S (1997) Appl Microbiol Biot 48:699

67. Kataoka M, Rohani LPS, Wada M, Kita K, Yanase H, Urabe I, Shimizu S (1998) Biosci Biotech Bioch 62:167
68. Kataoka M, Yamamoto K, Kawabata H, Wada M, Kita K, Yanase H, Shimizu S (1999) Appl Microbiol Biot 51:486
69. Kizaki N, Yasohara Y, Hasegawa J, Wada M, Kataoka M, Shimizu S (2001) Appl Microbiol Biot 55:590
70. Yasohara Y, Kizaki N, Hasegawa J, Wada M, Kataoka M, Shimizu S (2001) Tetrahedron-Asymmet 12:1713
71. Haberland J, Hummel W, Dausmann T, Liese A (2002) Org Process Res Dev 6:458
72. Haberland J, Kriegesmann A, Wolfram E, Hummel W, Liese A (2002) Appl Microbiol Biot 58:595
73. Endo T, Koizumi S (2000) Curr Opin Struct Biol 10:536
74. Tabata K, Koizumi S, Endo T, Ozaki A (2002) Enzyme Microb Tech 30:327
75. Endo T, Koizumi S, Tabata K, Kakita S, Ozaki A (2001) Carbohyd Res 330:439
76. Koizumi S, Endo T, Tabata K, Nagano H, Ohnishi J, Ozaki A (2000) J Ind Microbiol Biot 25:213
77. Endo T, Koizumi S, Tabata K, Ozaki A (2000) Glycobiology 10:90
78. Makkee M, Kieboom A, Bekkum H, Roels J (1980) Chem Commun 930
79. Pamies O, Bäckvall J (2003) Chem Rev 103:3247
80. Pamies O, Bäckvall J (2001) Adv Synth Catal 343:726
81. Rouhi A (2002) Chem Eng News 43
82. Steckhan E (1994) Top Curr Chem 170:83
83. Schmid A, Hollmann F, Bühler B (2002) In: Drauz K, Waldmann H (eds) Enzyme catalysis in organic synthesis, vol 3, 2nd edn. VCH-Wiley, p 1108
84. Steckhan E, Arns T, Heineman WR, Hilt G, Hoormann D, Jörissen J, Kröner L, Lewall B, Pütter H (2001) Chemosphere 43:63
85. Genders JD, Pletcher D (1996) Chem Ind–London 682
86. Wong C-H, Whitesides GM (1994) Enzymes in synthetic organic chemistry. Elsevier Science, Oxford
87. Hollmann F, Schmid A, Steckhan E (2001) Angew Chem Int Edit 40:169
88. Hollmann F, Witholt B, Schmid A (2002) J Mol Catal B–Enzym 19:167
89. Frede M, Steckhan E (1991) Tetrahedron Lett 32:5063
90. Brielbeck B, Frede M, Steckhan E (1994) Biocatalysis 10:49
91. Ruppert R, Herrmann S, Steckhan E (1987) Tetrahedron Lett 28:6583
92. Westerhausen D, Herrmann S, Hummel W, Steckhan E (1992) Angew Chem Int Edit 31:1529
93. Steckhan E, Herrmann S, Ruppert R, Dietz E, Frede M, Spika E (1991) Organometallics 10:1568
94. Schmid A, Hofstetter K, Feiten HJ, Hollmann F, Witholt B (2001) Adv Synth Catal 343:732
95. Delecouls-Servat K, Basseguy R, Bergel A (2002) Bioelectrochemistry 55:93
96. Hilt G, Steckhan E (1993) J Chem Soc Chem Commun 1706
97. Hilt G, Jarbawi T, Heineman WR, Steckhan E (1997) Chem–Eur J 3:79
98. Hilt G, Lewall B, Montero G, Utley JHP, Steckhan E (1997) Liebigs Ann-Recl: 2289
99. Schroeder I, Steckhan E, Liese A (2003) J Electroanal Chem 541:109
100. Degenring D, Schröder I, Liese A, Greiner L (2004) Org Process Res Dev (in press)
101. van de Velde F, van Rantwijk F, Sheldon RA (2001) Trend Biotechnol 19:73
102. Adam W (1999) Adv Biochem Eng/Biotechnol 63:73
103. Colonna S, Gaggero N, Richelmi C, Pasta P (1999) Trend Biotechnol 17:163
104. van Deurzen MPJ, van Rantwijk F, Sheldon RA (1997) Tetrahedron 53:13183

105. Allain EJ, Hager LP, Deng L, Jacobsen EN (1993) J Am Chem Soc 115:4415
106. Dexter AF, Lakner FJ, Campbell RA, Hager LP (1995) J Am Chem Soc 117:6412
107. Lakner FJ, Hager LP (1996) J Org Chem 61:3923
108. Seelbach K, Dreuzen MPJv, Rantwijk Fv, Sheldon RA, Kragl U (1997) Biotechnol Bioeng 55:283
109. Seelbach K (1997) Chloroperoxidase–Ein industrieller Katalysator? Regio- und enantioselektive Oxidationen. PhD Thesis, Rheinische Friedrich-Wilhelms-Universität, Bonn
110. Okrasa K, Guibé-Jampel E, Therisod M (2000) J Chem Soc Perk T 1:1077
111. van de Velde F, Lourenco ND, Bakker M, van Rantwijk F, Sheldon RA (2000) Biotechnol Bioeng 69:286
112. Laane C, Weyland A, Franssen M (1986) Enzyme Microb Tech 8:345
113. Biade A-E, Bourdillon C, Laval J-M, Mairesse G, Moiroux J (1992) J Am Chem Soc 114:893
114. Butt JN, Filipiak M, Hagen WR (1997) Eur J Biochem 245:116
115. Gros P, Zaborosch C, Schlegel HG, Bergel A (1996) J Electroanal Chem 405:189
116. Smith ET, Odom LD, Awramko JA, M.Chiong, Blamey J (2001) J Biol Inorg Chem 6:227
117. Morozov SV, Karyakina EE, Zorin NA, Varfolomeyev SD, Cosnier S, Karyakin AA (2002) Bioelectrochemistry 55:169
118. Delecouls K, Saint-Aguet P, Zaborosch C, Bergel A (1999) J Electroanal Chem 468:139
119. Delecouls K, Basseguy R, Bergel A (1998) Actual Chimique 91
120. Bergel A, DevauxBasseguy R (1996) J Chim Phys PCB 93:753
121. Jandel L, Schulte B, Bückmann AF, Wandrey C (1980) J Membrane Sci 7:185
122. Flaschel E (1983) Adv Biochem Eng/Biotechnol 26:73
123. Kula M-R, Wandrey C (1987) Method Enzymol 136:9
124. Buchholz K, Kasche V (1997) Biokatalysatoren und Enzymtechnologie. VCH Verlagsgesellschaft mbH, Weinheim
125. Bayer E, Schurig V (1975) Angew Chem 87:484
126. Bayer E, Gatfield I, Mutter H, Mutter M (1978) Tetrahedron 34:1829
127. Kragl U, Dreisbach C (1996) Angew Chem 108:684
128. Felder M, Giffels G, Wandrey C (1997) Tetrahedron Asymmetr 8:1975
129. Giffels G, Beliczey J, Felder M, Kragl U (1998) Tetrahedron Asymmetr 9:691
130. Wöltinger J, Bommarius AS, Drautz K, Wandrey C (2001) Org Process Res Dev 5:241
131. Wöltinger J, Drauz K, Bommarius AS (2001) Appl Catal A–Gen 221:171
132. Tsogoeva SB, Woltinger J, Jost C, Reichert D, Kuhnle A, Krimmer HP, Drauz K (2002) Synlett 707
133. Wöltinger J, Henniges H, Krimmer H-P, Bommarius AS, Drauz K (2001) Tetrahedron Asymmetr 12:2095
134. Laue S, Greiner L, Wöltinger J, Liese A (2001) Adv Synth Catal 343:711
135. Kragl U, Dreisbach C, Wandrey C (1996) In: Cornils B, Herrmann WA (eds) Applied homogeneous catalysis with organometallic compounds, vol 2. VCH, Weinheim, p 832
136. Rissom S, Beliczey J, Giffels G, Kragl U, Wandrey C (1999) Tetrahedron Asymmetr 10:923
137. Kragl U, Dwars T (2001) Trend Biotechnol 19:442
138. Bergbreiter DE (2002) Chem Rev 102:3345
139. Bayer E, Schurig V (1975) Angew Chem 87:484
140. Steckhan E, Herrmann S, Ruppert R, Thömmes J, Wandrey C (1990) Angew Chem 102:445
141. Leadbeater NE, Marco M (2002) Chem Rev 102:3217
142. Köllner C, Pugin B, Togni A (1998) J Am Chem Soc 120:10274
143. Brinkmann N, Giebel D, Lohmer G, Reetz MT, Kragl U (1999) J Catal 183:163

144. Hovestad NJ, Eggeling EB, Heidbüchel HJ, Jastrzebski JTBH, Kragl U, Keim W, Vogt D, van Koten G (1999) Angew Chem 111:1763
145. Sablong R, Schlotterbeck U, Vogt D, Mecking S (2003) Adv Synth Catal 345:333
146. Smet K, Aerts S, Ceulemans E, Vankelecom I, Jacobs P (2001) Chem Commun 7:597
147. De Smet K, Pleysier A, Vankelecom IFJ, Jacobs PA (2003) Chem–Eur J 9:334
148. Wandrey C, Flaschel E (1978) Chem Ing Tech 50:231
149. Wandrey C, Flaschel E (1979) Adv Biochem Eng 12:147
150. Wandrey C, Flaschel E, Schuegerl K (1977) Chem Ing Tech 49:257
151. Fodor K (1999) Enantiomer 4:497
152. De Vos WE, Vankelecom IJF, Jacobs P (2000) Chiral catalyst immobilization and recycling. Wiley-VCH, Weinheim
153. Blaser H-U (1991) Tetrahedron Asymmetr 2:843
154. Cornils B, Herrmann WA (2000) In: Cornils B, Herrmann WA (eds) Applied homogeneous catalysis with organometallic compounds. Wiley-VCH, New York, p 575
155. Sym EA (1936) Biochem J 30:609
156. Kvittengen L, Halling PJ (1999) Trends Biotechnol 17:343
157. Klibanov A (2001) Nature 409:241
158. Griengl H, Klempier N, Pöchlauer P, Schmidt M, Shi N, Mackova A (1998) Tetrahedron 54:14477
159. Bauer M, Griengl H, Steiner W (1999) Enzyme Microb Tech 24:514
160. Villela-Filho M, Wolberg M, Muller M, Hummel W, Liese A, Wandrey C (2002) Chem Ing Tech 74:657
161. Villela Filho M, Stillger T, Mueller M, Liese A, Wandrey C (2003) Angew Chem Int Edit 42:2993
162. Rosche B, Sandford V, Breuer M, Hauer B, Rogers PL (2002) J Mol Catal B–Enzym 19:109
163. Rosche B, Leksawasdi N, Sandford V, Breuer M, Hauer B, Rogers P (2002) Appl Microb Biot 60:94
164. Gröger H, Hummel W, Rollmann C, Chamouleau F, Hüsken H, Werner H, Wunderlich C, Abokitse K, Drauz K, Buchholz S (2004) Tetrahedron 60:633
165. Schöfer SH, Kaftzik N, Wasserscheid P, Kragl U (2001) Chem Commun 425–426
166. Park S, Kazlauskas R (2001) J Org Chem 66:8395
167. Reetz M, Wiesenhöfer W, Francio G, Leitner W (2002) Chem Commun 992
168. Sun Y, Wang J, LeBlond C, Landau RN, Laquidara J, Sowa JR, Blackmond DG (1997) J Mol Catal B–Enzym 115:495
169. Sun Y (1996) J Am Chem Soc 118:1348
170. Bommarius A, Krimmer H-P, Reichert D, Almena J, Karau A, Wöltinger J, Drauz K, Liese A, Greiner L, Wandrey C (2001) Volumenbegasung DE 101 63 168.5 (21.12.2001, German patent application)
171. Greiner L, Mueller DH, van den Ban ECD, Woeltinger J, Wandrey C, Liese A (2003) Adv Synth Catal 345:679
172. Noll T, Biselli M, Wandrey C (1996) BIOSpektrum 1:65
173. Rissom S, Schwarz-Linek U, Vogel M, Tishkov V, Kragl U (1997) Tetrahedron Asymmetr 8:2523
174. Bongs J, Hahn D, Schörken U, Sprenger GA, Kragl U, Wandrey C (1997) Biotechnology Lett 19:213
175. Schwab GM, Rudolph LM (1932) Naturwissenschaften 20:362
176. Lipkin D, Stewart TD (1939) J Am Chem Soc 61:3295
177. Nozaki H, Moriuti S, Takaya H, Noyori R (1966) Tetrahedron Lett 5239
178. Knowles WS, Sabacky MJ (1968) Chem Commun 1445
179. Horner L, Siegel H, Büthe H (1968) Angew Chem 80:1034

180. Izumi Y (1971) Angew Chem 83:956
181. Knowles WS (1983) Acc Chem Res 16:106
182. Katsuki T, Sharpless KB (1980) J Am Chem Soc 102:5974
183. Itsuno S, Nakano M, Ito K, Hirao A, Owa M, Kanda N, Nakahama S (1985) J Chem Soc Perk T 1 I:2615
184. Corey EJ, Bakshi RK, Shibata S (1987) J Am Chem Soc 109:5551
185. Oguni N, Omi T (1984) Tetrahedron Lett 25:2823
186. Jacobsen EN, Marko I, Mungal WS, Schröder G, Sharpless KB (1988) J Am Chem Soc 110:1968
187. Jacobsen EN, Zhang W, Muci AR, Ecker JR, Deng L (1991) J Am Chem Soc 113:7063
188. Wan K, Davis ME (1983) Tetrahedron Asymmetr 4:2461
189. Noyori R, Hashigushi S (1996) In: Cornils B, Herrmann WA (eds) Applied homogeneous catalysis with organometallic compounds. VCH, New York, p 575
190. Folienserie (1985) Folienserie des Fonds der Chemischen Industrie, vol 20. See http://www.biologe.de/Nuetzliches/FCI-CD/
191. Frost & Sullivan (2003) Analysis of developments in global chiral technology markets (Report B105). Frost & Sullivan, San Antonio, TX
192. Liese A, Lütz S (2002) GDCh Monographie der GDCh-Fachgruppe Angewandte Elektrochemie (Elektronentransfer in Chemie und Biochemie). GDCh-Monographie, Frankfurt 23:305

Received: March 2004

Adv Biochem Engin/Biotechnol (2005) 92: 225 – 260
DOI 10.1007/b98911

Cofactor Regeneration at the Lab Scale

R. Wichmann (✉)[1] · D. Vasic-Racki[2]

[1] Biochemical Engineering Group, Department of Biochemical and Chemical Engineering, Universität Dortmund, 44221 Dortmund, Germany
wichmann@bci.uni-dortmund.de
[2] Faculty of Chemical Engineering and Technology, University of Zagreb, Savska c.16, 10000 Zagreb, Croatia
durda.vasic-racki@public.srce.hr

Abstract Progress made in lab-scale applications of various coenzyme regeneration systems over the last two decades has mainly focused on the applications of NAD^+/NADH- and $NADP^+$/NADPH-dependent oxidoreductase reactions. In situ regeneration systems for these reactions, as well as whole cell, enzymatic, electro-enzymatic, chemical, and photochemical reactions are presented, including details about their efficiency and novelty. The progress of enzyme reaction engineering is also reported.

Keywords Regeneration of nicotinamide cofactors · Enzymes · Oxygenase · Dehydrogenases · Hydrogenases · Enzyme membrane reactors · Total turnover number · Retention

1 Introduction

The use of biocatalysts for preparative purposes is the subject of current research throughout the world [34]. Numerous industrial processes have already been established where biocatalysts are employed in the form of whole cells of microorganisms or in the form of purified (isolated) enzymes [45, 64, 68, 69].

As the isolation of enzymes employs laborious, time consuming and expensive procedures, making enzymes expensive, the use of whole cells for biocatalysed reactions (without isolating enzymes) have been explored since the 1950s.

The majority of these commercially explored biologically catalysed reactions leading to valuable products are mostly hydrolytic reactions. These reactions are catalysed by enzymes, which are applied either within their natural source of origin or with isolated enzymes in a soluble or immobilised state. Enzymes that belong to the classes of hydrolases, transferases, isomerases, or lyases either do not require a cofactor for their specific activity, or a cofactor like a metalion or a coenzyme is firmly bound. Such a cofactor helps to stabilise the correct three-dimensional structure of the enzyme required for its catalytic activity or it actually takes part in the catalytic activity, being modified along the way. As these cofactors are strongly bound to their respective enzyme, no special care has to be taken to maintain their function other than the addition of some free cofactor to the substrate medium to compensate for the loss of some of it due to limited binding to the enzyme.

On the other hand, oxidoreductases, which catalyse oxidative and reductive reactions, as well as ligases, which catalyse the formation or the splitting of complex compounds, often require so-called "free coenzymes". These coenzymes act as transport metabolites, transporting hydrogen, oxygen or electrons on the one hand, or other atoms or molecules on the other, between different parallel reactions. This means that the efficiency of the maintenance of biological energy is greatly enhanced, leading to a resource effective biochemical metabolism required for the high growth and survival rate of living beings.

The most important coenzymes are AMP/ADP/ATP and NAD^+/NADH or $NADP^+$/NADPH. While AMP/ADP/ATP are required for biochemical energy transfer, most reaction networks they are used in are too complex for economical applications in cell free systems, and so hardly any product of economic importance has emerged that requires these coenzymes in cell free synthetic reactions so far. Therefore, this article concentrates on reviewing the progress made in lab-scale applications of NAD^+/NADH- and $NADP^+$/NADPH-dependent oxidoreductase reactions that have been used in various fields, particularly for the production of various valuable chiral compounds, such as hydroxy acids [76], amino acids [10, 35], steroids [17], or alcohols [38, 43, 44, 63, 93] from prochiral precursors. Almost one fifth of all enzymes registered at the International Union of Biochemistry require dissociable coenzymes. Therefore, an efficient and economical cofactor regeneration system is indispensable for the

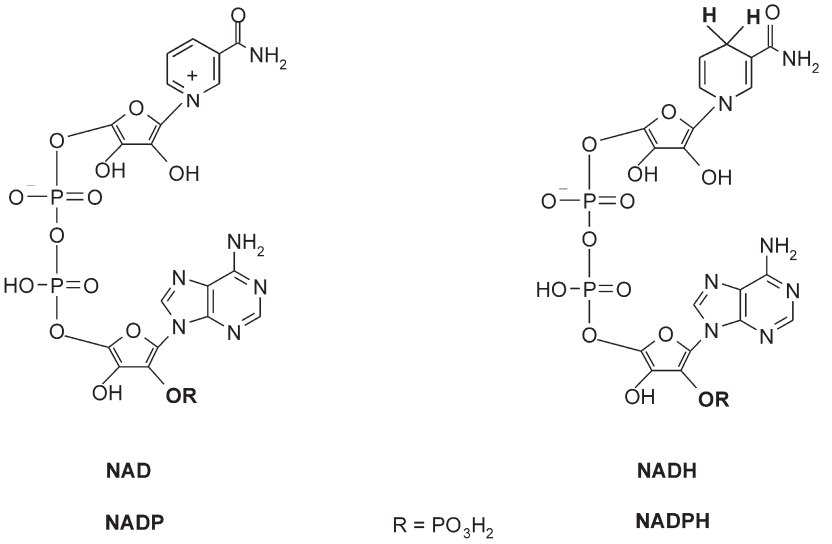

Fig. 1 Structures of the cofactors NAD(P)$^+$ and NAD(P)H

synthesis of bioactive compounds, because cofactors such as NAD(H) and NADP(H) are complex (Fig. 1), unstable [16], and quite expensive (Table 1).

Some review articles have already been published on this subject: Wandrey and Wichmann [80] report on "coenzyme regeneration in membrane reactors", Chenault and Whitesides [16] report on "regeneration of nicotinamide cofactors for use in organic synthesis" very extensively, Adlercreutz [2] summarises "cofactor regeneration in biocatalysis in organic media", while Kula and Kragl [40] review "dehydrogenases in the synthesis of chiral compounds". Therefore the aim of this review is to report the progress made in the last two decades in lab-scale applications of various coenzyme regeneration systems, including aspects of their efficiency and novelty.

The pyridine nucleotide cofactors NAD$^+$ and NADP$^+$ are essential components of the cell, where they act as electron carriers in reduction and oxidation reactions. Therefore whole-cell biocatalysts provide a continuous source of enzymes and cofactors, which could in some cases simplify reactions. It is known that whole-cells have some reserves of cofactors, but cofactor depletion can be

Table 1 Costs of cofactors

Cofactor	€/mol, from Juelich Fine Chemicals (2003)
NAD$^+$	2655
NADH	8868
NADP$^+$	11,417
NADPH	167,846

Table 2 Advantages and disadvantages of various strategies for cofactor regeneration [16]

Strategy	Advantages	Disadvantages
Biological-Microbiological	Inexpensive, self-assembling enzyme activity Inexpensive regenerating reagents (O_2, glucose) High selectivity	Relatively primitive state of development Low reactor volume productivity Complicated product isolation Limited or unknown stability Reduced enantiomeric purity of product in some systems Difficulty in controlling relative activities of enzymes Possible incompatibility with some chemical or biochemical components
Enzymatic: Substrate-coupled Enzyme-coupled	High selectivity, especially for NAD(P) → NAD(P)H Compatibility with enzyme-catalysed synthesis High rates for some systems Easy monitoring of reaction progress	Enzyme cost and instability Immobilization in some cases Complexity of product isolation in some cases Low rates for some systems Low reactor volume productivities for some systems
Electrochemical	Low cost of electricity No stoichiometric regenerating reagent Readily controlled redox potential Easy product isolation Easy monitoring of reaction progress	Incompatibility with many biochemical systems Poor selectivity (especially for reductive regeneration) Complex apparatus and procedures Rapid fouling of electrodes Requirement in many systems for mediating redox dyes or enzymes
Chemical	Generally inexpensive and commercially available reagents No requirement for added enzymes High redox potentials	Limited compatibility with biochemical systems Complexity of product isolation in some cases Low product yields Low TTN Slow rates for some systems (especially for oxidative regeneration)
Photochemical	No stoichiometric regenerating reagent in some systems No requirement for added enzymes	Complex apparatus Limited compatibility with biochemical systems Limited stabilities Requirement for photo-sensitizers and redox dyes

a problem. Within cells cofactors are synthesized and regenerated as a part of cellular metabolism. In processes that use isolated enzymes to catalyse synthetic reactions, another reaction system has to be used for the cofactor regeneration. Strategies for nicotinamide cofactor regeneration have been classified by Chenault and Whitesides [16] into four general categories: biological, enzymatical, electrochemical, chemical and photochemical (Table 2). The enzymatical strategies can be further divided into two groups. The first group consists of substrate-coupled systems where only one enzyme catalyses both the main reaction and the regeneration reaction. In the regeneration reaction, the enzyme uses mostly organic solvents as a substrate [2, 95]. This method is well suited to all systems that use enzymes in organic media [2, 7, 8, 52, 77]. Unfortunately, the choice of the co-substrate is limited by the enzyme's substrate specificity. The second group consists of enzyme-coupled systems, where a second enzyme and a second substrate are used to catalyse a cofactor regeneration reaction. This method has been widely explored, especially through the use of formate dehydrogenase as the cofactor-regenerating enzyme for NADH [39, 94], as well as for NADPH [29]. The enzyme uses formate as a substrate. Formate is cheap, most enzymes can tolerate it, and it is a strong reducing agent. The product of the regeneration reaction is CO_2, which hardly has any effect on enzymes at all and drives the reaction to completion, as it is easily removed from the reaction system as gas or by a consecutive conversion to hydrogencarbonate, which also simplifies product recovery. The German Future Prize was awarded to Professor Maria-Regina Kula and Dr. Martina Pohl for this finding in 2002 [94].

2
Cofactor Regeneration by Whole-Cell Biocatalysts

Whole-cells of baker's yeast – *Saccharomyces cerevisiae* – have been used as a cofactor regeneration system, while baker's yeast has been used for nearly a century to carry out organic reactions [65, 74] due to its ease of handling, nontoxicity, broad substrate tolerance, constant quality; a result of its use in the baking industry and very low price. The most common application of baker's yeast, even in industrial processes [17], is the asymmetric reduction of ketones. Although baker's yeast has been widely used to supply reducing power, even in gas-phase reactions [48, 55] it is rather difficult to freely combine it with the desired reactions. Unfortunately, baker's yeast-catalysed biotransformations also sometimes result in low optical purities, due to the presence of enzymes with overlapping substrate specificities, but different stereoselectivities. Furthermore, it has a low productivity, requiring the use of large amounts of cells in highly diluted media, causing slow recovery of the product from the reaction medium, particularly via a filtration stage. Recently [74] genetic engineering has made it possible to construct a new yeast strain to simplify the use of cofactor-requiring enzymes by introducing heterologous genes.

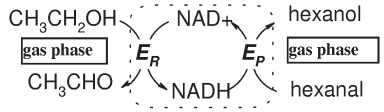

baker's yeast
E_R – Regenerating enzyme
E_P - Producing enzyme
Alcohol dehydrogenase [55]

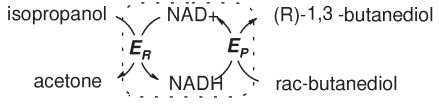

recombinant E.coli
E_R – Regenerating enzyme
E_P - Producing enzyme
(S)-1,3-Butanediol dehydrogenase [53], [54]

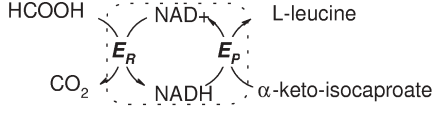

recombinant E.coli
E_R – Regenerating enzyme
Formate dehydrogenase
E_P - Producing enzyme
Leucine dehydrogenase [24]

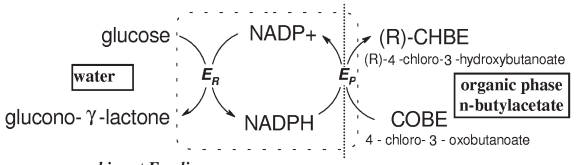

recombinant E.coli
E_R – Regenerating enzyme [32], [33]
Glucose dehydrogenase
E_P - Producing enzyme
Aldehyde reductase

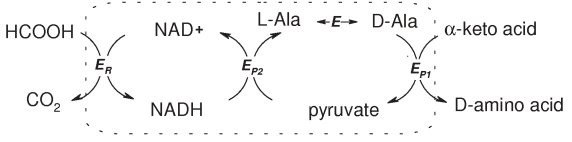

recombinant E.coli
E_R – Regenerating enzyme
Formate dehydrogenase
E_{P1} – Producing enzyme 1
D-Amino acid transferase
E_{P2} – Producing enzyme 2 [24]
L-Alanine dehydrogenase
E – Alanine racemase

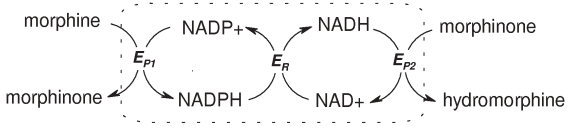

recombinant E.coli
E – Regenerating enzyme
Pyridine nucleotidetranshydrogenase
E_{P1} – Producing enzyme 1
Morphine dehydrogenase [11]
E_{P2} – Producing enzyme 2
Morphinone reductase

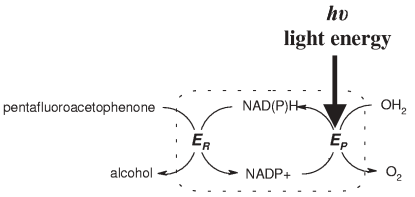

***Synechococcus elongatus PCC* 7942**
E_P – Producing enzyme
E_R – Regenerating enzyme [57]

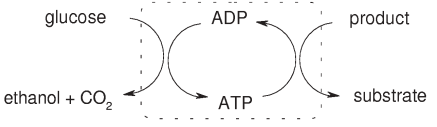

yeast

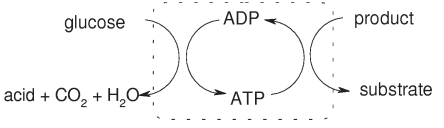

Corynebacterium ammonigenes [20]

Fig. 2 Cofactor regeneration by whole-cells

In general, whole-cell processes are employed when enzymatic activity does not require cofactor regeneration [86], because it is rather difficult to construct whole-cell processes with enzymes that require a cofactor, such as dehydrogenases, when cofactor regeneration has to accompany the bioconversion. Genetic engineering has made it possible through heterologous enzyme systems that are able to achieve the necessary level of cofactor regeneration [20]. An *Escherichia coli* strain expressing a heterologous NAD^+-dependent amino acid dehydrogenase and a formate dehydrogenase has been constructed. In the presence of α-keto acids, ammonium ions, and formate, the strain efficiently synthesized L-amino acids corresponding to the α-keto acids [24]. It should be noted that the amount of intracellular NAD^+ is sufficient for coupling between the amino acid dehydrogenase and formate dehydrogenase. Some of the microbial biotransformations with cofactor regeneration are presented in Fig. 2.

The asymmetric reduction of ethyl 4-chloro-3-oxobutanoate to (*R*)-4-chloro-3-hydroxybutanoate was achieved using recombinant *E.coli*, overcoexpressing the aldehyde reductase gene from *Sporobolomyces salmonicolor* and the glucose dehydrogenase gene from *Bacillus megaterium* as a catalyst [32, 33]. To produce (*R*)-1,3-butanediol, the (*S*)-1,3-butanediol dehydrogenase gene (cpSADH) was cloned from *Candida parapsilosis* and overexpressed in *E. coli* [53, 54]. Various L-amino acids were produced from α-keto acids with *E. coli* cells overexpressing heterologous genes of thermostable L-amino acid dehydrogenases such as leucine dehydrogenase from *Bacillus sphaericus* and formate dehydrogenase from *Candida boindini* with only the intracellular pool of NAD^+ available for the regeneration of NADH [24]. D-amino acids were also produced from α-keto acids with *E.coli* cells overexpressing thermostable heterologous genes of D-amino acid aminotransferase such as alanine racemase, L-alanine dehydrogenases and formate dehydrogenases [20]. The soluble pyridine nucleotide transhydrogenase of *Pseudomonas fluorescenes* was overexpressed in *E.coli* and applied for regeneration of both NADH and NADPH in the production of the important semi-synthetic opiate drug hydromorphone [11].

The development of an efficient and economical ATP regeneration system is also very important for the synthesis of many bioactive compounds. The whole-cells ATP regeneration process has been reported that uses either *yeast* or *Corynebacterium ammoniagenes* [20].

3
Cofactor Regeneration Using Isolated Enzymes as Biocatalysts

Processes catalysed by isolated enzymes result in higher volumetric productivities compared to whole-cell processes. The apparatus used and product recovery from the reaction medium is simpler. In such a cell-free process, the production of the biocatalysts, and hence the growth of the production organism, is decoupled from the biotransformation. This allows separate optimisation of

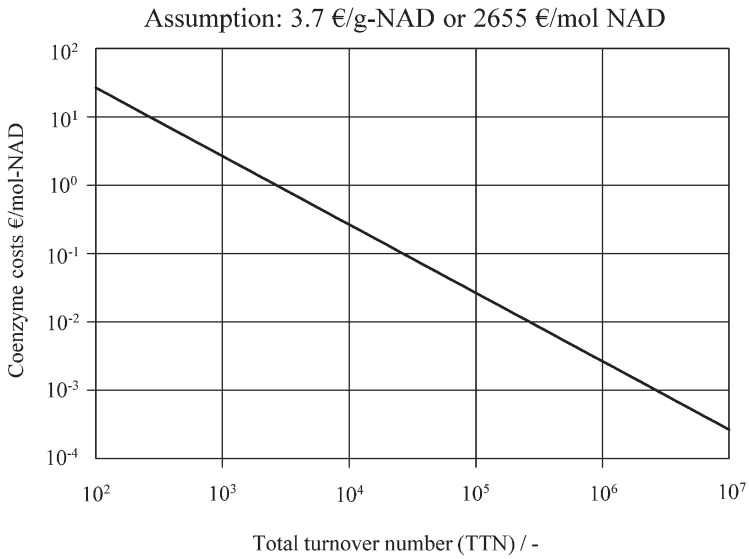

Fig. 3 Cofactor costs as a function of total turnover number (TTN)

both processes, which is clearly advantageous over the application of especially whole living cells, because the conditions for optimal cell growth and enzyme production in cells themselves can be very different from the reaction conditions used for biotransformations. The cell-free processes are mainly established for hydrolytic enzymes. The application of oxidoreductases (like dehydrogenases and oxygenases), in isolated form on a preparative scale and depending on the coenzyme NADP(H), is only economical if a suitable coenzyme regeneration system is used. Cofactor-requiring reactions are often uneconomical because of the cofactor costs. These costs may be drastically reduced if a high Total Turnover Number (TTN) for the cofactor can be reached [28, 35–37]. Figure 3 presents the costs of coenzymes as a function of TTN. The TTN is defined as the molar amount of synthesised product n_p per molar amount of consumed cofactor $n_{NAD(H)}$.

$$\mathrm{TTN} = \frac{n_p}{n_{NAD(H)}} \tag{1}$$

The TTN rises steeply with decreasing cofactor concentration at the expense of the volumetric productivity, since the cofactor concentration gradually becomes limiting for the total reaction system [35]. Redox biocatalysis by means of reductive amination is a suitable process for obtaining, say, L-tert leucine, while the regeneration of NADH is done using formate dehydrogenase and ammonium formate, yielding a TTN of 125,000 [35]. This process of the in situ regeneration of cofactors, brought to scale by Degussa in cooperation with professors Kula and Wandrey, is now considered the method of choice for running

reductive amination reactions [10]. Currently, the highest TTN of 600,000 appears to have been achieved by continuous lab-scale production of L-phenylalanine catalysed by phenylalanine dehydrogenase with polymer-coupled NADH retained in a membrane reactor using formate dehydrogenase for cofactor regeneration [28].

4 Substrate-Coupled Cofactor Regeneration

Some recently published systems that use the substrate-coupled method (Table 3) for cofactor regeneration [67] were applied mainly in unconventional enzyme reaction media, such as a gas/solid phase where yeast alcohol dehydrogenase was used with higher activity and stability than in water [66], or in an organic phase using the NAD(H)-dependent horse liver alcohol dehydrogenase [47, 77] and the NADP(H) dependent alcohol dehydrogenase from *Thermoanaerobium brockii* (TBADH) [7, 8, 52]. High TTNs were achieved with both enzymes. Alcohol dehydrogenase from *Thermoanaerobium brockii*, a NADP(H)-dependent enzyme, is increasingly being used as a catalyst in chiral synthesis because of its high enantioselectivity, its broad substrate specificity, and its extraordinary tolerance to high concentrations of organic solvents such as 2-propanol (20% (v/v) [95–97]. All of these features have attracted much technological interest [8]. The systems investigated earlier are summarised elsewhere [2]. In these investigations, horse liver alcohol dehydrogenase was mainly used in organic systems. Due to the high cost of this enzyme, an economical application of it is difficult to envisage, and it is therefore only of academic interest as a model system, especially for reactions in organic media.

5 Enzyme Coupled Cofactor Regeneration

Table 4 presents various enzyme coupled cofactor regeneration systems performed in water as well as in unconventional enzyme reaction media. Some of the systems developed earlier are summarised elsewhere [16, 35]. Besides well-established and known systems, new ones with the enzymes transhydrogenase [11] and NADH oxidase [25] used as cofactor regenerating enzymes were developed. Transhydrogenase of *Pseudomonas fluorescens* is an enzyme that can catalyse the transfer of reducing equivalents according to the following equation:

$$NAD^+ + NADPH \leftrightarrow NADH + NADP^+ \quad \text{(a)}$$

The applicability of cofactor regeneration using a soluble pyridine nucleotide transhydrogenase was tested, both as a cell-free system using isolated and

Table 3 Enzymatic – Substrate coupled cofactor regeneration

Production/Regeneration system	Enzyme		Reactor type	Volume ml	Productivity g $L^{-1}d^{-1}$	TTN	Reference
	E_p	E_R					
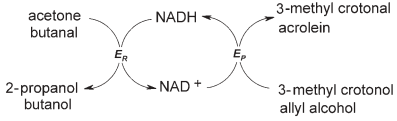	Yeast alcohol dehydrogenase	Yeast alcohol dehydrogenase	Fixed – bed (gas phase/ solid)				[66]
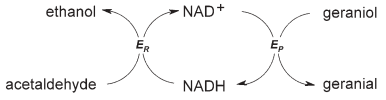	Yeast alcohol dehydrogenase (immobilized)	Yeast alcohol dehydrogenase (immobilized)	Fixed – bed	12 (1 cm^2 × 12 cm)		16326–41309	[47]
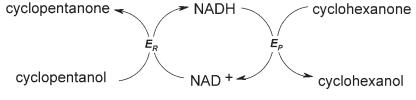	Horse liver alcohol dehydrogenase	Horse liver alcohol dehydrogenase	Batch	4		100000	[77]
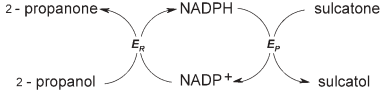	*Thermoanaerobium brokii* alcohol dehydrogenase	*Thermoanaerobium brokii* alcohol dehydrogenase	Batch (non-conventional media)	3		125	[7], [8]
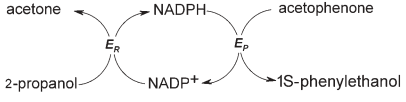	*Thermoanaerobium* alcohol dehydrogenase	*Thermoanaerobium* alcohol dehydrogenase	Batch	5		10–23	[52]

Table 4 Enzymatic – Enzyme coupled cofactor regeneration (part 1 of 5)

Production/Regeneration system	Enzyme		Reactor type	Volume ml	Productivity g $L^{-1}d^{-1}$	TTN	Reference
	E_p	E_R					
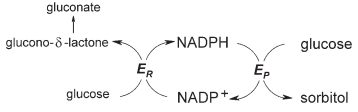	*Candida Tropicals* aldolase reductase (NAD(P)H)	Glucose dehydrogenase	Charged membrane CSTR	50	114	106000	[30]
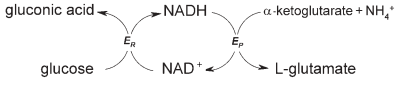	Glutamate dehydrogenase	Glucose dehydrogenase	Enzyme membrane	2	119–530	1200–62000	[46]
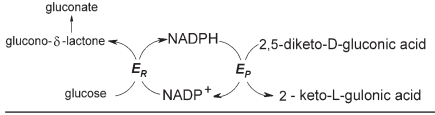	*Corynebacterium sp.* – ATCC31090 5-keto reductase	Glucose dehydrogenase	Batch		16.5		[3], [4]
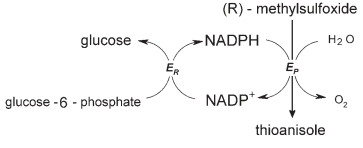	Cyclohexanone monooxygenase ($NADP^+$)	Glucose-6-phosphate dehydrogenase	UF-membrane reactor Batch (non-conventional media)	100			[84]
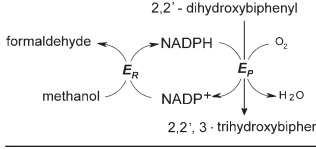	Monooxygenase	Yeast alcohol dehydrogenase	Batch	25	0.33–0.75	7–34	[49]

Table 4 Enzymatic – Enzyme coupled cofactor regeneration-extension (continuation – part 2 of 5)

Production/Regeneration system	Enzyme		Reactor type	Volume ml	Productivity g $L^{-1}d^{-1}$	TTN	Reference
	E_p	E_R					
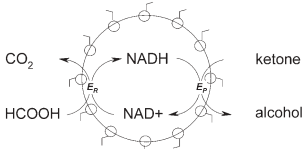	Horse liver alcohol dehydrogenase	Formate dehydrogenase	Batch microcapsule			2029	[59]
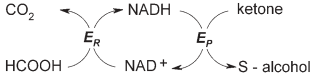	*Rhodoccocus* alcohol dehydrogenase	Formate dehydrogenase	UF-membrane reactor-CSTR	50		8-1350	[38]
	Phenylalanine dehydrogenase	Formate dehydrogenase	UF-membrane reactor-CSTR	10	12.5–761	~ 32	[72]
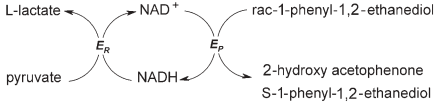	Glycerin dehydrogenase	Lactate dehydrogenase	UF-membrane reactor Differential circulation reactor	500			[44]
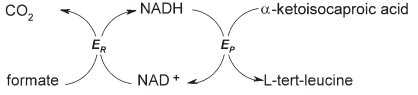	Leucine dehydrogenase	Formate dehydrogenase	UF-membrane reactor CSTR Cascade	70 and 46 + 46	336 and 260 + 290	2325 and 2400 + 4230	[36], [37]

Table 4 Enzymatic – Enzyme coupled cofactor regeneration-extension (continuation – part 3 of 5)

Production/Regeneration system	Enzyme		Reactor type	Volume ml	Productivity g $L^{-1}d^{-1}$	TTN	Reference
	E_p	E_R					
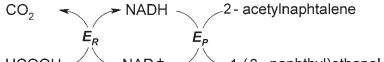	*Candida parapsilosis* Carbonyl reductase	Formate dehydrogenase	UF-membrane (cyclodextrin media) Batch CSTR	50–300 and 10	120		[85]
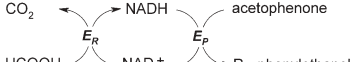	*Candida parapsilosis* Carbonyl reductase	Formate dehydrogenase	UF-membrane reactor-CSTR	10	88	1600	[63]
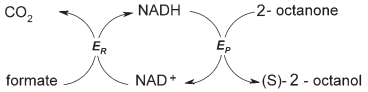	*Candida parapsilosis* Carbonyl reductase *Candida parapsilosis*	Formate dehydrogenase	Emulsion membrane reactor	100	119	124	[44]
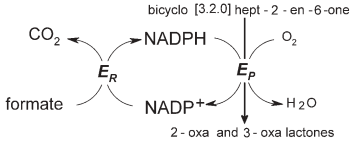	Diketocamphane monooxygenase	Formate dehydrogenase	Membrane reactor, Repetitive batch	10			[60]
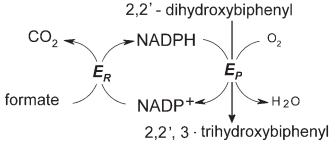	Monooxygenase	Formate dehydrogenase	Batch	200	11	503	[49]

Table 4 Enzymatic – Enzyme coupled cofactor regeneration-extension (continuation – part 4 of 5)

Production/Regeneration system	Enzyme		Reactor type	Volume ml	Productivity g $L^{-1}d^{-1}$	TTN	Reference
	E_p	E_R					
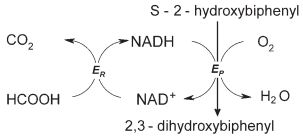	Monooxygenase	Formate dehydrogenase	Batch (non-conventional media) organic/ aqueous emulsion	250	10.8	403	[68], [69]
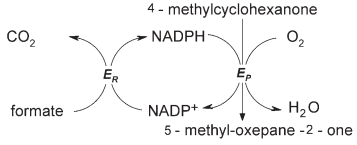	Cyclohexanone monooxygenase ($NADP^+$)	Formate dehydrogenase	Repetitive Batch (membrane integrated bubble free aeration)	30		160	[62]
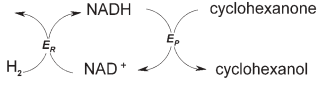	Horse liver alcohol dehydrogenase	Hydrogenase	Batch Membrane reactor (non-conventional media) organic/ aqueous	4			[5]
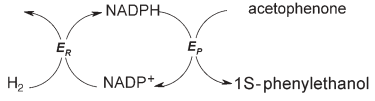	*Thermo-anaerobium* alcohol dehydrogenase	Hydrogenase	Batch Repetitive Batch	5	10	100	[52]

Table 4 Enzymatic – Enzyme coupled cofactor regeneration-extension (continuation – part 5 of 5)

Production/Regeneration system	Enzyme		Reactor type	Volume ml	Productivity g $L^{-1}d^{-1}$	TTN	Reference
	E_p	E_R					
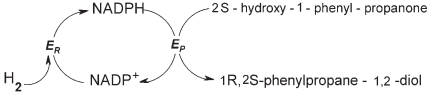	*Thermo-anaerobium* alcohol dehydrogenase	Hydrogenase	Repetitive Batch	5		160	[52]
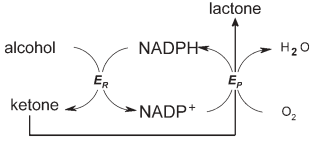	Monooxygenase ($NADP^+$)	*Thermo-anaerobium brokii* alcohol dehydrogenase	Batch (non-conventional media)	40	4.4	2.85	[82]
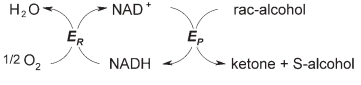	R-alcohol dehydrogenase	NADH-oxidase *Lactobacillus brevis*					[25]
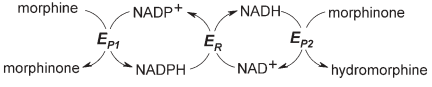	Morhine dehydrogenase Morphinone reductase	Pyridine nucleotide transhydro-genase	Batch	0.2	14.4		[11]

purified enzyme and as a whole-cell system for the production of hydromorphone. The results showed that soluble pyridine nucleotide transhydrogenase is able to cycle the cofactors, allowing the efficient transformation of morphine to take place in two-step reactions in the presence of catalytic amounts of cofactors. When using three enzymes in the reaction system, critical parameters are required for an optimum yield. The use of the pyridine nucleotide transhydrogenase within the whole-cell biocatalyst clearly improved the biotransformation of morphine and resulted in a reusable biocatalyst, implying that pyridine nucleotide transhydrogenase is able to recycle the cofactors and to maintain a useful intracellular cofactor balance [11].

A new method of regenerating NAD^+ using NADH oxidase from *Lactobacillus brevis,* which forms water H_2O as a by-product, has been developed. NADH oxidase (EC 1.6.99.3) is a flavoprotein and reacts with oxygen to produce water, enabling an easier product recovery than with other regenerating enzymes such as glucose dehydrogenase, lactate dehydrogenase or alcohol dehydrogenase. Therefore, the enzyme is well suited for the cofactor regeneration of NAD^+ when dehydrogenases are applied; for example, for the racemic resolution of alcohols [25].

It seems that NAD(P)-dependent dehydrogenases are well on the way to becoming a useful tool for the large-scale production of chiral compounds. The most convenient and useful methods for regenerating reduced nicotinamide coenzymes are enzymatic methods with formate/formate dehydrogenase for NADH, isopropanol/alcohol dehydrogenase (*L. brevis*/*T. brockii*) for NADPH, and glucose/glucose dehydrogenase (from *Bacillus*) for both NADH and NADPH [29]. A modified formate dehydrogenase accepting $NADP^+$ was recently produced by protein engineering [75].

One particularly exciting biocatalyst is cyclohexanone monooxygenase from *Acinetobacter calcoaceticus*, which is a flavoenzyme capable of catalysing the nucleophilic oxygenation of aldehydes, ketones (Bayer-Villiger oxidation), and also boron, as well as the electrophilic oxygenation of various hetero-atoms such as sulphur, selenium, nitrogen, and phosphorous. What makes cyclohexanone monooxygenase attractive for synthetic purposes is the fact that both types of reactions can proceed with high selectivity with a wide variety of natural and synthetic substrates. Furthermore, these biocatalytic oxidations are less hazardous, polluting, and energy consuming, than the conventional chemistry-based methodologies. Cyclohexanone monooxygenase has been used both as a whole-cell preparation and as an isolated enzyme [62]. The major disadvantages of the use of purified cyclohexanone monooxygenase are the time and expertise needed to purify the enzyme and the expense of the NADPH cofactor. Approximately 0.75 mg of pure enzyme can be isolated from a one-litre culture of cyclohexanol-grown *Acinetobacter* cells. This amount is sufficient to oxidise 0.5 mmol of ketone under typical conditions. Cofactor regeneration is another obstacle to using the purified enzyme as a synthetic reagent. Cyclohexanone monooxygenase catalyses substrate oxidation, through stoichiometric consumption of the expensive cofactor NADPH.

Therefore, for preparative purposes, it is essential to regenerate NADPH in situ at the expense of a cheap co-substrate by means of a second enzymatic reaction. Three NADPH regenerating systems coupled to the cyclohexanone monooxygenase-catalysed oxidation of thioanisole have been compared. 2-propanol/TBADH was selected as the NADPH regenerating system due to the low cost of the second substrate and high regeneration rate. A weakness of this system is represented by the high cost of commercial ADH, which, however, might be drastically reduced in the future by enzyme overexpression [73, 83, 84].

A clever closed-loop strategy has been developed, in which *Thermoanaerobium brockii* alcohol dehydrogenase catalyses the oxidation of a secondary alcohol to a ketone that becomes the substrate for cyclohexanone monooxygenase with concomitant production of NADPH [82].

6
Electrochemical, Chemical and Photochemical Coenzyme Regeneration

6.1
Electrochemical Regeneration

To date, enzymatic regeneration methods have been preferred. Although the association between enzymatic and electrochemical reactions, "enzymatic electrocatalysis" or "electroenzymatic reactions", has proven to be a very powerful tool to both the analytical and synthetic fields [71, 98], for most of the commercially attractive oxidations catalysed by dehydrogenases, the reaction is thermodynamically unfavourable. The introduction of an irreversible electrochemical reaction – in other words the electrochemical oxidation of NADH in order to perform coenzyme regeneration – therefore appears to be a good method of driving enzymatic reactions. Two cases have been experimentally and theoretically developed with the enzyme either in solution or immobilised onto the electrode's surface. In both cases, the electrochemical reactions drove the enzymatic reaction by consuming the NADH in solution or directly in the enzyme's environment [56]. So thermodynamically unfavourable reactions can only be used in a process if efficient NAD^+ regeneration and product elimination are simultaneously carried out within the reactor [42].

The direct amperometric oxidation of NADH suffers from large overpotentials (and consequently from the risk of interferences in complex samples) and electrode fouling. These limitations can be solved through the use of chemically modified electrodes that contain mediators which substantially lower the high overvoltage for NADH oxidation. Therefore, the electrochemical oxidation of NADH is promoted by these immobilised mediators, involving two steps at the electrode-solution interface, one chemical reaction between the oxidised form of the immobilized mediator (Med_{ox}) and NADH, and one electrochemical

reaction between the reduced form of the immobilized mediator (Med_{red}) and the electrode.

$$NADH^+ + Med_{ox} \rightarrow NAD^+ + Med_{red}$$
$$Med_{red} \xrightarrow{E_{appl} > E^{o'}} Med_{ox} + H^+ + 2e^- \qquad \text{(b)}$$

The reduced form of the mediator is electrochemically reoxidised if the applied potential E_{appl} is higher than the normal potential $E^{o'}$ of the immobilised mediator. The mediator therefore dictates the potential at which the electron transfer occurs. Consequently, the oxidation of NADH can now take place at a much lower potential, minimising the risk from interferences and electrode fouling. The coupling of both reactions may offer an elegant alternative to driving unfavourable chemical equilibria. The applied potential and reaction rate of the electrode reaction will become the new thermodynamic and kinetic driving force of the whole system. The redox mediator will bridge the catalytic transfer of electrons between the NAD^+/NADH pair and the electrode material at chemically modified electrodes. This demands intimate contact between the cofactor, the mediator and the electrode material. By allowing very close contact between enzyme, cofactor, and mediator, and thus the reaction sites, by co-immobilising them into a carbon paste electrode by adding poly-ethylene-amine to the reaction mixture, a favourable approach was obtained [19].

An interesting system for cofactor regeneration has been developed where the second enzyme, a hydrogenase from *Alcaligenes eutrophus* H16 (E.C.1.12.1.2), catalyses the electrochemical reduction of NAD^+ [99].

$$NAD^+ + H^+ + 2e^- \xrightarrow{\text{Hydrogenase}} NADH \qquad \text{(c)}$$

The advantages of such a regeneration method are numerous: the reductive power is directly supplied from inexpensive electrical energy. The catalysis does not require the use of a mediator in solution, avoiding problems with product recovery. The electrochemical reduction conditions induce a stabilising effect on the otherwise very unstable enzyme hydrogenase. The regeneration system was coupled with the synthesis of L-glutamate. Unfortunately, the performance of the enzyme is limited and a very low TTN is obtained, mainly due to the rapid denaturation of the hydrogenase. Obviously this needs to be improved considerably [15].

Non-enzymatic redox catalysts have been developed and successfully applied to NAD(P)H-dependent dehydrogenases. In this case, only the producing enzyme, a mediator, and the electrode as a source of reducing equivalents, are needed. An isolated monooxygenase with an indirect electrochemical regeneration of NADH has been reported. This was the first time that a flavine-dependent monooxygenase reaction has been coupled to an indirect electrochemical regeneration of NADH. The space/time yield of the non-optimised process (204 mg L^{-1} h^{-1}) already is about 50% of both the in vivo process

(390 mg L^{-1} h^{-1}) and the in vitro process with enzymatic regeneration of the coenzyme (405 mg L^{-1} h^{-1}) [26]. Viologenes were reported to be acting as electron shuttles between the cathode and a NAD(P)$^+$ reducing enzyme. The toxicity of viologenes, and the need for an enzyme to transfer the reduction equivalents from viologene to NAD(P)$^+$ are disadvantages. In addition, the regeneration reaction is quenched by molecular oxygen, making this concept inapplicable to mono-oxygenase reactions. Pentamethylcyclopentadienyl rhodium bipyridine complexes $[Cp^*Rh^{III}(bpy)(H_2O)]^{2+}$ can be utilized as a enzyme-free regeneration concept for reduced nicotinamide coenzymes, even in oxygen-containing reaction mixtures. Therefore, a productive coupling to mono-oxygenase was characterised using this concept. This characterisation was done in order to enlarge the applicability of this concept to an even broader range of preparative-scale biotransformations [27].

Although direct electrochemical oxidation of NAD(P)H can be performed, the reduction of NAD(P)$^+$ has not given results that would call for its application in organic synthesis until now. However, the use of a mediator and enzymes which catalyse the reduction of NAD(P)$^+$, the direct electrochemical reduction of NAD$^+$ by hydrogenases, and the formation of enzymatically active NADH by a direct electrochemical procedure appear to be promising approaches. The optimisation of the conditions for NAD(P)$^+$ regeneration in an electrochemical reactor, from the point of view of enzyme stability and coenzyme regeneration rate, was recently investigated. Preparative scale experiments with a graphite-felt electrode were done with glucose dehydrogenase (GDH) as a model enzyme because it is specific to NAD(P)$^+$. The enzyme converts β-D-glucose to D-glucono-δ-lactone while utilizing both coenzymes at similar rates. The equilibrium is shifted towards product formation at neutral pH by the spontaneous hydrolysis of D-glucono-δ-lactone to gluconic acid. Therefore, the reversibility of the enzymatic reaction does not limit NAD(P)H formation. Typical enzyme activity stabilisers (NaCl, sorbitol and BSA) did not have an effect on glucose dehydrogenase deactivation in the electrochemical reactor. However, polyethylene-amine can be used to protect glucose dehydrogenase from deactivation in preparative-scale electrochemical reactors [58].

The advantages of electrochemical methods explain the numerous attempts at new regeneration techniques, with new electrochemical mediators and modifications to the electrode surface among the possibilities envisaged. Of particular interest in applied biocatalysis is the electroanalytical oxidation of NADH at low overpotentials that can be achieved through a proposed variety of redox mediators. There are difficulties with many mediators due to their poor stability or due to electrode modification procedures. The electrooxidation of 3,4-dihydroxybenzaldehyde on glassy carbon electrodes is an exception, and gives rise to stable redox-active films, which exhibit high and persistent electrocatalytic activity. Enzyme immobilisation onto the electrode surface not only leads to an increased enzyme stability, but also to enzyme reutilisation, both of which are helpful for reactor design. A preparative-scale electrochemical reactor was used to enable the biotransformation of glucose into

gluconic acid. The reactor performance was studied using the enzyme covalently immobilised onto an electrode surface modified with 3,4-dihydroxybenzaldehyde in different ways. As a continuous substrate feed was lacking, a low TTN was obtained for the coenzyme (TTN_{max}=100) independently of the operation at 0.7 or 0.2 V; this maximum value was also attained more rapidly when the bioreactor was operated at 0.7 V [50].

The electrochemical regeneration of redox coenzymes avoids the use of any additional reagent, is simple, and presents high enough regeneration numbers for preparative-scale applications. The association between enzymatic and electrochemical reactions has proven to be a very powerful tool in analytical and synthetic fields, and has led to tremendous successes in the field of electrochemical biosensors in particular. Table 5 summarizes some of the recently developed electrochemical systems for cofactor regeneration.

6.2 Chemical Regeneration

Regenerating NAD(P)H using dihydrogen (H_2) is preferred, because H_2 is the cheapest reducing agent and it yields no by-products (both atoms of hydrogen are delivered to the reduction products). Previous reports on such a use of H_2 involved highly air-sensitive hydrogenase enzymes or complex systems in which H_2 first reduced an intermediate "hydride carrier", which subsequently reduced a nicotinamide coenzyme. Recently, simple transition-metal catalysts for the direct reaction between H_2 and $NADP^+$ under conditions (listed below) appropriate to the in situ coupling of NADPH regeneration to an enzymatic reduction have been introduced, with the following advantages: (i) high selectivity for reduction of the nicotinamide coenzyme versus the enzymatic substrate; (ii) high regioselecivity yielding 1,4-dihydropyridine; (iii) mild reaction temperature, preferably 25–65 °C, and; (iv) reaction in an aqueous medium in the pH range 6.5–8.5. [78]. The reduction of 2-heptanone to (*S*)-2-heptanol using *Thermoanaerobium brockii* alcohol dehydrogenase was performed with catalytic amounts of $NADP^+$ and $[RuCl_2(TPPTS)_2]_2$. It was demonstrated that ruthenium (II) and rhodium (III) complexes are effective catalysts for the reduction of nicotinamide coenzymes with hydrogen, under conditions that are appropriate for in situ coupling with enzymatic reductions. The TTN of both $NADP^+$ and ruthenium was 10. This TTN, though not impressive, demonstrates that the reduction is catalysed for both $NADP^+$ and ruthenium.

The use of a platinum carbonyl cluster for the catalytic reduction of NAD^+ to NADH by dihydrogen has been described [9]. By using the enzyme L-lactate dehydrogenase (L-LDH), the scope of this reaction has been extended to include reduction of pyruvate to L-lactate. Since both NAD^+ and L-LDH are soluble only in water, and the platinum carbonyl cluster is soluble only in organic solvents, a biphasic system consisting of water and dichloromethane was used.

To be viable, a cofactor regeneration system must generate reduced coenzyme with very high chemical yield and 1,4-regioselectivity under con-

Table 5 Electrochemical coenzyme regeneration (part 1 of 3)

Production/Regeneration system	Enzyme E_p	Electro-chemical system	Reactor type	Volume ml	Productivity g $L^{-1}d^{-1}$	TTN	Reference
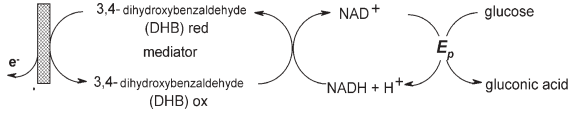	Glucose dehydrogenase	Mediator-DHB (3,4-dihydroxy-benzaldehyde)	Batch	28		max. 100	[50]
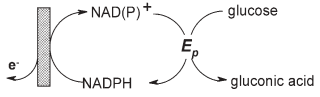	Glucose dehydrogenase	direct	Batch, Three electrodes configuration	28			[58]
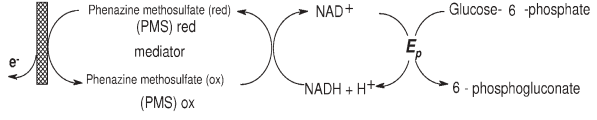	Glucose-6-P-dehydrogenase	Mediator-PMS (phenazine methosulfate)	Batch, Rotating disk graphite electrode	200		2.3	[88]
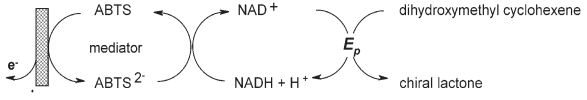	Horse liver alcohol dehydrogenase	$ABTS^{1-}$/ $ABTS^{2-}$ Mediator (2,2′-azinobis-(3-ethylbenzo-thiazoline-6-sulfonate	Batch, Stirred electro-chemical cell	30	3.24		[89]

Table 5 Electrochemical coenzyme regeneration (continuation – part 2 of 3)

Production/Regeneration system	Enzyme	Electro-chemical system	Reactor type	Volume ml	Productivity g $L^{-1}d^{-1}$	TTN	Reference
	E_p						
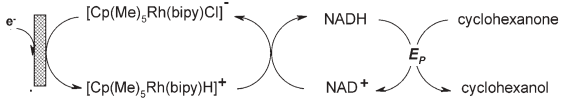	Horse liver alcohol dehydrogenase	Rh-complex-Mediator	Membrane reactor (Dialysis or UF-CSTR)	100			[18]
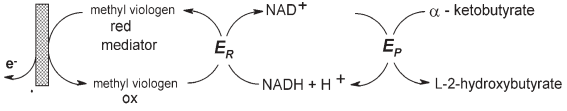	L-Lactate dehydrogenase	Viologen-Mediator Diaphorase	Membrane electro-chemical reactor, Batch	~15			[90]
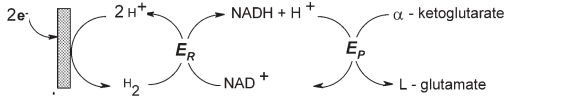	Glutamate dehydrogenase	Hydro-genase/H_2	Batch	5		992 1034	[15]
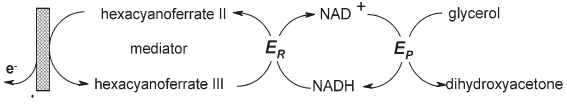	Glycerol dehydrogenase	Hexacyano-ferrate Diaphorase	Fixed bed, separate electro-chemical-cell				[91]

Table 5 Electrochemical coenzyme regeneration (continuation – part 3 of 3)

Production/Regeneration system	Enzyme E_p	Electro-chemical system	Reactor type	Volume ml	Productivity g $L^{-1}d^{-1}$	TTN	Reference
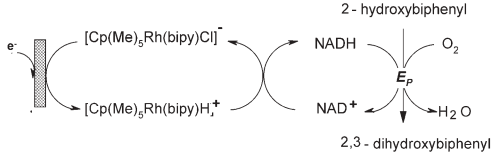	Monooxygenase	Rh-complex	Batch	27	4.9		[26]
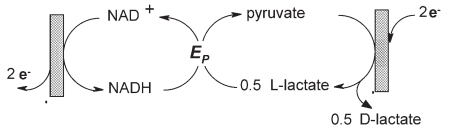	L-Lactate dehydrogenase		Two coupled compact reactors	50			[92]
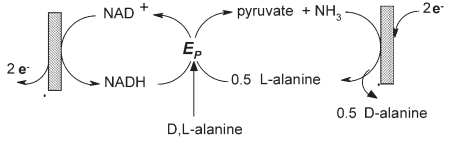	L-alanine dehydrogenase		Compact reactor plug flow				[6]
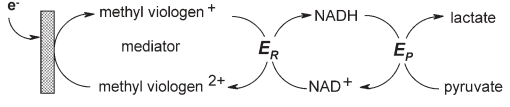	L-lactate dehydrogenase	Methyl-viologen Lipoamide dehydrogenase	Compact reactor-differential mode				[22]

Table 6 Chemical and photochemical coenzyme regeneration

Production/Regeneration system	Producing Enzyme	Chemical system	Reactor type	Volume ml	Productivity g $L^{-1}d^{-1}$	TTN	Reference
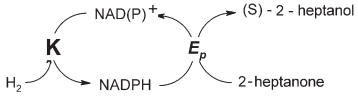	*Thermo-anaerobium brokii* alcohol dehydrogenase ($NADP^+$)	Chemical H_2/Ru-complex-catalyst	Batch			10	[78]
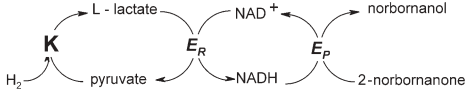	Horse liver alcohol dehydrogenase L-lactate dehydrogenase	Chemical H_2/Ru-complex-catalyst	Batch	300		49	[1]
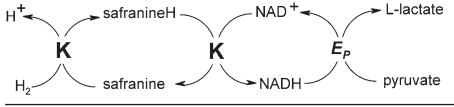	L-lactate dehydrogenase	Pt-carbonyl-cluster	Batch				[9]
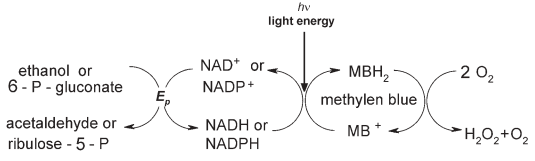	Yeast alcohol dehydrogenase (Immobilized)	Photochemical MB^+/MBH_2 (methylene blue)	Batch	60		1125	[31]
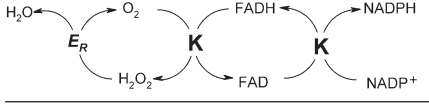	–	Catalase/FAD/Rh-complex					[27]

ditions that are compatible with both the coenzyme and the enzyme of the production's reaction. Likewise, the preferred recycling reagent must be inexpensive and should not yield by-products, which complicate product recovery. It seems that chemical methods at present tend to suffer from cumbersome reaction conditions, expensive and/or toxic reagents, and/or unwanted side products, and therefore have been not preferred for commercial or preparative applications. This is probably the reason that very few examples of chemical methods of cofactor regeneration have been found in the literature (Table 6).

6.3 Photochemical Regeneration

The irradiation of photosensitiser dyes (like methylene blue or *N*-methylphenazonium methyl sulfate) with visible light leads to the oxidation of reduced coenzymes such as pyridine nucleotides (NADH or NADPH). This photoredox reaction can be used to regenerate the oxidised form of this coenzyme in enzymatic reactions, and total consumption of the substrate with catalytic amounts of enzyme, coenzyme and photosensitizer can be obtained. The process has been studied with two common enzymatic reactions: ethanol oxidation and gluconate-6-phosphate oxidation. In the first case, a TTN of 1125 was obtained for the photo-regeneration of NAD^+ from NADH. This system operates with a dye (like methylene blue, MB) as the electron acceptor, which is able, in its excited state, to oxidise NADH or NADPH:

$$NADH + MB^+ + H^+ \xrightarrow{2e^-} NAD^+ + MBH + H^+ \qquad (d)$$

The sequence of electron transfer reactions that occurs in these aerobic enzymatic oxidations allows catalytic cycles to be performed with catalytic amounts of enzyme, coenzyme and dye [31].

The direct use of light energy for the reduction of substrate by biocatalysts has recently been demonstrated by the use of phototrophic organisms. Phototrophic organisms, such as algae and plants, capture light energy in order to generate NADPH from $NADP^+$ through photosynthetic electron-transfer reactions. CO_2 is then converted into sugar, generally using NADPH. It was proposed that the reducing power of NADPH generated through photosynthesis could also be used in the reduction of exogenous substrates such as unnatural ketones to yield useful optically active alcohols. Cofactor recycling is therefore no problem when photosynthetic living cells are used as biocatalysts for reduction. Accordingly, solar energy can be used directly for the bioconversion of artificial substrates. The focus was on cyanobacteria (micro algae), since they belong to both phototrophic and microbic categories. In other words, they are plant-like photosynthetic bacteria, so the growth rate of cyanobacteria is as high as that of typical microbes.Therefore, a new system for cofactor recycling in which cyanobacteria convert light energy to reducing power was proposed. The advantage of this reaction is that light energy, which is a cheap resource,

can be used since the microalgae possess a system that is required for the production of reduced coenzymes, NADPH. Under illumination, the reduction of ketones using the cyanobacteria was successfully demonstrated [57].

7
Reaction Engineering Aspects

7.1
Cofactor Retention

Besides the need for an efficient, economical, cofactor regeneration system, they also have to be retained within the reaction medium while the product is removed. At the same time the cofactor must be mobile enough to diffuse to the active site of the regenerating enzyme and to the active site of the enzyme that catalyses the primary reaction. A breakthrough for the reusability of cofactors was the synthesis of molecular weight-enlarged active cofactors, like NAD^+ coupled to a large inert molecule such as dextran or polyethylene glycol [14]. Enzymes and molecular weight-enlarged cofactors are much bigger than substrates and products so they can be separated by membrane technology. One approach is to use a membrane reactor [81], where enzymes and cofactors are retained in a compartment separated by a membrane with a cut-off of 5–10 KD through which the reaction medium is pumped. Another possibility is to enclose enzymes and molecular weight-enlarged cofactors within semipermeable microcapsules [72], or to co-immobilise cofactors and related enzymes [41, 51, 61, 87].

7.2
Cofactor Regeneration in Enzyme Membrane Reactors

The natural reactor for coenzyme regeneration is the microbial cell, which has some drawbacks. The main one is the danger that secondary reactions will occur, complicating product recovery. Therefore, in practice attempts are being made to replace the natural cell by an artificial cell – the enzyme membrane reactor [39, 80]. In the enzyme membrane reactor, the enzymes present in solution are retained either by means of a regular ultrafiltration membrane from the continuous flow leaving the reaction vessel [35–38, 43, 60, 81, 84, 85], by a nanofiltration membrane [46, 63, 70], or by means of charged membranes [30]. This exploits the fact that biopolymers like enzymes are very much larger in size than the substrate and product molecules, and are usually highly charged on their surface. Therefore continuous homogeneous catalysis is possible with very good exploitation of the biocatalyst. To avoid mass transport limitation, the operation of an enzyme membrane reactor with enforced flow is preferable. An essential advantage of this system is that the reactor can be operated under sterile conditions even in the continuous mode. This is possible

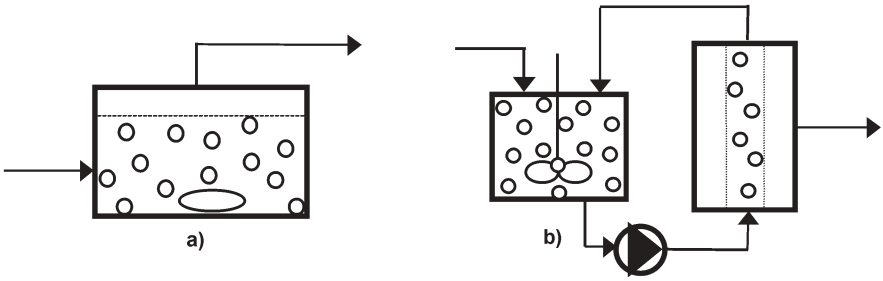

Fig. 4 Enzyme membrane reactors: **a** flat-membrane reactor; **b** hollow-fibre reactor

because the enzyme as well as the substrate solution can be fed into a presterilised reactor through a sterile filter. The product solution is ultrafiltrated and pyrogen free. An enzyme membrane reactor can be designed as a flat membrane reactor (Fig. 4a) or a hollow-fibre reactor (Fig. 4b). A flat membrane reactor prevents concentration polarisation by intensive stirring. This reactor, with a volume of 2–50 ml, is usually used for process development [35], and is commercially available with a 10 ml volume from Bioengineering AG, Wald (Zh.), Switzerland and Jülich Fine Chemicals, Jülich, Germany. A hollow-fibre reactor uses membranes in the form of hollow-fibre modules [23, 61, 79]. Using a circulating pump to achieve an enforced flow parallel to the membrane reduces the concentration polarisation in this reactor to a tolerable level.

The enzyme membrane reactor with soluble enzyme is particularly beneficial for the cofactor regeneration system when an enlarged cofactor [81] or a charged membrane [30] is used.

The enzyme membrane reactor can be operated in various modes: batch reactor [44, 84, 85]; repetitive batch reactor [52, 60, 63]; continuous stirred tank reactor (CSTR [35, 38, 63, 72]); plug flow reactor; cascade reactor [36]; as a reactor with recycle of reaction media [43], and so on.

The retention R of the cofactor within the reactor is very important, particularly for continuous operation as in the case of an ideal CSTR, where it is defined as:

$$R = \frac{C_{\text{cofactor in reactor}} - C_{\text{cofactor in outlet}}}{C_{\text{cofactor in reactor}}} \tag{2}$$

In a continuously operated reactor, the decrease in the cofactor concentration in the reactor is described by a function of operating time t and residence time τ as follows:

$$C_{\text{cofactor in reactor}}\,(t = t) = C_{\text{cofactor in reactor}}\,(t = 0) \cdot \exp\left(-\frac{1-R}{\tau} \cdot t\right) \tag{3}$$

It can be seen (refer to Figs. 5 and 6) that the elution of the cofactor from the reactor depends both on the retention of the membrane and the residence time of the liquid in the continuous reactor. Even at rather high retention, washout

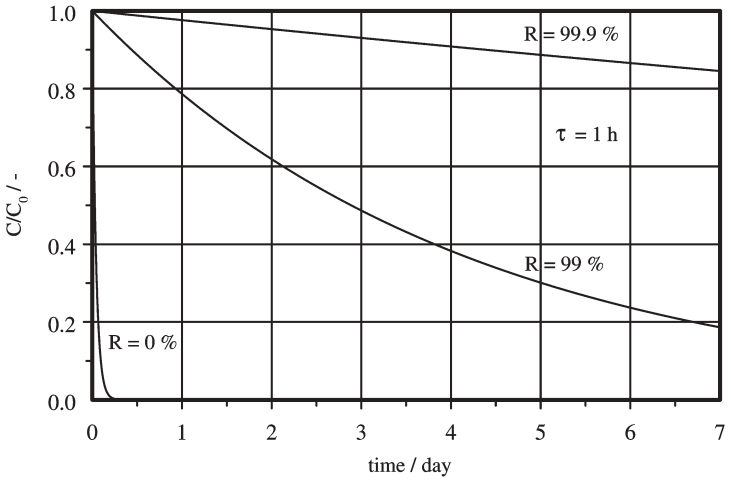

Fig. 5 Effect of the retention on the cofactor loss from a reactor

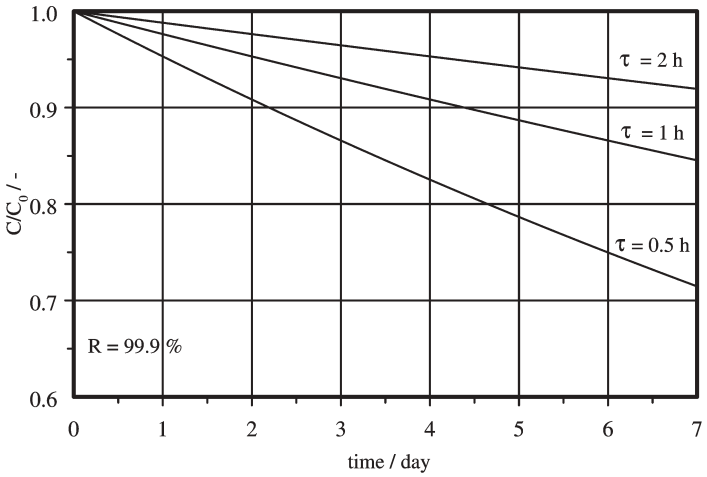

Fig. 6 Effect of the residence time on the cofactor loss from a reactor

becomes critical at low residence times. On the other hand, the active concentration of the cofactor also depends on its stability. PEG-10000 NAD(H) displays a retention of 99.82% and PEG-20000 NAD(H) 99.93% [80]. To achieve a high retention, the choice of the correct membrane depends on the average molecular weight of the coenzyme derivative and also on the pore size distribution that determines the actual retention of a given membrane. The performance of the membrane selected should be checked by experiments lasting for a sufficient number of residence times in order to allow an assessment of the data with sufficient confidence [39].

As can be seen from Fig. 5, if an enzyme membrane reactor is operated for a residence time of 1 hour over a period of a week, even at 99% retention much coenzyme (~80%) is eluted, so that a retention of about 99.9% is required to reduce the amount of cofactor eluted from the enzyme membrane reactor. Only in this case can a high TTN number be reached in a continuous enzyme membrane reactor. If an ultrafiltration cell is used instead for the recovery of the enzymes and coenzyme from the solution of a batch experiment, only 5–7 volumes of a rinsing solution is required to wash out products with a retention of 0%. If in this case the retention for the cofactor is only 99%, then only a few percent of the cofactor is eluted along with the product.

In Figure 6, the influence of the residence time of the substrate solution in an enzyme membrane reactor on the cofactor concentration is shown for a retention of 99.9%. Even at very short residence times, a significant elution of the cofactor is already evident. In principle, the higher operating cost of a membrane with high retention must be balanced with the cost of the fraction of cofactor lost due to its incomplete retention.

Figure 7 demonstrates the performance of a laboratory enzyme membrane reactor for producing L-leucine using a YM5 membrane from Amicon [39] during an experiment performed over a period of three months. A total turnover number of 80,000 was obtained for PEG – 20000 NAD(H). Figure 7 shows that the TTN increases from the start of the experiment and levels off after approximately 20 days while the reactor was operated at rather low stationary coenzyme concentrations.

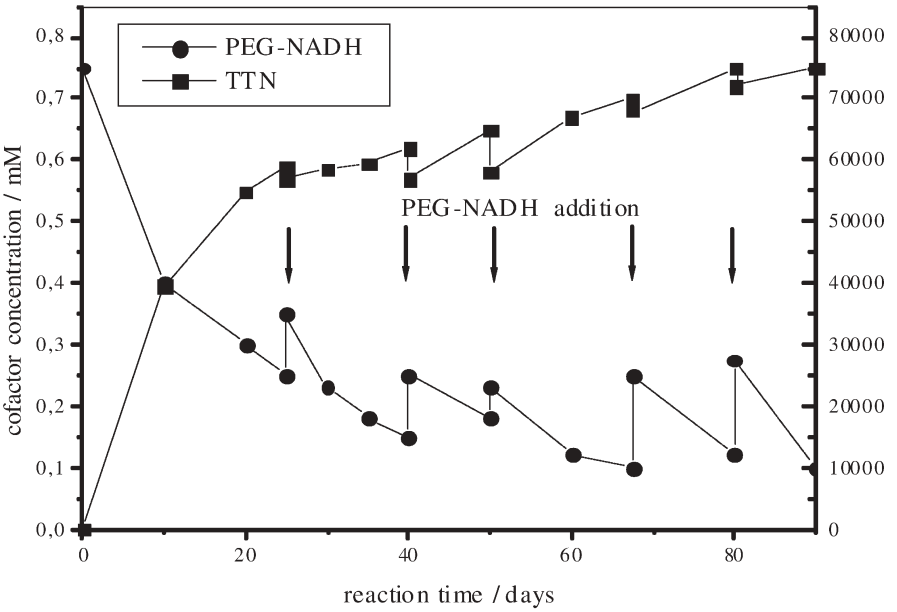

Fig. 7 Development of TTN during L-leucine production (from [39])

7.3 Cofactor Regeneration in Electrochemical Reactors

Electrochemical reactors with enzymes are important applications of electrochemical technology in bioprocess engineering. The electrochemical regeneration of redox coenzymes avoids the use of any additional reagent, is simple, and presents high enough regeneration numbers for preparative-scale applications.

Stabilisation of the enzyme is a crucial parameter to be taken into account when designing a new type of electro-enzymatic reactor. Generally, immobilisation is known to stabilise enzymes, but the different steps required to immobilise enzymes may drastically decrease the initial activity of fragile enzymes. For this reason, membrane reactors have been instead used to carry out enzyme-catalysed synthesis. However, the combination of electrochemical reactors with membrane techniques has rarely been used. Only a few examples of electrochemical membrane reactors have been found in the literature dealing with enzyme-catalysed synthesis.

In general, two types of electrochemical reactors can be distinguished:

1. The electrochemical and membrane reactors are separated. In this case the membrane reactor allows us to continuously remove the product, and to keep the enzyme in the working loop [13].
2. The electrochemical and enzymatic reactors are contained within the same device. This is the so-called "compact reactor". The principle of the reactor is shown in Fig. 8. There are two main designs for the reactor: a reactor with the producing enzyme immobilised on the electrode surface (Fig. 9), and

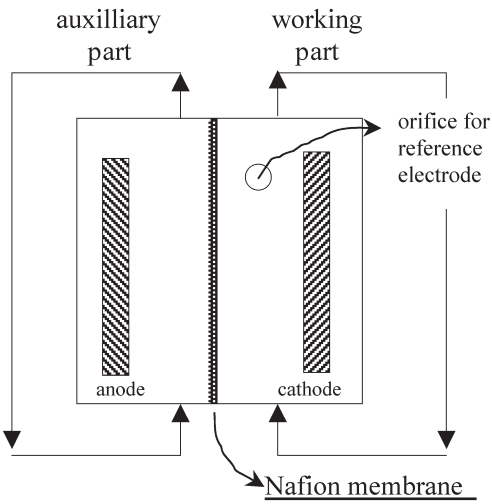

Fig. 8 Principle of the electrochemical reactor in the three electrode configuration (cathode, anode and reference electrode)

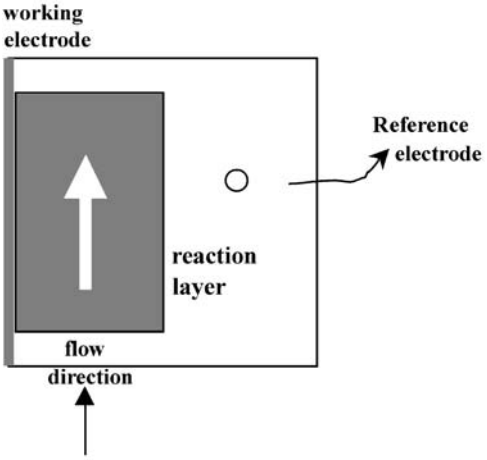

Fig. 9 The working part of the compact electrochemical reactor, with the producing enzyme immobilised on to the electrode surface

a membrane reactor (Fig. 10). A reactor with an immobilised producing enzyme can operate in batch mode [12, 42] or in continuous mode either as a plug flow reactor, a plug flow reactor with an included recycle loop [21], or as a stirred tank reactor, which is how a membrane reactor (Fig. 10) behaves. The direct electrochemical oxidation of NAD(P)H delivers an almost fully active coenzyme offering a high TTN (>10000) [58] in compact batch reactors. Although direct electrochemical oxidation of NAD(P)H is feasible, the reduction of $NAD(P)^+$ has not given good enough results for it to be applied in organic synthesis until now. Enzyme immobilisation onto

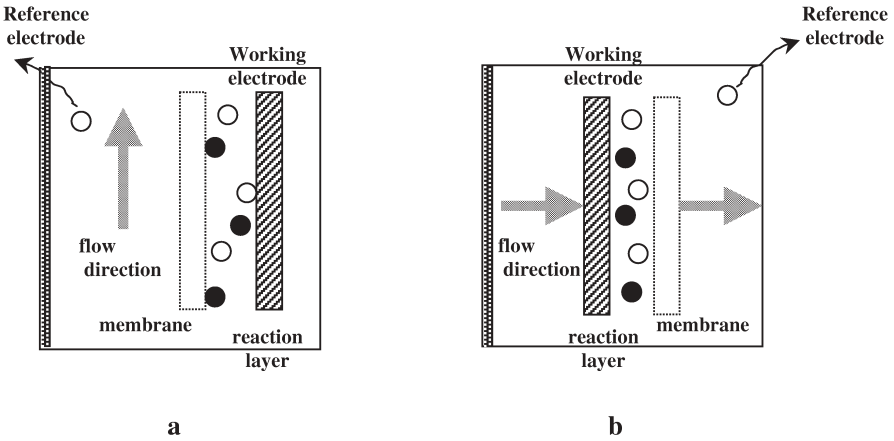

Fig. 10 The working part of the compact membrane electrochemical reactor: **a** dialysis reactor, **b** ultrafiltration membrane reactor

the electrode surface could allow not only an increase in enzyme stability, but also enzyme reutilisation, both of which are useful for reactor design.

The membrane reactor can be operated in either a diffusive or an enforced flow mode using dialysis (Fig. 10a) or ultrafiltration membranes (Fig. 10b) [18] respectively. In an ultrafiltration membrane electrochemical reactor (UF-MER), the solution circulates perpendicular to the electrode and so crosses the electrode and then the UF-membrane. The UF-MER can be used in two different modes: continuous and recycling. The reactor confines the enzyme near the electrode due to the membrane. The main problem with electrochemical reactors is that only a fraction of the producing enzyme (that which is close to the electrode surface) is really efficiently utilized. It should be emphasised that the reactors proposed can be utilised in a "plug and play" fashion; this means that when the best parameters for the desired reaction are determined (concentration, potential, pH, enzyme activity, and so on), it is only necessary to introduce the substrates and enzymes into the reactor to start the synthesis. No preliminary enzyme preparation or immobilisation steps are required.

8 Conclusion

A variety of potential useful enzymes require nicotinamide cofactors: alcohol dehydrogenases with their ability to reduce a ketone to a chiral alcohol, keto-acid dehydrogenases for the syntheses of aminoacids or monooxygenases that catalyse epoxidation or hydroxylation. Cofactors are too expensive to be added in stoichiometric amounts. Over the last few decades, there has been substantial progress in cofactor regeneration as well as in retention technology. Currently it seems that the best method that is also widely explored is enzymatic regeneration by the use of formate dehydrogenase as the cofactor-regenerating enzyme for NADH [39] as well as for NADPH [29]. The enzyme uses formate as a substrate. Formate is cheap, most enzymes can tolerate it, and it is a strong reducing agent. The product of the regeneration reaction is CO_2, which hardly has any effect on enzymes at all, thermodynamically drives the reaction to completion, and is easily removed from the reaction system as gas or by a consecutive conversion to hydrogencarbonate which simplifies product recovery. In Table 7 we present the current costs of the most extensively investigated regenerating enzymes for the use on the lab-scale. Of course, the higher the required quantity of enzyme, the lower its costs per enzyme unit will be.

Since the interest in biocatalysts that are able to hydroxylate organic compounds, such as oxygenases, has significantly increased in recent years, some progress is evident, especially in NAD(P)H regeneration on the lab-scale. A new NADP-dependent formate dehydrogenase [75], as well as a new NADH oxidase [25] have been found, enhancing the efficiencies of methods of cofactor regeneration.

Table 7 Costs of the enzymes used for NAD(P)(H)

Enzymes	€/1000 U, from Juelich Fine Chemicals (2003)	€/1000 U, from the Fluka Catalog (2003)
Formate dehydrogenase *Candida boidini*	(NAD^+-specific) 290	(NAD^+-specific) 437
Formate dehydrogenase *Pseudomonas s.* (mutant in *E.coli*)	(NAD^+-specific) 95 ($NADP^+$-specific) 680	(NAD^+-specific) 220 ($NADP^+$-specific) 1038
Glucose-6-P dehydrogenase *L. mesenteroides*		67
Glucose-6-P dehydrogenase *S. cerevisiae*		176
D-Glucose dehydrogenase *B. megaterium*	($NADP^+$-specific) 125	1159
D-Glucose dehydrogenase *Pseudomonas s.*	(both NAD^+ and NADPH-specific) 10.6	30
Alcohol dehydrogenase *S. cerevisiae*		2
Alcohol dehydrogenase *Horse liver*		615
Alcohol dehydrogenase *Thermoanaerobium brockii*		1526
D-Lactate dehydrogenase *Lactobacillus cellobiosus*	(NAD^+-specific) 3.5	
D-Lactate dehydrogenase *Lactobacillus s.*		6.5

The first coenzyme regeneration system to be commercialised up to the production stage, the production of L-tert leucine [10], is still in use.

Finally, the application of electrochemical reactors coupled to enzyme-catalysed processes has been expanded from analytical to preparative scale.

References

1. Abril O, Whitesides GM (1982) J Am Chem Soc 104:1552
2. Adlercreutz P (1996) Biocatal Biotransfor 14:1
3. Ammon K (1999) Dissertation. Universität Dortmund, Germany
4. Ammon K, Phan M, Wichmann R (1998) Chem Ing Tech 70:1126
5. Andersson M, Holmberg H, Adlercreutz P (1998) Biotechnol Bioeng 57:79
6. Anne A, Bourdillon C, Daninos S, Moiroux J (1999) Biotechnol Bioeng 64:101

7. Bastos FM, dos Santos AG, Jones Jr J, Oestreicher EG, Pinto GF, Paiva LMC (1999) Biotechnol Tech 13:661
8. Bastos FM, França TK, Machado GDC, Pinto GF, Oestreicher EG, Paiva LMC (2002) J Mol Catal B–Enzym 19–20:459
9. Bhaduri S, Mathur P, Payra P, Sharma K (1998) J Am Chem Soc 120:12127
10. Bommarius AS, Schwarm M, Drauz K (1998) J Mol Catal B–Enzym 5:1
11. Boonstra B, Rathbone DA, French CE, Walker EH, Bruce NC (2000) Appl Env Microbiol 66:5161
12. Bourdillon C, Lortie R, Laval JM (1988) Biotechnol Bioeng 31:553.
13. Brielbeck B, Frede M, Steckhan (1994) Biocatalysis 10:49
14. Bückmann AF, Kula MR, Wichmann R, Wandrey C (1981) J Appl Biochem 3:301
15. Cantet J, Bergel A, Comtat M (1996) Enzyme Microbiol Tech 18:72
16. Chenault HK, Whitesides GM (1987) Appl Biochem Biotech 14:147
17. Crocq V, Masson C, Winter J, Richard C, Lemaitre G, Lenay J, Vivat M, Buendia J, Prat D (1997) Org Process Res Dev 1:2
18. Délécouls-Servat K, Basséguy R, Bergel A (2002) Chem Eng Sci 57:4633
19. Dominiguez E, Lan PD, Okamoto Y, Hale PD, Skotheim TA, Gorton L, Hahn-Hägerdal B (1993) Biosens Bioelectron 8:229
20. Endo T, Kozumi A (2001) Adv Synth Catal 343:521
21. Fassouane A, Laval JM, Moiroux J, Bourdillon C (1990) Biotechnol Bioeng 35:935
22. Fisher RJ, Fenton JM, Iranmahboob J (2000) J Membrane Sci 177:17
23. Flaschel E, Wandrey C, Kula MR (1983) Adv Biochem Eng Biotechnol 26:73
24. Galkin A, Kulakova LJ, Yoshimura T, Soda K, Esaki N (1997) Appl Environ Microbiol 63:4651
25. Geueke B, Riebel B, Hummel W (2003) Enzyme Microbiol Tech 32:205
26. Hollmann F, Schmid A, Steckhan A (2001) Angew Chem Int Edit 40:169
27. Hollmann F, Witholt B, Schmid A (2003) J Mol Catal B–Enzym 19–20:167
28. Hummel W, Schütte H, Schmidt E, Wandrey C, Kula MR (1987) Appl Microbiol Biot 26:409
29. Hummel W (1999) TIBTECH 17:487
30. Ikemi M, Koizumi N, Ishimatsu Y (1990) Biotechnol Bioeng 36:149
31. Julliard M, Le Petit J (1982) Photochem Photobiol 36:283
32. Kataoka M, Rohani LPS, Yamamoto K, Wada M, Kawabata H, Kita K, Yanase H, Shimizu S (1997) Appl Microbiol Biot 48:699
33. Kataoka M, Yamamoto K, Kawabata H, Wada M, Kita K, Yanase H, Shimizu S (1999) Appl Microbiol Biot 51:486
34. Koeller KM, Wong CH (2001) Nature 409:232
35. Kragl U, Vasic-Racki D, Wandrey C (1993) Ind J Chem 32:103
36. Kragl U, Kruse W, Hummel W, Wandrey C (1996) Biotechnol Bioeng 52:309
37. Kragl U, Vasic-Racki D, Wandrey C (1996) Bioprocess Eng 14:291
38. Kruse W, Hummel W, Kragl U (1996) Recl Trav Chim Pays-B 115, 239
39. Kula MR, Wandrey C (1987) Method Enzymol 136:9
40. Kula MR, Kragl U. (2000) Dehydrogenases in the synthesis of chiral compounds. In: Patel RN (ed) Stereoselectice biocatalysis. Marcel Dekker, New York, pp 839–866
41. Larsson PO, Mosbach K (1974) FEBS Lett 46:119
42. Laval JM, Moiroux J, Bourdillon C (1991) Biotechnol Bioeng 38:788
43. Liese A, Karutz M, Kamphuis J, Wandrey C, Kragl U (1996) Biotechnol Bioeng 51: 544
44. Liese A, Zelinski T, Kula MR, Kierkels H, Karutz M, Kragl U, Wandrey C (1998) J Mol Catal B–Enzym 4:91

45. Liese A, Seelbach K, Wandrey C (2000) Industrial biotransformations. Wiley-VCH, Weinheim
46. Lin SS, Harada T, Hata C, Miyawaki O, Nakamura K (1997) J Ferment Bioeng 83:54
47. Lortie R, Villaume I, Legoy MD, Thomas D (1989) Biotechnol Bioeng 33:229
48. Lamare S, Legoy MD (1993) TIBTECH 11:413
49. Lutz J, Mozhaev VV, Khmelnitsky YL, Witholt B, Schmid A (2002) J Mol Catal B-Enzym 19–20:177
50. Manjón A, Obón JM, Casanova P, Fernández VM, Ilborra JL (2002) Biotechnol Lett 24:1227
51. Månsson MO, Larsson PO, Mosbach K (1979) FEBS Lett 98:309
52. Mertens R, Greiner L, van den Ban ECD, Haaker HBCM, Liese A (2003) J Mol Catal B-Enzym 24–25:39
53. Matsuyama A, Yamamoto H, Kawada N, Kobayashi Y (2001) J Mol Catal B–Enzym 513
54. Matsuyama A, Yamamoto H, Kobayashi Y (2002) Org Process Res Dev 6:558
55. Maugard T, Lamare S, Legoy MD (2001) Biotechnol Bioeng 73:164
56. Mayhew MP, Reipa V, Holden MJ, Vilker VL (2000) Biotechnol Prog 16:610
57. Nakamura K, Yamanaka R (2002) Chem Comm 1782
58. Obón JM, Casanova P, Manjón A, Fernández VM, Ilborra JL (1997) Biotechnol Prog 13:557
59. Orlich B, Berger H, Lade M, Schomaecker (2000) Biotechnol Bioeng 70:638
60. Pasta P, Carrea G, Gaggero N, Grogan G, Willetts A (1996) Biotechnol Lett 18:1123
61. Persson M, Månsson MO, Bülow L, Mosbach K (1991) Bio/Technology 9:280
62. Rissom S, Schwarz-Linek U, Vogel M, Tishkov IV, Kragl U (1997) Tetrahedron Asymmetr 8:2523–2526
63. Rissom A, Beliczey J, Giffels G, Kragl U, Wandrey C (1999) Tetrahedron Asymmetr 10, 923
64. Roberts SM (1999) J Chem Soc Perk T 1:1
65. Rodriguez S, Schroeder KT, Kayser MM, Stewart JD (2000) J Org Chem 65:2586
66. Russell AJ, Yang FX (1996) Chemtech 24
67. Schenkels P, de Vries S, Straathof AJJ (2001) Biocatal Biotransform 19:191
68. Schmid A, Vereyken I, Held m, Witholt B (2001) J Mol Catal B–Enzym 11:455
69. Schmid A, Dordick JS, Hauer B, Kiener A, Wubbolts M, Witholt B (2001) Nature 409:258
70. Seelbach K, Kragl U (1997) Enzyme Microbiol Tech 20:389–392
71. Somers WAC, van Hartingsveldt W, Stigter ECA, van der Lugt JP (1997) TIBTECH 15:495
72. Stengelin M, Patel RN (2000) Biocatal Biotransform 18:373
73. Stewart JD (1998) Curr Org Chem 2:195
74. Stewart JD (2000) Curr Opin Biotechnol 11:363
75. Tishkov VI, Galkin AG, Fedorchuk VV, Savitsky PA, Rojkova AM, Gieren H, Kula MR (1999) Biotechnol Bioeng 64:187
76. Vasic-Racki D, Jonas M, Wandrey C, Hummel W, Kula MR (1989) Appl Microbiol Biot 31:215
77. Virto C, Svensson I, Adlercreutz P, Mattiasson B (1995) Biotechnol Lett 17:877
78. Wagenknecht PS, Penney JM, Hembre RT (2003) Organometallics 22:1180
79. Wandrey C, Flaschel E, Schügerl K (1977) Chem Ing Tech 49:257
80. Wandrey C, Wichmann R (1985) Coenzyme regeneration in membrane reactors. In: Laskin A (ed) Enzymes and immobilized cells in biotechnology. Benjamin/Cummings, Co Menlo Park, CA, pp 177–208
81. Wichmann R, Wandrey C, Bückmann AF, Kula MR (1981) reprint (2000) Biotechnol Bioeng 67:791
82. Willetts J. Knowles CJ, Levitt MS, Roberts SM, Sandey H, Shipston NF (1991) J Chem Soc Perk T 1:1608

83. Willetts A (1997) TIBTEC 15:55
84. Zambianchi F, Pasta P, Carrea G, Colonna S, Gaggero N, Woodley JM (2002) Biotechnol Bioeng 78:489
85. Zelinski T, Liese A, Wandrey C, Kula MR, (1999) Tetrahedron Asymmetr 10, 1681–1687.
86. Hashimoto SI, Ozaki A, (1999) Curr Opin Biotechnol 10:604
87. Ukeda H, Imabayashi M, Matsumoto K, Osajima Y (1989) Agric Biol Chem 53:2909
88. Miyawaki O, Yano T (1992) Enzyme Microbiol Tech 14:474
89. Schröder I, Steckhan E, Liese A (2003) J Electroanal Chem 541:109–115
90. Grimes MT, Drueckhammer DG (1993) J Org Chem 58:6148
91. Kronkvist K, Wallentin K, Johansson G (1994) Anal Chim Acta 290:335
92. Biade AE, Bourdillon C, Laval JM, Mairesse G, Moiroux J (1992) J Am Chem Soc 114:893
93. Röthig TR, Kulbe KD, Buckmann F, Carrea G (1990) Biotechnol Lett 12:353
94. Kula MR, Pohl M (2002) Deutscher Zukunftspreis homepage. http://www.deutscher-zukunftspreis.de/archiv/02.htm
95. Villela MF, Stillger T, Müller M, Liese A, Wandrey C (2003) Angew Chem Int Edit 42:2993
96. Stampfer W, Kosjek B, Kroutil W, Faber K (2003) Biotechnol Bioeng 81:865
97. Schubert T, Hummel W, Müller M (2002) Angew Chem Int Edit 41:634
98. Steckhan E, Arns T, Heineman WR, Hilt G, Hoormann D, Jörissen J, Kröner L, Lewall B, Pütter H (2001) Chemosphere 43:63
99. De Lacey AL, Detcheverry M, Moiroux J, Bourdillon C (2000) Biotechnol Bioeng 68:1

Received: April 2004

Adv Biochem Engin/Biotechnol (2005) 92: 261–287
DOI 10.1007/b98910

Enzyme-Catalyzed Regio- and Enantioselective Ketone Reductions

Michael Müller (✉)[1] · Michael Wolberg[1] · Thomas Schubert[1] · Werner Hummel[2]

[1] Forschungszentrum Jülich GmbH, 52425 Jülich, Germany
mi.mueller@fz-juelich.de
[2] Heinrich-Heine Universität Düsseldorf, Institut für Enzymtechnologie, Forschungszentrum Jülich, 52426 Jülich, Germany

Dedicated to Prof. Dr. Christian Wandrey on the occasion of his 60th birthday.

Abstract In this chapter, examples are given of the application of highly reactive prochiral ketones as substrates for enzymatic reductions. 3,5-Dioxocarboxylates are polyketide-like compounds that can be used to synthesize all of the possible stereoisomers of the corresponding 1,3-diols by means of regio- and enantioselective enzymatic reduction. The results obtained from an investigation into the usefulness of the resulting hydroxyl ketones and 1,3-diols in organic synthesis led to the development of non-natural functionalized ynones as

a starting material for the enzymatic route to enantiopure propargylic alcohols. A broad variety of substituted acetylenic ketones can be reduced enantioselectively by the oxidoreductases *Lactobacillus brevis* ADH (LBADH), *Candida parapsilosis* carbonyl reductase (CPCR), horse liver ADH (HLADH) and *Thermoanaerobium brockii* ADH (TBADH). The resulting propargylic alcohols can be obtained in either enantiomeric form, since (*R*)- and (*S*)-specific oxidoreductases can be applied. By varying the size of the substituents, the enantiomeric excess can be tuned, or the enantioselectivity can even be reversed. The obtained highly functionalized enantiopure alcohols are synthetically flexible chiral building blocks that offer new synthetic strategies for target- and diversity-oriented synthesis.

Keywords Alcohol dehydrogenase · Chiral building blocks · Diols · Diversity-oriented synthesis · Stereoselective catalysis

Abbreviations

ADH	alcohol dehydrogenase
aq	aqueous
Ar	aromatic, aryl
CSA	camphorsulfonic acid
cat	catalytic
CPCR	*Candida parapsilosis* carbonyl reductase
DBU	1,8-diazabicyclo[5,4,0]undecen-7-ene
DMP	2,2-dimethoxypropane
dr	diastereomeric ratio
ee	enantiomeric excess
eq	molecular equivalents
FDH	formate dehydrogenase
g	gram
HLADH	horse liver alcohol dehydrogenase
HMG-CoA	3-hydroxy-3-methylglutaryl coenzyme A
HPLC	high performance liquid chromatography
L	liter
LBADH	*Lactobacillus brevis* alcohol dehydrogenase
LDA	lithium diisopropylamide
LKADH	*Lactobacillus kefir* alcohol dehydrogenase
NAD(H)	nicotinamide adenine dinucleotide (hydride)
NADP(H)	nicotinamide adenine dinucleotide phosphate (hydride)
NMR	nuclear magnetic resonance
rec	recombinant
SADH	*Thermoanaerobacter ethanolicus* alcohol dehydrogenase
TBADH	*Thermoanaerobium brockii* alcohol dehydrogenase
TEADH	*Thermoanaerobacter ethanolicus* alcohol dehydrogenase
TFA	trifluoroacetic acid
TsOH	*para*-toluenesulfonic acid
U	unit (μmol min^{-1})
UV	ultraviolet spectroscopy

1 Introduction

The metabolic diversity generated by nature through evolution is enormously broad: about 200,000 different secondary metabolites have been structurally described so far [1]. Members of this pool of metabolites are as simple as ethylene, an important phytohormone with a diverse bioactivity profile [2], and as complex as maitotoxin, the largest non-biopolymer (M=3422) and the most potent nonproteinaceous toxin known [3–5] (see Fig. 1).

However, the theoretically possible number (10^{62} to 10^{63}) of potentially bioactive low-molecular mass compounds ($M_R \leq 500$ g mol^{-1}) [6] is exceedingly large in comparison to the number of compounds actually realized by nature. What chemists and biochemists have found so far is that a simple combinatorial approach cannot be used to mimic the diversity observed in natural products. This holds true for low-molecular mass compounds [7] as well as for de-novo proteins [8]. Various strategies have recently been developed to overcome these limitations, including dynamic combinatorial chemistry [9], diversity-oriented synthesis [10], and natural-product-based combinatorial chemistry [11], to name just a few. According to our present understanding, the combination of combinatorial synthesis and screening by selection seems to be the most promising approach [12], but we are far from entirely understanding the mechanisms responsible for the evolution of enzymatic activity, regulation and metabolic diversity.

From an evolutionary point of view, nature has developed efficient methods for biosynthesizing a broad diversity of metabolites possessing pronounced, diverse, and specific biological activity, by employing biocatalysts that also display broad diversity in terms of activity and specificity. Nevertheless, this diversity is initially generated at the metabolic level from a few general building blocks like acetate, mevalonate (isopentyl and dimethylallyl pyrophosphates), chorismate and amino acids.

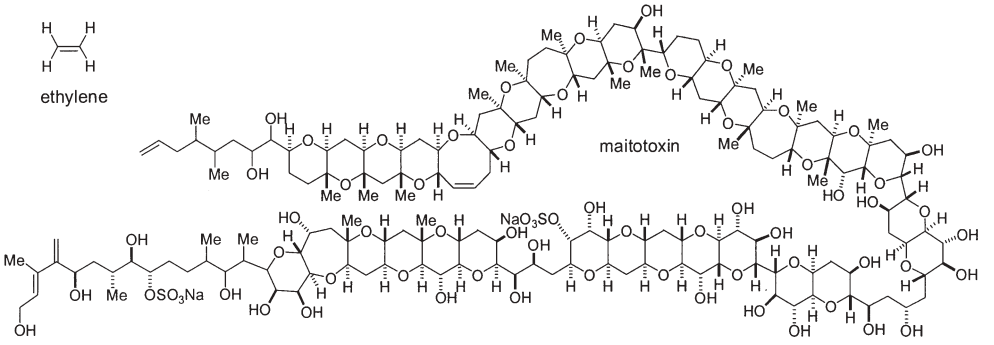

Fig. 1 Structures of the secondary metabolites ethylene and maitotoxin, illustrating the diversity that exists within this pool of compounds

Attention is drawn here to some concepts found during an investigation into chemoenzymatic synthesis that focused on aspects of bio-inspired diversity. The use of highly flexible and reactive prochiral substrates, that enabled access to various enantiopure secondary alcohols, was demonstrated.

3,5-Dioxocarboxylates are polyketide-like compounds which can be used to synthesize all of the possible stereoisomeric 1,3-diols derived from them via regio- and enantioselective enzymatic reduction. The propargylic alcohols introduced in the second part of the chapter lead to highly flexible C-4 building blocks that offer new synthetic strategies for target- and diversity-oriented synthesis.

2
Diversity-Oriented Access to 1,3-Diols through the Regio- and Enantioselective Reduction of 3,5-Dioxocarboxylates

2.1
Working Strategy

The biosynthesis of many hydroxylated natural products proceeds through regio- and enantioselective modification of polyketides, which are assembled through chain elongation via acetate or propionate units [13–15]. The enzymes responsible for the chain elongation and subsequent reduction, elimination, aromatization, and further modifications are classified as polyketide synthases [16, 17]. These multifunctional enzymes have been recently used for whole-cell biotransformations into "unnatural" metabolites, within the scope of combinatorial biosynthesis [18, 19].

We envisaged the biocatalytic regio- and stereoselective modification of polyketide-like compounds. This mimics the biosynthetic strategy of starting from a single substrate, which, after modification(s), affords a variety of different products. The regio- and enantioselective reduction of β,δ-diketo esters **A** signifies such a straightforward and flexible approach. All four stereoisomers of a dihydroxy ester **C** can be derived via hydroxy keto esters **B** from the same precursor **A** by this strategy (see Scheme 1) [20].

Only a few publications dealing with this subject can be found in the literature. Hydrogenation of diketo esters **A** with chirally modified ruthenium catalysts resulted in mixtures of *syn*- and *anti*-dihydroxy esters **C** with varying enantiomeric excess [21–24]. A notable exception to this is represented by the recent work of Carpentier et al, who succeeded in controlling the reduction of methyl 3,5-dioxohexanoate at the initial step, namely the reduction of the β-keto group. The enantiomeric excess achieved was, nevertheless, limited to 78% at best [21].

Highly enantioselective reduction of ethyl 6-benzyloxy-3,5-dioxohexanoate (**1**) by ADH of *Acinetobacter calcoaceticus* has been reported (97–99% ee) [25, 26]. Regioselectivity was not encountered, however, as was the case in the

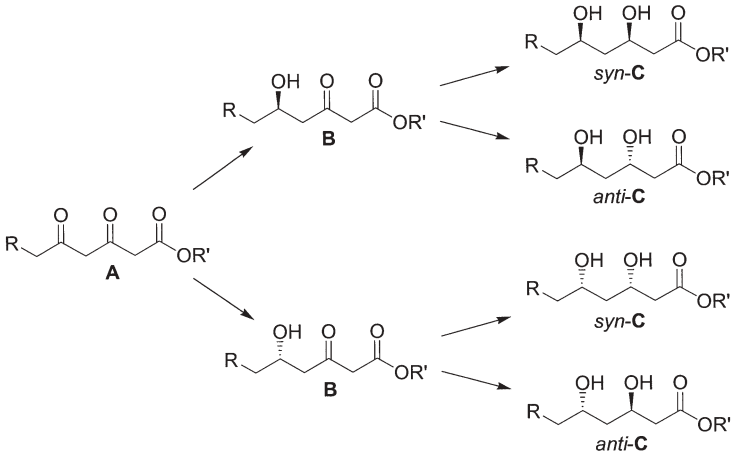

Scheme 1 Anticipated regio- and enantioselective reduction of β,δ-diketo esters **A**

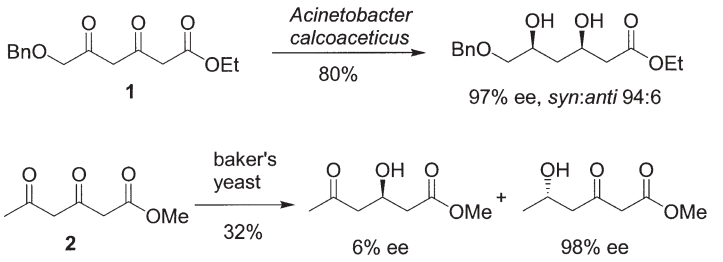

Scheme 2 Microbial reduction of diketo esters **1** and **2** [25–27]

reduction of a variety of β,δ-diketo hexanoates **A** (for example, compound **2**) with baker's yeast (see Scheme 2) [27].

The application of isolated enzymes in an anticipated regio- and enantioselective reduction of β,δ-diketo esters **A** seemed most promising to us, since alcohol dehydrogenases are generally known to operate in a highly selective manner [28].

2.2 Regio- and Enantioselective Reduction

In a photometric assay, an NADP(H)-dependent ADH of *Lactobacillus brevis* (LBADH) was identified as a suitable catalyst for accepting a broad range of diketo esters **A** as substrate [29]. This stable enzyme is readily available in the form of a crude cell extract (recLBADH) from a recombinant *Escherichia coli* strain [30–32].

To identify the keto group(s) reduced by recLBADH, reaction with diketo esters **3a–c** was performed on a preparative scale, using substrate-coupled re-

Table 1 Products of the recLBADH catalyzed reduction of the diketo esters **3a–c** [29] (see also Scheme 3)

Compound	R	Yield [%]	ee [%]	$[\alpha]_D^{25}$	lit. $[\alpha]_D$ (% ee)
(*S*)-**4a**	Cl	72	>99.5	−24.9	−23.0 (>97) [33, 34]
(*R*)-**4b**	H	77	99.4	−40.1	−39.6 (99) [35]
(*R*)-**4c**	Me	61	98.1	−36.0	−35.6 (99) [36]

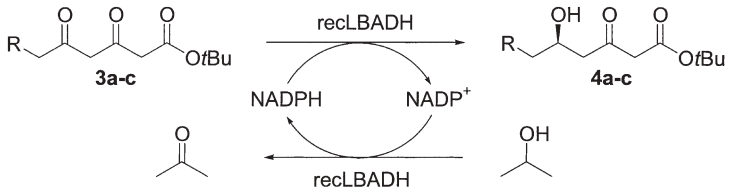

Scheme 3 The recLBADH catalyzed reduction of diketo esters **3a–c** (see also Table 1) [38]

generation of NADPH. Comparison of analytical data on the products (*R*)-**4b** and (*R*)-**4c** with literature data (NMR, [α]) clearly established the formation of (*R*)-configurated δ-hydroxy-β-keto isomers of high optical purity (see Table 1 and Scheme 3).

The enzyme recLBADH is the first catalyst that allows the highly regio- *and* enantioselective synthesis of δ-hydroxy-β-keto esters by reduction of the respective β,δ-diketo esters. This enzymatic reaction is of enormous preparative value. The substrates are readily available by acylation of β-keto ester bisenolates, and the reaction only requires a simple batch technique, which is easy to scale up. Reduction of the chlorinated compound **3a** has been routinely performed on a 75 g scale in our laboratory (8 L fed batch, final substrate concentration 34 mM), producing the hydroxy keto ester (*S*)-**4a** in an isolated yield of 84% [37].

In order to synthesize the (*R*)-enantiomer of hydroxy keto ester **4a** we reinvestigated the baker's yeast reduction of β,δ-diketo esters described by Tsuboi et al [27]. The chlorinated diketo ester **3a,** which had not been investigated by Tsuboi et al, was reduced with high regioselectivity at C-5 by baker's yeast, in contrast to its unchlorinated analogues **3b** and **3c** which gave mixtures of regioisomers in this reaction [38]. The enantiomeric excess of the product (*R*)-**4a** was greatly enhanced by application of a biphasic system (hexane/water and Amberlite XAD-7/water; for some recent applications of XAD-7 in bioconversions, see [39–41]). Additionally, it was found that the use of dried baker's yeast and a high yeast/substrate ratio (10 g yeast per mmol **3a**) gave the best results with regard to enantioselectivity. A combination of these optimized parameters enhanced the enantiomeric excess of the product (*R*)-**4a** from 48% to 90–94% (Scheme 4). Application of the resin considerably aided the isolation

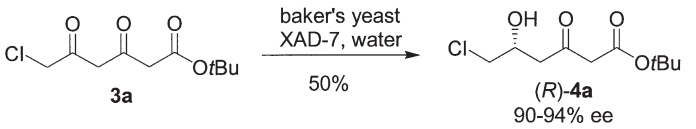

Scheme 4 Reduction of diketo ester **3a** by baker's yeast [38]

of the product, and so the reaction was carried out at gram scale without difficulty (1 mmol substrate/g resin XAD-7) [38].

When the enzymatic reduction of the heptanoate **3c** was performed in suspension on a preparative scale comparable to the recLBADH-catalyzed reduction of diketo ester **3a**, conversion difficulties became apparent, most likely due to the low solubility of heptanoate **3c** in the buffer. As in the case of the whole-cell biotransformation with baker's yeast, application of XAD-7 greatly facilitated substrate distribution, work-up and product recovery. After enzymatic reduction (recLBADH) of heptanoate **3c** in such a biphasic system, the product (*R*)-**4c** was obtained in an isolated yield of 66%. Furthermore, after ultrafiltration of the buffer solution, about two-thirds of the enzyme activity utilized was recovered, which again was applied in a repetitive manner [42]. It has therefore been shown that the enzyme-catalyzed regio- and enantioslective reduction of β,δ-diketoesters can be applied to lipophilic members of this class of compounds on a preparative scale, too.

2.3 Dynamic Kinetic Resolution

The enzyme-catalyzed regio- and enantioselective reduction of α- and/or γ-alkyl-substituted β,δ-diketoesters would enable the simultaneous (or successive, respectively) introduction of up to four fixed stereogenic centers into the molecule by two consecutive reduction steps through dynamic kinetic resolution [43], with a theoretical maximum yield of 100%. Although the dynamic kinetic resolution of α-substituted β-keto esters by chemical [44] or biocatalytic [45] reduction under neutral conditions has proven to be broadly applicable to stereoselective synthesis, the corresponding dynamic kinetic resolution of 2-substituted 1,3-diketones is rarely found in the literature [46–48].

By enzymatic reduction of branched diketo ester **5** with recLBADH in an aqueous buffer system, hydroxy keto ester **6** was isolated with a 66% yield (Scheme 5). NMR data for the major product *syn*-(4*S*,5*R*)-**6** clearly proved the regioselective single-site reduction of the keto group at C-5 [49].

This indeed verifies the dynamic kinetic resolution of the diketo ester *rac*-**5** through enzymatic reduction, indicating that the (*S*)-enantiomer of this substrate is accepted preferentially by recLBADH, and that under the conditions applied, racemization is faster than the enzymatic reduction of the (*R*)-enantiomer of diketo ester **5**.

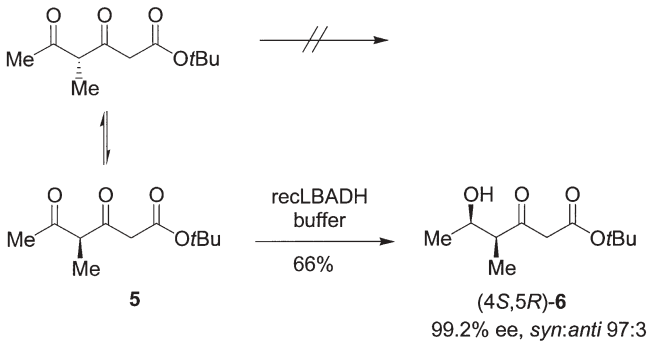

Scheme 5 Reduction of diketo esters **5** by recLBADH via dynamic kinetic resolution [49]

This methodology enables a novel approach to the chemistry of polypropionates based on a biomimetic approach via polyketides. Apparently, this method could be extended to the dynamic kinetic resolution of other 2-alkyl-substituted unsymmetrical 1,3-diketones through enzymatic and chemical reduction methods, applying non-basic conditions. Indeed, very recently Cossy et al applied non-enzymatic catalysis to the dynamic kinetic resolution of such 1,3-diketones through enantioselective monoreduction mediated by chiral ruthenium catalysts [50].

For some examples of the reduction of 2-alkyl-substituted ketones under basic conditions via dynamic kinetic resolution, see [51, 52].

2.4 Stereoselective Access to 1,3-Diols

Substituted 1,3-diols are valuable intermediates in the synthesis of drugs and natural products [53–55]. These useful building blocks are often obtained as mixtures of *syn*- and *anti*-diastereomers in varying diastereomeric ratios. Starting from the regio- and enantioselective reduction of β,δ-diketo esters, different methods of obtaining enantiomerically pure 3,5-dihydroxy esters were employed.

2.4.1 Diastereoselective Reduction by Chemical Methods

Prasad's *syn*-selective borohydride reduction was applied for the preparation of both enantiomers of dihydroxy ester *syn*-**7** [33, 56]. This method gave dihydroxy esters *syn*-**7** in a diastereomeric ratio *syn*-**7**/*anti*-**7** ($dr_{s:a}$) of 28:1 to 45:1. The enantiomers of dihydroxy ester *anti*-**7** were synthesized according to Evans' method [57], which resulted in a $dr_{a:s}$ (*anti*-**7**/*syn*-**7**) of 14:1 to 18:1 (Scheme 6) [38].

Advantageously, the diastereomeric ratios could be raised to ≥200:1 for all of the dihydroxy esters **7** using a single crystallization step. In the case of

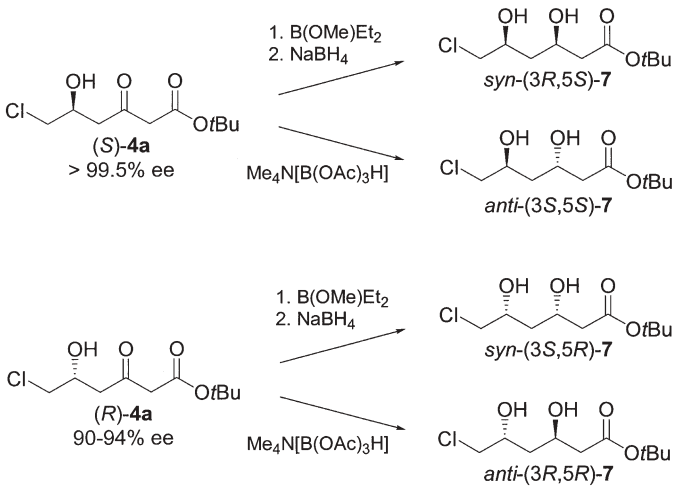

Scheme 6 Diastereoselective reduction of hydroxy keto esters (*S*)-**4a** and (*R*)-**4a** [38]

the two dihydroxy esters derived from the baker's yeast reduction product (*R*)-**4a**, most of the minor enantiomer was removed by this procedure as well [38].

2.4.2 Diastereomer-Differentiating Hydrolysis of 1,3-Diol-Acetonides

The separation of 1,3-diol diastereomers can be a difficult task, even at the stage of cyclic derivatives like the corresponding acetals [58–60]. This applies especially to non-crystallizing 1,3-diols and when the separation has to be conducted on a large scale.

On deprotecting a *syn*/*anti*-mixture of acetonide **8** with a catalytic amount of diluted aqueous hydrochloric acid in dichloromethane solution, we observed that the *anti*-diastereomer hydrolyzes much faster than the *syn*-diastereomer. Premature quenching of the acid catalyst with aqueous sodium bicarbonate solution resulted in a mixture of the diols *syn*-(3*R*,5*S*)-**7** and *anti*-(3*S*,5*S*)-**7** and highly enriched *syn*-acetonide *syn*-(3*R*,5*S*)-**8** (Scheme 7) [61].

Because of the great differences in polarity, the diastereomeric diols **7** can easily be removed from the corresponding acetonides **8** by flash chromatography. Therefore, the diastereomer-differentiating acetonide hydrolysis turns the difficult *syn*/*anti*-diastereomer separation into a separation of non-stereoisomeric compounds, which show great differences in their physical properties and so can be readily separated.

The differences in the hydrolysis rates of diastereomeric 1,3-diol-acetonides were known in principle [62]. However, any intended utilization of these differences for the separation of *syn*- and *anti*-1,3-diols or *syn*- and *anti*-1,3-diol-acetonides has not yet been described in the literature.

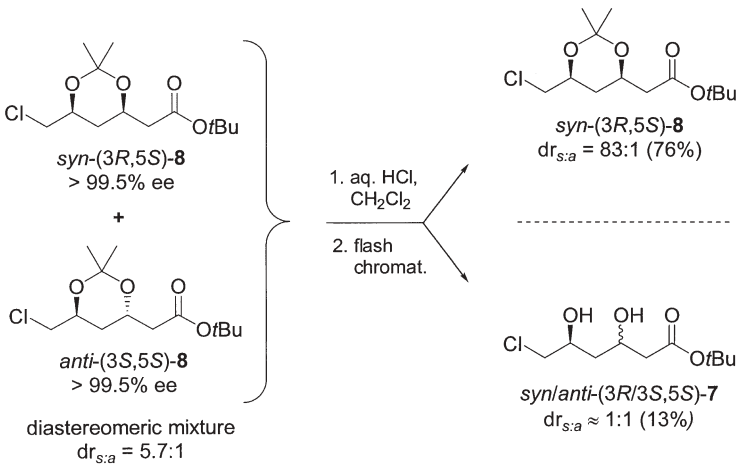

Scheme 7 Diastereomer-differentiating hydrolysis of the *syn*- and *anti*-acetonide **8** (isolated yields shown) [61]

The highly selective diastereomer-differentiating hydrolysis of 1,3-diol-acetonides described here has a general scope and can be easily applied on a large scale. Moreover, it can also be applied to generate highly enriched *anti*-1,3-diols from a diastereomeric mixture of 1,3-diol-acetonides [61].

2.5 Nucleophilic Substitution of Chlorine

In the previous sections it was shown that all four stereoisomers of the chlorinated dihydroxy ester **7** can be synthesized in an enantiopure form on a preparative scale by a flexible stereoselective two-step reduction sequence. In order to extend the applicability of these compounds a nucleophilic substitution of chlorine was envisaged.

A two-step conversion of acetonide *syn*-(3*R*,5*S*)-**8** to hydroxy compound *syn*-(3*R*,5*S*)-**9** is known from the patent literature [33].This compound is an advanced intermediate in the synthesis of HMG-CoA reductase inhibitors [63]. Iodide *syn*-(3*R*,5*S*)-**10** has been utilized for this purpose, too [64]. We were able to displace the chlorine of acetonide *syn*-(3*R*,5*S*)-**8** by iodine in a single step under advanced halogen exchange conditions (52% yield; Scheme 8) [65, 66]. However, conversion was incomplete (86%), and the remaining starting material could not be removed from the product *syn*-(3*R*,5*S*)-**10** [38]. Furthermore, complete decomposition was encountered in several experiments.

Alternatively, epoxide (3*R*,5*S*)-**11** was regioselectively opened with lithium iodide on silica [67]. The crude product was immediately subjected to acetonide protection, which afforded the desired iodide *syn*-(3*R*,5*S*)-**10** with a 58% yield (44% from *syn*-(3*R*,5*S*)-**7**; Scheme 9). Epoxide (3*R*,5*S*)-**11** was easily

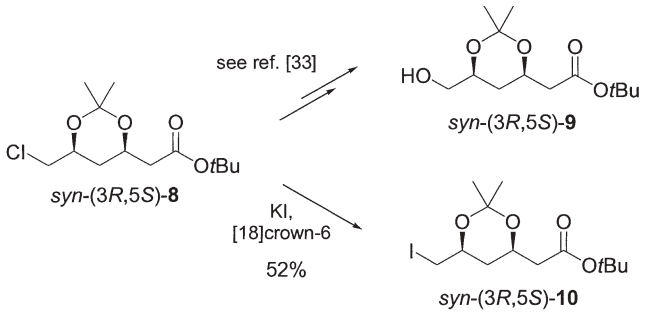

Scheme 8 Nucleophilic substitution of the chlorine of acetonide *syn*-(3*R*,5*S*)-**8** [38]

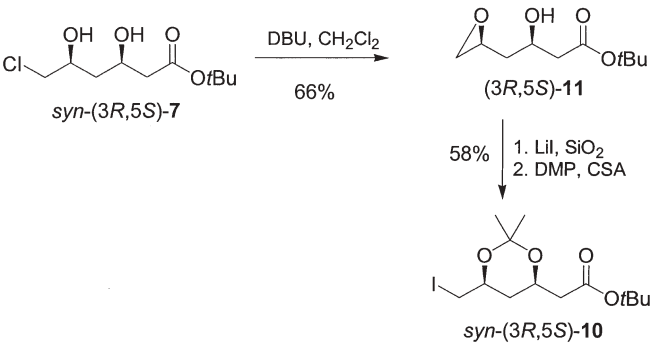

Scheme 9 Synthesis and regioselective opening of epoxide (3*R*,5*S*)-**11** [38]

obtained from dihydroxy ester *syn*-(3*R*,5*S*)-**7** by treatment with DBU (66% yield) [38].

Epoxy esters like (3*R*,5*S*)-**11** are also favorable intermediates in the synthesis of HMG-CoA reductase inhibitors, since the epoxide can be regioselectively opened by carbon nucleophiles, like cuprates [68, 69].

Therefore, starting from diketo ester **3a**, highly functionalized building blocks were obtained in only three reaction steps. Since the functional group manipulations described in this section should be applicable to the *anti*-dihydroxy ester **7** as well, this highly flexible strategy enables new applications in natural product synthesis.

2.6 Application in Natural Product Syntheses

The (*R*)-enantiomer of lactone **12** was required for the enantioselective synthesis of naturally occurring (*R*)-*semi*-vioxanthin. To this end, hydroxy keto ester (*R*)-**4b** was lactonized to (*R*)-5,6-dihydro-4-hydroxy-6-methyl-2*H*-pyran-2-one by treatment with trifluoroacetic acid [42, 70], followed by *O*-methylation with dimethyl sulfate, affording lactone (*R*)-**12** (Scheme 10) [71].

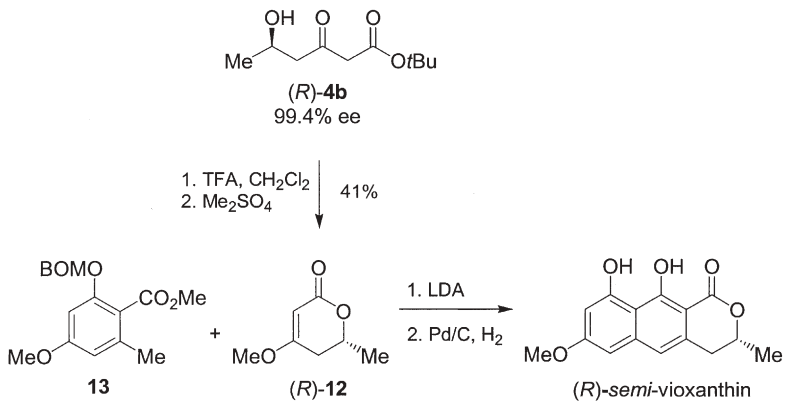

Scheme 10 Synthesis of (*R*)-*semi*-vioxanthin [71]

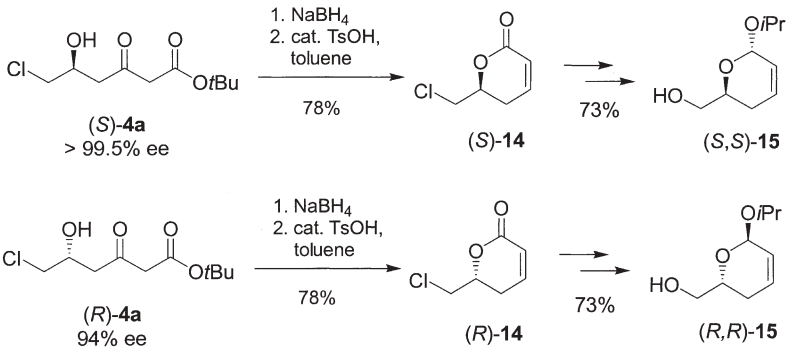

Scheme 11 Synthesis of δ-lactone equivalent **15** [78]

The aromatic ring system of (*R*)-*semi*-vioxanthin was built up through a tandem Michael-Dieckmann reaction of orsellinate **13** and pyranone (*R*)-**12** with a 27% yield. Selective cleavage of the benzyloxymethyl group was achieved by hydrogenolysis to give (*R*)-*semi*-vioxanthin in a 44% yield (Scheme 10) [71].

The α,β-unsaturated δ-lactone moiety occurs in many highly bioactive substances [72, 73], including callystatin A (cytotoxic) [74, 75] and ratjadone (cytotoxic) [76, 77], and is frequently introduced by a Wittig-type reaction. To provide a useful building block for natural product syntheses, an asymmetric synthesis via lactone **14** of both enantiomers of the δ-lactone equivalent lactol **15** was developed in collaboration with the Enders group, University of Aachen, based on the regio- and enantioselective biocatalytic reduction of diketo ester **3a** (Scheme 11) [78].

Protected lactol **15** has been used as an advanced intermediate in the asymmetric synthesis of (*S*)-argentilactone, (*S*)-goniothalamin [78] and (–)-callystatin [79] (Scheme 12).

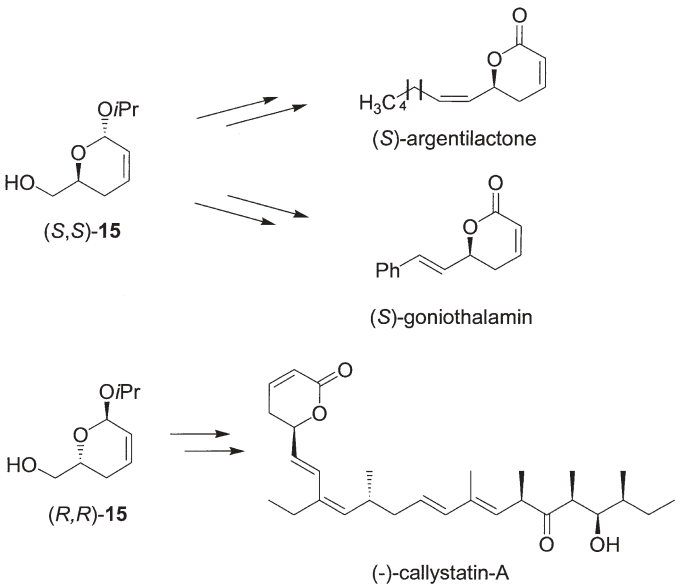

Scheme 12 Synthesis of (*S*)-argentilactone, (*S*)-goniothalamin and (–)-callystatin [78, 79]

2.7 Conclusions and Outlook

The regio- and enantioselective reduction of β,δ-diketo esters **A** (see Scheme 1) with ADH of *L. brevis* is a reaction of broad applicability. A wide variety of diketo esters are accepted by this readily available enzyme, and the required reaction technique is remarkably simple. Due to the mild reaction conditions, the reaction can be carried out without special care, even for highly sensitive compounds like the diketo ester **3a**. No serious limitations in terms of further scale-up are apparent. The hydroxy keto esters like (*S*)-**4a** made available by this reaction are compounds of high functionalization (Scheme 13), and many chemical modifications and applications of them are known from the literature. New applications in natural product syntheses have been developed using, for instance, the lactone equivalent (*S*,*S*)-**15**.

Since baker's yeast reduction of the diketo ester **3a** enables the formation of enantiomeric products, a diversity-oriented approach towards all possible stereoisomers of the compounds depicted in Scheme 13 is conceivable.

Thus, it was shown that the regio- and enantioselective enzymatic reduction of polyketide-like compounds represents a valuable alternative to the more classical approach starting from chiral β-hydroxy butyrates followed by chain elongation. It will be interesting to see whether non-enzymatic catalysts can be developed which enable the biomimetic regio- and enantioselective reduction of β,δ-diketo esters.

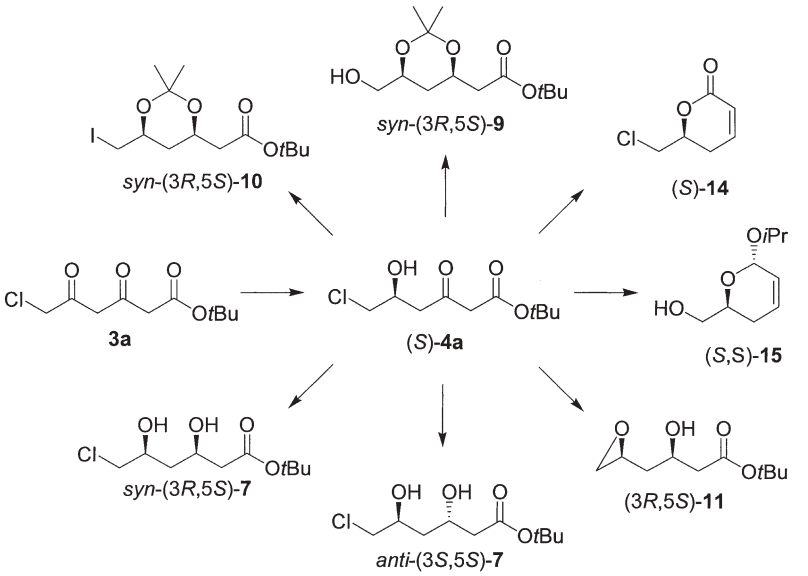

Scheme 13 Chiral building blocks produced from the hydroxy ketoester (*S*)-**4a**

3
Chemo- and Enantioselective Reduction of Propargylic Ketones: Towards a General Chiral Building Block

3.1
Working Strategy

Chiral, non-racemic propargylic alcohols are important synthetic intermediates in the synthesis of natural products and biologically active compounds. Since the C≡C triple bond allows flexible and wide-ranging functional group modifications, enantiopure propargylic alcohols are quite general chiral building blocks. An impressive example of the flexibility of the propargylic alcohols **D** was given by Schreiber et al in a diversity-oriented organic synthesis (Scheme 14) [80].

Asymmetric reduction of α,β-acetylenic ketones is a straightforward approach to this class of compounds. A number of chemical reducing reagents has been developed which provide chiral propargylic alcohols in good yields [81–84] (for a review of the enantioselective reduction of ketones, see [85]). Nevertheless, all of these reagents afford only a small range of propargylic alcohols in high enantiomeric excess, and most of them are limited to either hindered or unhindered alkynones. Furthermore, if hydrolytic enzymes like lipases are used, only a few of these alcohols are obtained with an enantiomeric excess higher than 99% [86–93], and only a small number of α,β-acetylenic ketones are reduced by isolated oxidoreductases at all [94–99] (LKADH: ADH

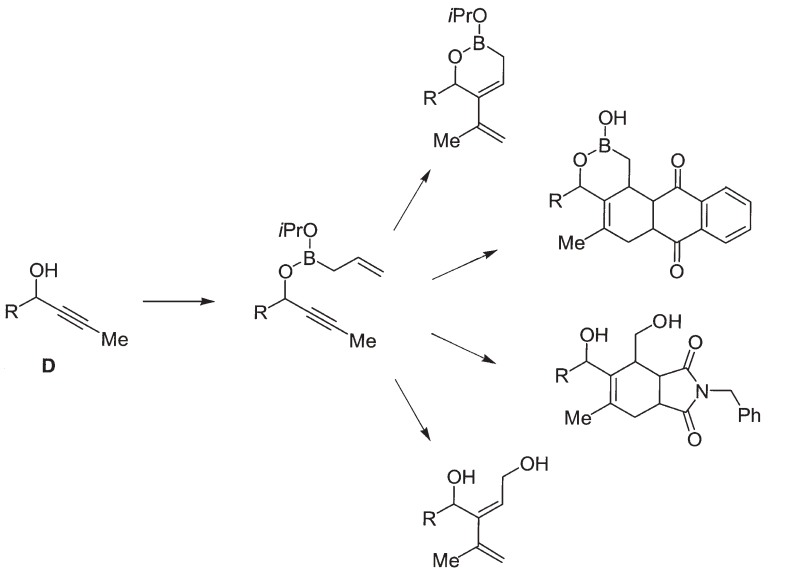

Scheme 14 Application of propargylic alcohols in diversity-oriented organic synthesis [80]

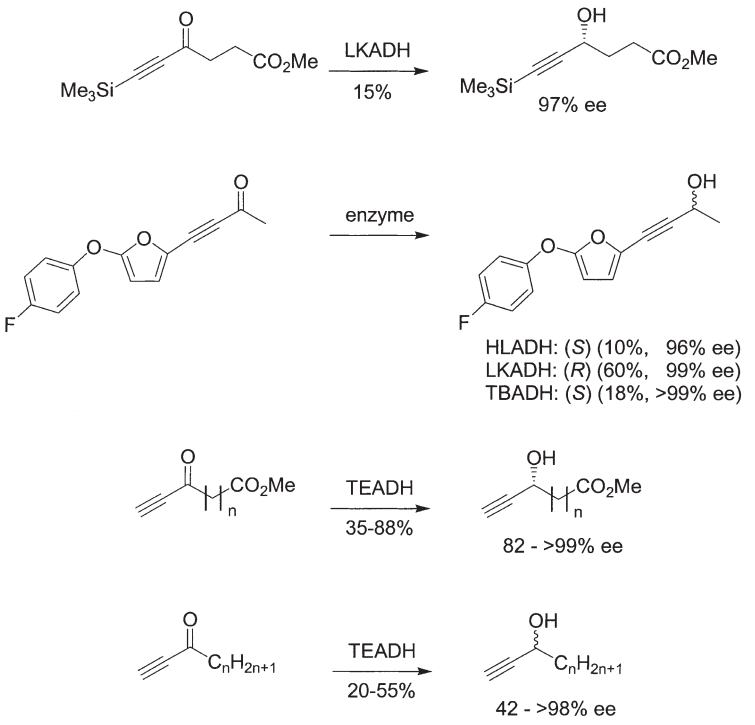

Scheme 15 Enzymatic reduction of ynones [94–99]

from *Lactobacillus kefir* [94]; HLADH: horse liver ADH [97]; TBADH: ADH from *Thermoanaerobium brockii* [98]; TEADH: ADH from *Thermoanaerobacter ethanolicus* [96, 99]) (Scheme 15).

As alcohol dehydrogenases can react stereo- and chemoselectively under very mild conditions, they should provide good access to enantiopure propargylic alcohols. This strategy provides the ability to start from a single substrate, which after enzymatic reduction produces either enantiomer of propargylic alcohol, and after further modifications a variety of different enantiopure products in only two to three steps.

3.2 Enantioselective Reduction of Aryl Alkynones

In a photometric assay, NADP(H)-dependent ADH of *Lactobacillus brevis* (LBADH) [30–32] and NAD(H)-dependent *Candida parapsilosis* carbonyl reductase (CPCR) [100] were identified as suitable catalysts for accepting a broad range of ynones as substrates. Both enzymes catalyze the reduction of various aryl alkynones **16** with high enantioselectivity and efficiency (Scheme 16) [101].

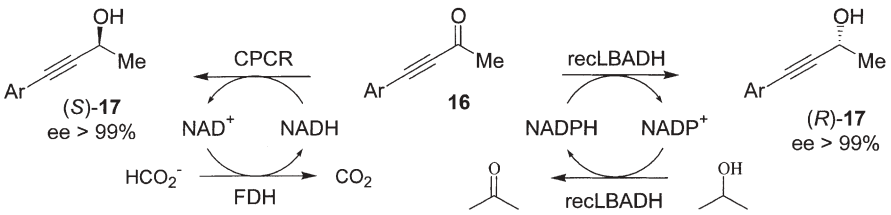

Scheme 16 Enzymatic reductions of aryl alkynones **16** with cofactor regeneration [101]

Since these two biocatalysts possess complementary stereoselectivity, they enable the syntheses of both enantiomers of the desired products. To demonstrate the applicability of enzymatic reduction of aryl alkynones on a preparative scale, we optimized the reaction parameters of the recLBADH-catalyzed reduction of 4-phenyl-3-butyn-2-one (**16**, Ar=phenyl). On a 2 gram scale (50 mM substrate concentration), in the presence of 0.05 mol-% $NADP^+$, recLBADH (250 U) catalyzed reduction afforded a 94% yield of enantiomerically pure (*R*)-4-phenyl-3-butyn-2-ol [(*R*)-**17**, Ar=phenyl]. Conversion was determined as >99% [101].

3.3 Synthesis of Enantiopure 3-Butyn-2-ol

(*R*)- and (*S*)-3-butyn-2-ol (**19**) are important intermediates, for example in syntheses of 5-lipoxygenase inhibitors [90]. The methyl and ethynyl residue of 3-butyn-2-one (**18**) shows a similar steric demand [102], making it difficult

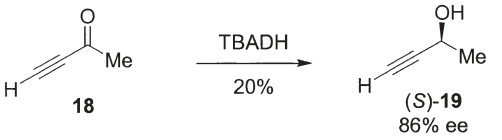

Scheme 17 Enzymatic reduction of 3-butyn-2-one (**18**) with TBADH [103]

for reducing reagents to distinguish between the two enantiofacial sides of the substrate. Therefore, all methods of reducing **18** failed to produce the enantiopure alcohol **19**. The best result with regard to the enantioselective reduction of **18** was obtained with *Thermoanaerobium brockii*-ADH (TBADH), to give (*S*)-**19** (86% ee) (Scheme 17) [103].

As expected, enzymatic reduction of **18** with recLBADH and CPCR resulted in unsatisfactory results (60% and 49% ee, respectively). The aforementioned results indicate that a bulky substituent at the alkyne moiety results in a higher selectivity of the reduction. Therefore, we required a functional group that could be easily attached to and removed from the alkyne unit. Silyl groups appeared to be suitable since they fulfill these requirements [104, 105] and their size can also be varied. Furthermore, Bradshaw et al reported that *Lactobacillus kefir*-ADH, an enzyme highly homologous to LBADH, affords (*R*)-4-trimethylsilyl-3-butyn-2-ol [(*R*)-**21a**] with an ee of 94% in 25% yield (Scheme 15) [95]. In our investigations, ketone **20a** was reduced by recLBADH with >99% conversion. The enantiomeric excess and absolute configuration of the product were determined by desilylation with borax converting alcohol (*R*)-**21a** into enantiopure (*R*)-3-butyn-2-ol [(*R*)-**19**] (Scheme 18).

The synthesis of enantiomerically pure (*S*)-3-butyn-2-ol [(*S*)-**19**] was achieved by introducing a silyl group with an aromatic substituent into the substrate (compound **20b**). In conclusion, we found easy access to both enantiomers of **19** in high enantiomeric excess simply by introducing an appro-

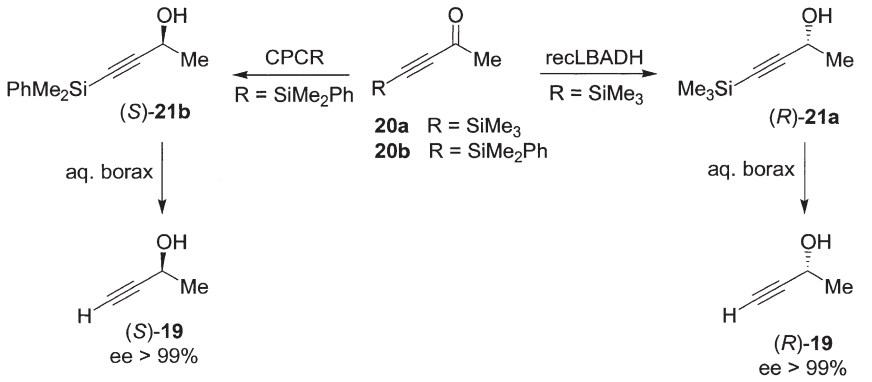

Scheme 18 Enzymatic reduction of silylalkynones, affording enantiopure 3-butyn-2-ol (**19**) [101]

priate silyl derivative and subsequently detaching the ee-enhancing group (Scheme 18) [101].

When recLBADH was tested with the *n*-alkyl ethynyl ketones **22a–c** (Table 2 and Scheme19), homologues of 3-butyn-2-one (**18**), it was observed that the preferred stereochemistry of the resulting propargylic alcohol depends on the size of the alkyl unit [101]. A similar observation was reported by Phillips et al. for SADH from *Thermoanaerobacter ethanolicus* [99]. In the case of recLBADH, a reversal of the enantioselectivity of the reduction was already known from using 1-pentyn-3-one (**22a**) as a substrate. Higher homologues like 1-hexyn-3-one (**22b**) and 1-octyn-3-one (**22c**) are even reduced with complete enantioselectivity. The enzymatic activity increases strongly for those substrates bearing longer alkyl chains.

Table 2 Screening results for the recLBADH-catalyzed reduction of *n*-alkyl-alkynones[101] (see also Scheme 19)

Alcohol;	R=	recLBADH	
		% activity (% conv.)	% ee (config.)
19	H	66 (100)	60 (*R*)
23a	CH_3	41 (90)	34 (*S*)
23b	C_2H_5	28 (100)	>99 (*S*)
23c	C_4H_9	85 (100)	>99 (*S*)

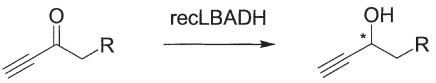

18, 22a-c **19, 23a-c**

Scheme 19 The recLBADH-catalyzed reduction of *n*-alkyl-alkynones (see also Table 2) [101]

Ethynyl ketones decompose in amine buffer, resulting in only moderate yields of 20–55% after enzymatic reduction [99]. We found that ketones with a terminal triple bond, as well as the corresponding alcohols, are stable in phosphate buffer, so propargylic alcohol (*S*)-**23b** (ee>99%) was easily obtained on a gram scale (69% yield) [101].

Thus, it was shown that substrate engineering can be successfully used to adjust the absolute configuration and the enantiomeric excess of the resulting propargylic alcohols by enzymatic reduction. Whereas the introduction of silyl-groups at C-4 of 3-butyn-2-one (**18**) resulted in enantiopure 3-butyn-2-ol (**19**) after reduction and deprotection, chain-elongation at C-1 afforded enantiopure higher homologues of opposite configuration.

3.4 Enzymatic Reduction of α-Halogenated Propargylic Ketones

Our interest in a general approach for obtaining enantiomerically pure building blocks as intermediates for organic synthesis encouraged us to continue our studies towards the reduction of α-halogenated propargylic ketones. Wong et al published two examples of observed enzymatic activity with α-halogenated propargylic ketones **24c** and **24e** (UV assay) [94, 95]. However, since it is known that α-halogenated ketones can undergo dehalogenation through a radical mechanism in the presence of NAD(P)H [106, 107], proof of product formation still has to confirm the presumed enzyme-catalyzed reduction to propargylic alcohols. Moreover, there has been only one report of a chiral, non-racemic α,β-alkynyl α-chloro- or α-bromohydrin. Corey and coworkers obtained (*R*)-4-triisopropylsilyl-1-chloro-3-butyn-2-ol (**27**) by oxazaborolidine reduction of the corresponding ketone **26**. However, the authors indicated that the bulky triisopropylsilyl group was essential for an ee of 95% (Scheme 20) [82].

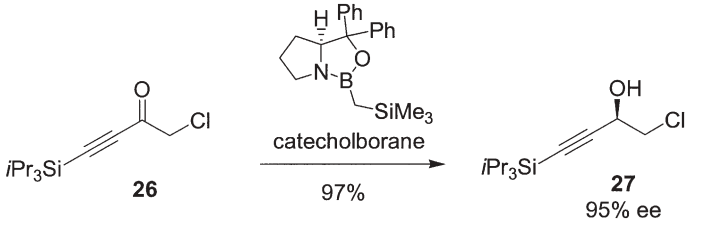

Scheme 20 Oxazaborolidine-catalyzed reduction of the ketone **26** [82]

In our own work, three ADHs were identified accepting propargylic substrates with substituents of the size of chloro- and bromo-methyl groups in a UV assay. The α-halogenated propargylic ketones **24**, which were easily synthesized in one step [108, 109], were reduced by HLADH, TBADH and recLBADH (see Table 3 and Scheme 21) [110].

Table 3 Relative enzymatic activities of HLADH, TBADH and recLBADH [110, 111] (see also Scheme 21)

Alcohol		% Activity (config.)		
		HLADH	TBADH	recLBADH
25a	X=Cl, R=Phe	32 (*R*)	53 (*R*)	70 (*S*)
25b	X=Cl, R=TBS	24 (*R*)	51 (*R*)	37 (*S*)
25c	X=Cl, R=TMS	15 (*R*)	74 (*R*)	28 (*S*)
25d	X=Br, R=TMS	35 (*R*)	4 (*R*)	18 (*S*)
25e	X=Cl, R=H	not determined	not determined	28 (*R*)
25f	X=Br, R=H	not determined	not determined	18 (*R*)
17	X=H, R=Phe	6 (*S*)	47 (*S*)	142 (*R*)

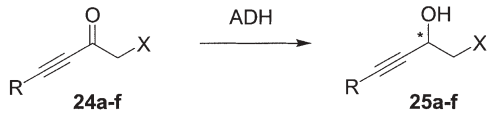

24a-f **25a-f**

Scheme 21 Structures and syntheses of alcohols from Table 3

All of these oxidoreductases reduce aromatic and aliphatic α-chloro-propargylic ketones (**24a–c**) with high activity. The α-bromo-propargylic ketone **24d** is also accepted as a substrate; however, the enzymatic activity of TBADH and recLBADH decreases, probably due to steric reasons. Because of the low solubility of substrate **24a**, about 25% of a short-chained alcohol was added as a cosolvent. The large excess of the short-chained alcohol shifted the substrate/product equilibrium towards the desired propargylic alcohol **25a**, resulting in almost quantitative conversions with high total turnover numbers of the cofactor.

Therefore, millimole quantities of substrate **24a** were converted using cofactor quantities as low as 0.005 mol% and small amounts of enzyme (100 units recLBADH/g substrate; 200 units HLADH/g substrate, respectively). The analytically pure products (*S*)- and (*R*)-**25a** were easily obtained by extraction in an isolated yield of >95%. HPLC analysis revealed >99% conversion and in each case only one single enantiomer could be detected (ee>99%).

Reduction of 1-(chloro or bromo)-3-butyn-2-one (**24e,f**) with recLBADH affords the enantiopure (*R*)-alcohols **25e,f**, resulting in an interesting switch in the enantioselectivity of the enzymatic reduction. As the enantiomers (*S*)-**25e,f** can be obtained by the recLBADH catalyzed reduction of **24b–d** and subsequent removal of the silyl-protecting group, this enzyme offers access to a pair of enantiomers. Due to the high volatility of the substrates (**24e,f**) these transformations were only performed on an analytical scale [111]. Nevertheless, application of an advanced technique should enable this transformation to be performed on a preparative scale, too. In this case, the transformation might be performed advantageously in a gas phase biotransformation [112, 113].

Two divergent conclusions can be drawn from the results obtained in the substrate screening using α-chlorinated versus nonchlorinated ketones with different enzymes. For the CPCR-catalyzed reductions, a loss of activity is observed for α-halogenated substrates, whereas HLADH gains in activity relative to the non-halogenated substrates (see Table 3 and Scheme 21). For the former case, steric reasons can be assumed for the negative results, whereas the effect observed in the latter case indicates a strong electronic influence that results in an activation of the substrate [114–116]. A more detailed investigation of this effect using different kinds of activated and non-activated substrates with different alcohol dehydrogenases will result in new insights, giving access to more prolific substrate engineering.

3.5 Modification of α-Halogenated Propargylic Alcohols

In the preceding section, it was shown that enantiomerically pure α-halogenated propargylic alcohols can easily be obtained in both enantiomeric forms by enzymatic reduction. Although the high functionality of these compounds makes them ideal precursors for further modification, the application of these chiral building blocks in target-oriented synthesis has not yet been described.

Propargylic alcohols **25** can easily be converted in good yields to their corresponding epoxides **28** without racemization. Ring closure was achieved by treatment with DBU in EtOH:H_2O (Scheme 22). After work-up by extraction, no further purification was necessary since no by-products were detected. This general approach to enantiomerically pure terminal propargylic epoxides [117–119] offers multifaceted applications in organic chemistry, as has been shown, for instance, by Hiyama and coworkers in the synthesis of the HMG-CoA-reductase inhibitor NK-104 (Pitavastatin) [120].

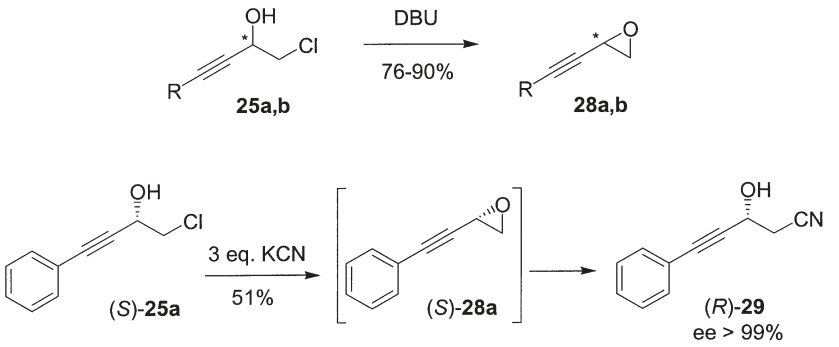

Scheme 22 Conversion of chlorohydrins **25** into epoxides **28** and nitrile (*R*)-**29** [111]

Regioselective openings of the epoxides **28** were realized with different nucleophiles (CN^-, N_3^-, OH^-) [111, 120]. Instead of a two-step process, direct conversion of chlorohydrin (*S*)-**25a** into cyanohydrin **29** was accomplished with a yield of 51% (Scheme 22) [121].

The propargylic terminal epoxides that are easily prepared from the corresponding halohydrins represent highly flexible and reactive building blocks. The potential of these compounds is emphasized by the most recent publication from Jacobsen's group. They applied the hydrolytic kinetic resolution of terminal epoxides by chiral (salen)Co(III) complexes to alkynyl epoxide **28b**, which afforded either the corresponding highly enantioenriched diol or the unreacted starting material (ee>99%) with a 41% yield [122].

As mentioned above, the C≡C triple bond in propargylic alcohols allows all-round access to different functional groups at C-3 and/or C-4. As an example,

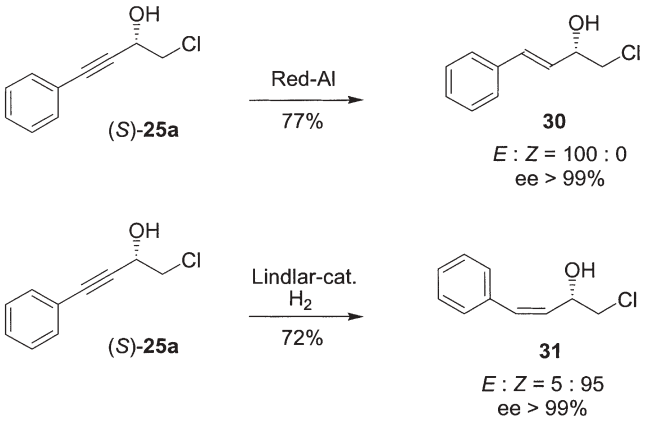

Scheme 23 Stereoselective synthesis of enantiopure (*E*)- and (*Z*)-olefins **30** and **31** [111]

the chlorohydrin (*S*)-**25a** was highly stereoselectively transformed into the corresponding enantiopure (*E*)- and (*Z*)-olefins **30** and **31** in high yields (Scheme 23) [110, 111].

3.6 Conclusions and Outlook

In conclusion, it has been shown that a broad variety of differently substituted acetylenic ketones can be reduced enantioselectively by the oxidoreductases recLBADH, CPCR, HLADH and TBADH. Most propargylic alcohols were obtained with ee values higher than 99%, making this method superior to non-enzymatic reduction techniques. In the majority of cases, the alcohols can be obtained in either enantiomeric form, since either (*R*)- or (*S*)-specific oxidoreductases can be applied. The substrate spectrum includes aromatic ynones as well as aliphatic derivatives. By varying the size of the substituents, the enantiomeric excess can be tuned, and even a reversal in enantioselectivity be achieved. Last but not least, the enzymatic reductions were scaled up using low amounts of enzyme and cofactor, making this method highly attractive in ecological and economic terms.

The use of α-halogenated substrates like **24** enables the synthesis of a new class of synthetically flexible enantiopure C-4-building blocks in only two steps. By applying these building blocks in further syntheses it was demonstrated that the biomimetic strategy of using a single substrate to obtain a broad variety of totally different compounds could be adopted successfully for propargylic alcohols (Scheme 24).

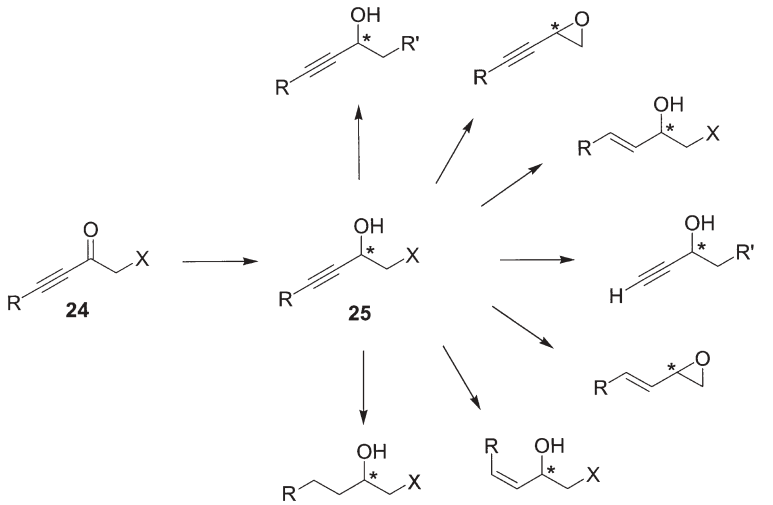

Scheme 24 Chiral building blocks produced from the enantiopure propargylic alcohols **25**

4 Summary

As an outcome of the investigation of the chemoenzymatic strategies described in this chapter, several new synthetic routes that have broad applicability in synthetic organic chemistry have been established:

- Regio- and enantioselective reduction of β,δ-diketo esters
- Dynamic kinetic resolution of 2-substituted 1,3-diketones
- Diastereomer-differentiating hydrolysis of 1,3-diol-acetonides
- Halogenated propargylic alcohols as versatile C-4 building blocks

Additionally, new biocatalytic concepts have been established:

- Use of highly sensitive substrates in enzyme-catalyzed reactions
- Large-scale biotransformations using NAD(P)H-dependent enzymes
- Adjustment of the product's stereochemistry by the use of directing groups
- Mimicry of diversity-oriented biosynthetic strategies using substrate engineering

By using this interdisciplinary approach, both, synthetic organic chemists and biochemists can gain valuable new insights into the strategies nature has evolved for metabolic diversity.

In the two sections of this chapter, examples were given of the use of highly reactive prochiral ketones as substrates for enzymatic reductions. In the case of β,δ-diketo esters, polyketides, obviously, are the natural prototypes for the chemistry developed. The results obtained from the elucidation of the regio- and enantioselective enzymatic reduction of these highly versatile compounds

led us to the development of non-natural functionalized ynones as starting material for the enzymatic access to enantiopure propargylic alcohols.

Recent work by others and by us aims at microbial access to other multipurpose building blocks in order to use them in a natural-product-based diversity-oriented synthesis. For example, in the group of Keasling, microbial production of isoprene-derived compounds has been developed [123]. We are involved in the development of the diversity-oriented access of compounds derived from chorismate [124–126]. It remains to be seen in the future whether the strategies (or parts thereof) evolved by nature to develop metabolic diversity in connection with biological activity can be copied successfully by man-made approaches.

References

1. Buckingham J (2000) Dictionary of natural products (on CD-ROM). Chapman & Hall/CRC, Boca Raton, FL
2. Lürssen K (1981) Chem Unserer Zeit 15:122
3. Murata M, Iwashita T, Yokoyama A, Sasaki M, Yasumoto T (1992) J Am Chem Soc 114:6594
4. Sasaki M, Matsumori N, Maruyama T, Nonomura T, Murata M, Tachibana K, Yasumoto T (1996) Angew Chem 108:1782; (1996) Angew Chem Int Edit 35:1672
5. Nonomura T, Sasaki M, Matsumori N, Murata M, Tachibana K, Yasumoto T (1996) Angew Chem 108:1786; (1996) Angew Chem Int Edit 35:1675
6. Bohacek RS, McMartin C, Guida WC (1996) Med Res Rev 16:3
7. Henkel T, Brunne RM, Müller H, Reichel F (1999) Angew Chem 111:688; (1999) Angew Chem Int Edit 38:643
8. Moffet DA, Hecht MH (2001) Chem Rev 101:3191
9. Lehn JM (1999) Chem Eur J 5:2455
10. Schreiber SL (2000) Science 287:1964
11. Breinbauer R, Vetter IR, Waldmann H (2002) Angew Chem 114:3002; (2002) Angew Chem Int Edit 41:2879
12. Ganesan A (1998) Angew Chem 110:2989; (1998) Angew Chem Int Edit 37:2828
13. Moore BS, Hertweck C (2002) Nat Prod Rep 19:70
14. Staunton J, Weissman KJ (2001) Nat Prod Rep 18:380
15. Rawlings BJ (2001) Nat Prod Rep 18:231
16. Various (1997) Chem Rev 97(7):2463–2706
17. Moore BS, Hopke JN (2001) Chembiochem 2:35
18. Leadlay PF (1997) Curr Opin Chem Biol 1:162
19. McDaniel R, Ebert-Khosla S, Hopwood DA, Khosla C (1995) Nature 375:549
20. Müller M (1991) The aim of this project in our group originated from truly biosynthetic roots. During work done on the diploma thesis (under the supervision of Prof. Steglich), for which the synthesis of polyketide-derived natural products was intended, I was faced with the problem of the regioselective addition of nucleophiles to highly enolizable dialkyl 3-oxo-glutarates possessing 1,3,5-trioxofunctionality, which is found in compounds **A** as well. Diplomarbeit, University of Bonn, Germany
21. Blandin V, Carpentier JF, Mortreux A (1999) Eur J Org Chem 12:3421
22. Shao L, Kawano H, Saburi M, Uchida Y (1993) Tetrahedron 49:1997

23. Shao L, Seki T, Kawano H, Saburi M (1991) Tetrahedron Lett 32:7699
24. Sayo N, Saito T, Kumobayashi H, Akutagawa S, Noyori R, Takaya H (1989) EP-A 297 752; Chem Abstr 111:114745n
25. Patel RN, Banerjee A, McNamee CG, Brzozowski D, Hanson, RL, Szarka LJ (1993) Enzyme Microbiol Tech 15:1014
26. Patel RN, McNamee CG, Banerjee A, Szarka LJ (1993) EP-A 569 998; (1994) Chem Abstr 120:52826q
27. Uko M, Azuma H, Sakai T, Tsuboi S (1991) JP-Kokai 03–48641; Chem Abstr 115:28713b
28. Kula MR, Kragl U (2000) In: Patel RN (ed) Stereoselective biocatalysis. Marcel Dekker, New York, p 839
29. Wolberg M, Hummel W, Wandrey C, Müller M (2000) Angew Chem 112:4476; (2000) Angew Chem Int Edit 39:4306
30. Hummel W (1997) Adv Biochem Eng Biotechnol 58:145
31. Hummel W (1999) Trend Biotechnol 17:487
32. Riebel B (1996) A 10 L fermentation of *E. coli* strain recADH-HB101+ yields approximately 600 kU of recLBADH. Dissertation, University of Düsseldorf, Germany
33. Thottathil, JK, Pendri Y, Li WS, Kronenthal DR (1994) US 5 278 313; (1994) Chem Abstr 120:217700j
34. Kizaki N, Yamada Y, Yasohara Y, Nishiyama A, Miyazaki M, Mitsuda M, Kono N, Ueyama N, Inoue K (2000) EP-A 1 024 139; (2000) Chem Abstr 132:166230
35. Masoni C, Deschenaux PF, Kallimopoulos T, Jacot-Guillarmod A (1989) Helv Chim Acta 72:1284
36. Kallimopoulos T, Deschenaux PF, Jacot-Guillarmod A (1991) Helv Chim Acta 74:1233
37. Wolberg M (2001) Dissertation, University of Oldenburg, Germany
38. Wolberg M, Hummel W, Müller M (2001) Chem Eur J 7:4562
39. Nakamura K, Fujii M, Ida Y (2000) J Chem Soc Perk T 3205
40. D'Arrigo P, Fantoni GP, Servi S, Strini A (1997) Tetrahedron Asymmetr 8:2375
41. Vicenzi JT, Zmijewski MJ, Reinhard MR, Landen BE, Muth WL, Marler PG (1997) Enzyme Microbiol Tech 20:494
42. Wolberg M, Ji A, Hummel W, Müller M (2001) Synthesis 937
43. Faber K (2001) Chem Eur J 7:5005 (and refs cited therein)
44. Noyori R, Tokunaga M, Kitamura M (1995) Bull Chem Soc 68:36 (and refs cited therein)
45. Stecher H, Faber K (1997) Synthesis 1 (and refs cited therein)
46. Tsuboi S, Nishiyama E, Furutani H, Utaka M, Takeda A (1987) J Org Chem 52:1359
47. Fujisawa T, Mobele BI, Shimizu M (1992) Tetrahedron Lett 33:5567
48. Hayakwa R, Shimizu M (1999) Synlett 8:1298
49. Ji A, Wolberg M, Hummel W, Wandrey C, Müller M (2001) Chem Commun 57
50. Eustache F, Dalko PJ, Cossy J (2002) Org Lett 4:1263
51. Noyori R, Ohkuma T (2001) Angew Chem 113:40; (2001) Angew Chem Int Edit 40:40 (and ref cited therein)
52. Ohkuma T, Koizumi M, Muniz K, Hilt G, Kabuto C, Noyori R (2002) J Am Chem Soc 124:6508
53. Oishi T, Nakata T (1990) Synthesis
54. Rychnovsky SD (1995) Chem Rev 95:2021
55. Schneider C (1998) Angew Chem 110:1445; (1998) Angew Chem Int Edit 37:1375
56. Chen KM, Hardtmann GE, Prasad K, Repič O, Shapiro MJ (1987) Tetrahedron Lett 28:155
57. Evans DA, Chapman KT, Carreira EM (1988) J Am Chem Soc 110:3560
58. Tamaru Y, Hojo M, Kawarmura S, Sawada S, Yoshida Z (1987) J Org Chem 52:4062
59. Jung ME, Kretschik O (1998) J Org Chem 63:2975

60. Trieselmann T, Hoffmann RW (2000) Org Lett 2:1209
61. Bode SE, Müller M, Wolberg M (2002) Org Lett 4:619
62. Pihlaja K (1967) Ann Univers Turkuensis Ser A1:114; (1968) Chem Abstr 69:76439
63. Wess G, Kesseler K, Baader E, Bartmann W, Beck G, Bergmann A, Jendralla H, Bock K, Holzstein G, Kleine H, Schnierer M (1990) Tetrahedron Lett 31:2545
64. Jendralla H, Granzer E, v. Kerekjarto B, Krause R, Schacht U, Baader E, Bartmann W, Beck G, Bergmann A, Kesseler K, Wess G, Chen LJ, Granata S, Herchen J, Kleine H, Schüssler H, Wagner K (1991) J Med Chem 34:2962
65. Richardson TI, Rychnovsky SD (1996) J Org Chem 61:4219
66. Rychnovsky SD, Griesgraber G (1992) J Org Chem 57:1559
67. Kotsuki H, Shimanouchi T (1996) Tetrahedron Lett 37:1845
68. Guindon Y, Yoakim C, Bernstein MA, Morton HE (1985) Tetrahedron Lett 26:1185
69. Roth BD, Roark WH (1988) Tetrahedron Lett 29:1255
70. Tabuchi H, Hamamoto T, Miki S, Tejima T, Ichihara A (1994) J Org Chem 59:4749
71. Drochner D, Müller M (2001) Eur J Org Chem 1:211
72. Davies-Coleman MT, Rivett DEA (1989) Fort Chem Org Nat 55:1
73. Collett LA, Davies-Colemann MT, Rivett DEA (1998) Fort Chem Org Nat 75:181
74. Kobyashi M, Higuchi K, Murakami N, Tajima H, Aoki S (1997) Tetrahedron Lett 38:2859
75. Murakami N, Wang W, Aoki M, Tsutsui Y, Sugimoto M, Kobayashi M (1998) Tetrahedron Lett 39:2349
76. Schummer D, Gerth K, Reichenbach H, Höfle G (1995) Liebigs Ann 685
77. Christmann M, Bhatt U, Quitschalle M, Claus E, Kalesse M (2000) Angew Chem 112:4535; (2000) Angew Chem Int Edit 39:4364
78. Job A, Wolberg M, Müller M, Enders D (2001) Synlett 1796
79. Enders D, Vicario JL, Job A, Wolberg M, Müller M (2002) Chem Eur J 8:4272
80. Micalizio GC, Schreiber SL (2002) Angew Chem 114:160; (2002) Angew Chem Int Edit 41:152
81. Matsumura K, Hashiguchi S, Ikariy T, Noyori R (1997) J Am Chem Soc 119:8738
82. Helal CJH, Magriotis PA, Corey EJ (1996) J Am Chem Soc 118:10938
83. Parker KA, Ledeboer MW (1996) J Org Chem 61:3214
84. Ramachandran PV, Teodorovic AV, Rangaishenvi MV, Brown HC (1992) J Org Chem 57:2379
85. Helmchen G, Hoffmann RW, Mulzer J, Schaumann E (1995 In: Houben-Weyl Methods of Organic Chemistry. Thieme Verlag, Stuttgart, vol E21d, p 4049
86. Waldinger C, Schneider M, Botta M, Corelli F, Summa V (1996) Tetrahedron Asymmetr 7:1485
87. Nakamura K, Takenaka K, Ohno A (1998) Tetrahedron Asymmetr 9:4429
88. Xie SX, Ogawa J, Shimizu S (1998) Biotechnol Lett 20:935
89. Kurihara M, Ishii K, Kasahra Y, Miyata N (1999) Tetrahedron Lett 40:3183
90. Burgess K, Jennings LD (1991) J Am Chem Soc 113:6129
91. Marshall JA, Chobanian HR, Yanik MM (2001) Org Lett 3:3369
92. Ghanem A, Schurig V (2003) Tetrahedron Asymmetr 14:57
93. Xu D, Li Z, Ma S (2003) Tetrahedron Lett 44:6343 (and refs cited therein)
94. Bradshaw CW, Fu H, Shen GJ, Wong CH (1992) J Org Chem 57:1526
95. Bradshaw CW, Hummel W, Wong CH (1992) J Org Chem 57:1532
96. Zheng C, Pham VT, Phillips RS (1994) Catal Today 22:607
97. Fang JM, Lin CH, Bradshaw CW, Wong CH (1995) J Chem Soc Perk T 976
98. Kolasa T, Stewart AO, Brooks CDW (1996) Tetrahedron Asymmetr 7:729
99. Heiss C, Phillips RS (2000) J Chem Soc Perk T 2821
100. Peters J, Minuth T, Kula MR (1993) Enzyme Microbiol Tech 15:950

101. Schubert T, Hummel W, Kula MR, Müller M (2001) Eur J Org Chem 22:4181
102. White DP, Anthony JC, Oyefeso AO (1999) J Org Chem 64:7707
103. De Amici M, De Micheli C, Carrea G, Spezia S (1989) J Org Chem 54:2646
104. Stang PJ, Dixit V (1985) Synthesis p 962
105. Look G (1995) Silylating agents. Fluka Chemie AG, Buchs, Switzerland
106. Tanner DD, Stein AR (1988) J Org Chem 53:1642
107. Aleixo LM, de Carvalho M, Moran PJS, Rodrigues JAR (1993) Bioorg Med Chem Lett 3:1637
108. Birkofer L, Ritter A, Uhlenbrauck H (1963) Chem Ber 96:3280
109. Nahm S, Weinreb SM (1981) Tetrahedron Lett 22:3815
110. Schubert T, Hummel W, Müller M (2002) Angew Chem 114:656; (2002) Angew Chem Int Edit 41:634
111. Schubert T (2002) Dissertation, University of Bonn, Germany
112. Pulvin S, Legoy MD, Lortie R, Pensa M, Thoms D (1986) Biotechnol Lett 8:783
113. Yang F, Russell AJ (1996) Biotechnol Bioeng 49:700
114. Peters J (1993) Dissertation, University of Düsseldorf, Germany
115. Zelinski T (1995) Dissertation, University of Düsseldorf, Germany
116. Itoh N, Mizuguchi N, Mabuchi M (1999) J Mol Catal B–Enzym 6:41
117. Lopp M, Kanger T, Müraus A, Pehk T, Lille Ü (1991) Tetrahedron Asymmetr 2:943
118. Kanger T, Niidas P, Müürisepp AM, Pehk T, Lopp M (1998) Tetrahedron Asymmetr 9:2499
119. Sánchez-Obregón, Ortiz B, Walls F, Yuste F, Garcia Ruano JL (1999) Tetrahedron Asymmetr 10:947
120. Takahashi K, Minami T, Ohara Y, Hiyama T (1995) Bull Chem Soc Jpn 68:2649
121. Schubert T, Hummel W, Müller M (2001) DE 101 05 866.7
122. Schauss SE, Brandes BD, Larrow JF, Tokunage M, Hansen KB, Gould AE, Furrow ME, Jacobsen EN (2002) J Am Chem Soc 124:1307
123. Martin VJJ, Pitera DJ, Withers ST, Newman JD, Keasling JD (2003) Nature Biotechnol 21:796
124. Franke D, Sprenger GA, Müller M (2001) Angew Chem 113:578; Angew Chem Int Edit 40:555
125. Franke D, Sprenger GA, Müller M (2003) Chembiochem 4:775
126. Franke D, Lorbach V, Esser S, Dose C, Sprenger GA, Halfar M, Thömmes J, Müller R, Takors R, Müller M (2003) Chem Eur J 9:4188

Received: April 2004

Adv Biochem Engin/Biotechnol (2005) 92: 289 – 316
DOI 10.1007/b98909

Membrane Reactors at Degussa

Jens Wöltinger (✉) · Andreas Karau · Wolfgang Leuchtenberger · Karlheinz Drauz

Degussa AG, Business Unit Exclusive Synthesis & Catalysts, Rodenbacher Chaussee 4, 63457 Hanau-Wolfgang, Germany
jens.woeltinger@degussa.com, andreas.karau@degussa.com, wolfgang.leuchtenberger@degussa.com, karlheinz.drauz@degussa.com

Abstract The review covers the development of membrane reactor technologies at Degussa for the synthesis of fine chemicals. The operation of fed-batch or continuous biocatalytic processes in the enzyme membrane reactor (EMR) is well established at Degussa. Degussa has experience of running EMRs from laboratory gram scale up to a production scale of several hundreds of tons per year. The transfer of the enzyme membrane reactor from biocatalysis to chemical catalysis in the chemzyme membrane reactor (CMR) is discussed. Various homogeneous catalysts have been investigated in the CMR, and the scope and limitation of this new technique is discussed.

Keywords Enzyme membrane reactor · Chemzyme membrane reactor · Biocatalysis · Asymmetric catalysis · Amino acid · Continuous reaction

1 Introduction

One of the major challenges for process development chemists in the chemical industry is the economic application of chemical or biological catalysts. As well as a high turnover of a catalyst based on such intrinsic parameters as specific activity and stability, separation and recycling can increase the efficiency of the catalyst even further, resulting in lower catalyst costs per kg of product. Degussa has therefore developed a platform technology for catalyst recovery based on membrane reactors to separate and recycle the catalysts from the reaction mixture. This simplifies the work-up protocol and leads to high turnover numbers by recycling the catalyst in situ.

This review describes the development of membrane reactors used at Degussa for the production of fine chemicals. Starting with the enzyme membrane reactor as the initial technological innovation, and leading to the implementation of the chemzyme membrane reactor concept for continuous homogeneous chemical catalysis, all of the relevant technologies are discussed.

2 Membrane Reactors for Biocatalysis

2.1 Enzyme Membrane Reactor Technology

The use of soluble enzymes in biotransformations presents significant advantages over immobilized enzymes in terms of productivity, selectivity and economics [1–2]. Immobilization procedures often lead to reduced activity due to covalent or physical attachment to a carrier and additional mass transfer resistance within the particles. Furthermore, the immobilization step generates extra catalyst manufacturing costs. The volume activity achievable in the reactor is dependent on the specific activity of the carrier and the maximum concentration of the carrier in the reactor. For carriers with low specific activities, the volume activity in the reactor is often limited. Maximum carrier concentrations are achieved in fixed bed operations with up to 40–50 vol% carrier.

These drawbacks can be overcome by direct application of soluble enzymes in the reactor. To be economically competitive, the total turnover numbers of the soluble enzymes have to be in the same range as the immobilized ones. The application of soluble enzymes in simple batch biotransformations leads to the loss of the biocatalyst after each batch. The introduction of the enzyme

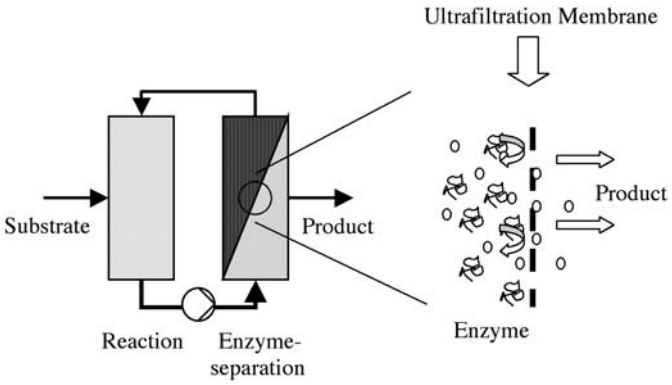

Fig. 1 Schematic concept of the enzyme membrane reactor

membrane reactor (EMR) made it possible to retain the biocatalyst in the reactor, which enables enzyme lifetimes of several batches and continuous process operation. Ultrafiltration membranes in the reactor reject the enzymes, and only the solvent (for example water) and product are able to pass through the membrane (Fig. 1). Depending on the reaction kinetics, the EMR can be operated in continuous, batch, or fed-batch mode.

Degussa introduced the first production scale EMR in 1981 after three years of intensive and successful cooperation with Wandrey et al. It was used for the production of enantiomerically pure amino acids via the acylase route [3–4]. In the meantime, Degussa has expanded this technology to different enzyme systems, and several products are now produced by this technology.

For the successful development and operation of EMR-based processes, several aspects of membrane technology, reaction engineering, and enzyme engineering must be considered. These areas are considered in more detail below.

2.2 Aspects of Membrane Technology

Membrane technology is one of the key factors for the successful development and operation of membrane reactor based processes. Rejection rates, specific flux rates, fouling effects, and long term operational stability all significantly influence the operating performance, capital investment and operating costs of the process.

Because most enzymes have molecular weights in the range of 10–150 kDa, a molecular weight cut-off of 10 kDa is sufficient to obtain rejection rates $\geqslant$99% for a large number of different enzymes. These very high enzyme rejection rates are necessary to minimize enzyme losses at the filtration step. Figure 2 shows the relative contribution of enzyme costs as a function of the rejection rate, *R*.

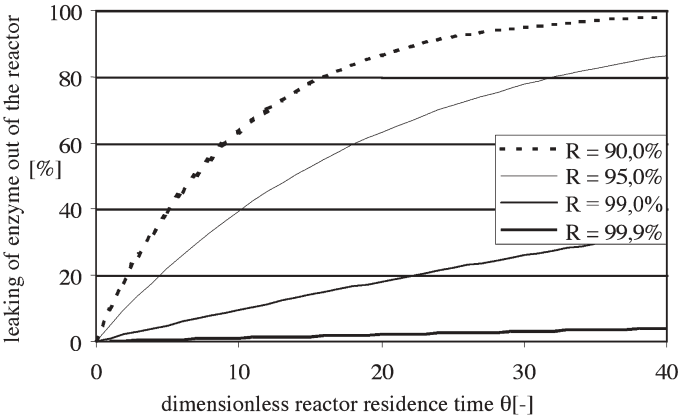

Fig. 2 Influence of retention rate on enzyme losses in a continuous process

Ultrafiltration membranes, which exclude macromolecules in the range of 1–500 kDa, are usually composite membranes, with an extremely thin layer of homogeneous polymer supported on a much thicker supporting substructure. The pores of the thin layer are much smaller than the pores of the rest of the membrane, so that the thin layer is responsible for the cut-off and the filtration resistance, while the substructure determines the mechanical strength of the membrane.

The best polymer to use for the thin layer depends on the properties of the enzyme. Reaction mixtures containing hydrophobic enzymes normally show better filtration characteristics with hydrophilic membrane materials such as regenerated cellulose or hydrophilized polyethersulfones. This is due to reduced unspecific protein adsorption on the membrane surface. Hydrophobic membrane materials such as polysulfone are preferred with hydrophilic proteins.

Two main types of reactor set-up are possible (Fig. 3). The first is a dead-end filtration, where the whole solution is pumped towards the membrane (Fig. 3b). In the second, the solution is pumped tangentially to the membrane (cross-flow filtration) (Fig. 3a). Cross-flow filtration is more suitable for scale-up, as complete filtration modules are commercially available and they can be operated in parallel, which reduces the space required to a minimum. For initial laboratory experiments, dead-end filtration is more suitable as the reactor volume is smaller than in the cross-flow system, thus minimizing the amount of starting material and solvent required.

Cross-flow filtration technology is often used for enzyme membrane reactors in order to minimize the build-up of material, which can cause membrane blocking. The liquid is circulated tangentially to the membrane surface and sweeps the membrane clean of deposited particles or proteins.

Different membrane configurations are available for cross-flow filtration. Plate and frame devices, tubular geometry, hollow-fiber cartridges, or spiral wound cartridges are available. Because of low investment costs, compact size

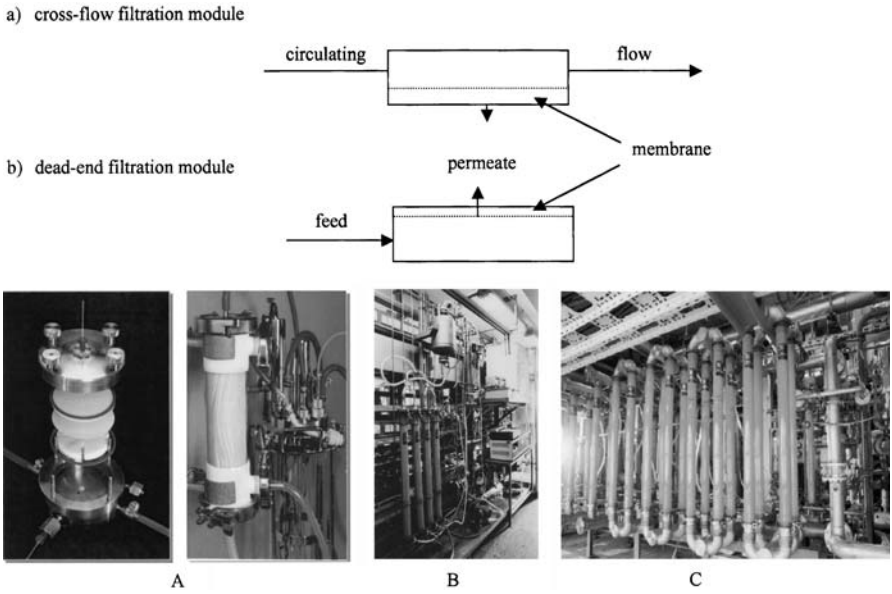

Fig. 3 Cross-flow and dead-end filtration modules for the membrane processes, and enzyme membrane reactors using hollow fiber membranes at different scales (**A**: lab scale, **B**: pilot scale, **C**: production scale)

and simple scale-up, hollow-fiber modules are often preferred for homogeneous reaction systems. In contrast to reaction mixtures containing high solid concentrations (whole cells, precipitated product, and so on), tubular membranes or plate and frame modules are used.

Operating conditions have a strong influence on the achievable specific flux rate. It is often believed that increasing the trans-membrane pressure ΔP will increase the flux through the membrane. This actually only holds for low ΔP; at higher ΔP there is no further flux increase. At high ΔP, the specific flux over time deteriorates faster than with low ΔP. This is due to the formation of a surface layer on the membrane, which is a function of ΔP and the specific flux rate. As well as leading to longer filtration times, the specific flux falls continuously over the filtration time. Furthermore, for maximum confidence in scale-up, it is helpful to keep the length of the membrane fibers and volume-to-area ratio V/A constant when scaling up from laboratory to plant scale. In contrast to the downstream part of the process, the reactor, including the membrane system, usually operates efficiently at the pilot and production plant scale, because it has been well studied and designed at the laboratory scale. Figure 3 shows the enzyme membrane reactor at Degussa at laboratory, pilot plant and production scale.

2.3 Scale-Up Challenges

Problems often occur if scale-up considerations and calculations are based on an insufficient data set from lab scale experiments. Successful scale-up requires proper process characterization and development at the laboratory scale, which for membrane reactors means optimizing the reaction kinetics and the membrane operation. The most critical areas for scale-up are enzyme inactivation in large scale reactors and the long term performance of the membranes. Higher inactivation rates at production scale can be due to higher shear forces during mixing, larger gas-liquid surfaces, and higher substrate or temperature gradients in the reactor. The effects of these parameters on the enzyme inactivation rates have to be studied carefully in the laboratory and the results applied to the process design. The long term filtration performances of the membranes depends mainly on fouling effects and the efficiency of the cleaning process. As well as the membrane material, the operating conditions, such as the trans-membrane pressure and the flow rate, influence the fouling characteristics. These parameters have to be optimized in the laboratory with filtration modules that have the same filtration length as those used at production scale. Scale-up of the membrane area should be performed by numbering-up of the filtration modules. If these aspects are considered during the development phase, the scale-up should be unproblematic.

2.4 Aspects of Enzyme Development for Membrane Reactor Applications

The soluble enzyme has to be very stable during the process for the process to be transferred successfully to production scale. In the event of insufficient enzyme stability, the enzyme has to be continually added to the process, leading to increased enzyme costs. In such cases the enzymes can either be immobilized to give improved process stability, or optimized by evolutionary or rational protein design methods. For large-scale production, the enzymes have to be available in large quantities at low cost. This is achieved by using recombinant strains with high expression levels and simplified downstream protocols. Crude enzyme formulations are often sufficient for an industrial process.

As an example, the acylase enzyme (acylase I; aminoacylase; *N*-acetyl amino acid amidohydrolase; E.C. 3.5.1.14.) is available in large, industrial amounts from two sources: porcine kidney, and from the mold *Aspergillus oryzae*. Results on the operational stability of both acylases in a recycle reactor demonstrated the high stability of the *Aspergillus* enzyme, whilst the renal enzyme was not stable enough for long-term operation [5–7]. Stability investigations on the acylase under process conditions showed that the enzyme concentration did not have an effect on stability, but that pH values of <7.0 were detrimental to the enzyme's operating stability.

The improvement in the process stability of formate dehydrogenase from *Candida boidinii* was achieved by site-directed mutagenesis. The stability of the wild type was limited because of oxidation of cysteine residues at the enzyme active site. Using site-directed mutagenesis, cysteines were replaced by serine at position 23 and by alanine at position 262. A positive side effect was an increased thermostability of 5–7 °C. The half-life of the new mutant in the reaction mixture was improved by a factor of four [8].

2.5 Aspects of Reaction Kinetics for Membrane Reactors

Membrane reactors can be operated in continuous, repetitive batch, or fed-batch mode. Optimal operation conditions depend on the enzyme kinetics and the required productivity and conversion. If maximum conversion rates are required, batch operations show higher productivity than continuous reaction schemes. This is due to the fact that in continuous processes the substrate concentrations are permanently low (often significantly below the K_m value) and product concentrations are high. From Michaelis-Menten kinetics it can be shown that reaction rates under these conditions are far below the maximum reaction rates. In batch reactions, the reaction rates are high at the beginning and decrease during the reaction. If maximum productivity is required, then continuous reaction schemes with only partial conversion are favorable. However, in these cases the downstream protocol is often more complicated and cost-intensive. The optimal operation mode has to be investigated for each individual process depending on the relevant constraints. All operational modes can be implemented using EMR technology at an industrial scale.

2.6 EMR Processes at Degussa

2.6.1 Acylase Process

The first industrial acylase process was performed by Tanabe Seiyaku using immobilized acylase in a fixed-bed reactor. Takeda scaled up the process using an immobilized enzyme in a fixed-bed column in 1968 [9]. Degussa introduced a continuous acylase process employing the enzyme membrane reactor, based on the work by Wandrey et al in 1981 [3–4], and transferred this technology using soluble acylase to production scale in 1982 [10]. Since then, Degussa has installed several membrane reactors for pilot, small, and large-scale production. A variety of proteinogenic (alanine, methionine, valine, tryptophan) and non-proteinogenic amino acids (*O*-benzlyserine, norleucine, norvaline) have been prepared at Degussa in bulk quantities by resolution of the respective *N*-acetyl amino acids [11].

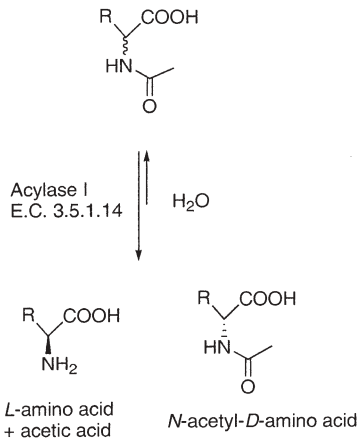

Scheme 1 Acylase route to L-amino acids

The D,L-amino acids are obtained via a Strecker reaction and acetylated under Schotten-Baumann conditions to yield the *N*-acetyl-D,L-amino acid, the substrate for the enzymatic resolution (Scheme 1). After the acylase resolution, the L-amino acid is isolated from the reaction mixture by ion chromatography and purified by crystallization. The nominal capacity of the plant dedicated to producing enantiomerically pure L-amino acids via enzyme membrane reactor technology using the acylase process is several hundreds of tons/yr. The industrial process is illustrated for L-methionine in Fig. 4.

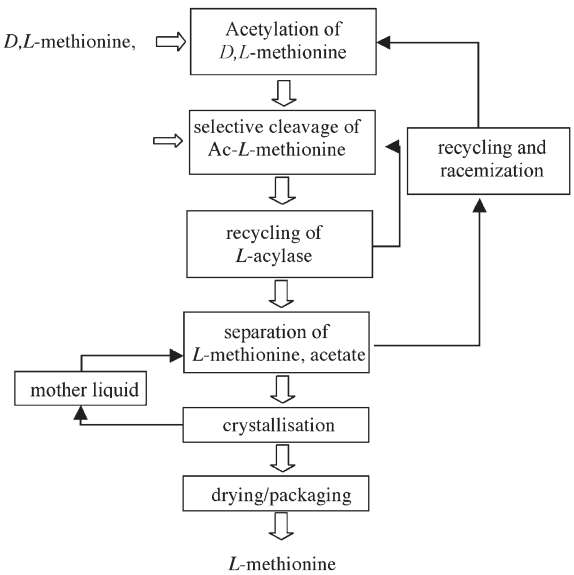

Fig. 4 Continuous production process via the acylase route

2.6.2
Dehydrogenase Technology with Integrated Cofactor Regeneration

Dehydrogenases offer the chance to produce enantiomerically pure components from prochiral compounds such as α-keto acids in a single step in quantitative yield. Thus L-amino acids may be obtained by reductive amination or optically pure alcohols by reduction. Racemization of the unreacted enantiomer, which is always a challenge when using simple hydrolysis systems, is no longer required. A disadvantage of the dehydrogenase technology is the requirement for cofactors (like NADH or NADPH) in equimolar amounts. This process can therefore only be operated on a large scale if the cofactor is regenerated. Wandrey and Kula have developed an elegant regeneration of NAD^+ to NADH using formate to reduce the NAD^+ generated by reductive amination. The formate is oxidized irreversibly to CO_2 by formate dehydrogenase (FDH, E.C. 1.2.1.2.) [12].

The quantitative reductive amination of an α-keto acid substrate catalyzed by an L-amino acid dehydrogenase coupled with FDH is very attractive, particularly for the production of unnatural amino acids or chiral alcohols, which cannot be produced efficiently by fermentation. This technology has been operated at a production scale at Degussa since 1999 for the production of (*S*)-*tert*.-leucine and (*S*)-neopentyl-glycine, important building blocks for a range of pharmaceutical products (Scheme 2).

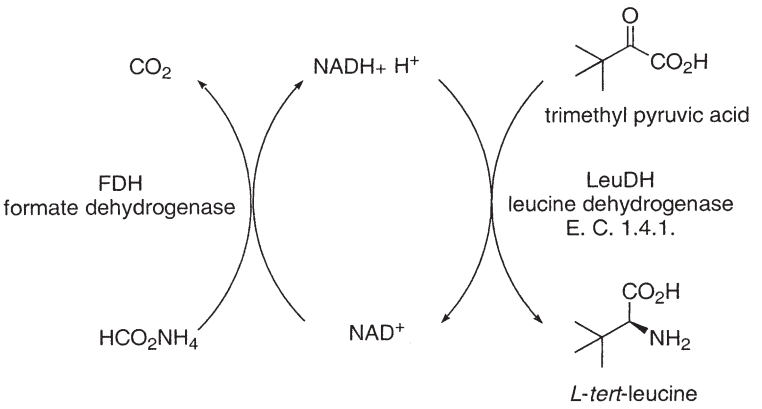

Scheme 2 (*S*)-*tert*-leucine process

Using a substrate concentration of 0.5 M, L-*tert*-leucine was produced in a continuous laboratory membrane reactor, with an average conversion of 85% and a space-time yield of 638 g/(l d). For continuous operation, because the molecular weight of NAD^+ is only ~600 Da, the size of the cofactor has to be enlarged in order to ensure retention by the UF membrane. The cofactor can be covalently bound to a water-soluble polymer such as poly(ethyleneglycol) (PEG) with a molecular weight of about 20 kDa [13]. The total turnover number

over a period of two months was 125,000. For higher conversion yields at a production scale, the reaction is run in a fed-batch mode to streamline the downstream process. After completion of the reaction, the enzymes are retained by an ultrafiltration (UF) membrane, while the product and unbound cofactor permeate through the membrane. Nevertheless, the total turnover number of the cofactor is so high that cofactor costs are still a negligible part of the total production costs.

2.6.3 L-Ornithine Salts from L-Arginine and Arginase

L-Ornithine and its salts are of growing importance for the pharmaceutical industry, in parenteral nutrition (L-Orn·HCl and L-Orn acetate), in the treatment of hepatic diseases (L-Orn·L-Asp and L-Orn α-ketoglutarate), or as starting materials for pharmaceutical building blocks. The enzymatic hydrolysis of L-arginine by L-arginase (L-arginine amidinohydrolase, E.C. 3.5.3.1.) is a very attractive route to the large-scale synthesis of L-Orn, and it is highly competitive with fermentative processes [14] (Scheme 3).

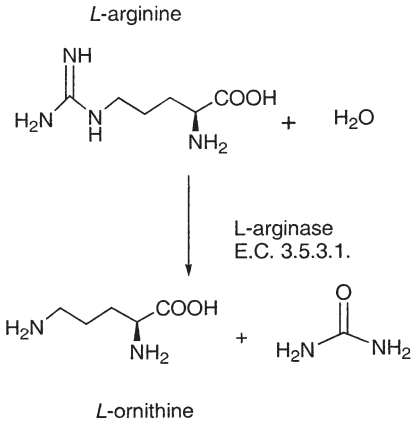

Scheme 3 Production of L-ornithine using arginase

In order to obtain sufficiently high activity levels, native arginase from calf or bovine liver is used instead of immobilized preparations. The enzyme membrane reactor was preferred for this process because of the high solubilities of reactants and products and because of the use of a soluble enzyme. Because of mammalian arginase's sensitivity to shear forces, the usual reactor concept with pumped recycling leads to rapid deactivation of the enzyme during production. To increase enzyme stability, a new reactor concept was developed using a quiescent medium with hydraulic transport of substrate and enzyme solution [15] (Fig. 5). Using stabilizing agents such as manganese ions and ascorbic acid, the deactivation of enzyme could be further decreased. The process was con-

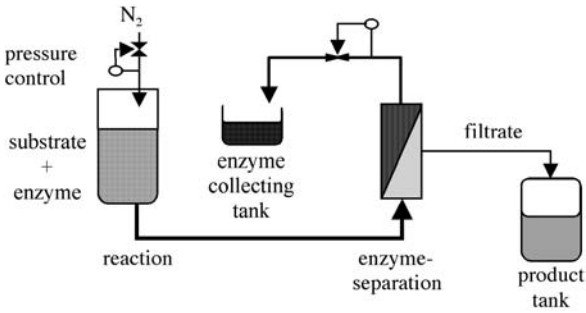

Fig. 5 Alternative process design of the enzyme membrane reactor without mechanical agitation

ducted on a pilot scale at enzyme consumption levels of less than 400 units per kg L-ornithine at 83–88% conversion.

3 Membrane Reactors for the Separation of Homogeneous Catalysts

In contrast to separations of biocatalysts, which are achieved by membrane technology using commercially-available ultrafiltration membranes which make use of the high molecular weight of the enzyme, homogeneous chemical catalysts cannot be separated by this process. As well as the low molecular weight of the catalyst, the nature of the solvent also comes into play. Reactions accelerated by biocatalysts are usually carried out in water, whereas reactions using homogeneous catalysts are run in organic solvents. The membranes used for the separation of biocatalysts are unstable in organic solvents, but recently nanofiltration and ultrafiltration membranes resistant to organic solvents have become commercially available, allowing the separation of homogeneous catalysts with membrane technology.

Chemical catalysts are separated from the product by three main techniques:

- Separation of the catalyst during work-up of the whole reaction solution
- Separation of a catalyst bound to a heterogeneous support by filtration
- Using a fixed-bed reactor with the catalyst bound to an insoluble polymer

All three approaches have their disadvantages. One is the loss of catalyst, the other is the reduced activity of a heterogeneously bound catalyst compared with a homogeneous one. However, one advantage of heterogeneous over homogeneous catalysts is their easy recovery.

In a membrane reactor, a combination of the advantages of homogeneous and heterogeneous catalysis can be achieved by attaching a low molecular weight catalyst to a high molecular weight polymeric support. To obtain similar activity to the native catalyst, the support has to be soluble in the reaction medium.

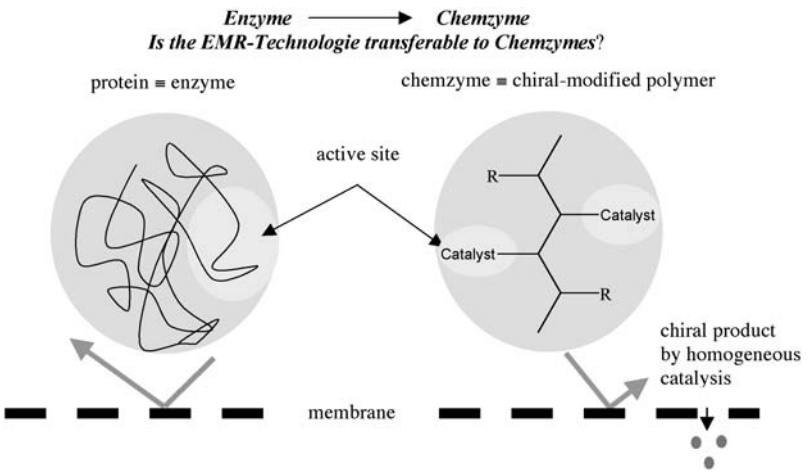

Fig. 6 A comparison between enzymes and molecular weight-enlarged homogeneous catalysts

The left hand side of Fig. 6 depicts the principle of an enzyme membrane reactor. The enzyme is held back by the low cut-off of the membrane, while low molecular weight compounds such as products and substrates can pass through the membrane easily. By setting a suitable residence time, the reaction runs to completion and only the product leaves the reactor with the permeate. The enzyme remains in the membrane reactor and is available for further transformation.

The right-hand side of this figure shows the chemzyme membrane reactor (CMR). In contrast to the single active site of the enzyme, an attachment of several homogeneous catalyst molecules to the polymeric support is possible. These perform the reaction and the product leaves the reactor via the membrane. Due to the high molecular weight, the chemzyme (chemical enzyme) cannot pass through the membrane and is retained. By applying this technique, it is not only easy to separate the catalyst from the product, but it is also possible to increase the total turnover number of the catalyst.

3.1 Research Scope

The key to the success of a chemzyme membrane reactor is in the combination of expertise from three separate research areas, as shown in Fig. 7.

3.2 Chemistry Research

The first area deals with the homogeneous catalyst. The catalyst has to meet requirements of stability and activity for the desired reaction but must also be

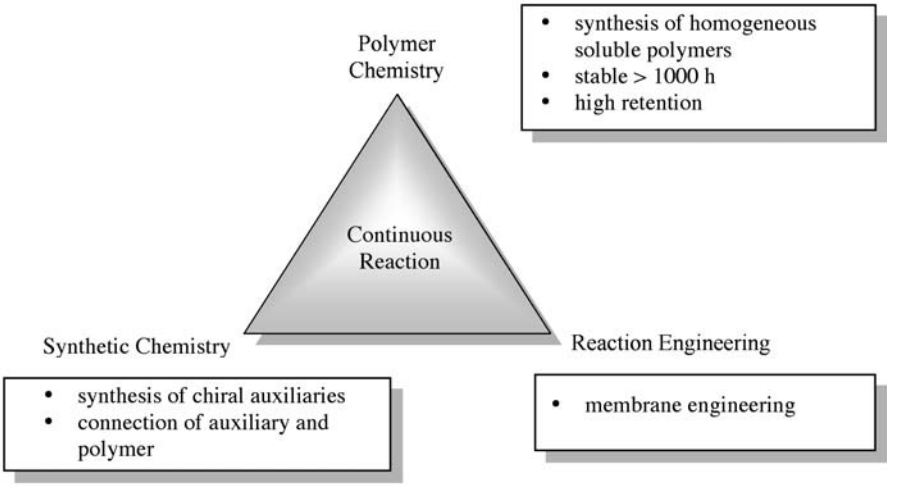

Fig. 7 Important research areas for continuous processing in a CMR

easy to synthesize. This is important for a commercial catalyst, as modification of the catalyst is usually required to enable connection to the polymer support. When using a metal-ligand system, such as is found in many hydrogenation catalysts, the binding of the metal to the ligand is also extremely important.

3.3 Polymer Research

The second requirement is a good knowledge of polymer chemistry. To use it in a CMR, the polymeric support has to be soluble in the reaction medium. The polymer has to be stable towards degradation and interaction of the support with the catalyst or the product, and the correct linker group has to be chosen to bind the catalyst to the polymer.

Three main polymer structures are possible. The architecture of the polymer is expected to play a major role in the retention of the polymer by the membrane.

The size of a linear polymer is correlated with the molecular weight (MW), so a high MW will lead to better retention for a given membrane (Fig. 8). However the viscosity of the polymer solution will also increase with MW, so that a balance between retention and ease of handling must be achieved. An example of a linear polymer is polystyrene prepared by radical polymerization, which can be run on a large scale. However the molecular weight distribution of polymer must be narrow to achieve a balance between solubility and viscosity.

Polymeric supports can also be prepared in the form of star-shaped structures or dendrimers. These tend to have a narrow molecular weight distribution, but a more complex manufacturing process (particularly for the star-shaped polymers). With a dendrimer, the catalyst active sites are arranged on

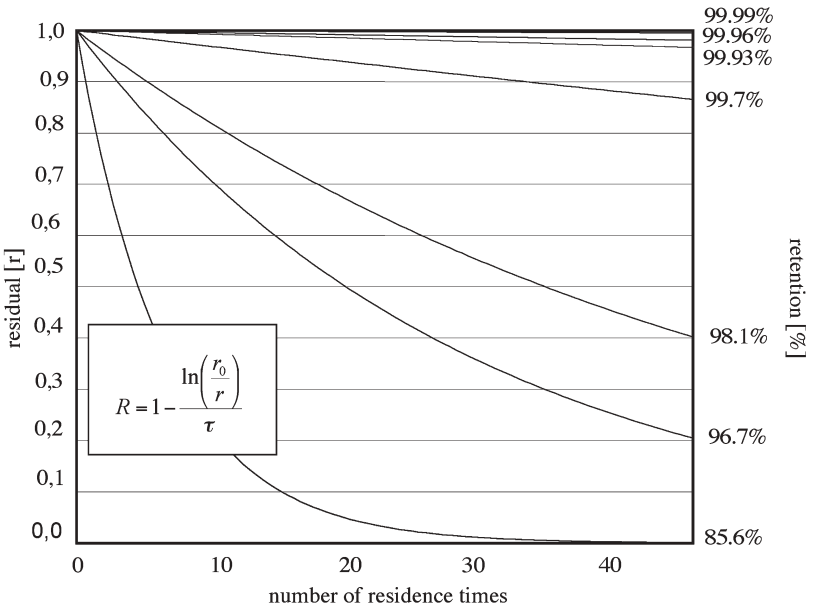

Fig. 8 Residue of a polymer with a certain retention after 48 residence times

the "surface" of the ball-shaped chemzyme. The accessibility of low molecular weight starting materials, or products, to the catalytic center is higher for a star-shaped polymer than for a linear polymer.

3.4 Engineering Research

A good engineering approach is also required for a successful chemzyme membrane reactor. The solution of the starting materials has to be pumped through the reactor under constant flow conditions, while the membrane is chosen so that >99.95% of the polymer bound catalyst will be retained. The membrane must also be stable in pure organic solvents. Fortunately, solvent-resistant membranes with a cut-off in the range 500–20,000 Da are now commercially available. It is necessary to adapt the MW of a polymer-supported catalyst to the membrane for a given cut-off.

The higher the cut-off, the larger the supported chemzyme. However a chemzyme that is too large leads to a higher viscosity solution in the membrane reactor and the need for a high trans-membrane pressure. On the other hand, a low cut-off can also result in a high trans-membrane pressure, even though the MW of the chemzyme can be reduced. The solvent or solvent mixture chosen also influences the trans-membrane pressure, depending on the membrane material used (ceramic or different types of cross-linked polymers).

3.5
Applications of the Chemzyme Membrane Reactor

One of the main types of homogeneous catalyst is a chiral or achiral ligand complexed to a metal; the presence of the metal being essential for the reaction. Most hydrogenation catalysts such as DuPhos, Deguphos, BiNAP, or PhanePhos are members of this group. The second group of homogeneous catalysts, which is much smaller, contain no metals. This second group is also very interesting in terms of the reactions catalyzed. Both are described in this chapter.

3.5.1
Borane Reduction

In 1997 Wandrey and co-workers published the synthesis of a modified prolinol and its coupling to a polysiloxane (Scheme 4) [16]. The polymer-bound prolinol was converted to the corresponding oxazaborolidine **1**, which was then used for the borane reduction of prochiral ketones. The yields and enantiomeric excesses obtained were the same as for those obtained with the monomeric oxazaborolidines.

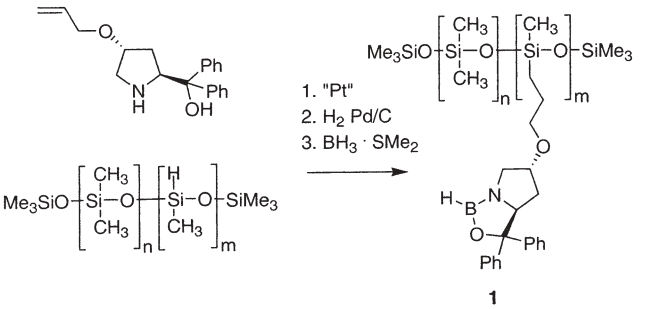

Scheme 4 Oxazaborolidine catalyst bound to a polysiloxane

Kragl and Wandrey published details of the first continuously operating chemical membrane reactor that operated with comparable enantiomeric excess and yields to monomeric catalysts in 1998 [17–19]. Running the membrane reactor in a dead-end mode, a range of prochiral ketones were reduced, using two different polymer-bound oxazaborolidines as catalysts (Scheme 5). The continuous process was run with optimal conversion and enantiomeric excess for a period of 60 h, and total turnover numbers (TTN) of up to 560 were obtained, compared to a TTN of between 5 and 20 for monomeric oxazaborolidines. This represented a significant improvement in catalyst utilization. The reactor works under stable conditions until the catalyst concentration drops below a critical value. There are two possible reasons for this:

a. leaching of the polymer-bound catalyst
b. deactivation of the catalyst

Both of these processes lead to first-order, negative exponential behavior.

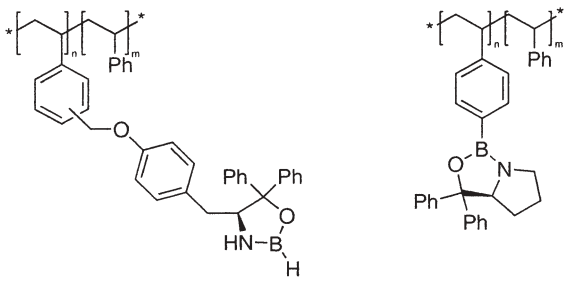

Scheme 5 Two different molecular weight-enlarged oxazaborolidine catalysts on a polystyrene backbone

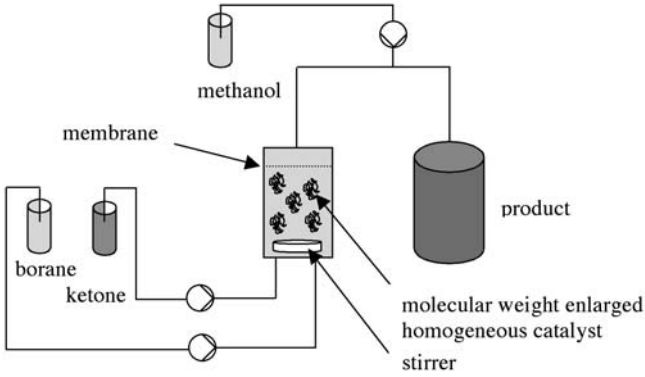

Fig. 9 Set-up for continuous ketone reduction with borane

The laboratory CMR arrangement is depicted in Fig. 9. A 10 ml stainless steel chemzyme membrane reactor, equipped with a nanofiltration membrane, is charged with catalyst, and the ketone and borane solutions are charged simultaneously via the dosing pumps. The residence time in the reactor can be varied by altering the flow rates. Methanol is added downstream of the reactor to quench the excess of borane and prevent uncatalyzed reduction of the ketone, which would lead to a degradation of the enantiomeric excess.

Further improvements were achieved by using more stable oxazaborolidines. It was found that the molecular weight-enlarged β-alkyl-oxazaborolidines were less moisture sensitive than the β-*H*-oxazaborolidines, mirroring the results found with the unsupported oxazaborolidines. Figure 10 shows the conversion and enantiomeric excess for the reduction of tetralone **4** with borane in the presence of a polysiloxane-bound stable β-methyl-oxazaborolidine **6** [20]. Constant values were found for conversions and enantiomeric excesses over more than 200 residence times, with a TTN of 321, assuming no catalyst leaching. The tetralone and borane feed concentrations were doubled after 143 residence times and again after 168 residence times, giving a final

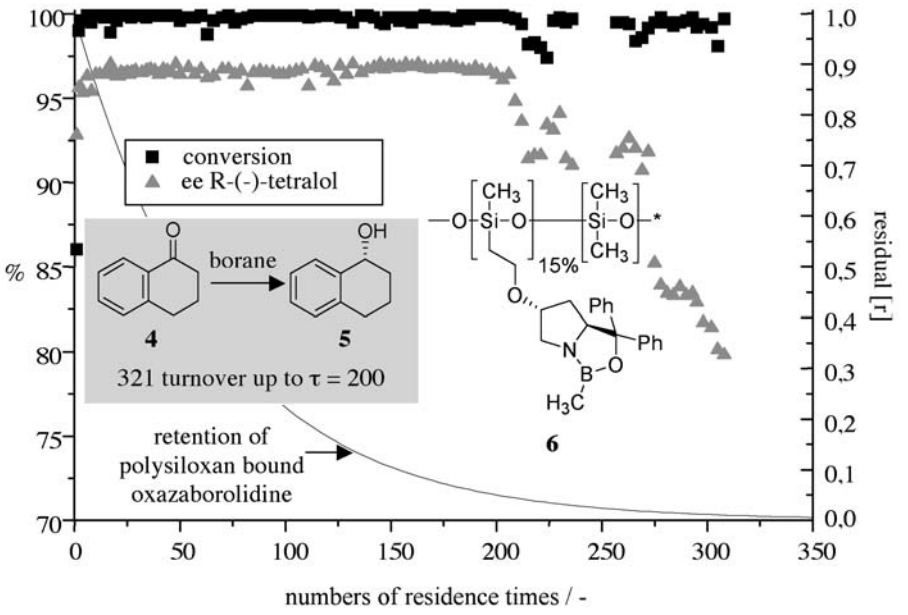

Fig. 10 Continuous reduction of tetralone using polysiloxane-bound oxazaborolidine as catalyst

tetralone feed of 2 mol/l. Again assuming no catalyst leaching, a space time yield of 1.42 kg/(l d) could be achieved.

Assuming the catalyst did not lose activity and selectivity, the main reason for the decrease in selectivity after 207 residence times is catalyst leaching. At this point, the uncatalyzed borane reduction of the ketone begins to dominate, and the enantiomeric excess decreases as the catalyst is lost through leaching. It can be calculated that an amount of 1.2 mol% of catalyst is required to run the borane reduction of tetralone with optimal conversion and enantiomeric excess. By using a polystyrene-bound molecular weight-enlarged catalyst 7 with a higher retention factor, optimal conversion was achieved over 355 residence times (Fig. 11). With a one-hour residence time, this gives a continuous operation period of more than two weeks, and a TTN of 1374 [21–22].

3.5.2 Juliá-Colonna Epoxidation

This second example uses a metal-free homogeneous oligopeptide catalyst bound to a polymer for the CMR reaction. The reaction catalyzed in this case is the Juliá-Colonna epoxidation of α,β-unsaturated ketones of the chalcone series [23].

The laboratory equipment for the epoxidation reaction is similar to that used for the borane reduction. The two reagent streams are charged to the 10 ml stainless steel reactor, using mass flow meters to control the flow rates better.

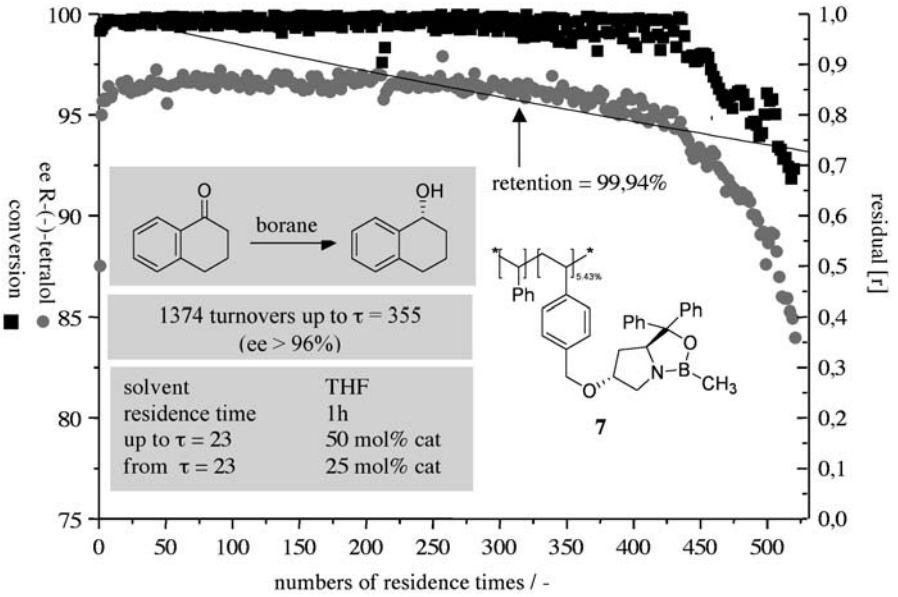

Fig. 11 Continuous reduction of tetralone using polystyrene-bound oxazaborolidine as catalyst

The standard poly-L-leucine catalyst, which is widely used for the Juliá-Colonna epoxidation, remains insoluble under all of the reaction conditions used. The first homogeneous version of this reaction using *trans*-chalcone **8** was only reported recently. However, the conversion observed was only 39% after 1 h and 80% after 24 h, with an ee of 95–98%. This is a good starting point for further development of the process in the chemzyme membrane reactor, as the catalyst concentration can be increased to speed up the reaction without a correspondingly large increase in the catalyst cost. Using the CMR technique, increasing the reaction rate, and recycling the catalyst in situ, the catalyst cost per kg of product and the total manufacturing cost can both be reduced.

As with the borane reduction, the work was focused on linear polymers. Two types of soluble polymer enlarged oligo(L-leucine) were prepared (Scheme 6). The approach to catalyst **12** involved the co-polymerization of one equivalent of commercially available *O,O*-bis(2-aminoethyl)-poly(ethyleneglycol) 20,000 **10** with 16 equivalents of L-leucine-*N*-carboxyanhydride **11** in $CHCl_3$. It was found that the resulting poly(ethyleneglycol)-supported oligo(L-leucine) **12** can act as an efficient homogeneous chiral catalyst in the epoxidation of *trans*-chalcone **8** using urea-hydrogen peroxide adduct as the oxidant. The optically active epoxyketone **9** was obtained with a conversion of 99% and an ee of 94% after 15 minutes of reaction.

When the polystyrene-supported catalyst **14** was used, an ee of up to 97% and a conversion of 92% after 60 min was observed. These remarkable results observed in batch reactions demonstrated the potential of the new catalysts

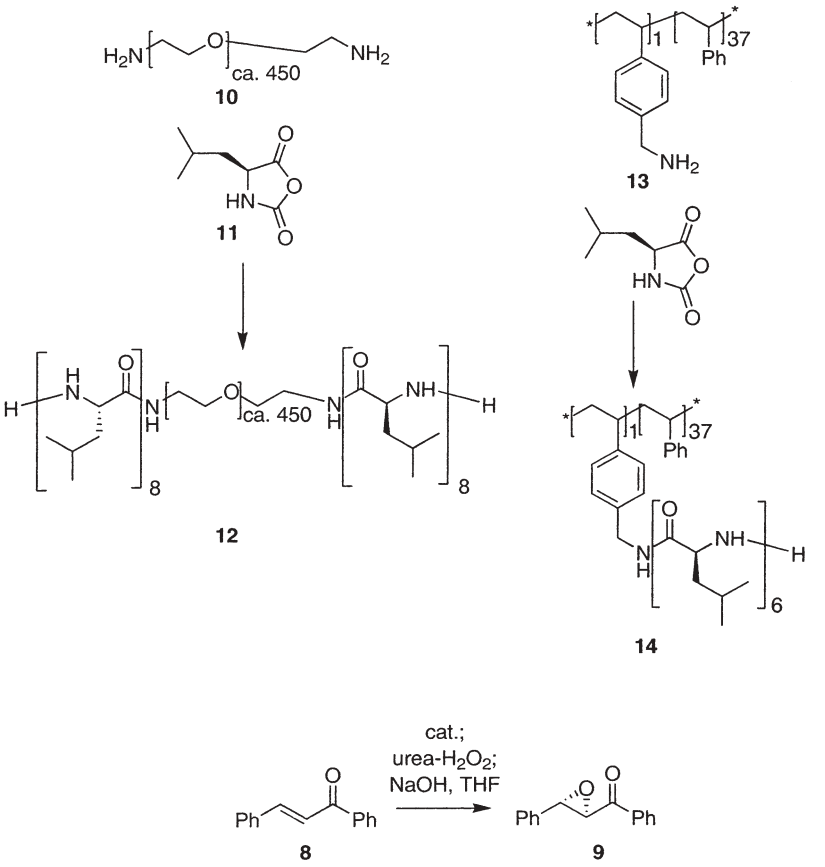

Scheme 6 Synthesis of homogeneous oligo(L-leucine) and its use in asymmetric epoxidation

for the continuous reaction, the results of which are presented in Fig. 12 for the catalysts **12** and **14.**

In the first experiment with catalyst **12,** a conversion of up to 86% and an ee of up to 90–95% were observed over 25 residence times. The addition of freshly prepared urea-H_2O_2 solution after 45 residence times leads to a renewed increase in conversion as well as in enantiomeric excess. The reason for the drop in enantioselectivity of catalyst 12 under the reaction conditions cannot be adequately explained. While the conversion of chalcone **8** using the polystyrene-supported catalyst **14** dropped significantly to 47% after 28 residence times, little loss of selectivity was observed (still over 90% ee). The reactor was operated until the concentration of active oligo(L-leucine) **12** or **14** dropped below the critical value at residence time 50. As the retention of catalyst **14** (98.99%) is comparable to, and even higher than, that of catalyst **12** (98.89%), it can be assumed that deactivation of catalyst **14** dominates over its leaching through the membrane.

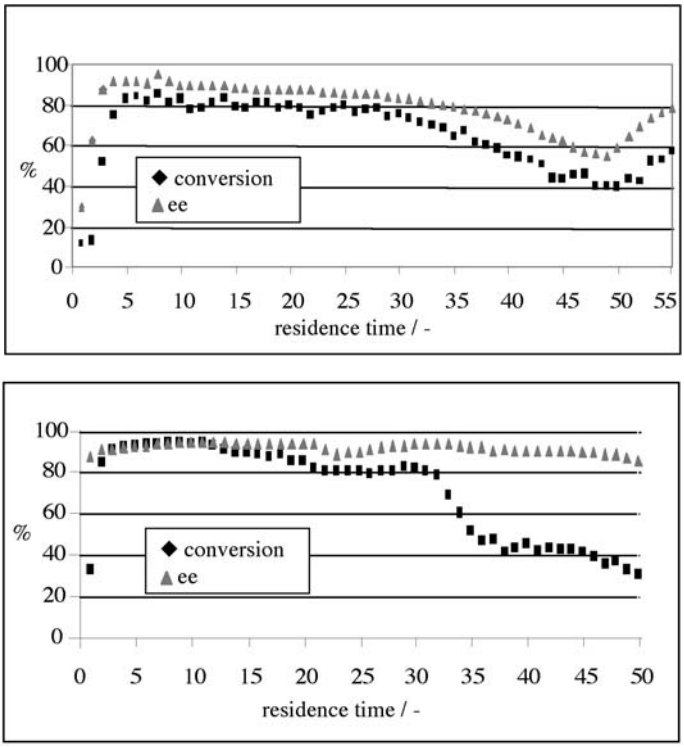

Fig. 12 Conversion plots for the continuous reactions using catalysts **12** and **14**

The polymer catalysts **12** and **14,** which were employed in the continuous reactions, were recovered and reused for batch epoxidations, and no decrease in ee (up to 97%) and conversion (around 85% after 60 min) was observed. It has been demonstrated that catalyst retention in the reactor solves catalyst recovery problems and provides a simple reaction procedure associated with high catalyst activity and selectivity.

3.5.3 Asymmetric Opening of Meso-Anhydrides

The third process for the membrane reactor was another metal-free catalytic process, the asymmetric ring opening reaction of *meso*-anhydrides [24]. The products of this reaction can be used, for example, as precursors for chiral β-amino acids. As with the borane reduction and the Juliá-Colonna epoxidation reaction, the asymmetric opening of anhydrides with cinchona alkaloids suffers from a requirement for long reaction times (>24 h) and large amounts of catalyst.

cis-4-Cyclohexene-1,2-dicarboxylic anhydride **15** was chosen as a model substrate, since it can be opened using the commercially available $(DHQD)_2$-

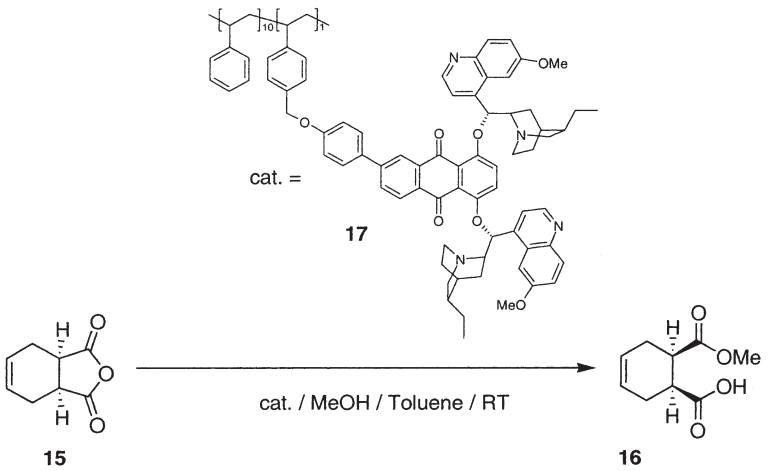

Scheme 7 Model reaction for the asymmetric opening of *meso*-anhydrides

AQN catalyst within 15 min at room temperature in methanol when 100 mol% of catalyst is used (Scheme 7).

The homogeneous polystyrene-attached catalyst **17** was less active than the native catalyst and full conversion was only reached after 1 h with, however, a high selectivity. The reaction arrangement was similar to that used for the epoxidation reaction; the two process streams being toluene/anhydride and toluene/methanol solutions.

The conversion and ee values for the continuous reaction are shown in Fig. 13a. The steep decline in both ee and conversion are not due to catalyst leaching, even though catalyst retention is poor at 95.4%. Batch experiments showed that the amount of catalyst **17** remaining within the reactor after 20 runs is sufficient for high conversion after 1 h. An increase of methanol from 10 to 20 equivalents increased the conversion from 60% to 90% after 20 residence times and a further methanol increase to 30 equivalents led to a conversion of 95%. In both cases, the ee value was almost unaffected and remained at a level of 50%. Furthermore, the decline in the ee value cannot be explained by catalyst leaching, since the uncatalyzed reaction between anhydride **15** and 10 equivalents of methanol, leading to racemic product, is slow (12% conversion after 24 h).

Batch experiments with different amounts of product present during the reaction showed that product inhibition was responsible for the decline in both ee and conversion, leading to the conclusion that this reaction is not suitable for a continuous process because of the high product concentration inside the reactor. A repetitive batch reaction is more suitable in this case, as the complete reaction volume is changed after completion of the reaction, and high values of conversion and ee should be achieved. The repetitive batch experiments showed that an improvement in ee and conversion was possible by changing

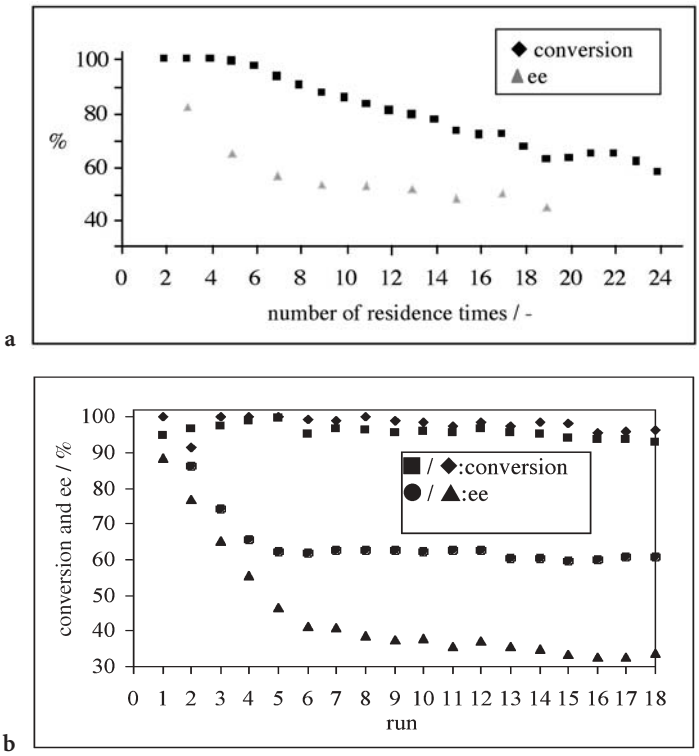

Fig. 13 **a** Conversion (filled diamonds) and ee (filled triangles) values for the continuous ring-opening of anhydride **15**. **b** Conversion and ee values for two repetitive batch reactions. Repetitive batch 1 (filled squares and filled triangles): catalyst not washed between runs; repetitive batch 2 (filled diamonds and filled circles): catalyst washed between runs. Conversion and ee values were determined by HPLC

from a continuous to a semi-batch process. Conversion was maintained at >90% over 18 cycles, but the ee-value dropped to below 40%. If a washing step between cycles is introduced, there is only a slight increase in conversion, but the ee increases significantly to 60% (Fig. 13b).

In both experiments, selectivity did not drop further after the initial decrease during the first few runs in the repetitive batch mode. This, together with NMR studies of recovered polymer-supported catalyst showing two molecules of product attached to each AQN-Ligand, provided further evidence for product inhibition. Enhancement of the washing procedure between cycles should result in reconstitution of the original catalyst, and high conversion and enantioselectivity should be possible throughout the repetitive batch cycle. Nevertheless, these results demonstrated the principle of the chemzyme membrane reactor, albeit in semi-batch mode. Over 18 cycles in this mode, the amount of catalyst required was 5.6 mol% per batch, and this would decrease further if subsequent cycles were run.

Transferring a metal catalyzed reaction to a continuous reaction system raises another question: will the metal remain bound to the polymer-attached ligand, or will the metal leach out through the reactor membrane? This question was examined by studying the transfer hydrogenation and the Sharpless dihydroxylation. Here the binding of the metal to the ligand is different in each case, and they are therefore appropriate for the study of continuous operation in a CMR.

3.5.4 Transfer Hydrogenation

The transfer hydrogenation was, like the borane reduction, evaluated in cooperation with Wandrey's group [25]. The well-known asymmetric reduction of acetophenone was chosen in order to obtain results that could be compared with a large number of batch reaction results. The tetradentate Gao-Noyori catalyst was attached via a linker to a polysiloxane, which is soluble in the isopropanol solvent. The solubility was additionally improved by attaching polar tris-(2-methoxyethoxy)silyl groups to the polysiloxane backbone (Scheme 8). The addition of a cosolvent (dichloromethane) permitted a high catalyst concentration to be used, which accelerated the completion of the reaction in the continuous mode.

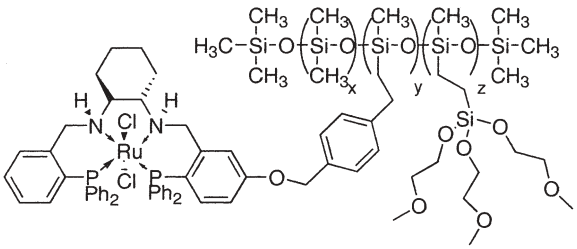

18

Scheme 8 Polymer-bound Gao-Noyori catalyst

The challenge in continuous transfer hydrogenation is the irreversible deactivation of the catalyst by oxygen, requiring the complete exclusion of oxygen from the reaction system. Because of the sensitivity of the catalyst to water this has to be excluded as well. However, catalyst deactivation by water is reversible and can be compensated for by continuous dosage of isopropanol.

The constant dosage of isopropanol into the reactor resulted in a slow but constant degradation of the polysiloxane backbone. Cyclosiloxane fragments were detected in the permeate by GC. This is not acceptable for a continuous system and the backbone has to be changed for industrial applications. Nevertheless, the loss of catalyst by degradation was compensated for by adding small amounts of polymer attached catalyst to the feed stream, and a TTN of 2880 with a space time yield of 560 g/(l d) was obtained, with stable conversion at ~80% and with ee at 94%. The results of this trial are presented in Fig. 14.

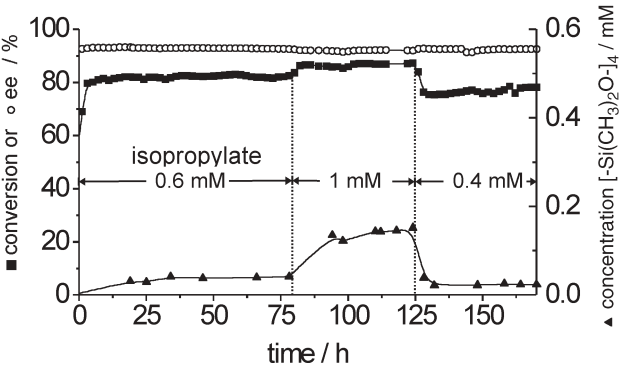

Fig. 14 Continuous transfer hydrogenation: enantiomeric excess/conversion versus time

3.5.5 Sharpless Dihydroxylation

Compared with the example above, where there is a defined tetradentate binding of the metal to the ligand, in the Sharpless dihydroxylation there is only a weak attachment of the metal to the alkaloid ligand. This reaction is therefore a good test of the scope and limitations of the chemzyme membrane reactor [26]. The conversion of homocinnamic acid **19** to the corresponding dihydroxy compound **20**, a building block for HIV-protease-inhibitors, was chosen as a model reaction (Scheme 9).

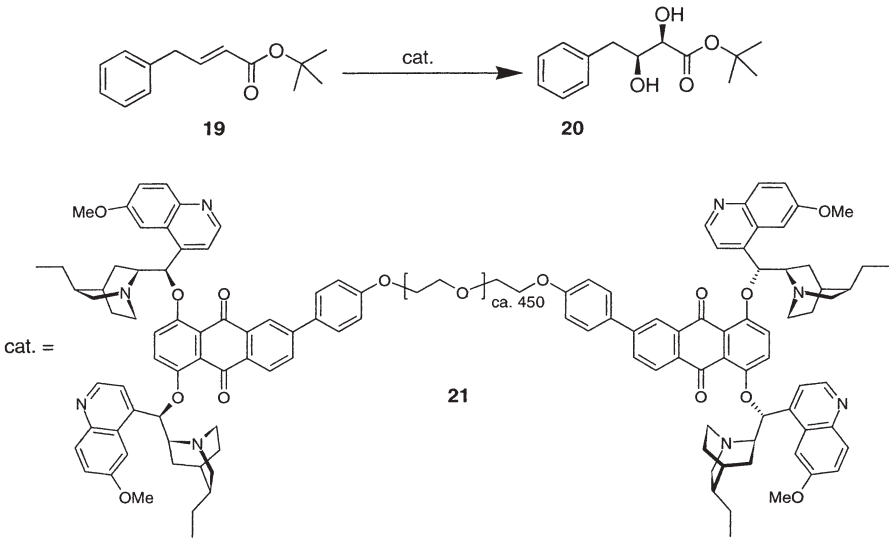

Scheme 9 Sharpless dihydroxylation of homocinnamic acid **19** with the molecular weight-enlarged AQN-catalyst

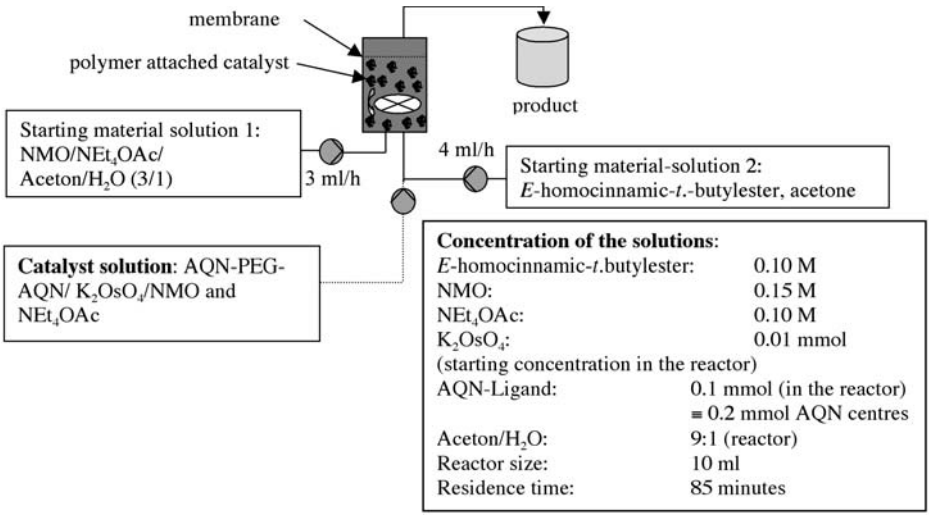

Fig. 15 Arrangement of the CMR reactor for continuous Sharpless dihydroxylation. The reaction vessel was rinsed with the solutions of raw materials 1 and 2 before dosing the catalyst solution. During Catalyst solution changing, the addition of raw material stream 2 was stopped briefly. As soon as the catalyst was in the reactor, solutions 1 and 2 were added continuously again

The Sharpless dihydroxylation reaction is run in a solvent mixture in the presence of a salt. Two protocols are available. The first is the use of potassium hexacyanoferrate in *tert*-butanol/water, while the second involves NMO as oxidant in a 9:1 acetone:water mixture. The second method was investigated in the CMR reactor since it is easier to perform, although the ee values reported are lower. The main aim of the study was to investigate the leaching of osmium from the ligand in the CMR.

Higher concentrations of osmium and ligand, and an increase in temperature from 0 °C to ambient temperature were used to reduce the reaction time to 2 h in the CMR. The high concentrations of catalyst can only be economic in a continuously operating CMR. No loss of selectivity and activity was found under these conditions. The apparatus used was similar to that used for the previous reactions, and is shown in Fig. 15. This demonstrates the flexibility of the CMR concept, which is able to accommodate a wide range of processes.

Figure 16 shows the course of one CMR experiment. The initial conversion and ee were both about 80%, only slightly less than in batch experiments. However, the conversion drops very quickly to only 18% after six residence times, without a change in the ee value. This is clearly due to leaching of osmium rather than of the ligand. After six residence times, 23% of the initial potassium osmate concentration was added continuously along with the NMO, which led to an increase in the conversion rate to the initial levels. The conclusion is that the polymer-bound ligand **21** could be retained by the membrane, but that the weakly bound metal was easily leached under the reaction conditions.

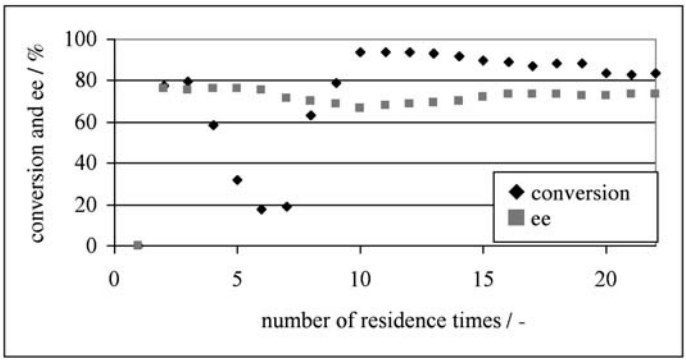

Fig. 16 Progress of the continuous dihydroxylation reaction, showing conversion and ee

3.6 Conclusion

These results highlight the scope and limitations of a chemzyme membrane reactor. A homogeneous catalyst retained by a membrane is only practical if the catalyst is required in large quantities, because of the increased synthetic work incurred. This is appropriate, for example, for the borane reduction or the asymmetric opening of anhydrides. The results of the transfer hydrogenation experiments indicate that a metal-bound catalyst can be used in a continuous system without deactivation by metal leaching, but only if there is strong binding between the metal and the ligand to prevent leaching. The Sharpless dihydroxylation demonstrated that weak metal-ligand binding results in the loss of the metal through the membrane. In this way, the CMR can be used to study the strength of the bond between ligand and metal in a practical set-up.

The practical advantage of a membrane reactor operating in a continuous mode is that it allows a large increase in catalyst loading, or in reaction temperature, to reduce the reaction time, while keeping the manufacturing cost at

Table 1 Comparison between batch and continuous mode processes

Catalyst	Product	Productivity (g/l/d)	TTN	Solvent
L-acylase	L-methionine	>10	–	water
FDH/LeuDH	L-*tert.*-leucine	638	125,000	water
PS-bound oxazaborolidine **7**	tetralone	1,420	1,374	THF
original Corey oxazaborolidine	tetralone	–	10	THF
polysiloxane-bound catalyst **18**	acetophenone	560	2,880	isopropanol
original Gao-Noyori catalyst	acetophenone	–	100	isopropanol

a low level. As the catalyst can be recycled in situ, the catalyst cost per kg of product can be reduced to a level below that achieved in a conventional system.

The advantages of a continuous system over batch operation are summarized in Table 1.

3.7 Summary and Outlook

Membrane reactors are a technological concept for the recycling of homogeneous catalysts. The limitations of using heterogeneous systems, such as reduced specific activities, impaired selectivity, and higher cost can be overcome by using homogeneous catalysis. This concept is suitable for both chemical and biocatalysis. The current focus of Degussa is to extend this technology platform to other chemical or biocatalysts in order to produce additional product classes, such as chiral alcohols or esters. Other reactor concepts are being tested which will allow the use of whole cells rather than the isolated enzyme.

Acknowledgements The authors wish to thank Dr. Ian Grayson for valuable help in the preparation of this manuscript.

References

1. Bommarius AS, Riebel BR (2004) Biocatalysis, 1st edn. Wiley-VCH, Weinheim
2. Drauz K, Waldmann H (2002) Enzyme catalysis in organic synthesis: a comprehensive handbook, 2nd edn. Wiley-VCH, Weinheim
3. Leuchtenberger W, Karrenbauer M, Plöcker U (1984) Ann NY Acad Sci (Enzyme Eng 7) 78434
4. Wandrey C, Wichmann R, Leuchtenberger W, Kula M-R (1981) Degussa AG/GBF, US 4 304 858
5. Genzen I, Löffler H-G, Schneider F (1980) Z Naturforsch 35c:544
6. Bommarius AS, Drauz K, Klenk H, Wandrey C (1992) Ann NY Acad Sci (Enzyme Eng XI) 67:126
7. Bommarius AS, Drauz K, Groeger U, Wandrey C (1992) Membrane bioreactors for the production of enantiomerically pure α-amino acids. In: Collins AN, Sheldrake GN, Crosby J (eds) Chirality in industry. Wiley, London 20:371
8. Slusarczyk H, Felber S, Kula M-R, Pohl M (2000) Eur J Biochem 267:1280
9. Takahashi T, Izumi O, Hatano K (1989) Takeda Chemical Industries, Ltd., European patent EP 0 304 021
10. Bommarius AS, Schwarm M, Drauz K (1996) Chim Oggi 14:61
11. Wöltinger J, Drauz K, Bommarius AS (2001) Appl Catal A 221:171
12. Kula MR, Wandrey C (1988) Method Enzymol 136:34
13. Kragl U, Vasic-Racki D, Wandrey C (1992) Chem Ing Tech 499
14. Bommarius AS, Makryaleas K, Drauz K (1991) Biomed Biochim Acta 50:249
15. Degussa AG (1992) German patent application DE 40 20 980
16. Felder M, Giffels G, Wandrey C (1997) Tetrahedron Asymmetr 8:1975
17. Giffels G, Beliczey J, Felder M, Kragl U (1998) Tetrahedron Asymmetr 9:691
18. Rissom S, Beliczey J, Giffels G, Kragl U, Wandrey C (1999) Tetrahedron Asymmetr 10:923

19. Kragl U, Beliczey J, Brinkmann N, Felder M, Giffels G, Wandrey C (1998) In: GVC Jahrbuch, VDI-Verlag, Düsseldorf, p 151
20. Wöltinger J, Bommarius AS, Drauz K, Wandrey C (1999) DECHEMA-Arbeitsausschüsse "Technische Reaktionen" und "Katalyse" und GVC-Fachausschuß "Technische Reaktionsführung", Frankfurt
21. Wöltinger J, Drauz K, Bommarius AS (2001) Appl Catal A–General 221:171
22. Wöltinger J, Bommarius AS, Drauz K, Wandrey C (2001) Org Process Res Dev 5:241
23. Tsogoeva SB, Wöltinger J, Jost C, Reichert D, Kühnle A, Krimmer H-P, Drauz K (2002) Synlett 707
24. Wöltinger J, Krimmer H-P, Drauz K (2002) Tetrahedron Lett 43:8531
25. Laue S, Greiner L, Wöltinger J, Liese A (2001) Adv Synth Catal 343:711
26. Wöltinger J, Henniges H, Krimmer H-P, Bommarius AS, Drauz K (2001) Tetrahedron Asymmetr 12:2095

Received: April 2004

Author Index Volumes 51 – 92

Author Index Volumes 1 – 50 see Volume 50

Subject Index